MUSCULOSKELETAL MODELLING OF THE SHOULDER DURING CRICKET BOWLING

Lomas Shiva Persad

Department of Bioengineering

Imperial College London

A thesis submitted in fulfilment of the requirements for a degree of
Doctor of Philosophy at Imperial College London and the Diploma of Imperial College

January 2016

Abstract

Shoulder injuries affect athletes who participate in overhead sports, such as swimming, baseball or basketball. This is due to the high loading, large range of motion and repetitive nature of the sporting task. Impingement has been identified as the most common cause of shoulder pain in overhead athletes. Cricket bowling involves one of the more complex sporting tasks where the arm goes through a large range of motion during circumduction to project the cricket ball at varying degrees of speed and spin where injury surveillance research estimates that over 20% of cricket injuries are related to the upper limb with the glenohumeral joint being the second most injured site. Similar to other overhead athletes, cricket bowlers have a prevalence of shoulder injury and pain with loss of internal rotation. It is hypothesised that this is due to large distraction forces and muscle imbalance at the glenohumeral joint. A second, specific hypothesis is that bowlers who have greater internal rotation after delivering the cricket ball are more likely to suffer from impingement. The motivation for this study is derived from these hypotheses. The aim of this thesis was to test the hypotheses above and investigate potential shoulder injury risk in cricket bowlers. A full body 3D kinematic analysis of fast and slow bowling actions was conducted and a musculoskeletal model used to investigate joint forces and muscle activations at the shoulder. Technical advances were made in musculoskeletal modelling; these included a new kinematic optimisation routine and improvements in the muscle wrapping method. The performance of a scapula tracker in full speed bowling trials showed good repeatability. There was however, significantly greater posterior/anterior tilt and internal rotation underlining the effect of speed of movement on the scapula tracker that was used. At ball release, the glenohumeral adduction angle for fast bowlers was between 36°- 80° and 59°- 66° for slow bowlers with the humerus externally rotated within a range of 90°- 140° and 71°- 131° for both sets of bowlers respectively. The analysis showed that one potentially vulnerable position was in the region between upper arm horizontal and ball release due to the location of the joint reaction force and its magntiude. A large distraction force was reported for bowlers where the superior shear forces was also a key factor in determining the risk on injuries at the joint. Predicted activation pattern for subscapularis substantiate the risk of impingement injuries due to overuse and fatigue during rotation of the arm from upper arm horizontal to ball release. In addition, internal/external glenohumeral joint torque values were similar for both sets of bowlers with the peak value occuring midway between upper arm horizontal and ball release. Further work should concentrate on the link between technique and musculoskeletal loads and thus allow training to mitigate the risk of shoulder injury.

Acknowledgements & Declarations

Firstly, I would like to thank my supervisor Professor Anthony Bull for his support, comments and unwavering enthusiasm throughout the duration of this thesis. I am also grateful to Dr. Eftaxiopoulou for her guidance, advice and knowledge imparted to me when it came to using the motion capture system and analysis.

I would like to acknowledge Mr. Fraser Stewart and the Marylebone Cricket Club for allowing me the use of their facilities and cricketers. In addition, I would like to thank both past and present members of the Imperial College Cricket Club for volunteering as test subjects throughout the years.

Thanks to everyone in the Musculoskeletal Biomechanics group for all the advice and encouragement throughout the years.

Finally, I am forever indebted to my parents Gyandeo and Judy and to my brother Artma, whose love and support throughout my life made this possible. I dedicate this thesis to you all.

Lomas Shiva Persad

Contents

Figures

Tables

Chapter 1

Introduction

This chapter describes the motivations and aims of this thesis.

1.1 Motivation

Shoulder injuries affect athletes who participate in over-head sports, such as swimming, cricket, baseball or basketball. This is due to the high loading, large range of motion or repetitive nature of the sporting task. Cricket bowling involves one of the more complex sporting task where the arm goes through a large range of motion during circumduction to project the cricket ball at varying degrees of speed and spin. A review of injuries in cricket has shown that shoulder injuries in bowlers are both prevalent, and amenable to biomechanical analysis (Orchard et al., 2006; Stretch, 2003; Ranson and Gregory, 2008).

A review of the literature highlighted that similar to other overhead athletes, cricket bowlers show signs indicating the onset of shoulder pain such as loss of internal rotation, large distraction forces and muscle imbalance at the glenohumeral joint, where impingement was described as the most common shoulder injury. Therefore, bowlers should also be considered at risk of shoulder injuries. The motivation for this thesis is derived from these hypotheses.

The shoulder complex has a large range of motion where the scapula rotates closely with the clavicle and has multiple muscle attachments connecting to the thorax. The humerus is tethered to the scapula by the action of the important rotor cuff muscles at the highly mobile but inherently unstable glenohumeral joint. The scapula forms the base of movement for the upper arm, where a stable joint allows effective transmission of loads generated in the torso and lower limbs through the kinematic chain of the shoulder. Therefore, key to understanding the risk of injuries at the glenohumeral joint is kinematics of the scapula, muscle forces and joint loads across the glenohumeral joint.

1.2 Aims

The aims of this thesis are as follows:

- Compare key shoulder kinematic and kinetic variables between faster and slower balls delivered by both fast and slow bowlers. This would involve analyse of the glenohumeral kinematics and muscles that generate this movement during bowling.
- Identify and describe phases in the bowling action that highlight a greater risk of impingement injuries and its relation to internal rotation during the bowling action.

These aims were achieved by fulfilling the following requirements:

- Develop a clinical kinematic description of the bowling technique. This would require developing a motion capture marker model and camera setup through empirical means.
- Dynamic tracking of the scapula during bowling. Using a scapula tracking device, experiments were done to capture the movement of the scapula and how its implementation could be optimised to provide better results.
- Use a previously validated musculoskeletal model (UKNSM) for simulating upper limb musculoskeletal loads during cricket bowling, making the necessary adaptations.
- Analyse the movement of scapula, muscle forces, joint loading and stability involved in the motion to determine the potential injury risk and how this aligns with the hypothesis and establish phases of the action which places the bowler at greater risk of injury.
- Verification of the musculoskeletal model outputs with the literature and its suitability for cricket bowling.

These requirements were achieved by firstly conducting experimental work for measuring scapula kinematics in this activity. Scapula kinematics were measuring during slow circumduction to allow for comparison and to quantify the accuracy and repeatability of the technique used during the circumduction motion. After which, the technique was used for full speed bowling trials where its performance was reassessed. An existing musculoskeletal model was further developed where changes to the kinematic optimisation and muscle wrapping methods where necessary to proceed with the analysis. Predicted muscle forces, joint stability and joint loading are then presented and discussed on a general level, due to major limitations of the musculoskeletal model.

1.3 Thesis outline

Chapter 2: Anatomy and Functional Kinematics

Musculoskeletal anatomy of the upper and lower limbs are presented with a focus on the functional kinematics of muscles and joints in the upper limb. Details of important concepts such as calculation of Euler angles, basic concepts of vectors and rotation matrices and definition of standardised anatomical coordinate frames are also presented as these were used throughout this work.

Chapter 3: Biomechanics of cricket bowling and a review of shoulder injury

The game of cricket is briefly described with relevant cricket jargon being explained. A review of current knowledge in the biomechanics of cricket bowling is presented where key variables used in describing the bowling technique are outlined.

A literature review of shoulder injuries in overhead athletes and commonality with cricket bowlers are presented within this chapter, where the role of the scapula in the overhead athlete is highlighted. Key publications that described the hypotheses under investigation in this thesis are also outlined in this chapter.

Chapter 4: Dynamic tracking of the scapula during slow circumduction

A review of scapula measurement techniques are presented followed by an experimental study with the aim of assessing the performance of a scapula-tracking device.

A skin fixed scapula tracking device was used during slow circumduction of the dominant arm in 12 subjects. The repeatability of the device in capturing scapula kinematics and its accuracy when compared to a scapula palpator was assessed. This work aims to utilise knowledge of the performance of the device so that any adjustments or improvements could be made to the device before it is used in full speed bowling trials. In addition, the results of this study provides a basis for comparison when the device is used in full speed bowling trials.

Chapter 5: Motion capture of bowlers and results

This chapter describes the material and methods involved in calculating bowling kinematics. The data obtained from this experimental study represent the cohort of subjects that will be used for analysis in subsequent chapters. Kinematic analysis of bowlers tested is presented with a focus on scapula kinematics, humerus kinematics and bowling technique variables.

Chapter 6: Upper limb musculoskeletal modelling of cricket bowling using the UKNSM

A technical description of the upper limb musculoskeletal model used in this thesis is presented in this chapter. Issues with the model and adaptations with the rationale for doing so are also presented. Improvements included correcting scapula kinematics that resulted in non-physiological positions and improving the muscle wrapping method for key muscles where the line of action of muscle elements are determined by a shortest path algorithm. Sensitivity of the model to the new changes and other variables are shown where the improvements to model

outputs is highlighted.

Chapter 7: Musculoskeletal forces at the shoulder during bowling

This chapter presents the results obtained from the modified UKNSM. Glenohumeral joint reaction force, mucsle forces, kinematics and joint stability are analysed and compared with the literature in establishing a link to impingement injuries. Muscle activities are compared to EMG measurements during bowling where there was agreement on the prime movers of the arm during the different bowling phases. This allows some verification of the muscle activation patterns and discussion presented even though the magnitude of forces may have been overestimated.

Chapter 8: Conclusions and future work

A summary of the outcomes of the work in this thesis is presented in this final chapter. Limitations are discussed highlighting key areas for future work in terms of musculoskeletal modelling of the cricket bowling action.

Chapter 2

Anatomy and Functional Kinematics

This chapter describes the functional anatomy of the upper limb and the mathematics use to describe joint kinematics of the upper limb in clinical terms. The conventions established for joint rotations are particularly important to note, as it is fundamental in understanding the kinematics involved in cricket bowling.

2.1 Introduction

The upper limb comprises of the shoulder complex, humerus and forearm. Figure 2.1 shows how each of these groups combine to form a chain link to the thorax connected along the way by the major joints of the upper limb. The shoulder complex has the largest range of motion of any articulation in the body where there exist a balance between mobility and stability. Integral to this balance is the scapula, which acts as a moveable base allowing for the large range of motion, like the circumduction motion of the humerus during cricket bowling. Furthermore, the scapula has more muscle attachments than any other bone in the upper limb and keeps the humerus tethered by the action of muscles and passive structures. This highlights the importance of the scapula in upper limb modelling.

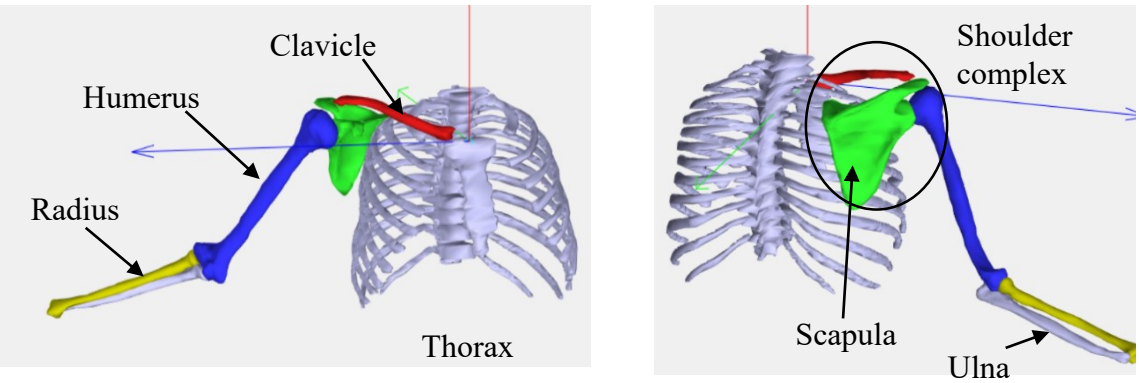

Figure 2.1 Bones of the upper limb

2.2 Clinical terms

Three fixed anatomical planes within the body are used in describing rotations and translational directions. Proximal and distal refer to the relative position of body segments where, proximal refers to the segment closer to the thorax and distal refers to further segment.

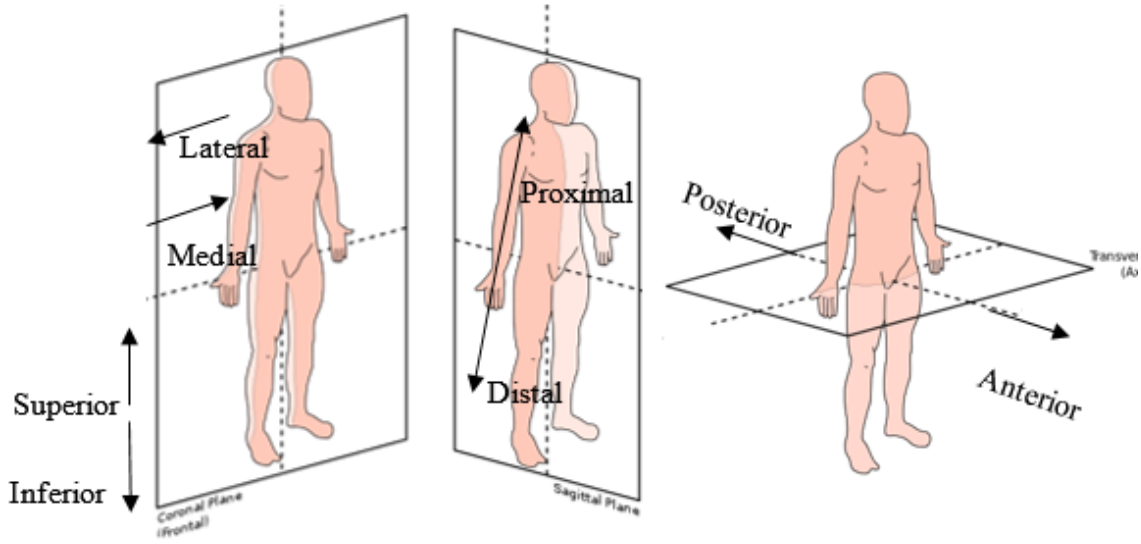

Figure 2.2 coronal, sagittal and transverse anatomic planes adapted from Edoarado (2013)

Generally, movement of the upper limbs relative to proximal segments can be described as shown in Figure 2.3 where clinical description of upper limb movement is based on rotations in anatomical planes. Abduction or adduction occur in the coronal plane rotating away or towards the body midline respectively. Flexion/extension is used to describe the relative rotation between proximal and distal segments in the sagittal plane. Internal/external rotation refer to rotations about the segment longitudinal axis.

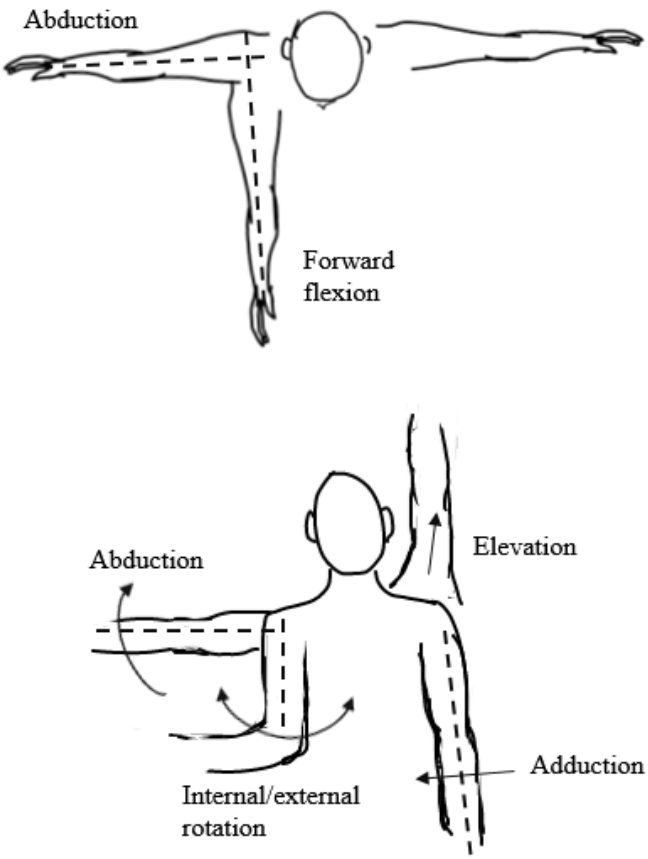

Figure 2.3 Description of upper limb motion

Scapula, clavicle rotation relative to the thorax and glenohumeral rotations are described in Section 2.6.3.

2.3 Upper limb Functional Anatomy

2.3.1 The shoulder complex

The shoulder complex contains the clavicle, scapula, rib cage and humerus (Figure 2.4). It connects the upper limb to the axial skeleton as well as provides attachment sites for many muscles that control the movement of the arm (Tortora & Derrickson, 2011). The shoulder complex is made up of four articulations: sternoclavicular (SC) joint, acromioclavicular (AC) joint, glenohumeral (GH) joint and scapulothoracic (ST) articulation.

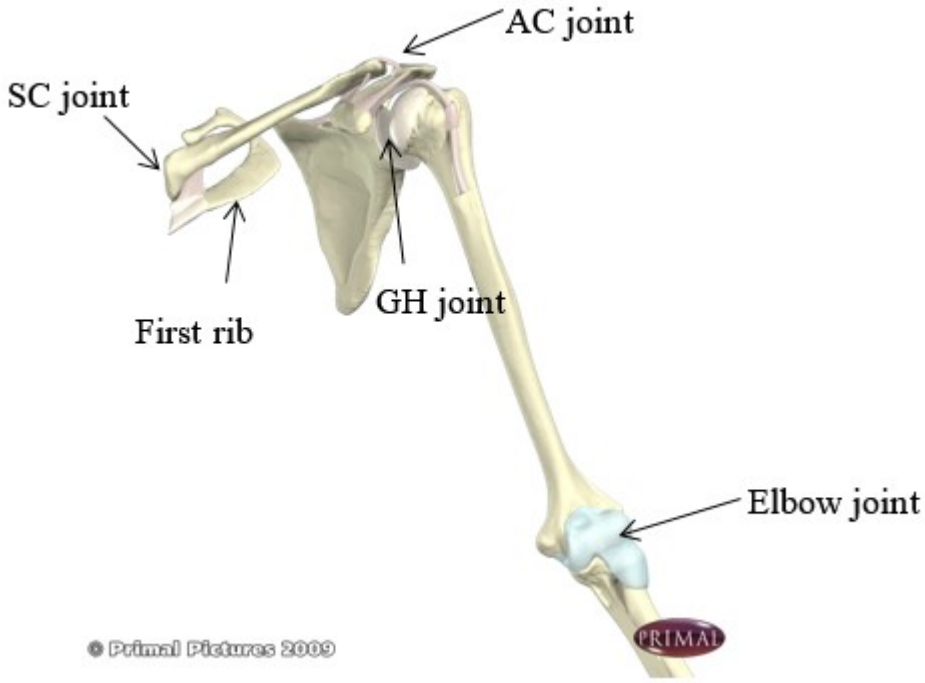

Figure 2.4 Shoulder complex and elbow joint (Primal, 2006)

2.3.2 Clavicle

The clavicle is the only bony attachment that links the thorax to the upper limb via the SC and AC joints where it is linked with the manubrium of the thorax and acromion process of the scapula respectively. These joint locations can easily be seen or palpated through the skin along its longitudinal axis (Tortora & Derrickson, 2011). The clavicle has three ligaments that help to constrain movement of the clavicle and by extension constrain scapula kinematics. These are the costoclavicular ligament at the proximal end as well as the conoid and trapezoid ligament at the distal end. Altering its length leads to altered kinematics at the shoulder complex (Charlton, 2003) and changes in shoulder strength (Ledger et al., 2005). The clavicle is also important in supporting axial loads as well as helps the humerus and scapula maintain their position relative to the rib cage.

2.3.3 Scapula

The scapula is a large triangular bone, located between the second and seventh ribs (Tortora & Derrickson, 2011) and is well suited to carry large number of muscle attachments. It has three

processes: the acromion, spine and coracoid process. Inferior to the acromion is the glenoid cavity. On the posterior surface of the scapula are two fossae: the supraspinatus fossa and the infraspinatus fossa located superior and inferior to the scapula spine. They both serve as attachment sites for tendons of the supraspinatus and infraspinatus muscles that are responsible for maintaining stability of the glenohumeral joint in addition to driving abduction and external rotation of the humerus respectively. Similarly, the subscapular fossa, which is located on the anterior surface of the scapula, serves as the attachment for the subscapularis the main instigator of humeral internal rotation.

The spine that runs medial to lateral on the posterior side serves as attachment sites for muscles as well as the medial border, which extends from the superior angle to the inferior angle. In all there are eighteen muscle attachments on the scapula (Grey, 2008).

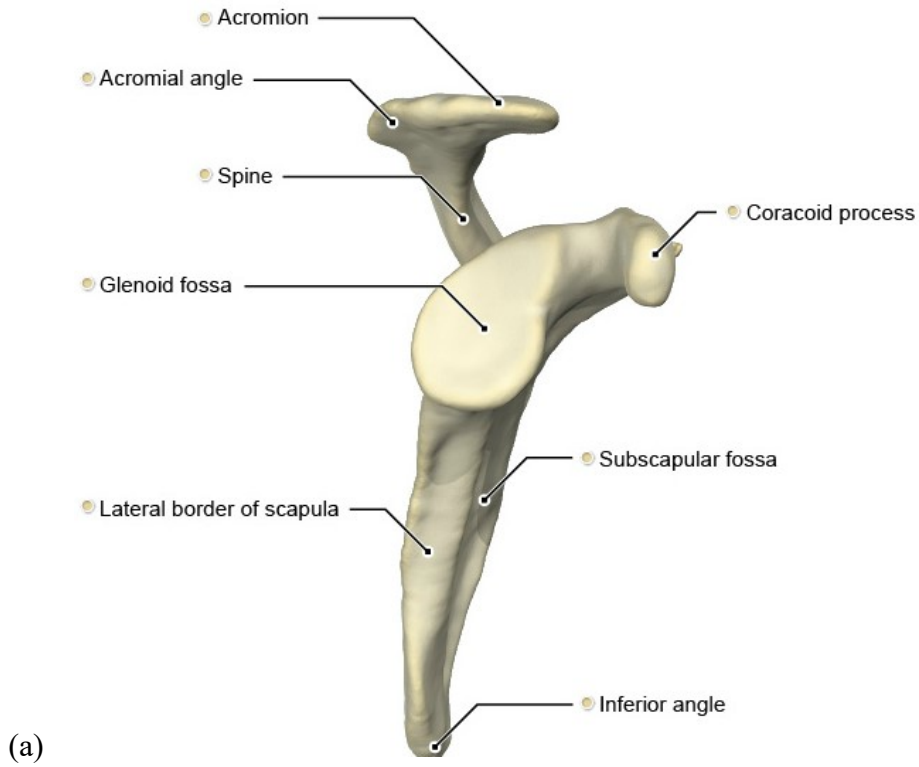

(a)

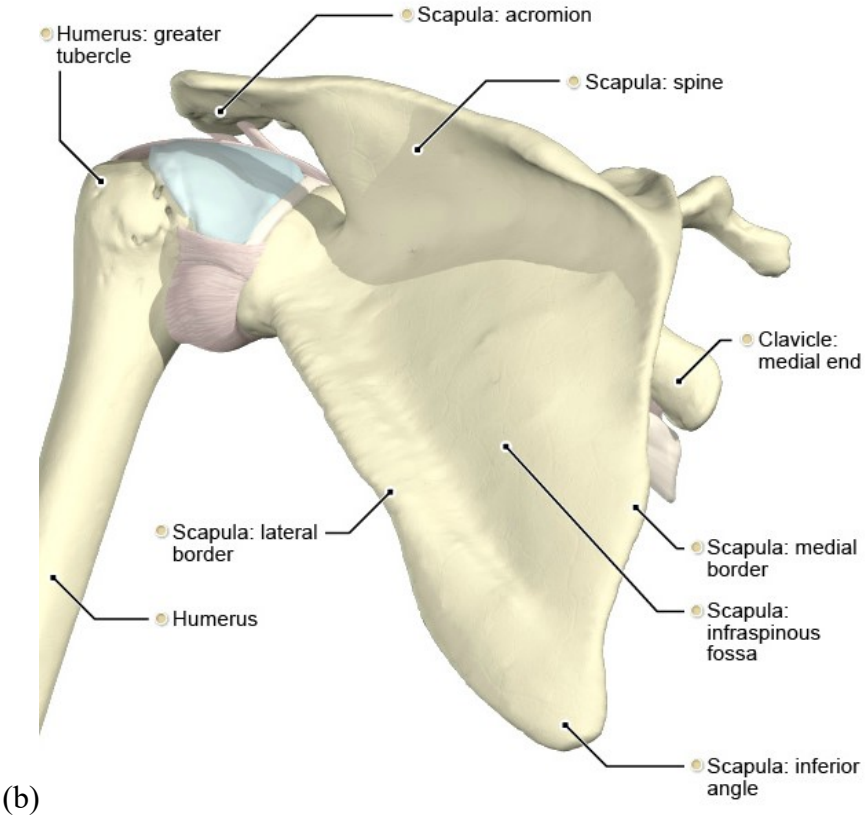

(b)

Figure 2.5 Anterior(left) and lateral (right) view of the left scapula (Primal, 2006)

The coracoid process is the hook-like projection that lies underneath the clavicle and serves as the attachment site for the conoid and trapezoid ligaments and two muscles. The scapula is mechanically supported by these ligamentous structures that connect to the clavicle. As the arm elevates, the clavicle also elevates allowing the scapula to rotate and elevate the glenoid fossa.

The spine forms into the acromion at the lateral end where it articulates with the clavicle forming the AC joint. The acromion arches over the glenohumeral joint allowing the attached middle deltoid to have a significant moment arm about this joint. The general shape of the scapula as well as the protruding structures allow for large scapulothoracic muscle moment arms around the SC and AC joints (Veeger & van der Helm, 2007). The projection of the acromion creates a space with the glenoid to allow the rotator cuff muscles to pass. This is called the subacromial space. The rotator cuff muscles that pass through this space are susceptible to wear and tearing due to a reduction of this space where, the rotator cuff is effectively pinched during movement, leading to injury. This problem is very common at the shoulder (Ludewig & Cook, 2000; Roberts et al., 2002) and is one of the topics of investigation in this thesis.

Finally, the glenoid cavity is a shallow cavity that articulates with the humeral head to form the glenohumeral joint. The combination of its surface being retracted, the retroverted humeral head, the scapula lying in a plane 30°-45° from the coronal plane and the low conformity of the interacting surfaces all aid in producing a large range of motion of the humerus (Terry & Chopp, 2000).

2.3.4 Humerus

The humerus is the largest bone of the upper limb. It articulates proximally with the scapula and distally at the elbow with the Ulna and Radius. Muscles that are attached to the humerus include the powerful deltoid, latissimus dorsi, pectoralis and rotator cuff to name a few. In all, there are twelve muscle attachments along its length. The greater tuberosity; a lateral projection at the proximal end, and the lesser tuberosity; an anterior projection at the proximal end, form the bicipital groove though which the long head of the bicep passes. At high arm elevations, the greater tuberosity together with an abnormal acromion shape may result in the pinching mechanism of muscle injury that was described earlier.

At the distal end, there are the medial and lateral projections known as the medial epicondyle (ME) and lateral epicondyle (LE) (Figure 2.8). They are easily palpable and are used as

identification landmarks for the humerus for defining the kinematic coordinate frame of the segment.

2.3.5 Forearm

The forearm is made up of the longer ulna that is on the medial side and the shorter radius on the lateral side. The radial head is located at the proximal end while the ulnar head is at its distal end. Situated at the distal end of the radius and distal end of the ulna are the styloid processes: radial styloid (RS) and ulna styloid (US) (Figure 2.8) which are used as palpable landmarks for the forearm for defining its coordinate frame when calculating kinematics.

2.4 Upper limb Joints

A brief description of each joint and how they are linked to form the upper limb kinematic chain is given in this section. A more detailed look at the muscles that crosses these joints and how they maintain the joint integrity is presented in Section 2.5. Generally, ligaments and other passive structures of the joint only apply constraining forces while the muscles are the active components for producing forces that leads to motion.

2.4.1 Sternoclavicular joint

The sternoclavicular joint (SC) is located between the manubrium of the thorax and clavicle. The SC joint allows for movement of the clavicle in three planes, allowing for clavicle anterior-posterior, elevation-depression and some axial rotation.

The costoclavicular ligament connects the proximal end of the clavicle to the thorax where it acts to limit the clavicle elevation (Pronk et al., 1993). Therefore, at high humeral elevation and by extension high clavicle elevation, this ligament would play an important role at the SC joint. One major limitation of modelling its behaviour is that strains maybe overestimated due to a shift in the effective rotation centre (Pronk et al., 1993).

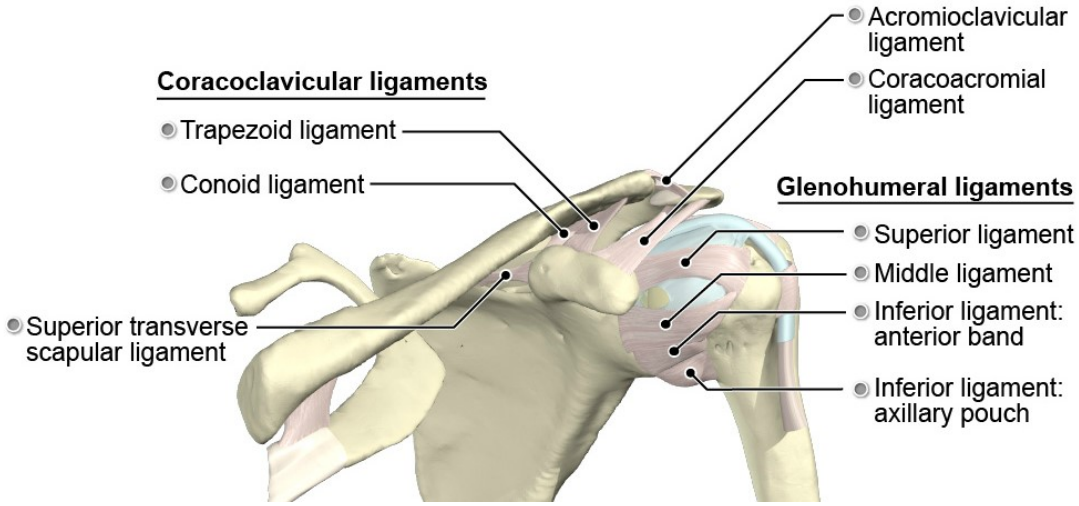

Figure 2.6 Costocalvicular ligament between thorax and clavicle and other ligaments at the glenohumeral joint (Primal, 2006)

2.4.2 Acromioclavicular joint

The joint is stabilised by three ligaments. They are acromioclavicular ligaments at the joint between the clavicle and acromion and the conoid (medial) and trapezoid ligaments (lateral) shown in Figure 2.6. The action of these ligaments reduce translations of the joint (Pronk et al., 1993) reduce shearing as well as limit axial rotation along the clavicle (Pronk et al., 1993).

2.4.3 Scapulothoracic gliding plane

This is an articulation of the anterior surface of the scapula and the posterior surface of the rib cage. Between these two bony segments, there are the subscapularis and serratus anterior muscles with the larger trapezius, latissimus dorsi on the posterior surface of the scapula. In this way these muscles and others form layers (Williams et al., 1999) with bursa in between to facilitate the movement of the scapula . While there is no physical joint, the scapula moves over this region known as the scapulothoracic gliding plane (STGP). The separation of the scapula over the rib cage is not fully understood and is one of the modelling challenges that will be discussed in this thesis.

2.4.4 Glenohumeral joint

The humerus and scapula form the GH joint. This joint is inherently unstable to allow for the large range of motion possible by the humerus. The high degree of freedom of the joint is due

to the looseness of the articular capsule and shallowness of the glenoid cavity in relation to the larger humeral head. The joint is held intact by passive structures like the GH ligaments and joint capsule as well as active muscles that originate from the scapula and wrap around the humeral head, called the rotator cuff muscles (Figure 2.11). These muscles play an important role in maintaining stability by providing compression of the joint at all shoulder positions (Lee et al., 2000; Southgate et al., 2009; Hughes & An, 1996). Their role is discussed at length in section 2.5.1. The glenoid labrum is a fibrocartilaginous ring that lines the glenoid cavity that helps to deepen the concavity of the glenoid adding to stability.

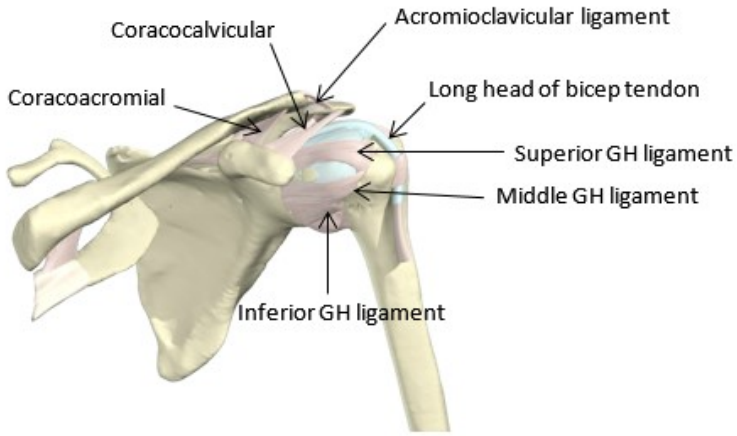

Figure 2.7 Acromioclavicular and glenohumeral joint anatomy (Primal, 2006)

2.4.5 Elbow

The elbow joint formed between the humerus and two bones of the forearm. During normal function, there are three articulations at this joint: humeroulnar, humeroradial and radioulnar (Figure 2.8).

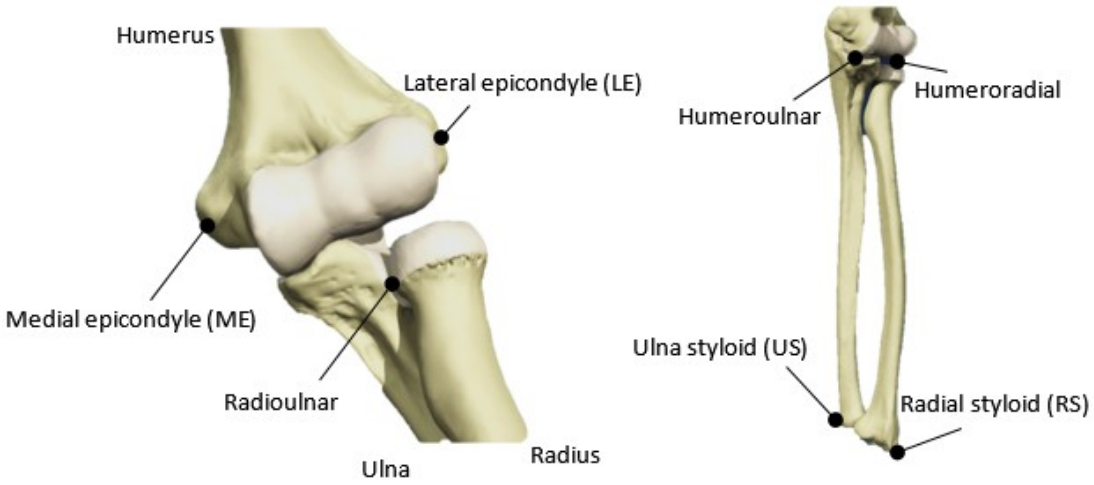

Figure 2.8 Elbow and forearm landmarks (Primal, 2006)

The two most important ligaments of the elbow are the medial and lateral collateral ligaments. They consist of the ulnar collateral ligament, which extends from the medial epicondyle of the humerus to the ulna, and the radial collateral ligament, which extends from the lateral epicondyle of the humerus to both the radius and ulna. Muscles that cross this joint are presented in the next section.

When the elbow joint is fully extended, the glenohumeral, elbow and wrist joints are not collinear. The deviation that occurs is known as the carry angle of the elbow (Steel & Tomlinson, 1958). It has been reported to be a function of age and gender where male subjects average 10° while female subjects average 13° (Van Roy et al., 2005).

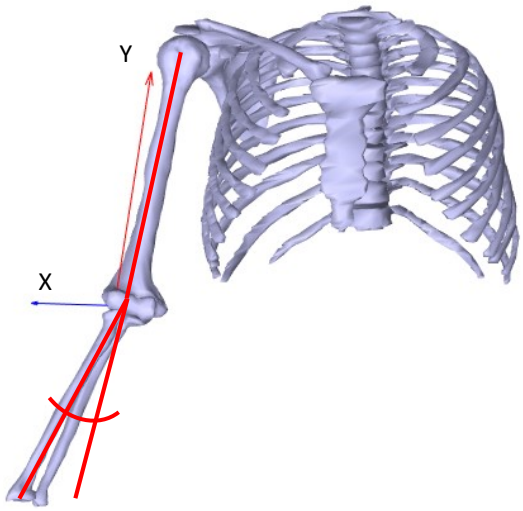

Figure 2.9 Anterior view of the right arm showing the carry angle

2.5 Upper limb muscles

The actuators that provide movement at joints are the muscles. An overview of some of the main muscles and prime movers for the upper limb is presented in Figure 2.10. They are usually superficial muscles with greater moment arms and larger cross-sectional area than the deeper lying muscles. Some of these superficial muscles originate from the thorax and attach to the scapula, clavicle or humerus where they may span the SC, AC and GH joints due to the close proximity of these joints contributing to moment arms about these joints.

The trapeziums, rhomboids and levator scapulae originate from the base of the skull or spine and connect the scapula or clavicle to the thorax of the body providing a strong basis for performing arm movements. Other muscles such as the pectoralis major, pectoralis minor, latissimus dorsi, teres major and deltoid connect to the proximal end of the humerus and anchor it to the body.

Important upper limb muscles are highlighted in this section.

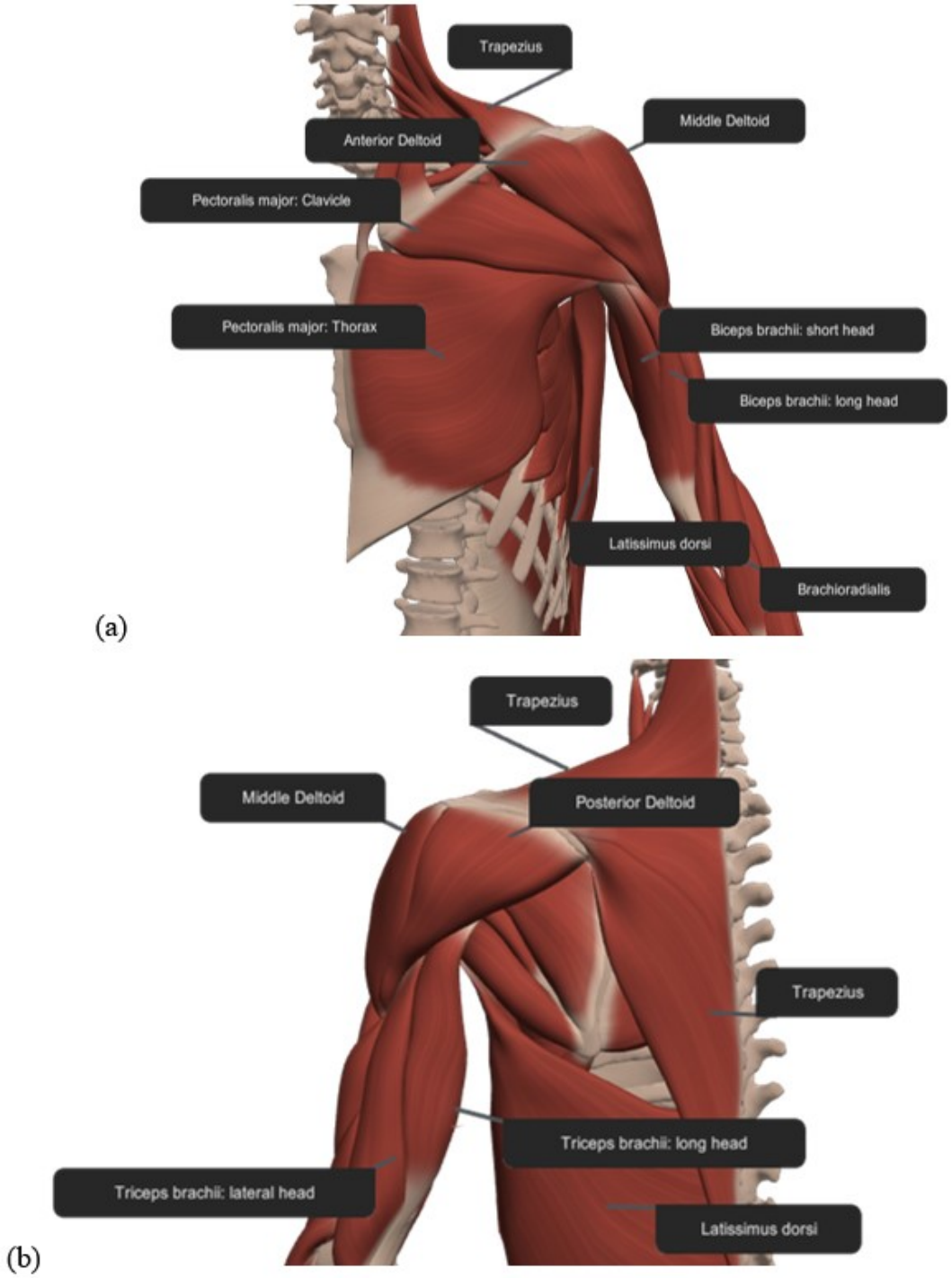

Figure 2.10 Summary of upper limb musculature and prime movers of the upper limb (a) anterior view (b) posterior view (Primal, 2006)

2.5.1 Rotator cuff muscles

The four most important muscles (and their respective tendons) of the GH joint are collectively known as the rotator cuff muscles: subscapularis, suprasinatus, infraspinatus, and teres minor (Figure 2.11). The rotator cuff muscles are constantly being recruited to stabilize the glenohumeral joint regardless of shoulder kinematics (Hurov, 2009; Terry & Chopp, 2000). They work as a group in unison in centring the humeral head within the glenoid fossa.

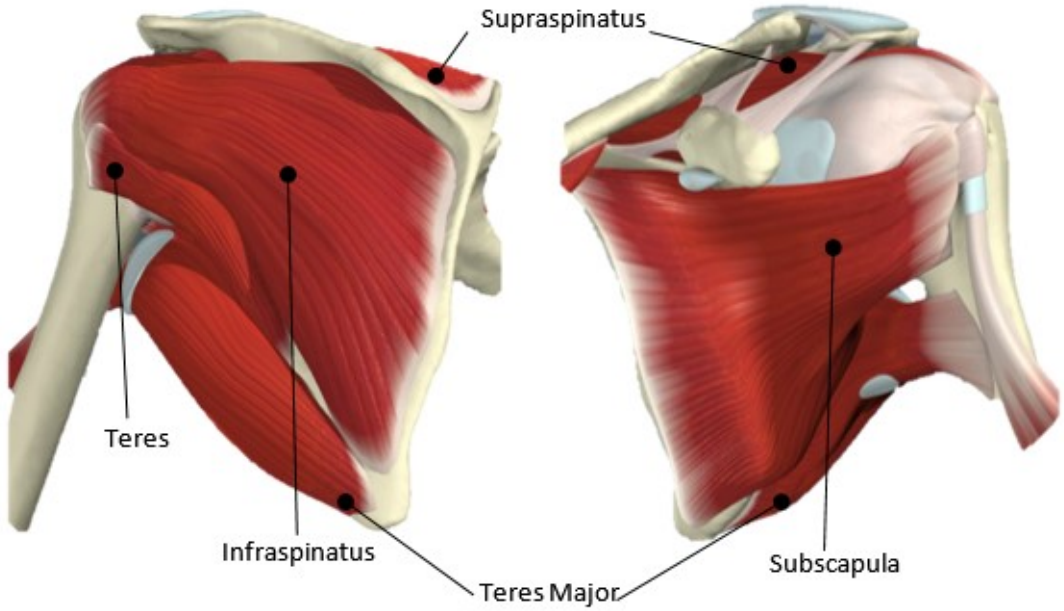

Figure 2.11 Posterior (left) and anterior (right) view of the scapula showing the rotator cuff muscles and teres major (Primal, 2006)

The arrangement of the rotator cuff muscles and the way they wrap around the humeral head allows them to have lines of action that are perpendicular to the glenoid (Figure 2.12). This means that they are well suited for keeping the GH joint reaction force within the glenoid and prevent dislocations (Veeger & van der Helm, 2007; Terry & Chopp, 2000; Ackland & Pandy, 2009). The action of the subscapularis/teres major oppose the infraspinatus /teres minor in controlling GH axial rotation (Terry & Chopp, 2000) while the suprasinatus and deltoid are used to elevate the arm.

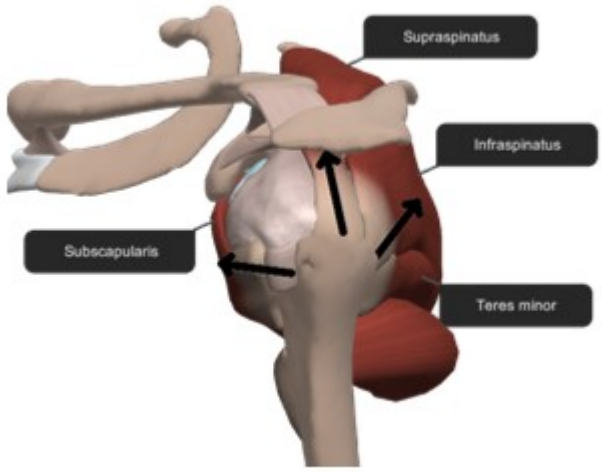

Figure 2.12 Action of the rotator cuff in stabilising the GH joint (Primal, 2006)

Weakening of the rotator cuff can cause superior translation of the humeral head due to the powerful deltoid muscle to pull on the humerus during elevation (Yanagawa et al., 2008). This results in impingement of the rotator cuff muscles causing injury (Ludewig & Braman, 2011) (Figure 2.13). This problem of impingement and its effects on overhead athletes is discussed in chapter 2.

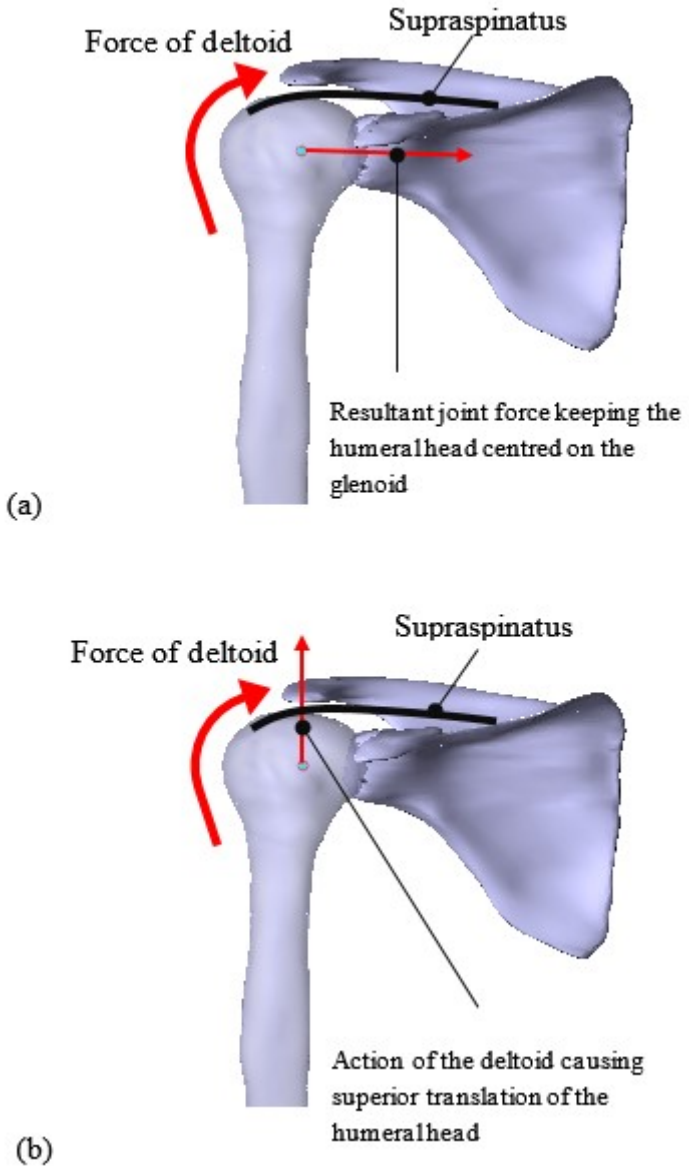

Figure 2.13 (a) Normal action of the rotator cuff muscles keeping the humeral head centred on the glenoid (b) muscle imbalances causing resulting in an unopposed deltoid force causing superior translation of the humerus impinging on the supraspinatus

2.5.2 Other important scapula muscles

The deltoid muscle is subdivided into the anterior, middle and posterior portions and all insert into the humerus. The anterior deltoid originates from the anterior boarder and distal third of the clavicle, the middle deltoid from the superior surface of the acromion and the posterior deltoid from the inferior border of the scapula spine. In this way, they encompass the GH joint and are important prime movers at the shoulder.

The functional role of the deltoid portions (Figure 2.14) is dependent on their location relative to the GH joint. For instance, the posterior portion is used in humerus external rotation and extension while, the anterior portions are used in flexion and internal rotation of the humerus and the middle portion is used primarily in abduction and flexion with a weak internal/external rotation moment arm (Ackland & Pandy, 2011).

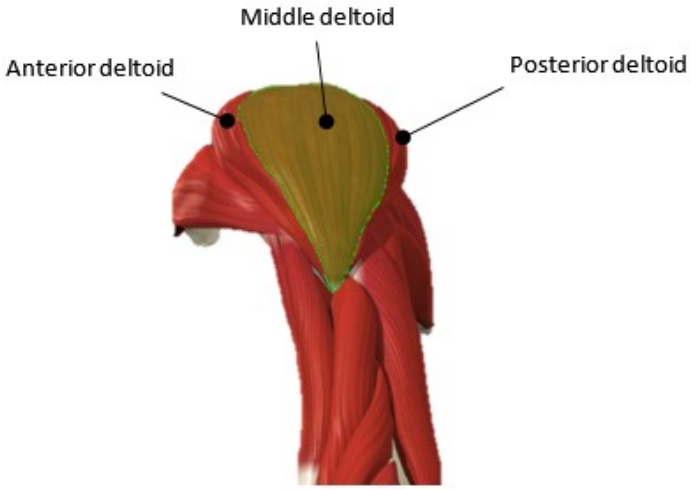

Figure 2.14 Lateral view of the shoulder showing the deltoid muscle (Primal, 2006)

The serratus anterior (Figure 2.15) originates from the anterior and lateral surface of the first nine ribs inserting into the inferior angle and medial border of the scapula. It lies in between the scapula and the ribcage on the scapulothoracic gliding plane with layers or bursa in between to reduce friction of moving segments. It has a very large moment arm when activated, pulling the medial border of the scapula towards the ribcage and in controlling upward rotation of the scapula.

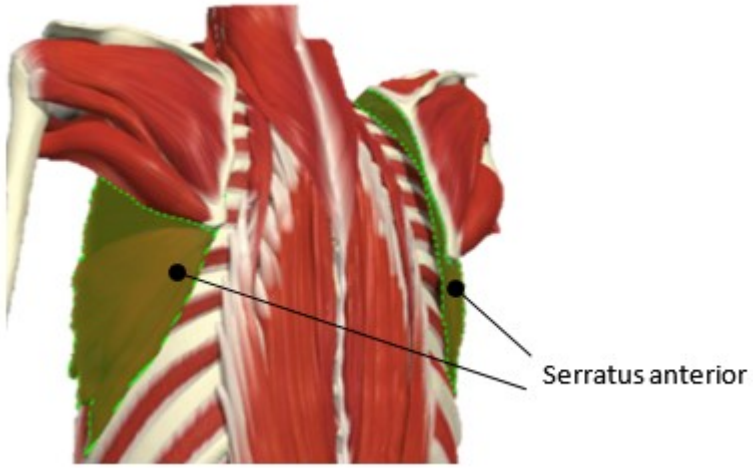

Figure 2.15 Posterior view of Serratus anterior (Primal, 2006)

The trapezius (Figure 2.16) has a large origin that spans from C1 at the base of the skull to T12 vertebra and insertion on the scapula spine, medial margin of the acromion and posterior surface of the distal third of the clavicle. The superior fibres help support the arm and in elevation of the shoulder complex, the middle retracts the scapula and the inferior medially rotates the scapula.

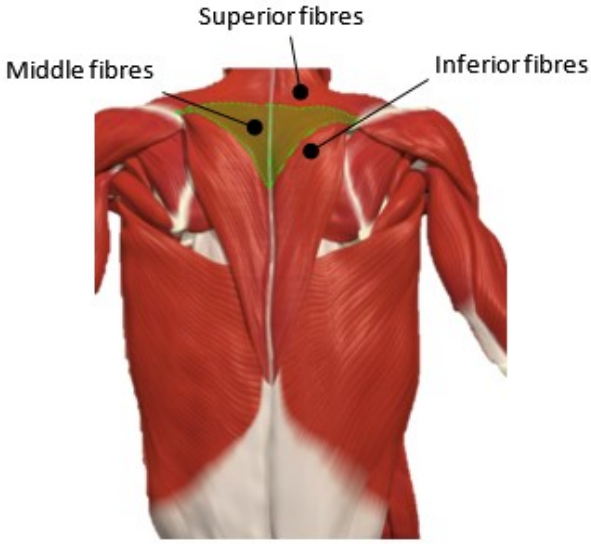

Figure 2.16 Posterior view of the Trapezius (Primal, 2006)

The major and minor rhomboid originate (Figure 2.17) from C7 to T5 vertebra and attach along the medial border of the scapula. The rhomboid is located just beneath the trapezius and is

responsible for retraction of the shoulder complex and downward rotation of the scapula.

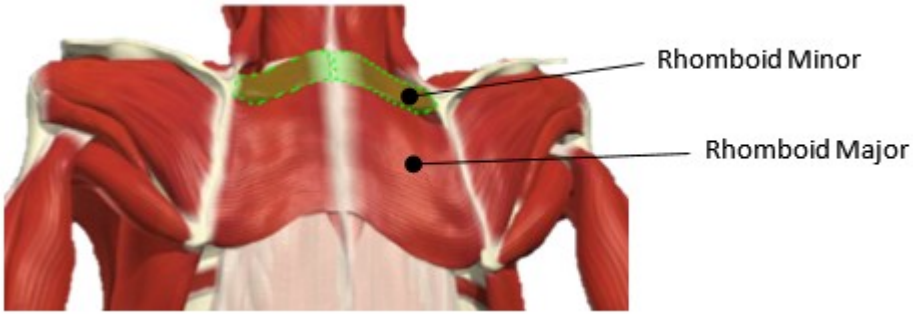

Figure 2.17 Posterior view of the Rhomboid (Primal, 2006)

The action of these three major muscles (trapezius, serratus anterior and rhomboid muscles) aid to stabilise and control scapula rotation (Figure 2.18) where the scapula is held against STGP while supporting the arm.

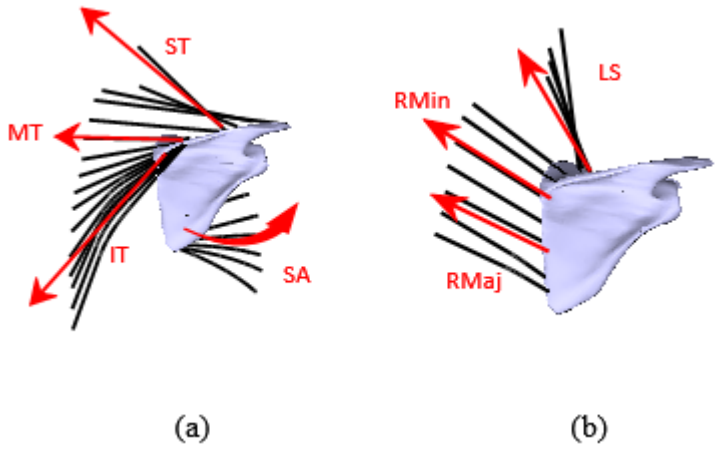

Figure 2.18 (a) Actions of the superior (ST), middle (MT) and inferior trapezius (IT) and serratus anterior (SA) (upward rotator) muscles that support that scapula (b) actions of the downward rotators of the scapula that include the levator scapulae (LS), rhomboid major (RMaj) and rhomboid minor (Rmin).

2.5.3 Musculature of the humerus and elbow joint

The pectoralis major (Figure 2.19) is divided in the sternal and clavicle head from where it originates and attaches onto the humerus. This muscle plays an important role in adduction and

internal rotation of the arm and flexion of the arm.

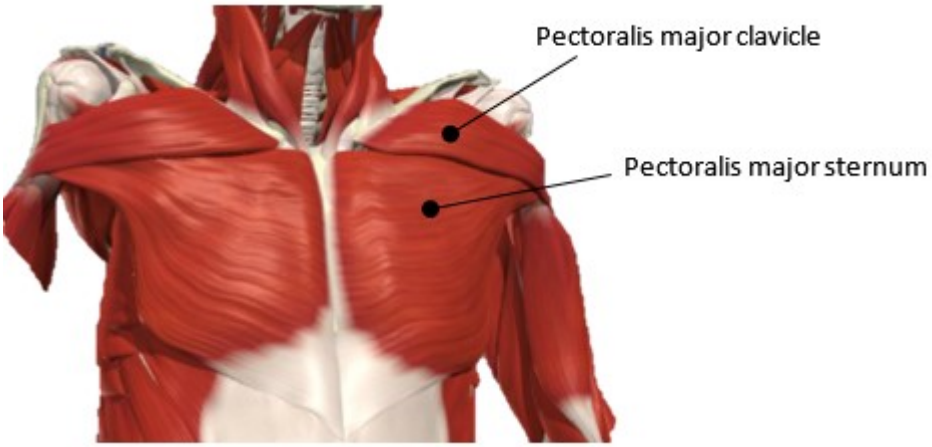

Figure 2.19 Anterior view of the pectoralis (Primal, 2006)

The latissimus dorsi (Figure 2.20) is a broad muscle that originates from T7 to T12 vertebra and pelvis where it ends as a flattened tendon attached to the humerus. The primary action of this muscle include adduction of the arm and less effectively in extension (Ackland et al., 2008).

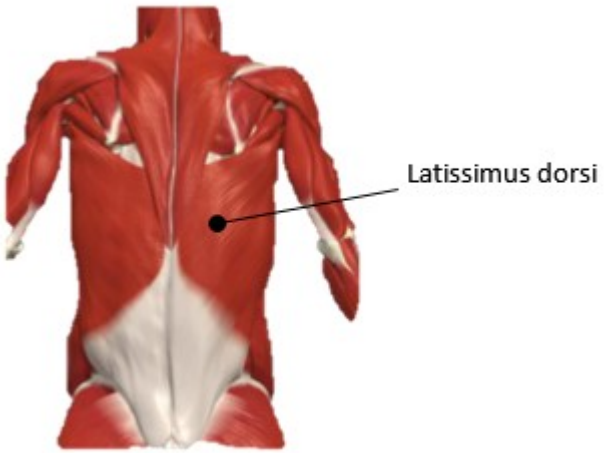

Figure 2.20 Posterior view of the latissimus dorsi (Primal, 2006)

The biceps brachii (Figure 2.21) is divided into the long head, which originates from within the GH joint capsule and the short head originating from the coracoid process of the scapula. Both heads combine to insert at the same location on the radius. The brachialis on the distal end of the humerus and inserts on the ulna. Both the brachialis and bicep brachii are flexors of the elbow with the bicep brachii is also a supinator of the forearm.

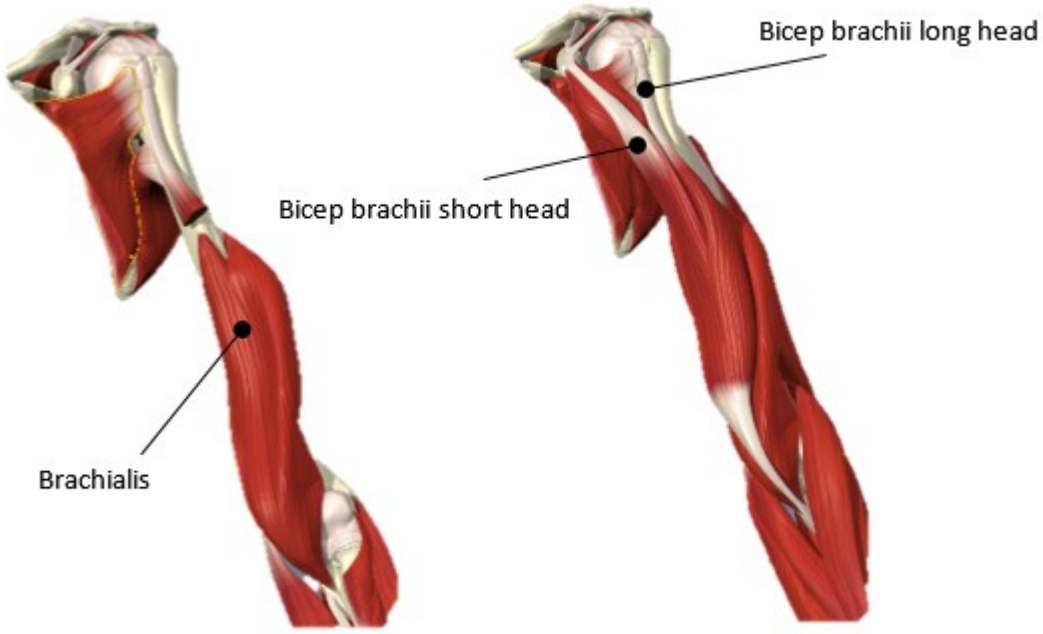

Figure 2.21 Bicep brachii and brachialis muscles (Primal, 2006)

The coracobrachialis (Figure 2.22) originates from the coracoid process of the scapula and inserts on mid shaft of the humerus. Its primary action is flexion of the arm and secondary action is assisting in adduction of the arm.

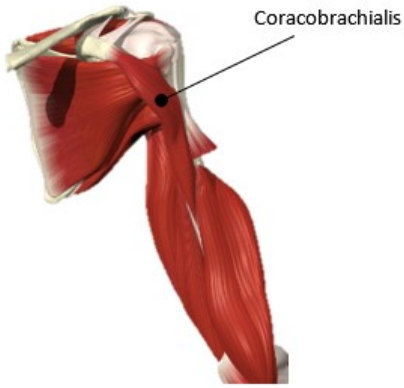

Figure 2.22 Coracobrachialis muscle (Primal, 2006)

The long head of the triceps brachii (Figure 2.23) originates from the scapula below the glenoid

where it extends inserting on the posterior surface of the ulna. On either side of the on head are medial and lateral head with insert onto the ulna via the same tendon.

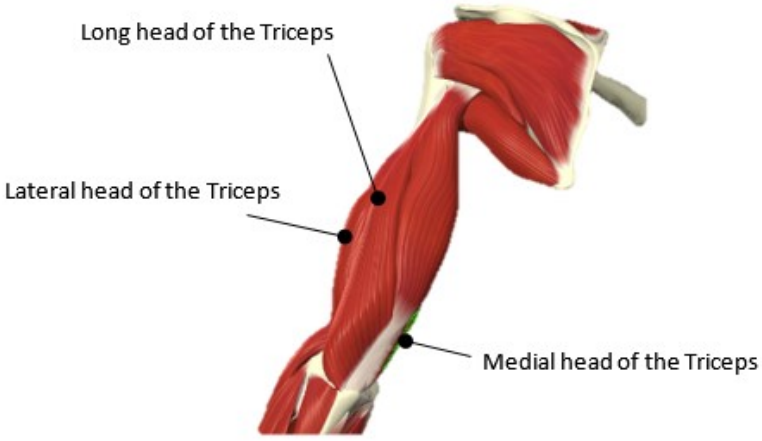

Figure 2.23 Triceps brachii (Primal, 2006)

As a general overview, the internal, external and abductors of the shoulder are presented in Figure 2.24.

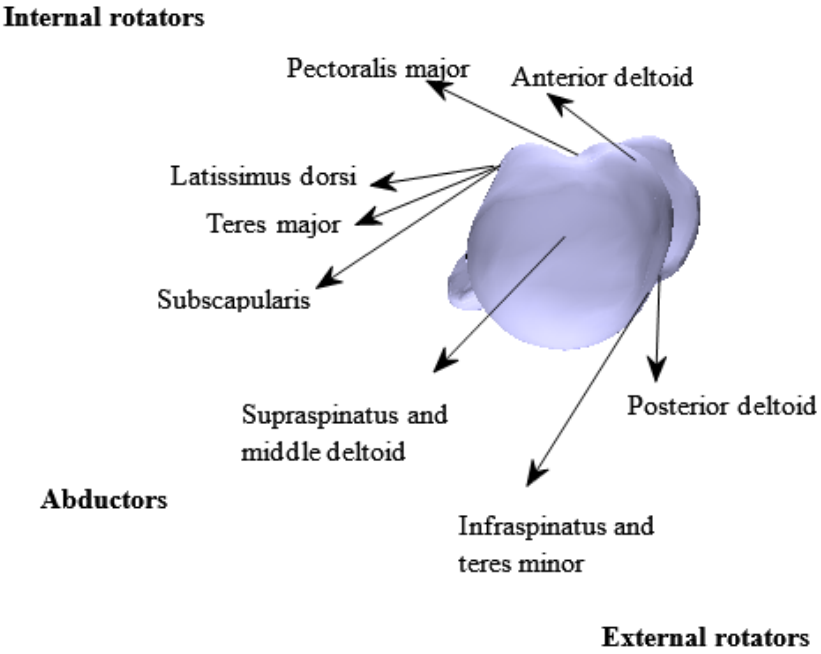

Figure 2.24 Superior view of the shoulder showing the action of key muscles on the humerus

2.6 Upper limb 3D joint kinematics and clinical description

All joints have a theoretical six degree of freedom however in modelling the upper limb it is common place to reduce to three degrees of freedom, neglecting translations. Joint rotations refer to the relative rotation of the distal to proximal segments that make up the joint. This relative movement between adjacent segments is described by a time varying rotation matrix, which is then decomposed into three successive angular rotations called Euler angles (Euler, 1776). The mathematics and methods involved in calculating Euler angles and how joint rotations are clinically described is presented in this section.

2.6.1 Vectors and rotation matrices convention

Before Euler angles can be calculated, segment embedded local [L] coordinate frames need to be established in addition to an understanding of how the vectors within these frames combine to form a transformation matrix that describes the position and orientation of one frame relative to another. The most fundament coordinate frame is the global [G] coordinate frame. Figure 2.25 shows a point p on segment B where its position from the origin of the [G] is represented by the following vector:

$$ {}^{G}\bar{p} = \begin{bmatrix} p_x \\ p_y \\ p_z \end{bmatrix} $$

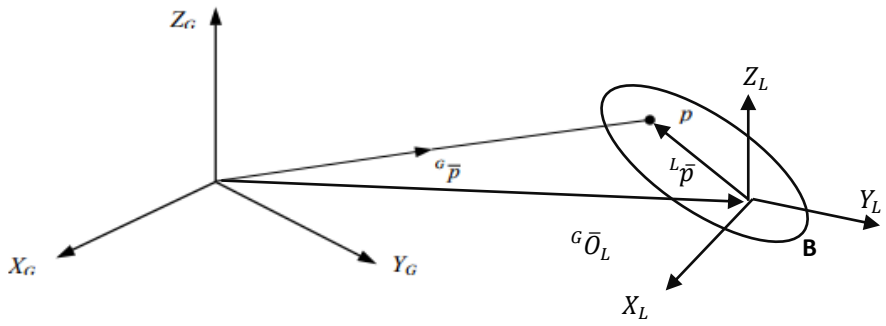

Figure 2.25 Position vector of a point P in the global frame

Using three fixed non-collinear points on a segment, three orthogonal axes can be defined to represent the local coordinate frame and calculate the position and orientation of the segment also known as the pose of the segment. Firstly, a rotation matrix is found by describing the vectors of the local frame in terms of the global frame. This is done by calculating the dot

product or direction cosines of the unit vectors of [L] with those of [G].

$$ {}^{G}_{L}R = \begin{bmatrix} {}^{G}X_L \vdots & {}^{G}Y_L \vdots & {}^{G}Z_L \end{bmatrix} = \begin{bmatrix} r_{1,1} & r_{1,2} & r_{1,3} \\ r_{2,1} & r_{2,2} & r_{2,3} \\ r_{3,1} & r_{3,2} & r_{3,3} \end{bmatrix} \quad \text{Equation 2.1} $$

Where ${}^{G}_{L}R$ is the rotation matrix between [L] and [G] and the elements are the dot products; $r_{1,1} = \bar{X}_L \cdot \bar{X}_G = \cos(\theta)$, where θ is the angle between both vectors. One important property of this rotation matrix is that its transpose is equal to its inverse meaning $R^T R$=I.

${}^{G}_{L}R$ describes rotation between both frames, so ${}^{G}\bar{p}$ is given by the following transformation

$$ {}^{G}\overline{p} = {}^{G}_{L}R \cdot {}^{L}\overline{p} + {}^{G}\overline{O}_L \quad \text{Equation 2.2} $$

Where, ${}^{L}\bar{p}$ is the position vector of p in [L] and ${}^{G}\bar{O}_L$ is the position vector or the origin of [L]. In this case, the transformation changes the position vector of p described in the [L] to being described in [G]. This can be reversed by finding the transposed of the rotation matrix and is given by:

$$ {}^{L}\overline{p} = {}^{L}_{G}R^T ({}^{G}\overline{p} - {}^{G}\overline{O}_L) \quad \text{Equation 2.3} $$

Where, ${}^{L}_{G}R^T$ describes the rotational transform from [G] to [L]. This forms the basis of transforming points from one frame to another that is used extensively in this study.

This two-step process described by Equation 2.2 and Equation 2.3 can be simplified as the following matrix-vector products:

$$ \begin{bmatrix} {}^{L}\bar{p} \\ 1 \end{bmatrix} = \begin{bmatrix} {}^{G}_{L}R & {}^{G}\bar{O}_L \\ 0 \quad 0 & 0 \quad 1 \end{bmatrix} \cdot \begin{bmatrix} {}^{G}\bar{p} \\ 1 \end{bmatrix} \quad \text{Equation 2.4} $$

For the case of multiple segment frames (Figure 2.26), we multiply the two rotation matrices yielding another rotation matrix whose application to a positional vector effects the same rotation as the sequential application of the original two rotation matrices. Additionally, this

resultant rotation matrix describes a rotational transform between the two original frames, when calculated for each frame of motion is the time varying rotation matrix between the segments from which the Euler angles are calculated.

The transformation between both frames is given by:

$$ {}^{A}_{B}R = {}^{G}_{A}R^{T} \cdot {}^{G}_{B}R \qquad \text{Equation 2.5} $$

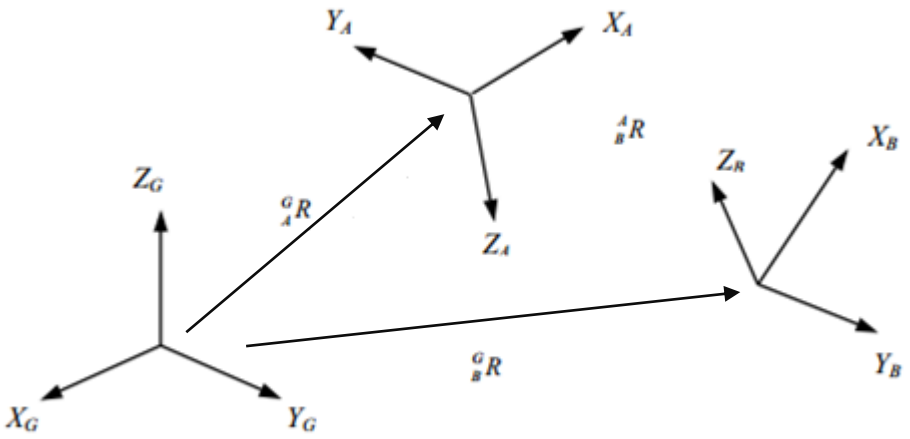

Figure 2.26 Rotation between segment local frames.

2.6.2 Euler angles

Euler angles are commonly used to represent joint angles in biomechanics mainly because it is simple to calculate and the angles can have clinical meaning if calculated correctly. Euler angles can describe rotations relative to a static or moving frame. In this way, there are twelve possible sequences of Euler angles since the three angles are sequence dependant. This thesis follows the standard set out by Wu et al. (2005) for biomechanical joint description and is presented in Section 2.6.3.

The sequence of Euler angle rotations describes the rotation about each axis of one frame relative to the other. Given that both frames are initially aligned, an example of this is shown below where there is a rotation about x-axis of α° followed by a rotation about the new y-axis of β° and lastly a rotation about the twice-changed z-axis of γ°.

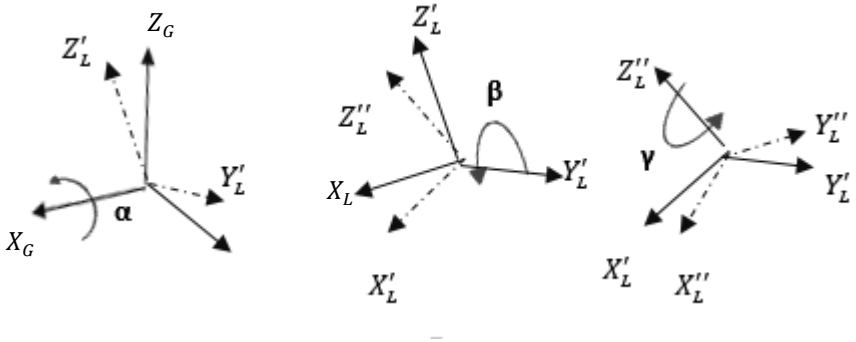

Figure 2.27 XY'Z" Euler sequence

Each rotation about the XYZ axes is given by:

$$R_x(\alpha) = \begin{bmatrix} 1 & 0 & 0 \\ 0 & c\alpha & -s\alpha \\ 0 & s\alpha & c\alpha \end{bmatrix} \quad \text{Equation 2.6}$$

$$R_y(\beta) = \begin{bmatrix} c\beta & 0 & s\beta \\ 0 & 1 & 0 \\ -s\beta & 0 & c\beta \end{bmatrix} \quad \text{Equation 2.7}$$

$$R_z(\gamma) = \begin{bmatrix} c\gamma & -s\gamma & 0 \\ s\gamma & c\gamma & 0 \\ 0 & 0 & 1 \end{bmatrix} \quad \text{Equation 2.8}$$

Where c is cosine and s is sine. The rotation sequence is defined by ${}^{G}_{L}R_{XYZ} = R_X(\alpha) \cdot R_Y(\beta) \cdot R_Z(\gamma)$, so multiplying these rotations in the same order gives

$${}^{G}_{L}R_{XYZ}(\alpha,\beta,\gamma) = \begin{bmatrix} c\beta c\gamma & -c\beta s\gamma & s\beta \\ s\alpha s\beta c\gamma + c\alpha s\gamma & -s\alpha s\beta s\gamma + c\alpha c\gamma & -s\alpha c\beta \\ -c\alpha s\beta c\gamma + s\alpha s\gamma & c\alpha s\beta s\gamma + s\alpha c\gamma & c\alpha c\beta \end{bmatrix} \quad \text{Equation 2.9}$$

Therefore, ${}^{G}_{L}R_{XYZ}$ is a function of the three Euler angles and maps it to the rotation matrix. Equating the matrices of Equation 2.1 and Equation 2.9, the X,Y',Z'' Euler angles can be calculated:

$$\beta = atan2\left(r_{1,3}, \sqrt{r_{2,3}^2 + r_{3,3}^2}\right) \quad \text{Equation 2.10}$$

$$\alpha = atan2\left(\frac{-r_{2,3}}{\cos\beta}, \frac{-r_{3,3}}{\cos\beta}\right) \quad \text{Equation 2.11}$$

$$\gamma = atan2\left(\frac{-r_{1,2}}{\cos\beta}, \frac{-r_{1,1}}{\cos\beta}\right) \quad \text{Equation 2.12}$$

One major limitation of using Euler angles is that there are singularities that may occur where the angles are undefined. This manifests mathematically when β in Equation 2.11 & Equation 2.12 is equal to ± 90° resulting in a division by zero. This issue is also known as gimbal lock where there is a loss of one degree of freedom due to two axes becoming aligned.

Changing how the coordinate frames are defined, using different Euler sequences (Šenk & Chèze, 2006) and using other methods such as floating axis method (Hill et al., 2008) or quaternions are some of the ways gimbal lock be avoided. The application of these solutions are very limited however, since the underlining idea that will be applied in the thesis is to get joint angles that are clinically relevant.

2.6.3 International Society of Biomechanics (ISB) standards.

ISB standards for the upper limb together with the clinical description of segment kinematics is presented in this section. The construction of these segment frames is based on the anatomical landmarks show in Figure 2.28. All the information is taken from the literature (Wu et al., 2002) unless stated otherwise.

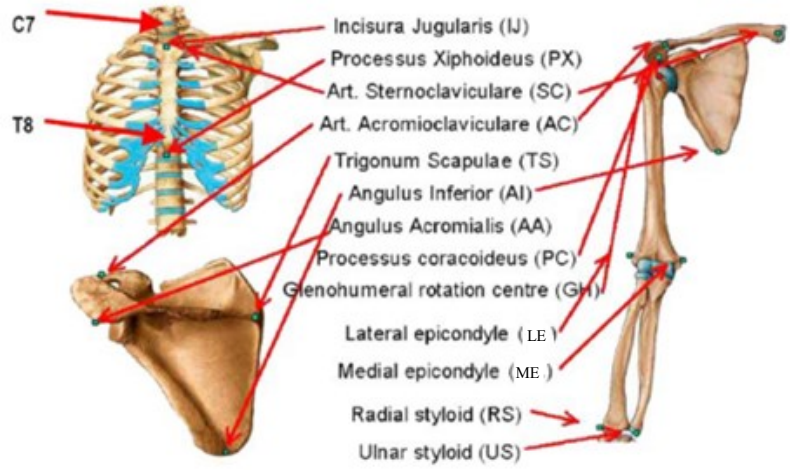

Figure 2.28 Anatomical landmarks of the upper limb adapted from Wu et al. (2002)

2.6.3.a Thorax

The thorax rotation with respect to the global frame is described using the ZX'Y'' Euler sequence.

Origin	The origin coincident with IJ
Y_t	The line connecting the midpoint between PX and T8 and the midpoint between IJ and C7, pointing upward
Z_t	The line perpendicular to the plane formed by IJ, C7, and the midpoint between PX and T8, pointing to the right
X_t	The common line perpendicular to the Z_t and Y_t axis, pointing forwards

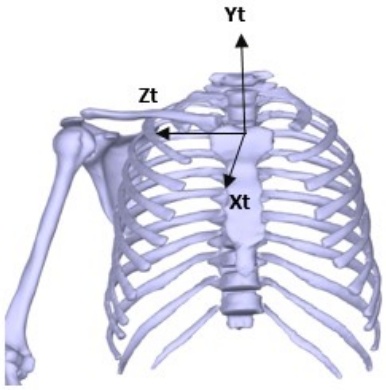

Figure 2.29 A Thorax frame. Its Clinical description about these axes are; flexion/extension about Zt, right/left lateral rotation about Xt, and left/right axial rotation about Yt

2.6.3.b Clavicle

Rotation of the clavicle with respect to the thorax is calculated using YX'Z'' Euler sequence. The clinical description of each angle is given in Figure 2.30

Origin	The origin coincident with SC
Z_c	The line connecting SC and AC, pointing to AC
X_c	The line perpendicular to Z_c and Y_t, pointing forward. Note that the X_c-axis is defined with respect to the vertical axis of the thorax (Y_t- axis) because only two bony landmarks can be discerned at the clavicle.
Y_c	The perpendicular to X_c and Z_c

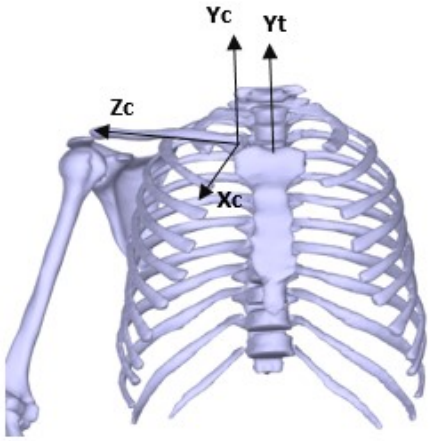

Figure 2.30 Clavicle frame. Its Clinical description about these axes are; Yc- pro/retraction, Xc-depression/elevation and Zc-axial rotation

2.6.3.c Scapula

Scapula rotations are described in a slightly different way from ISB even though the same coordinate frame is used. Instead of pro/retraction, rotations about the Y-axis are described as internal/external. Instead of lateral/medial, rotations about the X-axis is known as upward/downward rotation. Rotations about the Z-axis is called anterior/posterior tilt remain unchanged (Figure 2.31). It should be note that these clinical descriptions hold true for both the SC and scapulothoracic joints. The Euler sequence used at these joints is YX'Z''.

Origin	The origin coincident with AA
Z_s	The line connecting TS and AC, pointing to AC
X_s	The line perpendicular to the plane formed by AI, AA, and TS, pointing forward.
Y_s	The common line perpendicular to the X_s- and Z_s-axis, pointing upward

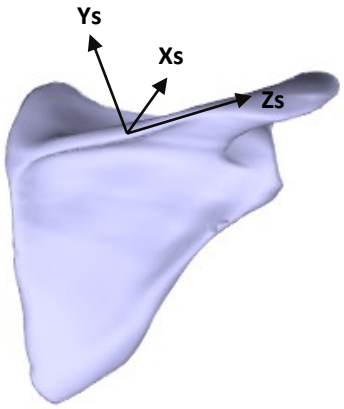

Figure 2.31 Posterior view of the scapula showing its coordinate frame. Its Clinical description about these axes are; Xs-down/upward rotation, YS- internal/external rotation and Zs-posterior/anterior tilt.

2.6.3.d Humerus

Glenohumeral and humerothoracic kinematics are described using YX'Y'' Euler sequence where the three angles represent elevation, plane of elevation and internal/external rotation.

Origin	GH
Y_h	The line connecting GH and the midpoint of LE and ME, pointing to GH
X_h	The line perpendicular to the plane formed by LE, ME and GH, pointing forward
Z_h	The common perpendicular to Y_h and X_h

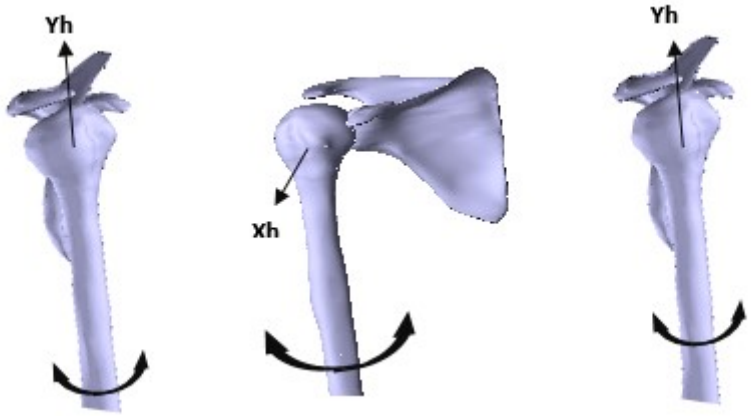

Figure 2.32 Humerus frame. The first rotation about Yh defines the plane of elevation, rotation about Xh is elevation/depression and the final rotation about Yh is internal/external rotation

2.6.3.e Forearm

Rotation of the forearm with respect to the humerus is described by a ZX'Y'' Euler sequence. The forearm undergoes flexion/extension about the Z-axis and pronation/supination about the Y-axis. It should be noted that the frame definition given here was abandoned for a more accurate method of measuring elbow joint kinematics and is presented in Chapter 2. The clinical description however, remains unchanged.

Origin US

Y_f The line connecting US and the midpoint between LE and ME, pointing proximally

X_f The line perpendicular to the plane through US, RS, and the midpoint between LE and ME, pointing forward

Z_f The common line perpendicular to the X_f and Y_f-axis, pointing to the right

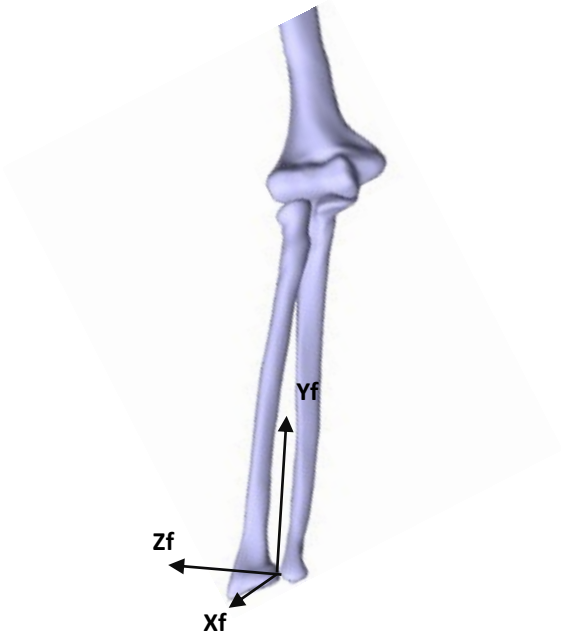

Figure 2.33 Forearm frame. Rotations about Yf is pronation/supination and Zf is flexion/extension

2.7 Lower limb bones and 3D joint kinematics

An overview of lower limb bony anatomy and kinematics is presented in this section. This is necessary as full body kinematics is calculated for cricket bowlers and the joint angles obtained from both lower and upper limb are used in the performance analysis.

2.7.1 Lower limb bones and anatomical landmarks

The lower limb includes the pelvis, femur, shank (which comprises the tibia and fibula) and bones of the foot with the hip, knee and ankle joints located between these segments (Figure 2.34). Similar to the make up the upper limb, there are medial and lateral projections on the Femur and shank that are used to define its respective local coordinate frame.

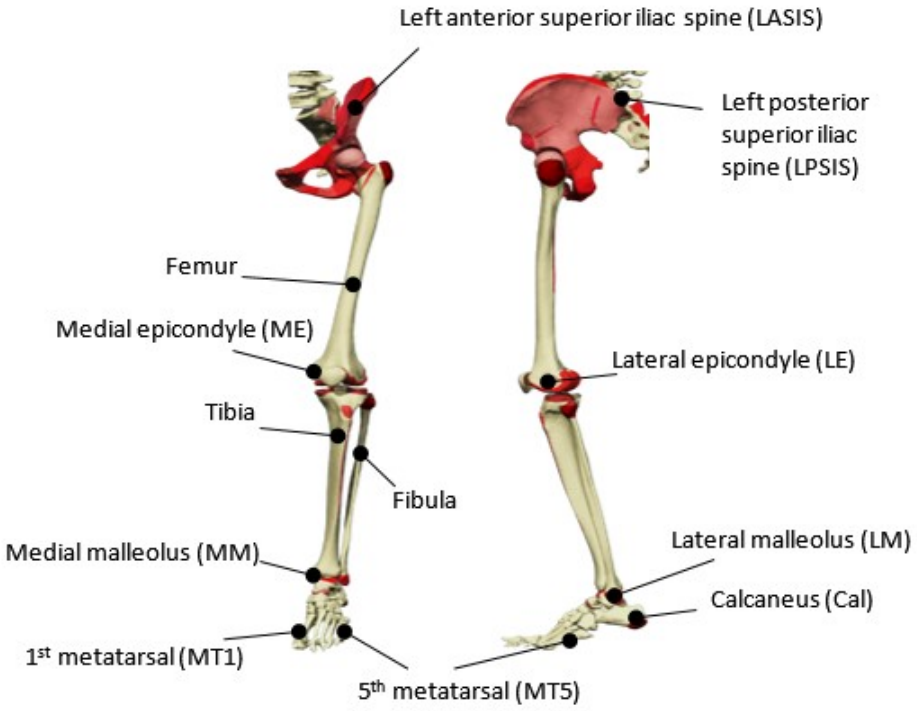

Figure 2.34 Lower limb bony anatomy (Primal, 2006)

2.7.2 Lower limb anatomical coordinate frames

Standards for lower limb segment coordinate frames are adapted from the literature (Wu et al., 2002). The primary focus of this thesis is the upper limb so only certain key kinematics of the lower limb is looked at. Therefore, these segment frame definitions do not represent the most accurate way of calculating kinematics. The anatomical frames retain their clinical descriptions.

2.7.2.a Pelvis

Origin	The origin coincident with the right (or left) hip center of rotation
Z	The line parallel to a line connecting the right and left ASISs, and pointing to the right
X	The line parallel to a line lying in the plane defined by the two ASISs and the midpoint of the two PSISs, orthogonal to the Z-axis, and pointing anteriorly
Y	The line perpendicular to both X and Z, pointing cranially

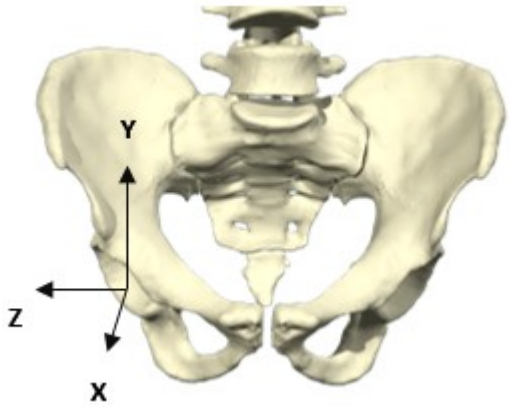

Figure 2.35 Anterior view of the pelvis showing its local coordinate frame (Primal, 2006)

Rotations of the thorax with respect this pelvis frame is calculated using ZX'Y'' Euler sequence.

2.7.2.b Femur

Origin	The origin coincident with the right (or left) hip centre of rotation, coincident with that of the pelvic coordinate system (O) in the neutral configuration
Y	The line joining the midpoint between the medial and lateral femur epicondyles (FE) and the origin, and pointing cranially
Z	The line perpendicular to the y-axis, lying in the plane defined by the origin and the two FEs, pointing to the right
X	The line perpendicular to both Y-and Z-axis, pointing anteriorly

Rotation of the femur with respect to the pelvis at the hip joint is calculated using ZX'Y'' Euler sequence where rotations about the X-axis is adduction/abduction, about the Y-axis is internal/external rotation and about Z-axis is flexion/extension.

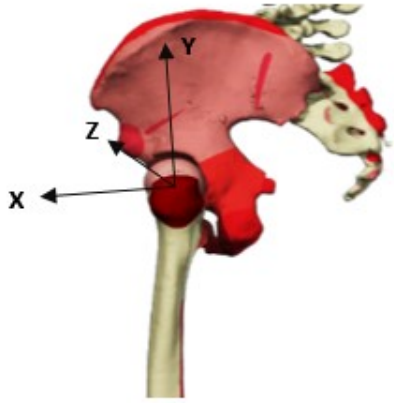

Figure 2.36 Lateral view of the left femur showing is local coordinate frame (Primal, 2006)

2.7.2.c Shank

Rotations of the shank with respect to the femur at the knee joint is calculated using ZX'Y'' Euler sequence. Rotation about the X-axis is adduction/abduction, about the Y-axis is internal/external and about the Z-axis is flexion/extension.

Origin	Midpoint between LM and MM
Y	The line connecting midpoint between MM and LM and midpoint between ME and LE of the femur, pointing to the upward
X	The line perpendicular to plane created by the midpoint at the knee, MM and LM pointing anterior
Y	The common line perpendicular to Y-and X-axis.

2.7.2.d Foot

Rotations of the foot with respect to the shank at the ankle joint is calculated using Z'X'Y'' Euler sequence. Rotation about the X-axis is inversion/eversion, about the Y-axis is internal/external rotation and about the Z-axis is dorsiflexion/plantarflexion. It should be noted that for subjects that were wearing shoes during testing the anatomical landmarks of the foot were approximated.

Origin	Cal
Y	The line perpendicular to plane created by Cal, MT1 and MT5
Z	The line perpendicular to plane created by the Y-axis and the midpoint at the between MT1 and MT5
X	The common line perpendicular to Y-and Z-axis.

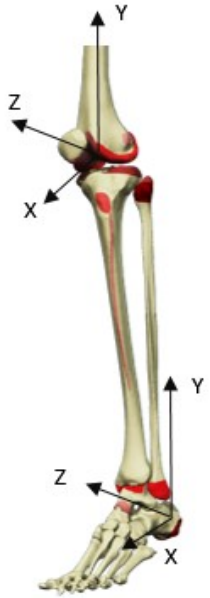

Figure 2.37 Femur and foot segment frames. Image adapted from (Primal, 2006)

2.8 Summary

This chapter introduces the upper and to a lesser extend the lower limb bony anatomy. Important muscles of the upper limb have been presented with the scapula being a key component in during arm movement. Mathematical description of Euler angles and how its use has been illustrated as well as the clinical descriptions of the upper and lower limb joint rotations.

The next chapter presents a literature review of injuries in cricket bowlers as well as the biomechanics of cricket bowling.

Chapter 3

Biomechanics of cricket bowling and a review of shoulder injury

A review of the biomechanics of cricket bowling is presented in this chapter together with a review of shoulder injuries in upper limb athletes with the focus on cricket bowlers. Concepts specific to the game, which are used in the performance and injury predisposition analysis, are also introduced.

3.1 Introduction

Documentation of injury is important as this helps to predict, reduce and prevent injuries. Injury reports can help to improve the system of epidemiological data collection and development of a cricket injury database. In addition, they highlight any injury trends that might have been caused due to changes in the sport; this might help to identify areas for further research.

3.1.1 The game of cricket

The International Cricket Council (ICC) is the highest governing body responsible for organising major international tournaments such as the Cricket World Cup, sanctioning umpires, enforcing the laws of the game and ensuring that it is played with the right spirit and is also a commercial success. Making and updating the laws of the game fall under the control of the Marylebone Cricket Club (MCC).

Dependant on a cricketer's ability and experience, that player may progress through these three playing levels:

- School cricket; which is associated with secondary school cricket.
- Domestic level; where clubs compete within a league at the state/county/provincial level.
- International level; the highest playing level where nations compete against each other.

Cricket is played between two teams of eleven players and is classified into three existing formats of the game. Test cricket is played over a span of five days while One Day Internationals (ODI) and Twenty-Twenty (T20) cricket has a length of 50 and 20 overs per side respectively. During play, one team bats while the other fields, reversing roles at the end of the innings. The objective of the fielding team is to get the opposition batsman out and this duty is primarily the responsibility of the bowlers (Figure 3.1).

Figure 3.1 Run-up of international fast bowler Mitchel Johnson adapted from (Vorndran, 2014)

3.2 Cricket bowling

Unlike other overhead sports that allow free manipulation of the arm to perform the specific sporting task, cricket bowling is unique in that there are strict regulations allowing for only limited elbow kinematics. Bowlers must do this act by propelling a 156-163gram cricket ball towards the batsman who is standing approximately 20 meters away in front of the wicket at the other end of the pitch. Bowlers deliver the ball with varying degrees of speed or spin in an attempt to deceive the batsmen to get him/her out. Bowlers who specialise in either of these disciplines are broadly classified as fast bowlers or slow bowlers. Slow bowlers are also known as spinners. Spinners can be further subdivided into off spinners who spin the ball turning it into the batsman from the off side or leg spinners who spin the ball turning it across the batsman from the leg side (Figure 3.2). In addition to their normal delivery type, bowlers may also develop variations that may help in getting the batsmen out. In reality, there are many types of bowlers and many variations in delivery types, however, for simplification bowlers are described in these two general ways: fast or slow bowlers.

Figure 3.2 Grip for (a) leg spin and (b) off spin where the arrow shows the direction of rotation of the ball driven by the action of the wrist and fingers.

3.3 Biomechanics of cricket bowling

Cricket bowling is a complex movement requiring the co-ordinated actions of the upper and lower limbs to deliver a ball with the right technique. It is different to that of throwers since bowlers are required to propel the ball by circumduction of the upper arm while limiting elbow extension during ball release near the top of the arc. Fast bowlers typically have a long run up, converting this momentum together with the high circumduction velocity of the arm with a rhythmic action to deliver the ball at speeds reaching 160km/h. Spin bowlers have a much shorter run-up. Depending on the technique used they, rely on rotations about their front foot, shoulder and wrist as well as the action of their fingers to impart spin on the ball, which is usually delivered around 65 to 90km/h. Irrespective of the type of bowler, the basics aspects of the bowling action are the same and can be broken down into five distinct phases (Woolmer et al., 2008).

1. The run-up and jump. This leads into the beginning of the gather with the body side-on and the head looking over the front shoulder with the ball tucked in near the chin pointing towards the batsman
2. The set-up. The hip begins to flex as the front knee is brought upwards, the body rocks back and the bowling arm begins to extend.
3. The unfold. As the bowler unwinds towards the target with the lower arm approximately parallel to the ground, the front foot comes down and forward with the front arm as the back foot makes contact with the ground (BFC).

4. The delivery. The head is level. The bowling arm is at approximately shoulder level and the front foot makes contact with the ground (FCC) as the bowling arm continues its circumduction with the ball being released in a region at the top of the arc. The front arm continues its downward motion.
5. The follow-through. The body pivots on the front foot as the bowling arm follows a similar path to the front arm as the trunk flexes. The back foot crosses the front foot making ground contact. This continues for a few steps as the bowler gradually slows down to reduce his momentum.

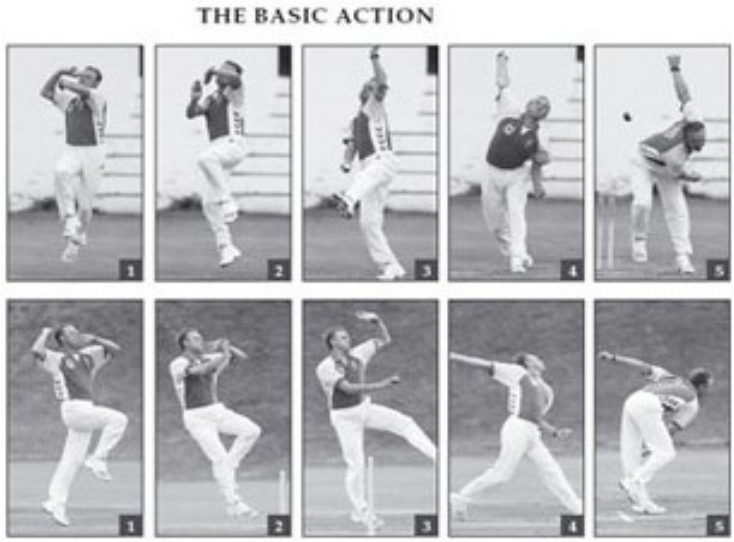

Figure 3.3 Front and lateral view of the bowling phases (Woolmer et al., 2008)

3.3.1 Side-on versus front-on bowling technique

Bowling techniques can be classified as either front-on or side-on depending on the direction of the bowling shoulder with respect to the batsman. In a perfect side-on action, the back foot is parallel to the crease with the bowling shoulder pointed in the opposite direction of the batsman, i.e. 180° (Figure 3.4a) and the hip-shoulder separation angles is less than 30°. In contrast, a front-on action which is a faster approach, requires the bowling shoulder alignment to be greater than 180° (Figure 3.4b) and the hip-shoulder separation angle is less than 30°. Cases where bowlers use a combination of these two techniques is referred to as mixed action and results in excessive twisting of the spine leading to lower back injuries (Finch et al., 1999; Bartlett et al., 1996).

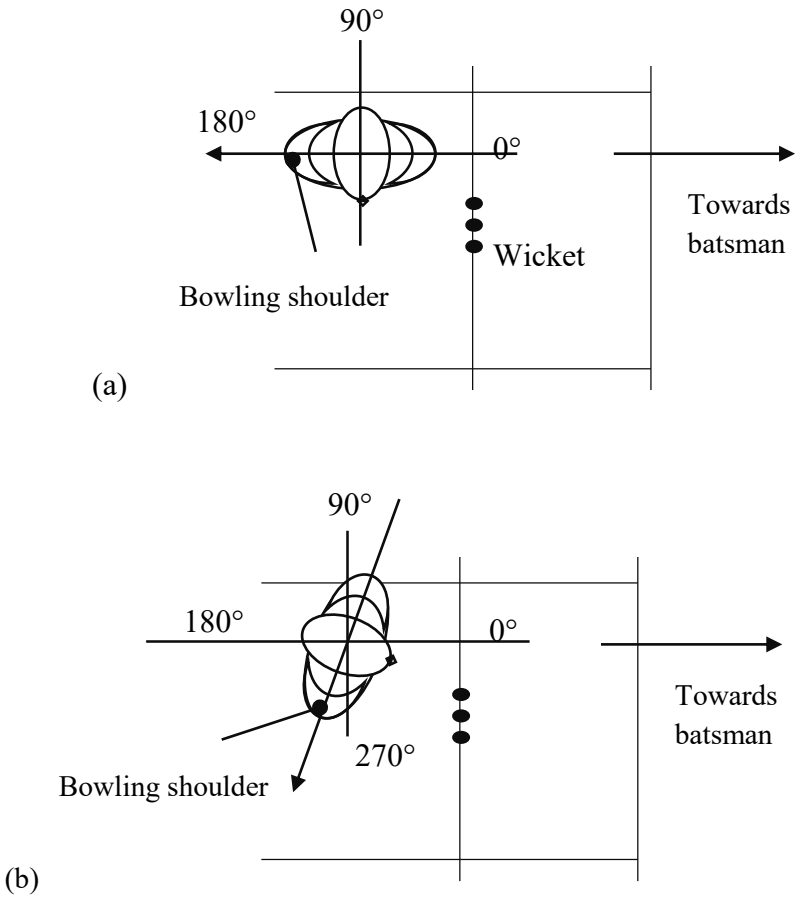

Figure 3.4 top-down view showing (a) side-on (b) front-on bowling techniques

3.3.2 Legality of deliveries

A key factor in the action leading up to ball release is the flexion/extension of the elbow and whether it is within the legal limit as stipulated by the International Cricket Council (ICC). Over the years the 'no-ball law' has undergone a number of iterations and revisions based on the findings of studies.

The no ball law (law 24.3) states:

"A ball is fairly delivered in respect of the arm if, once the bowler's arm has reached the level of the shoulder in the delivery swing, the elbow joint is not straightened partially or completely from that point until the ball has left the hand. This definition shall not debar a bowler from flexing or rotating the wrist in the delivery swing." (MCC, 2010)

The ICC went on to further define a throw, allowing for 15˚ straightening for all bowlers at

international level. This was based on the recommendations of Lloyd et al. (2000b), stating that the human eye could only detect a throw if the bowler exceeded the 15˚ mark.

The need for such a rule stems from the fact that bowlers can gain an unfair advantage by extending their elbow to increase ball speed or ball spin. Studies that have looked at the contribution of movements of different body parts to the generation of velocity at ball release showed that upper arm rotation contributes the greatest generation of ball speed (Woolmer et al., 2008; Zhang, 2011) . Thus, it is important when considering the legality of the delivery and the extension of the forearm to the circular rotation of the shoulder for generating ball speed.

3.3.3 Performance analysis and technique classification.

Studies have shown that there is a positive relationship between run-up velocity and ball release velocity where bowlers with a front-on action were able to approach the crease faster than if they were side-on (Bartlett et al., 1996). There was however a negative relationship between run-velocity and accuracy suggesting that a balance must be found between these two.

At back foot contact, the bowler is leaning backward either due to lateral flexion in side-on bowlers or hyperextension of the spine for front-on bowlers (Bartlett et al., 1996). While this happens, the arm continues to extend in the initial phase of circumduction to BR. This action of the trunk has been shown to have a significant contribution to ball release speed in fast bowlers (Bartlett et al., 1996).

At front foot contact, the angular displacement of the front knee during impact helps attenuate the ground reaction forces where these forces may reach up to 9 times body weight (Bartlett et al., 1996). Factors that affect the reaction forces felt depends on run-up velocity and the front knee angle. On the other hand, bowlers with a straight front knee and limited flexion occurring have been shown to have greater ball release velocity (Ranson et al., 2008) since there is a greater momentum transfer as the bowler pivots about the front leg with a greater effective lever arm. Furthermore, a straight front leg allows the bowler to quickly slow down which drives the trunk forward increasing ball speed (Worthington et al., 2013).

At ball release, the position of the arm at front foot contact (FCC) is a good predictor of ball release where bowlers who delay the bowling arm as long as possible (Bartlett et al., 1996) and are able to have their bowling arm further back relative to the trunk (Worthington et al., 2013) have greater ball release speed. The hip and shoulder alignment changes due to shoulder counter

rotation in the delivery stride where at FCC is another predictor of ball release speed. A misalignment between the hip and shoulder of less than 30° indicates pure front-on or side-on technique while greater than 30° indicates a mixed-technique with an increased risk of lower back injury (Foster et al., 1989).

The stride length of a bowler is the distance between back foot contact (BCC) and FCC and is usually normalised using the bowler's height. It depends on the approach speed with reported values of 1.3m and 1.67m for an approach speed of 3.8m/s and 4.6m/s respectively (Elliott & Foster, 1984). The alignment of both feet in the stride length is also important as it indicates the type of bowling technique.

The non-bowling arm plays a crucial role in both techniques of fast and spin bowlers. From its elevated position (Figure 3.6a), the non-bowling arm is accelerated down, together with the front foot, into the body to facilitate the rotation of the bowling arm as well as help in aiming. The accuracy of a bowler is measured in line and length of the ball delivered. Both these distances map the location where the ball bounces relative to the batsman's wicket and is used to discern types of deliveries as well as distinguish between good and bad balls.

Upper arm rotation is the largest (>60%) contributor to ball speed where internal rotation of the upper arm plays a major role (Zhang, 2011; Stronach et al., 2014). This is followed by contributions from thorax rotation, pelvis rotation, linear velocity of the pelvis and forearm rotation (Zhang, 2011). Hussain (2011) showed that the increase in ball speed was increasingly greater than the decrease in ball speed associated with shorter arm length when the elbow was flexed from 5° to 35° (Figure 3.5). In addition to this, Marshall and Ferdinands (2003) estimated that with an upper arm velocity of 1700°/s and the elbow flexed from 5° to 35°, there was increase in wrist speed ranging from 2.8 km/h to 28km/h. They also suggested that both fast and spin bowlers could benefit from bowling with a flexed elbow. The practicality of this however is limited since the bowling action is such a fast motion, it would be nearly impossible to keep the elbow flexed and not exceed the legal limit of a change in 15°. Still, this highlights how important upper arm internal rotation can be for bowlers who bowl with a slightly flexed elbow within the legal limit or even bowlers with a significant carry angle.

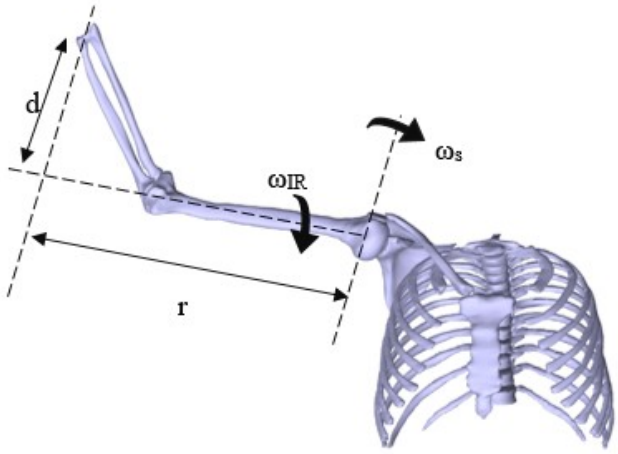

Figure 3.5 The associated reduction in linear wrist speed due to a shorter arm length (r) from the flexing the elbow is less than the gain in linear wrist speed due to internal rotation of the shoulder (ω_{IR}) about the long axis of the humerus at a distance d. ω_s is the resultant angular velocity of the shoulder during bowling.

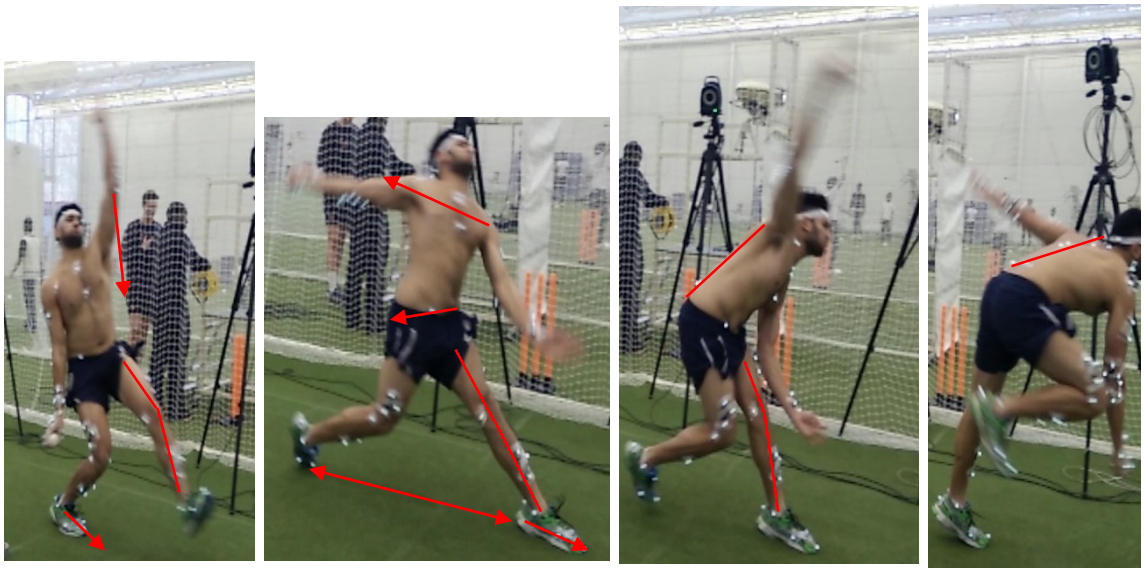

(a) (b) (d) (e)

Figure 3.6 key variables in bowling; (a) shows the action of the non-bowling arm and alignment of the back foot, (b) shows shoulder counter rotation and stride length while (c) & (d) shows thorax flexion and axial rotation. (a) to (c) shows the change of the front leg flexion angle

3.4 Review of shoulder injuries in overhead athletes

Shoulder injuries are very common in overhead athletes since the arm motion is repetitive, operating near its physiological limits at high angular velocity producing large forces that can compromise the joint (Hess et al., 2005; Wilk et al., 2009). As a result, there exist numerous studies with varying approaches that approach this problem. The following section summarises the state of shoulder problems in overhead athletes.

Overhead athletes may participate in sports such as badminton, tennis and baseball and although each sport has its distinctive technique, there are similarities in the muscle activations involved (Moynes et al., 1986). Furthermore, cricket bowlers can be included in this group as the arm action and range of motion are comparable. These sports involve repetitive overhead motions requiring well-coordinated action of the shoulder muscles (Ng & Lam, 2002; Wilk et al., 1993), especially the rotator cuff, to maintain stability and integrity of the glenohumeral joint. Any strength imbalance of the rotators can result in abnormal displacement of the humeral head leading to increasing the possibility of impingement (Section 3.4.1) and injury. In fact, rotator cuff impingement and instability have been shown to account for most of the shoulder pain in overhead athletes (Baltaci & Tunay, 2004).

Throwing has been described as mainly the internal rotator muscles acting concentrically during the acceleration phase and the external rotators acting eccentrically during the deceleration phase (Baltaci & Tunay, 2004; Noffal, 2003), where the external rotators are responsible for decelerating the arm while maintaining dynamic stability at the glenohumeral joint. There are similarities between this and other sports that facilitate comparison of the functional activity of the arm. For example, the cocking phase of a baseball pitch and tennis serve are analogous in that the arm is initially at maximum external rotation followed by rapid internal rotation during the acceleration phase concluding in deceleration of the arm in the follow through phase. Although the angular velocity of both activities differ where a pitcher velocity can reach 7000°/s while tennis are around 1500°/s (Williams & Kelley, 2000), they still produce considerable load that can damage the shoulder joint. It is during this phase of maximum external rotation and deceleration that it is reported that majority of injuries occur (Ng & Lam, 2002).

Noffal (2003), who investigated the eccentric external and concentric internal strength ratios (peak torques) of throwers and non-throwers, reported values of 1.17 & 1.48 for dominant and

non-dominant sides of throwers and 1.37 & 1.90 for non-throwers. These results support the importance of the external rotator muscles in decelerating the arm as their peak torques are greater than that of the internal rotator muscles, indicated by a functional ratio greater than 1. Comparing the ratio bilaterally for both groups, the dominant side of throwers had the lowest functional ratio indicating that their internal rotator muscles were almost as strong as their external rotators and stronger on their dominant side than non-dominant side.

Baltaci and Tunay (2004) conducted experiments to determine whether differences in peak torque existed between dominant and non-dominant sides of overhead athletes. Their results are similar showing that the muscles responsible for internal rotation, extension and adduction where stronger on both dominant and non-dominant sides. In fact, there is a good agreement in the literature that shows internal rotators of overhead athletes are stronger compared to the non-dominant side or sedentary individuals (Codine et al., 1997). Unilateral overhead sports athletes show as much as 15% greater strength on the dominant side muscle groups compared to the non-dominant side (Anderson, 1993). However differences greater than 20% are considered to be abnormal (Sapega, 1990).

In addition to this, the glenohumeral range of motion has been shown to be adaptive on the dominant side of overhead unilateral athletes. During the deceleration phase in the overhead motion, the posterior-inferior portion of the GH joint capsule may contract as a result of the repetitive micro trauma (Tyler et al., 2000). Other reseachers, particularly within baseball have attributed the change in axial rotation to osseous adaptations to the humeral head (Crockett et al., 2002), where there was greater humeral head retroversion. Either of these causative factors leads to a loss of internal rotation (glenohumeral internal rotation deficit or GIRD) with an increase in external rotation in some cases. This phenomenon is well documented in a variety of unilateral overhead sports (Ellenbecker et al., 2002; Myers et al., 2006). Both these issues of muscular imbalance and reduction in range of motion have known to be indicators of impingement syndrome (Section 3.4.1).

3.4.1 Impingement

Impingement is described as the rubbing of the rotator cuff against other structures of the shoulder like the anterioinferior aspect of the coracoacromial ligament or between the acromion and humeral head (Figure 3.7). The spectrum of pathological conditions that arise include full or partial rotator cuff tears, labral tears, and capsular injury (Bedi, 2011; Spindler et al., 2001).

Factors that contribute to impingement may be structural abnormalities of the scapula (Warner et al., 1992), muscle imbalance or overuse of the rotator cuff.

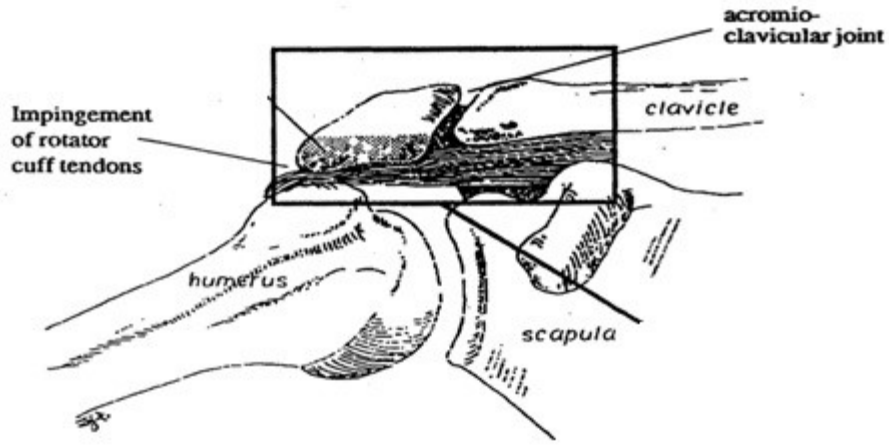

Figure 3.7 Impingement of the rotator cuff between the acromion and humeral head (Thompson, 2015)

The most common shoulder pain in the overhead athlete is known as internal glenoid impingement (Bedi, 2011; Spindler et al., 2001). It is postulated that this occurs when the under surface of the supra or infraspinatus tendons are entrapped with the posterosuperior aspect of the labrum during arm elevation and external rotation (Frost & Michael Robinson, 2006; Paley et al., 2000) although there is some disagreement in the literature about this.

In contrast, secondary impingement occurs when the rotator cuff is pinched in the subacromial space. This usually occurs due to instability in the GH joint where the weakened rotator cuff muscles cannot keep the humeral head centred on the glenoid, causing it to migrate superior reducing the subacromial space and impinging the rotator cuff. Furthermore, the dysfunction of the rotator cuff may increase the role of the bicep brachii in maintaining stability (Pagnani et al., 1996) leaving it susceptible to injury.

Hughes et al. (2012) measured impingement of the rotator cuff during full external and internal rotation for flexion, extension and abduction in cadavers. They found that the suprasinatus was impinged by the coracoacromial ligament when the arm was internally rotated in abduction, the

subscapularis muscle was impinged by the coracoid process in both internal and external rotation of arm flexion and the infraspinatus muscle was impinged by the posterior acromion when the arm was externally rotated in extension. Of these impinging positions, flexion and abduction while the arm was internally rotated showed significantly larger pressures being applied on the rotator cuff. Both these arm positions also occur during the bowling action in the region before and after ball release. Consequently, these findings provide a starting point in the biomechanical assessment of bowling within the context of likelihood of impingement.

3.4.2 Role of the scapula

The role of the scapula includes acting as a stable base during glenohumeral articulation, elevate the acromion to decreease the risk of rotator cuff imingement and finally provide the link in the proximal to distal sequencing of velocity, energy and forces during the sporting task (Kibler, 1998).

Studies have shown that the scapulothoracic joint contributes 20°-40° of upper arm elevation up to 90° (McClure et al., 2001; Yano et al., 2010). As the arm elevates, scapula upward rotation is necessary to elevate the lateral acromion and preventing impingement of the rotator cuff with the greater tuberosity of the humerus (Lukasiewicz et al., 1999). The ratio between scapula rotation and humeral elevation is known as the scapulohumeral rhythm (De Groot, 1998) with a value of 2:1 at the mid-range of elevation (Rockwood, 2009) where, up to 90° of elevation there is posterior tipping after which the scapula begins to anterior tip (Ebaugh et al., 2005). There is a clear relationship between scapula kinematics and shoulder impingement where altered scapulohumeral rhythm was found in subjects with subacromial impingement (Ludewig & Cook, 2000).

For young cricketers who experienced shoulder pain, Green et al. (2013) showed that a consistently downward rotated scapula predisposes cricketers to injury through impingement. This is in agreement with other research where the scapula position was found to be more upwardly rotated, internally rotated and retracted in throwing athletes as an adaptive mechanism to decrease likelihood of impingement (Myers et al., 2005). Dysfunction of the scapula can lead to changes in the tension of each muscle, adversely affecting stability in the joint where it is estimated that posterior and interior shear forces can range from 300-400N and compressive forces can be greater than 1000N (Meister, 2000) in overhead sports.

While it is clear that humerus elevation dictate scapula kinematics, exact three-dimensional

kinematic interaction between both segments is not well understood even though these rotations are evaluated clinically. Studies that look at the athletic shoulder make use of regression equations (Veeger et al., 1993; van Drongelen et al., 2011) to account for scapula movement, use markers attached to the skin (Nikooyan et al., 2010; Prinold & Bull, 2015) or simply do not include the movement of the scapula in their analysis.

3.5 Review of injuries in cricket

Within this section, a review of common injuries in cricket is presented. The incidence and impact of shoulder injuries on bowlers are also reported and comparisons are made between bowlers and other overhead athletes.

Bowling has been reported as exhibiting the highest chance of muscle injury for both spin and fast bowlers especially if they bowl frequently (Stretch, 2003). A review of the literature shows that on-going long-term surveillance into cricket related injuries have been conducted by the following nations: Australia, England and South Africa. In addition to this, there was a single season study conducted in the West Indies.

In the study of South African elite players (Stretch, 2003), injuries sustained for three seasons were surveyed. A total of 436 cricketers sustained 812 injuries during this period. Injuries frequently occurred to the lower limbs followed by the upper limbs, trunk, head and neck. Fast bowlers accounted for a large portion of injuries recorded. They were deemed to have a greater risk of injury because of the demands fast bowling places on the musculoskeletal system, incorrect technique, poor training and overwork. Other cricketers usually experience problems due to overuse or fielding (throwing and catching the ball).

In a study of acute injury incidence in professional county club cricket in the UK, over a 10 year span (Leary & White, 2000) reported that the Lower limb was most vulnerable to injury. Their study showed that 44.9% of all injuries (990) occurred to the lower limb, upper limb (29.4%), trunk (20%) and head and neck (5.7%) accounted for the remainder of injuries. Incidences of injury in bowlers were the greatest followed by all-rounders and then in batsmen.

A study conducted in the West Indies (Mansingh et al., 2006) reported that during the 2003-2004 season, injuries were greater to those playing international games (Test and ODI). A total of 33 international and 162 domestic cricketers sustained 79 injuries in that season. Bowlers sustained 43% of injuries while batsmen accounted for 40% of injuries.

Figure 3.8 represents the most likely injured body parts of a cricketer. These sites of injuries and rank were found to be consistent among the reviewed studies.

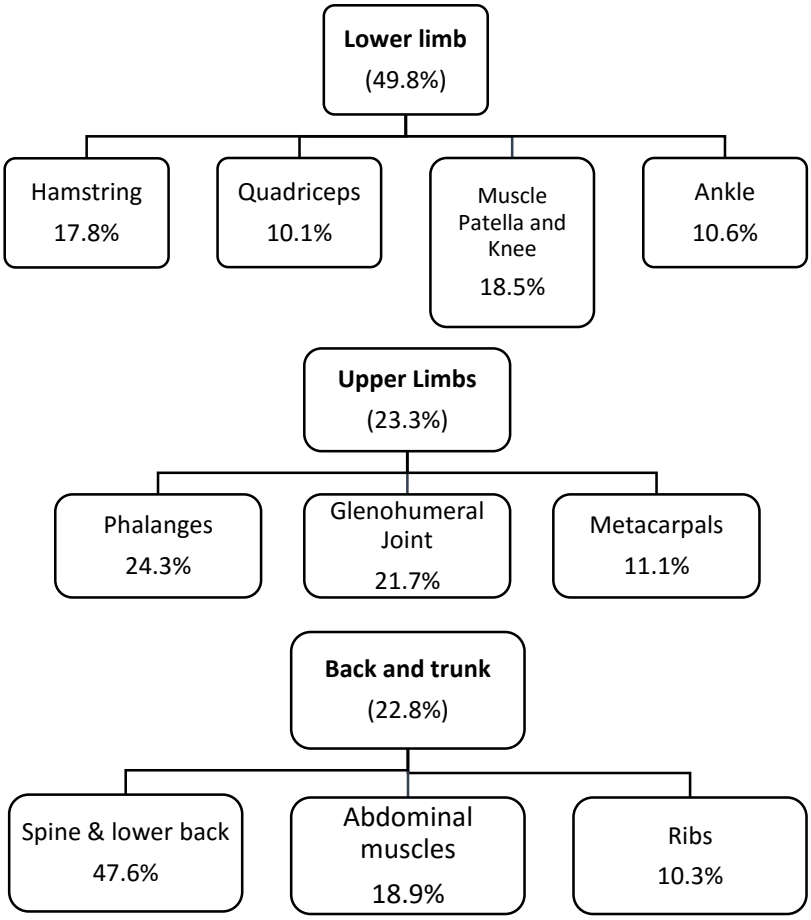

Figure 3.8 Frequently injured anatomical sites for cricketers

Injury in Australian men's cricket at the state and national level was studied for a period of 11 seasons concluding in the 2008-09 season (Orchard, 2010). It was reported that the introduction of T20 cricket has led to a hectic cricket schedule leading to greater injury prevalence rates. However, there were no significant changes to the injury profile in cricket other than what was reported above.

3.5.1 Shoulder injury in bowling

Shoulder injuries were particularly common in leg spinners as evident in a study of young cricketers (Gregory et al., 2002), where it was reported that 16.7% of spin bowlers developed shoulder injuries. They stated that the reason leg spinners had this problem was because they

rotate the bowling arm internally during the release phase thus placing the shoulder in an impinging position. There was no mention of this scenario in other research papers and this is under investigation in this thesis.

Stuelcken et al. (2010) reported a large peak shoulder distraction force during the early follow through phase of the bowling action in female fast bowlers. These researcher used a three-segment inverse solution model of the bowling arm to quantify the distraction force and reported a value 0.92 body weight and found to be within range of values reported in baseball pitchers, who are considered to be at high risk of shoulder injury (Werner et al., 2001) therefore, cricket bowlers should also be considered at high risk as well.

Bell-Jenje and Gray (2005) reported on the incidence, nature and risk factors of shoulder injuries in South African national academy cricketers. During the five-year study, ninety-six cricketers suffered a total of 165 injuries of which 40 were shoulder injuries. Bowlers and all-rounders accounted for 78% of shoulder injuries with 50% of these injuries occurring during fielding activities. Forty two per cent of shoulder injuries were associated with weak scapular stabilizers while 37% had limited glenohumeral internal rotation. In addition, 70% of shoulder injuries were classified as primary or secondary impingement.

Furthermore, 6% of bowling injuries were attributed to shoulder tendon injuries as reported by (Orchard et al., 2002) highligthing the need to establish the contribition of surround shoulder musculartur to joint stability.

3.5.2 Impact of shoulder injury on bowling

In a study conducted at the National Cricket Performance Centre in Loughborough University (Ranson & Gregory, 2008), the impact of shoulder injuries on professional cricketers in the 2005 England and Wales first Class cricket season was accessed. It was reported that of the 158 cricketers surveyed, 28% of spin bowers and 21% of fast bowlers experienced shoulder problems. The impact of these injuries on performance was determined by asking the affected cricketers how the injury impaired their ability to perform their cricketing role.

Ranson and Gregory (2008) investigated the impact of shoulder injuries on professional cricketers during one season and concluded that while shoulder injuries in cricketers are common, players generally carried on playing with the injury with some reduction in their performance. Thus, the incidence and prevalence of shoulder injuries was greater than what is

reported in injury survelliance studies. One limitation of this study was that the players themselves were allowed to determine the impact of shoulder injury on their batting, bowling, fielding. Ideally, Long-term surveillance of the players to determine the biomechanics of their action including kinematics of the ball when healthy and injured may provide more accurate results.

Giles and Musa (2008) found that healthy cricketers who regularly bowl or throw had significantly less internal and greater external rotation when comparing dominant to non dominant shoulders. Sundaram (2012) also reported similar findings in addition to reporting that spinners had a significantly greater external rotation than fast bowlers. Finally, cricketers who suffered from should pain had significantly greater loss in internal rotation than those who did not (Stuelcken et al., 2008).

Aginsky et al. (2004) looked at predisposing factors for shoulder injuries in fast bowlers. Test that were conducted included isokinetic strength measurement of the shoudler with both concentric and eccentric contractions performed as well as a leighton flexometer to measure the range of humerus axial rotation. The reported internal range of motion of $84° \pm 10.8°$ for injured and $89.8° \pm 17.26°$ for uninjuried while the external rotation ranges were $116.2 \pm 10.3°$ and $166.8° \pm 7.9°$ for injured and uninjured respectvely. Although these differences were not significant ($p>0.05$), they reported that fast bowlers who suffered from a muscle imbalance in the rotator cuff group and coupled with a front-on action suffered from chronic shoulder problems. From this, they hyptothesised that a front on action and rotator cuff imbalance predisposes a bowler to impingement syndrome.

Despite there being data on injury incidence and prevalence rates in cricket, information on the effects of shoulder injuries on a bowler's performance is scarce. As a result, there is not much empirical evidence that explain the effects of shoulder injuries on bowling even though the functional impairment of the shoulder has previously been reported.

3.6 Summary

Cricket bowling technique has been broken down showing the important phases in the action. Key performance parameters within the action have been discussed.

Shoulder injuries incidence and impact on cricket bowlers have been reported on where impingement is said to be the most common cause of shoulder pain. The role of the scapula was

highlighted in overhead activities.

It was revealed that the shoulder is the second most frequently injured site of the upper limbs. Shoulder problems usually occur because of the physical demands placed on the joint and are therefore biomechanical in nature. For instance, the range of motion required together with the repetitive nature bowling and any postural defects or poor technique may predispose bowlers to shoulder injuries.

Despite the availability of data describing the injury incidence in cricket, information on the impact of specific injuries is scarce. To date, there are few reports that address the connection between the biomechanics of a bowler's injured shoulder and the reduction in performance. For instance, impingement syndrome has been identified as the major cause of shoulder injuries in bowlers (Bell-Jenje and Gray, 2005; Aginsky et.al, 2004). However, the exact extent of the injury and factors such as whether a bowler can play without reduction in the playing skills (bowling or otherwise) has yet to be properly investigated. Studies usually report on the functional impairment of the shoulder due to injuries (Aginsky et al., 2004; Giles and Musa, 2008). Thus, the direct impact on a bowler's performance is unknown.

Furthermore, reports do not take into consideration the fact that those who experience shoulder injuries usually carry on playing (Ranson and Gregory, 2008) and injured players are at a high risk of experiencing future shoulder injuries. Hence, the real extent of shoulder injuries and their impact on performance of cricketers may be more serious than previously reported.

Finally, bowlers were shown to suffer from similar shoulder problems as other overhead athletes. A review of the literature highlighted predisposing factors for shoulder injuries in bowlers. These include a large distraction force in fast bowlers, a front on action with rotator cuff imbalances and internal rotation of the upper arm during ball release particularly in leg spinners.

The next chapter describes a pilot study used to assess the performance of a scapula tracker device that was used to measure scapula rotations during slow humeral circumduction.

Chapter 4

Dynamic tracking of the scapula during slow circumduction

This chapter describes the method that was used to track the scapula during bowling. A study is presented showing the practicality of using a scapula tracker device for slow circumduction of the upper arm in the range of motion used in cricket bowling.

4.1 Introduction

The previous chapter highlighted the importance of the scapula in overhead activities where, abnormal scapula movement is associated with different pathologies such as joint instability (Warner et al., 1992) and impingement syndrome (Ludewig & Cook, 2000; Aginsky et al., 2004). Consequently, it is important to accurately measure scapula kinematics as it provides important information in the fields of injury prevention (Prinold & Bull, 2015; Shaheen et al., 2013) and sports performance (Meyer et al., 2008; Myers et al., 2005). Furthermore, measurement of scapula kinematics allows for GH motion to be computed, which is important in upper limb biomechanical modelling (Charlton, 2003; Prinold, 2012).

A summary of marker methods used and their limitations for tracking the scapula during movement is presented in this chapter. Finally, details of a study looking at tracking the scapula during slow circumduction are presented.

4.1.1 Gold standard measurement techniques

Common techniques that have been used to record scapula motion include radiography and fluoroscopy. They are highly accurate and invasive techniques that are considered as a gold standard measurements against which other scapula measurement methods are validated. Radiography generally involves measuring rotations in one plane for single plane x-rays where 3D movement is projected onto a 2D plane. There is however high variability when trying to repeatedly obtain images at exactly the same angle to the plane. This method is also constrained by a limited capture volume and low sampling frequency. Fluoroscopy on the other hand has become more popular given that it uses a lower dose of radiation and has a significantly higher sampling frequency. Bi-planar fluoroscopy provides 3D data and is able to dynamically track movement. However, these methods also suffer from similar projection issues (De Groot, 1999), lower sampling frequency and limited capture volume when compared to motion capture systems.

Metal pins attached to the bone have, on occasion been used in the shoulder to record kinematics (Karduna et al., 2001; McClure et al., 2001; Ludewig et al., 2009). Similar to the other invasive methods, it offers a high degree of accuracy in addition to being able to track slow dynamic movement. Limitations of this method include ethical issues associated with invasive methods, altered kinematics of the shoulder due to pain being felt and also being unsuitable for use in athletic activities. Regardless of these issues, bone pins have been fairly widely used as a gold

standard measurement in validating non-invasive techniques like skin-fixed markers.

Magnetic resonance imaging (MRI) and palpation methods are two non-invasive gold standard measurement techniques, the latter of which offers a number of advantages over the previously mentioned techniques. MRI imaging is inherently three-dimensional where planes and axes are determined automatically and does not use ionising radiation. It is however limited by static measurement under current constraints, high cost associated with the MRI scanner and difficulty in allowing physiological motions under weight bearing due to scanner geometry.

In palpation methods, a device is used for identifying anatomical landmarks in order to measure 3D position of bones typically in static positions. The original palpation technique was developed for use in cadaveric studies where the device was composed of an open chain of four links connected by four hinges (Pronk & van der Helm, 1991). For the scapula, a palpation device also known as a scapula locator was developed by Johnson et al. (1993) and works by placing its three adjustable points on each of the three anatomical landmarks (acromial angle (AA), inferior angle (AI) and root of scapula spine (TS)) of the scapula to determine its position (Johnson et al., 1993) (Figure 4.1). The use of a rigid body with markers attached, ensures that the measured landmarks are rigid and therefore reduces measurement error when compared to individually palpating each point. Repeatability of this device for measuring intra-subject scapula rotations was found to be within 2° - 5° (Barnett et al., 1999; Shaheen et al., 2011a; De Groot, 1997; Meskers et al., 1998; Johnson et al., 1993).

The application of the scapula locator was extended for slow dynamic movement and was found to have similar repeatability with static measurements as reported by Shaheen et al. (2011a). In their study, the locator was adapted by placing force sensors at the points of contact and was used during slow bilateral scapula plane elevation. A mean variation of 3.6° was reported for the device (Shaheen et al., 2011a). Furthermore, an inter-observer variability of up to 6.6° was reported when using the locator with pressure-feedback. Other studies have found similar values ranging from 4°-8° (Meskers et al., 1998; Barnett et al., 1999).

The scapula locator has been used in various studies with good intra-subject and inter-observer repeatability with comparable accuracy with the previously mentioned imaging techniques and therefore can be classified as a gold standard measurement technique. Similar to the previously mentioned techniques it is also unsuitable for athletic activities but offer an easy and convenient scapula tracking method in a clinical setting for slow movement.

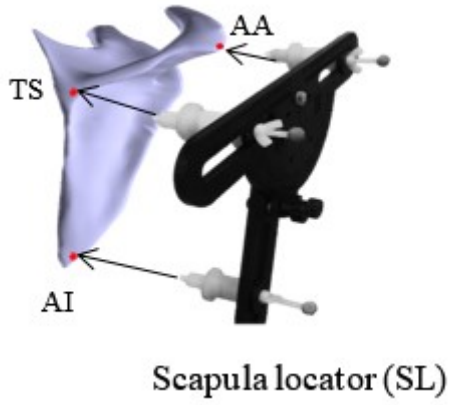

Figure 4.1 Scapula locator used to identify position of the scapula by locating its anatomical landmarks

Even though these techniques are accurate, the disadvantages of ethical issues of exposing subjects to risk and being impractical for use in tracking scapula movement in cricket bowling means that other non-invasive, less accurate methods must be used and validated against a gold standard measurement.

4.1.2 Non-invasive measuring techniques

Non-invasive methods that use skin mounted sensors are known as cutaneous marker methods. These marker methods work by attaching sensors on the skin in order to record movement of the underlying bone. Marker methods include the use of electromagnetic system (Karduna et al., 2001; Barnett et al., 1999; Meskers et al., 1998; Ebaugh et al., 2005; Ludewig et al., 2009) or passive markers (Lovern et al., 2009; van Andel et al., 2009; Lempereur et al., 2010; Senk & Cheze, 2010; Shaheen et al., 2011b; Prinold & Bull, 2015) in an optoelectronic system for studying scapula kinematics. The use of passive skin markers in particular have been popular in human motion analysis due to its non-invasive nature and are less obtrusive on the subject with no tethered wires. All marker methods however are limited as they suffer from inaccuracies relating to the placement of the markers or because of relative movement between the underlying bone and skin mounted markers known as soft tissue artefacts (STA) (Leardini et al., 2005). This is especially true for the scapula (Figure 4.2), because of the soft tissue covering the scapula and the fact that there is an average upward rotation of 50°, posterior tilting of 30° and external rotation of 24° during elevation (Rockwood, 2009). These large rotations results in a difference of up to 87mm between actual and measured scapula landmarks (Matsui et al., 2006).

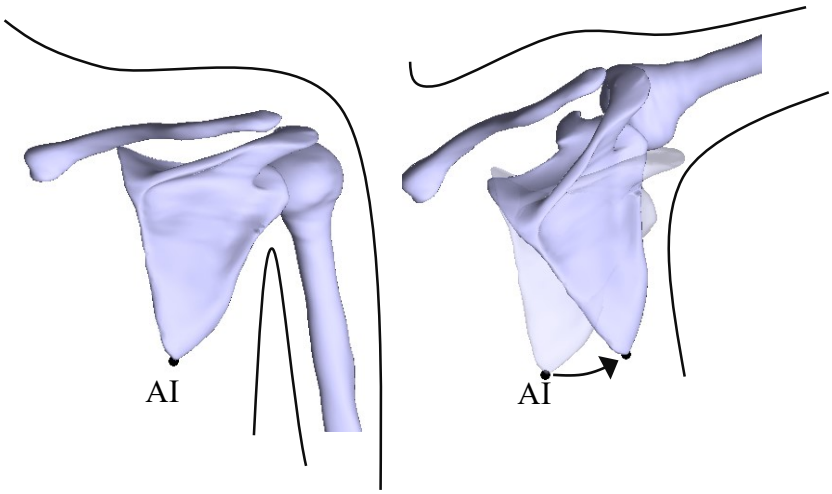

Figure 4.2 Posterior view of the shoulder showing the displacement of AI in it's palpated during arm elevation.

Electromagnetic systems offer the advantage of automatically creating coordinate frames, simpler digitisation processes and no need for direct line of sight of the sensor, when compared to optoelectronic systems. These systems use an electromagnetic sensor and receiver connected via a cable to record motion. For this reason, there are a number of drawbacks of using such a system in very fast dynamic motion. They typically have lower sampling rates where errors in recorded motion can arise from rapid changes in velocity and hindrance of subject leading to altered kinematics, both of which are caused by the connected cable (Meyer et al., 2008).

Optoelectronic systems also known as motion capture systems use retro-reflective markers attached to the skin where at least two infrared cameras must see the marker in order to track its position in 3D space. Two common methods that have been used to track scapula motion are Scapula Tracker (ST) and Acromial Method (AM). Both methods operate on the principle that scapula anatomical landmarks are digitised relative to the mounted sensors.

The AM involves a sensor placed directly on the flat part of the acromion on a rigid frame (McQuade & Smidt, 1998). The ST method was developed by Karduna et al. (2001) where an adjustable rigid tracker (Figure 4.3a) was attached on the scapula spine and acromion.

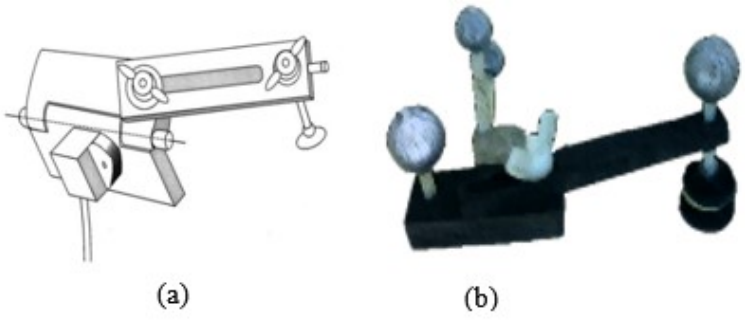

Figure 4.3 (a) Schematic drawing of scapula tracker designed by Karduna et al. (2001) (b) modified version (Prinold et al., 2011)

Both methods have been validated using bone pins implanted into the scapula by Karduna et al. (2001). They reported that both methods performed well within 120° of arm elevation. The ST was found to be the more accurate of the two methods where it had less error for external rotation and posterior tilt during humeral elevation in the scapula and sagittal planes (Table 4-1). However, it was found to underestimate upward rotation whereas the acromial method overestimated it.

Prinold et al. (2011) improved upon the design of the scapula tracker for use with a motion capture system (Figure 4.3b). The device consists of a base that is attached to the mid-range of the scapula spine and an adjustable foot attached at the junction between the spine and acromion. They found that their scapula tracker performed better for internal rotation and posterior tilt when compared to the acromial tracker method above 100° of humerothoracic elevation. In addition, it was found to be accurate within 3° with a single calibration and 2° when using multiple scapula calibrations during scapula plane elevation.

	Tracker method				**Acromial method**			
	Scapula plane elevtation	Sagittal plane elevation	Horizontal abduction	External rotation	Scapula plane elevtation	Sagittal plane elevation	Horizontal abduction	External rotation
Posterior tilt	4.7	6.2	3.8	4.6	6.6	8.6	7.3	3.7
Upward rotation	4.2	4.1	4.0	4.5	2.0	2.5	4.1	4.0
External rotation	3.2	3.8	5.0	4.4	9.4	11.4	10.0	6.2

Table 4-1 RMS errors in degrees for ST and AM methods when compared to bone pins. From Karduna et al. (2001) study

Multiple calibrations were chosen based on the level of humerothoracic elevation and ranged from 30° to 120° calibrated positions. It was reported that multiple calibration position reduced the mean error by distributing it more evenly over the full range of motion as the calibration that is used changes. If a single calibration were used then, the ideal single calibration position was found to be 90° of humerothoracic elevation for both ST and acromial methods. In previous studies, the ST was calibrated with no humeral elevation (van Andel et al., 2009; McClure et al., 2001; Karduna et al., 2001) and therefore suffer from increasing measurement errors as the scapula moves away from its calibration position during humerothoracic elevation therefore, the calibration position does make a significant difference when recording scapula kinematics with these devices.

Shaheen et al. (2011b) showed that the position of an acromial cluster significantly affected accuracy. Scapula measurements obtained from an AM were validated against Palpator measurements for up to 90° of humerothoracic elevation. They found that position C, the medial aspect of the acromion (Figure 4.4) was least affected by soft tissue deformation as the RMS value at this position was half that of position B. These findings were incorporated into the protocol for using the scapula tracker used by Prinold et al. (2011) where the adjustable foot in their tracker was placed at position C. This is generally accepted as the best location as it reduces errors by avoiding the bulge of the deltoid muscle during elevation.

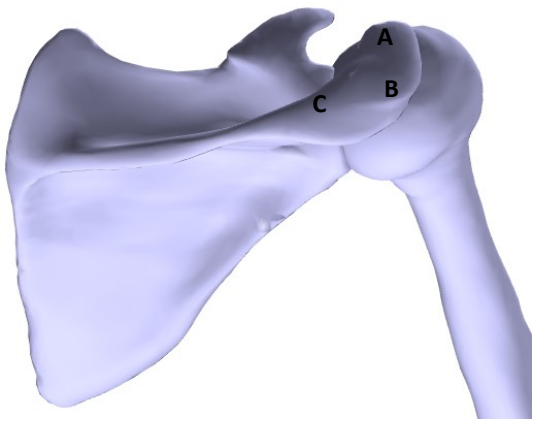

Figure 4.4 Three positions of the acromial method tested by Shaheen et al. (2011b)

4.1.3 Other considerations when measuring and reporting scapula kinematics

In an effort to reduce the variability of reported shoulder kinematics, the International Society of Biomechanics (ISB) published standards for the upper limb joint coordinate system and

rotation sequences (Wu et al., 2005). Ludewig et al. (2010) found this proposed standard interprets scapula motion with less internal and upward rotation and more posterior tilt when using its recommended anatomical mediolateral axis definition of TS to AA instead of TS to acromioclavicular joint (AC) (Figure 4.5). In addition to the anatomical coordinate system used, scapula rotations are also affected by the choice of Euler sequence.

Euler sequences used for shoulder kinematics have been investigated where it was reported that there were differences up to 50° for scapulothoracic rotations (Karduna et al., 2000). In addition, for humerothoracic rotations the XZY sequence was recommended over the ISB standard as it avoids gimbal lock issues (Bonnefoy-Mazure et al., 2010) and the choice of sequence of glenohumeral rotation would depend on the aims of experiment and motion being captured (Šenk & Chèze, 2006). While these findings provide an alternative method for calculating and reporting scapula kinematics, ISB standards were chosen in this thesis, as it is commonly used and allows comparisons with others in the literature.

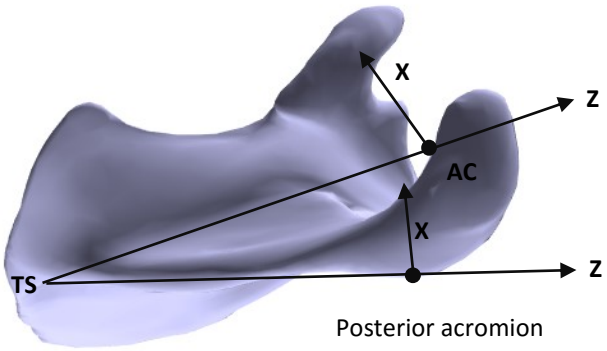

Figure 4.5 Superior view of the scapula showing the difference in x (anteroposterior) and z (mediolateral) axis derived from the root of the spine (TS) to the acromion and acromioclavicular joint (AC) that was illustrated in Ludewig et al. (2010)

For fast overhead activities such as those studied in this thesis, the speed of movement is an important consideration when measuring scapula kinematics. There is however limited literature looking at this since the accurate measures mentioned in Section 4.1.1 cannot be used. There is also variability in reporting the effect due to changes in speed of motion. While investigating changes in sub maximal speed it was found that the glenohumeral and scapulothoracic ratios were not fixed and were significantly different to those at lower speeds

(Sugamoto et al., 2002). Fayad et al. (2006) used 3D recording methods and concluded that scapula rotation did not differ between fast and slow movements. There were however, differences in scapula rotation among three planes of elevation. More importantly, they found that interpolation of statically measured data did not represent dynamic scapula rotations. Since the speeds used in such studies are not close to athletic movements, the applicability of these findings is limited.

4.2 Aim

The aim of this study was to investigate the performance of the best-available method, the scapula tracker (Prinold et al., 2011) during a range of motion that is used in cricket bowling: slow circumduction of the upper arm. This was achieved by comparing the scapula rotations calculated from the scapula tracker (ST) and those obtained from a scapula locator (SL).

4.3 Materials and Methods

Scapula kinematics was measured for twelve male subjects (age: 25.6± 3.9 years, height: 1.76 ± 0.07 meters, mass: 69.98 ± 8.31 kg) who had no reported shoulder pain. The local ethics committee granted approval of this study and consent was obtained from each subject.

4.3.1 Model

Anatomical reference frames for each segment were constructed in accordance with ISB standards (Wu et al., 2005). Scapula rotations - Internal/external (IE), downward/upward (UD) rotation and posterior/anterior (PA) tilt - were calculated with respect to the thorax using the Euler sequence YX'Z''. Humerothoracic kinematics was found using YX'Y'' Euler sequence. Figure 4.6 illustrates the anatomical frames used.

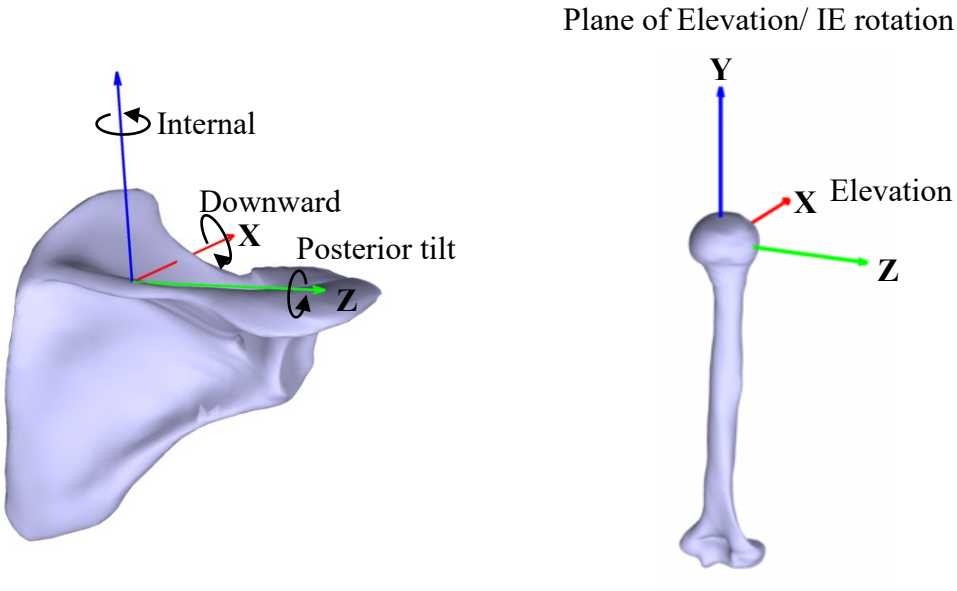

Figure 4.6 Scapula and humerus anatomical frames and rotations

4.3.2 Data collection

Fifteen markers were placed on the truck and dominant arm (Table 4-2). Anatomical landmarks of the scapula, elbow and wrist (Table 4-3) were digitised with respect to a technical cluster on each of the respective segments as described by Cappozzo et al. (1995).

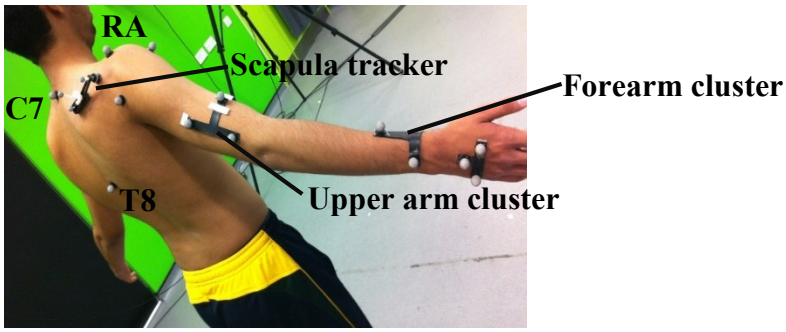

Figure 4.7 Marker model

Thorax	C7	Spinous process of the 7th cervical vertebra
	T8	Spinal process of the 8th thoracic verebra
	IJ	Incisura Jugularis
	PX	Xiphoid process
	RA	Right Acromion
	LA	Left Acromion
Scapula	ST1	Marker 1, scapula tracker
	ST2	Marker 2, scapula tracker
	ST3	Marker 3, scapula tracker
Humerus	U1	Marker 1, Upper arm cluster
	U2	Marker 2, Upper arm cluster
	U3	Marker 3, Upper arm cluster
Forearm	F1	Marker 1, Forearm cluster
	F2	Marker 2, Forearm cluster
	F3	Marker 3, Forearm cluster

Table 4-2 Marker model used for the upper limb

Scapula	AA Acromial angle
	AI Inferior Angle
	TS Root of scapula spine
Humerus	LE Lateral epicondyle
	ME Medial epicondyle
Forearm	US Ulnar styloid
	RS Radial styloid

Table 4-3 Digitised landmarks

Technical clusters for each segment were located (Eftaxiopoulou et al., 2013) in areas that minimised errors caused by soft tissue artefact while the scapula tracker was placed on the midpoint of the scapula spine and extending to the junction between the spine and acromion. A passive marker, 9-camera optical tracking system (Vicon, Oxford, UK) was used to capture marker trajectories at 100Hz.

The scapula position was digitised with the arm near the top of the circumduction arc and was used as the calibration position in the dynamic trials. This position was chosen since scapula calibration done with the arm at this elevation would result in more accurate scapula rotations in this region. This is important because the upper region of the bowling arc is of greater significance when looking at the risk of impingement.

Dynamic trials involved controlled-slow circumduction (approx. 1.1 rad/s) of the subject's

dominant arm (Figure 4.8a), starting and ending with the arm along the side of the thorax and with the elbow extended. The position of the scapula was recorded using the scapula locator and scapula tracker simultaneously (Figure 4.8b) with the locator being readjusted at the start of each trial. Six trials for each subject were recorded and used in calculating average humeral and scapula kinematics.

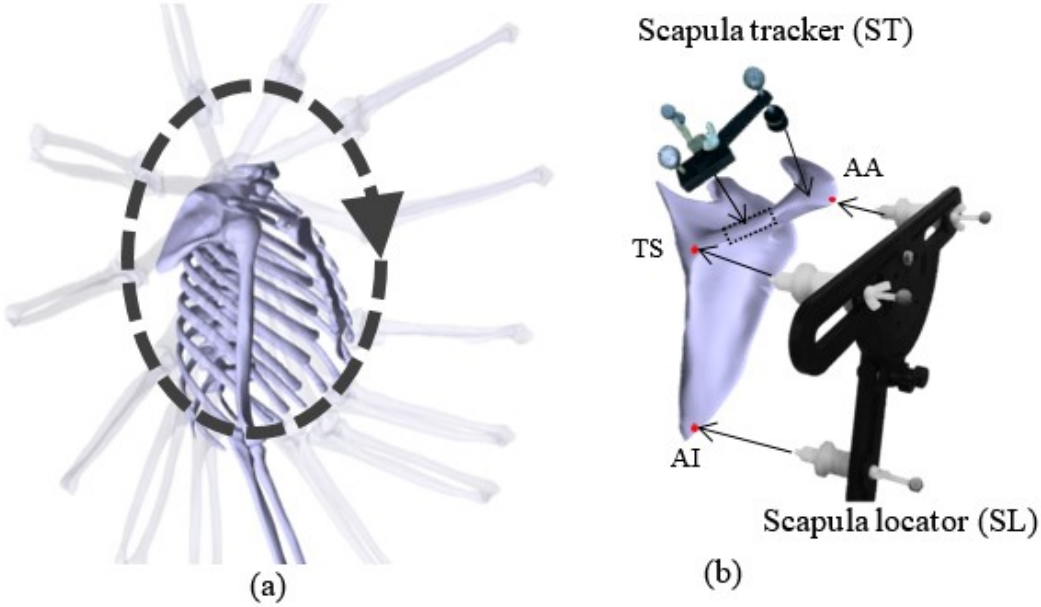

Figure 4.8(a) Upper arm slow circumduction, (b) Scapula locator and tracker location on the scapula during dynamic tracking

The centre of rotation (COR) of the glenohumeral joint was found using a spherical fitting method (Gamage & Lasenby, 2002) in which the subject was asked to explore the region below 45° of upper arm elevation and flexion, performing random humeral rotations with the elbow flexed at 90°.

4.3.3 Statistical analysis and data processing

Average scapulothoracic rotations obtained using the locator across all subjects were used to formulate a set of regression equations that predicted scapula kinematics based on the plane of elevation and elevation humerothoracic angles. The feasibility of the regression results were quantified by recalculating the regression angles for each subject but leaving out their scapulothoracic rotations each time in formulating the regression equations. Both regression and scapula tracker methods were then compared to the locator method.

The new coefficient of multiple correlation (CMC) (Ferrari et al., 2010) method was used to compare how similar kinematic curves from both methods (the ST and the regression) were to the ones obtained using the SL. A one-way ANOVA was conducted to compare the range of motion for scapula about its three axis of rotation for both ST and regression methods and against the SL method.

4.4 Results

CMC and RMSE confirmed that the scapula tracker is in very good agreement with the locator results for IE and UD rotations but poor for PA tilt, where it generally overestimates the amount of posterior tilt (Figure 4.9 and Figure 4.10). A one way ANOVA test showed that the range of motion of both methods for scapula PA tilting were significantly different ($p<0.05$). Regression analysis did not further improve what could be achieved with the ST for IE and UD.

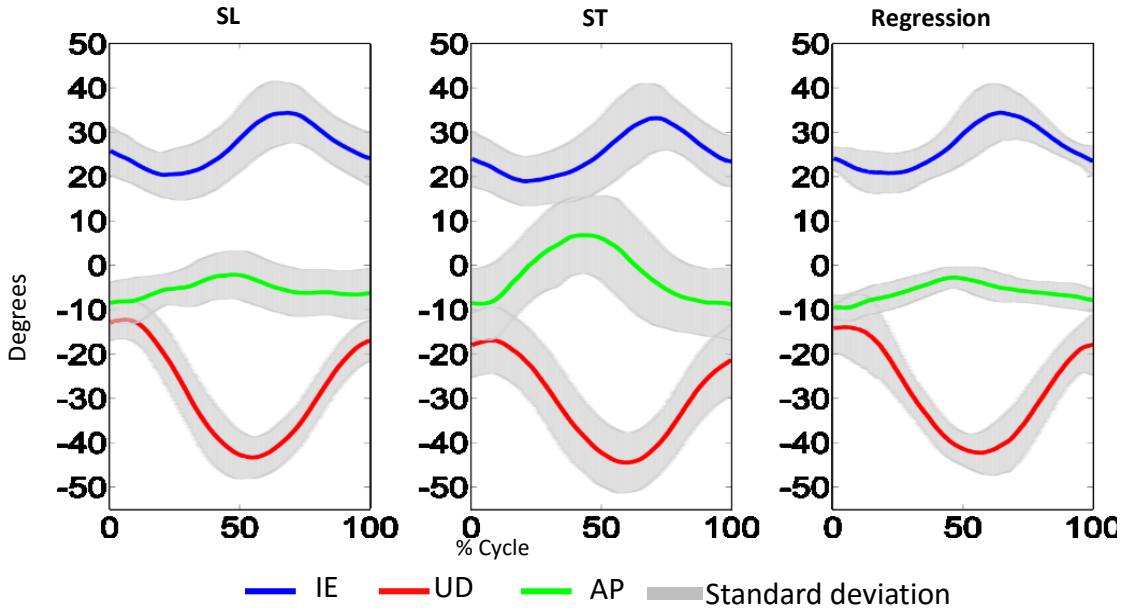

Figure 4.9 Average scapulothoracic kinematics during circumduction for three methods across all subjects

The average error of a leave-one-out regression analysis is 5.19°, 6.69° & 3.08° respectively for each rotation angle. A summary of other regression model parameters is shown in Table 4-6. The regression model is given by Equation 4.1-Equation 4.3.

Average maximum humeral elevation among subjects was generally consistent, ranging from 120° to 150° (Figure 4.11). There was however, some variation in average IE humeral rotation, indicating that subjects performed the motion in slightly different ways, which coupled with variations in angular velocity of the humerus at both inter and intra subject levels, may have had a negative impact on the development of the regression model.

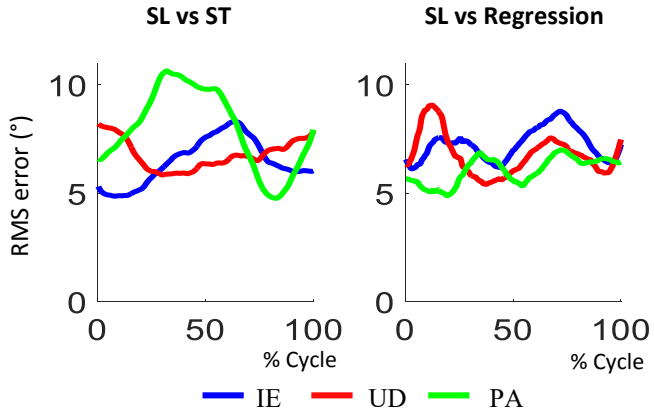

Figure 4.10 RMS error for ST and regression vs SL

	Scapula tracker			Regression		
	IE	**UD**	**PA**	**IE**	**UD**	**PA**
1	0.60	0.97	0.68	0.77	0.98	0.91
2	0.96	0.91	**0.48**	0.92	0.96	**0.00**
3	0.86	0.99	0.93	0.84	0.95	0.72
4	0.80	0.96	**0.46**	0.73	0.94	**0.00**
5	0.95	0.94	0.83	0.90	0.93	0.64
6	0.89	0.97	**0.30**	0.82	0.90	**0.28**
7	0.80	0.93	0.73	0.77	0.89	**0.23**
8	0.94	0.96	0.73	**0.54**	0.89	**0.44**
9	0.71	0.94	0.69	0.70	0.94	**0.43**
10	0.95	0.96	0.61	0.89	0.93	**0.26**
11	0.80	0.97	**0.45**	**0.00**	0.91	**0.00**
12	0.92	0.88	**0.53**	0.77	0.98	**0.49**

Table 4-4 CMC values for SL vs. ST and SL vs. regression, values below 0.6 are highlighted showing a poor agreement

Intra-subject repeatability was determined using the CMC values calculated for kinematic curves of the scapula and humerus across the six trials. The mean values across the subjects for

IE rotation, UD rotation and PA tilt for the scapula tracker were 0.82 (SD 0.13), 0.94 (SD 0.03) & 0.86 (SD 0.08) and for the locator were 0.78 (SD 0.17), 0.95 (SD 0.02) & 0.56 (SD 0.23) respectively. Humeral kinematics repeatability was 0.98 (SD 0.01), 0.97 (SD 0.02) and 0.94 (SD 0.04) for plane of elevation, elevation and IE rotation respectively.

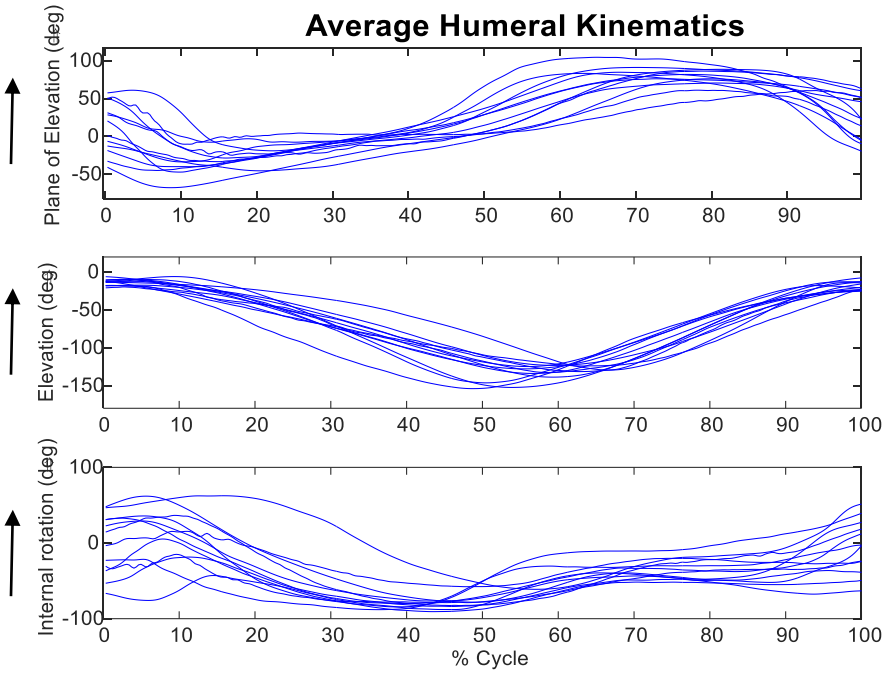

Figure 4.11 Average Humerothoracic kinematics for all subjects.

Average RMSE (standard deviation)					
SL vs ST			SL vs regression		
IE	UD	PA	IE	UD	PA
6.2° (2.8)	6.2° (3.0)	8.4° (2.9)	6.6° (2.1)	6.1° (3.1)	5.5° (2.3)

Table 4-5 Average RMSE values and Standard deviations for ST and regression compared to SL

	IE (Y)	UD (X)	PA (Z)
Adjusted R^2	0.99	0.99	0.99
RMSE	0.143	0.140	0.165

Table 4-6 Regression fit Parameters

The regression model is given by the following equations where Y, X and Z are the predicted IE, UD and PA scapula rotations. x_1 and $x_2$are humerothoracic plane of elevation and elevation angles.

$$Y = 29.6877 - 0.1219 * x_1 + 5.32 \times 10^{-4} * x_1^2 + 0.230 * x_2 - 1.73 \times 10^{-4} * x_2^2 - 0.0011 * x_1 x_2 \quad \text{Equation 4.1}$$

$$X = -49.3376 + 0.0622 * x_1 + 9.44 \times 10^{-4} * x_1^2 - 0.019 * x_2 + 0.0011 * x_2^2 - 4.39 \times 10^{-4} * x_1 x_2 \quad \text{Equation 4.2}$$

$$Z = 5.2711 - 0.11329 * x_1 + 2.039 \times 10^{-4} * x_1^2 - 0.1372 * x_2 + 2.45 \times 10^{-4} * x_2^2 + 9.02 \times 10^{-4} * x_1 x_2 \quad \text{Equation 4.3}$$

4.5 Discussion

Dynamic measurement of overhead shoulder activities is made possible with the scapula tracker presented here. Scapula IE and UD rotations are accurate to within 6.21° and 6.24° respectively (Table 4-5) and show a better consistency with the gold standard measure when based on CMC values. Anterior-posterior tilt values have higher errors (8.41°), and therefore the recommendation is that these are derived using the regression equations presented here. However, while the regression model reduced the overestimation of the posterior tilt, CMC values (Table 4-4) were still generally low, which indicated it did not follow the same trend set by the SL. Therefore, future work should focus on improving the dynamic measure of anterior-posterior tilt. This may be done by further optimising the attachment of the tracker device or including the use of multiple calibration points.

The range of motion obtained for the scapula tracker were in agreement with the literature (Karduna et al.,2001, McClure et al.,2001, Shaheen et al., 2011b), where the range of values for scapula rotations during humerothoracic elevation up to 120° were: 5° to 25° of anterior tilt, 20° to 64° of upward rotation and 37 to 30° of internal rotation. The RMS errors for scapula rotations (Figure 4.10) were within comparable ranges reported by Karduna et al., (2001) and Prinold et al. (2011) when looking within the same humerothoracic elevation range. They showed a similar trend of an increasing error (up to 20° and 10° for PA and IE in both studies) as the humerus elevation angle approached 120°. This higher error is expected as they were

comparing against bone pins, which are more accurate than the locator method used in this study. It should also be noted that the circumduction motion done in this study is different to the planar elevations typically done in other studies when measuring scapula kinematics therefore comparisons are limited to analysing scapula kinematics within similar humerothoracic range.

The performance of the scapula tracker illustrates its potential for use in full speed bowling action especially if only IE and UD rotations were being considered. There are however, certain limitations that are not well understood when measuring scapula kinematics during high-speed movement. These include the effects of measurement errors on the force prediction capabilities of musculoskeletal models and the importance of one scapula rotation over another during bowling that is necessary for preventing impingement injuries. Studies have shown that subjects who suffer from impingement syndrome have a lower posterior tilting of 8°-9.5° when compared to healthy subjects (Ludewig & Cook, 2000; Lukasiewicz et al., 1999). While it is expected the errors would increase in full speed trials, there is no better alternative and therefore this method will be used and its performance reassessed during these trials.

Limitations of the study include the assumption that kinematics obtained using the locator was accurate. While this may be true for static conditions, there were difficulties in manoeuvring the SL while the ST was attached to the subject. These difficulties were mitigated through the use of protocols described in the literature (Shaheen et al., 2011b). In addition, the bulge of the posterior deltoid near maximum elevation would have affected the posterior tilt measurement and thus further optimisation of the ST placement as well as the use of multiple calibration locations may further reduce errors.

4.6 Conclusion

In this study, scapula rotations calculated from a scapula tracker (ST) and a regression model during slow circumduction of the dominant arm were compared to those obtained from a scapula locator (SL). The results show that the scapula tracker was found to be accurate for IE and UD rotation and shows good repeatability during slow overhead circumduction thus highlighting its potential in the field of shoulder biomechanics during overhead activities.

The next chapter chapter presents the materials, methods, and results of the main study that was conducted to capture full body kinematics of cricket bowlers where the scapula tracker was used.

Chapter 5

Motion capture of bowlers

This chapter describes the methods and materials that were used for the main experimental study. This includes the marker model used to capture full body kinematics of cricket bowlers and a description of the motion capture process. The data obtained represents the cohort of subjects that will be used for analysis in subsequent chapters. Kinematic results are presented in this chapter prior to analysis of the shoulder forces in the subsequent chapters.

5.1 Introduction

A prerequisite to understanding and analysing human movement is the collection of data that would allow for the reconstruction of bone position and orientation in 3-D space at each instant in time throughout the entire motion. This chapter describes the methods used in 3D motion capture of the bowling action and how these data are processed. In addition, the data collected will be used in upper limb biomechanical model to look at the likelihood of shoulder injury in bowlers where, the results of scapula kinematic data in particular is an important consideration during the musculoskeletal modelling process. Steps involved in the data collection, processing and analysis from the kinematic model are presented in this chapter. Kinematic results that are presented include scapulothoracic and humerothoracic data for all subjects together with a description and classification of the bowling techniques.

5.1.1 Aim and objectives

The aim of the study was to develop a full body kinematic model for cricket bowlers, which was used to assess the performance for the scapula tracker and to classify the bowling technique employed by each subject. This was done using recommendations set out by the International Society of Biomechanics (Wu et al., 2005; Wu et al., 2002) and building upon the work done by Eftaxiopoulou (2011) who looked at measuring elbow kinematics in bowlers.

5.2 Materials and methods

The study was designed to collect full body kinematics from bowlers using an optical motion tracking system. Eighty-one reflective markers were used, mostly in clusters of three, attached to the subjects' head, thorax, upper and lower limbs. Healthy subjects were recruited for one testing session lasting approximately one hour. Testing was conducted over four consecutive days with five researchers present each day to assist in setting up and preparing the subjects for the bowling trials in addition to packing up the equipment at the end of each day. All testing was done at the MCC indoor academy at Lord's cricket ground. Ethics were applied for and informed written consent was obtained from each subject.

5.2.1 Equipment and set-up

A 10-camera optical motion tracking system (Vicon, Oxford, UK) was used at an acquisition rate of 400 Hz to track reflective markers attached to the subject. Three reflective markers of

14 mm in diameter were fixed to aluminium T-frames forming a cluster, which were then attach to upper and lower limbs using double-sided tape. A custom-made headband with four markers attached was used for the head while markers on the thorax and pelvis were directly attached on the skin at the anatomical landmarks for both segments. The specially designed marker cluster (Prinold et al., 2011) that was described in Chapter 4, was used to track movement of the scapula.

Two digital high speed cameras were also used at an acquisition rate of 100 Hz to record the timings of upper arm vertical (UAV), upper arm horizontal (UAH) and ball release (BR) in the bowling action. The high-speed cameras were used simultaneously with the optical motion tracking system allowing for the data captured from both sets of cameras to be synchronised.

Camera positions (Figure 5.1) used by Eftaxiopoulou (2011), who cited the work of Aginsky and Noakes (2010), were used as a template from which the final setup was finalised after testing in the motion laboratory at Imperial College London. Key to this decision making process was making use of the space given at the indoor school, placement of the two high-speed video cameras for capturing movement of the upper arm and ball release and placement of the 10 motion capture cameras for capturing full body kinematics whilst minimising the chances of marker occlusion. The system was calibrated prior to testing each subject, ensuring the an accuracy within 0.3mm was always obtained

Post-processing the data such as labelling and gap filling was done in *Vicon nexus 1.8.5* (Vicon, Oxford, UK) whereas calculation of joint angles and other kinematic parameters were done in *Matlab 8.6* (The Mathworks Inc, Natick, USA). During the gap filling, in the case where there was a significant gap (more than 20 frames), visual checks were done to ensure that the occluded maker predicted trajectory followed the expected path of motion. An open-source biomechanical toolkit (Barre & Armand, 2014) was used extensively for importing the data from nexus into Matlab for further processing.

(a) (b)

Figure 5.1 showing camera setup used at the MCC indoor academy and (b) showing the location of the subject within the capture volume

5.2.2 Subjects

Subjects were recruited from the MCC indoor academy, from county teams who also trained at the facility and from Imperial College. Seventeen healthy subjects were recruited and tested. Due to problems with the quality of the data captured, only 15 subjects were included in the study. Eleven were fast bowlers, two were off spinners and two were leg spinners. The 15 subjects were 1.82 ± 0.05 metres in height, 79.45 ± 13.12 kg in mass with an average age of 23 years (range: 19-34). Full details of each subjects is presented with the results in Section 5.4.

5.2.2.a Inclusion criteria

Healthy bowlers and no history of chronic shoulder injury and no current shoulder injury.

5.2.2.b Exclusion criteria

Any history of serious shoulder, elbow or lower back injuries. Any surgery to the elbow or shoulder. Any other injury that would normally prevent their selection to play cricket.

5.2.3 Marker model

Seven markers were used for the thorax: on the left and right acromion process just after the AC joint, seventh cervical vertebra, eighth thoracic vertebra, jugular notch, xiphoid process and manubrium. Two clusters were used for the bowling side upper and lower arms. Details of the placement of clusters for the upper and lower limbs are given in Section 5.3.1. The full marker model is shown in Table 5-1 and Figure 5.3

Researchers were approached about sharing the marker model and protocol used in capturing cricket bowling kinematics. The intention was to make the dataset open so that comparison and further studies could be done in a spirit of openness and collaboration. Researchers at the University of Western Australia (Chin et al., 2009) and Loughborough University (Worthington et al., 2013) agreed and as such additional markers were included to accommodate for the other marker models. These included two markers on the thorax at the 10^{th} thoracic vertebra and 1^{st} lumbar vertebra, markers anterior and posterior to the humeral head and extra clusters on the bowling arm. The reason for doing this was to allow comparison of kinematics calculated based on a marker model familiar to these researchers. Full details of the marker model used by these researchers are documented in the above cited publications.This comparison of calculation methods is not within the scope of this thesis.

In addition, a cluster was placed on the bowling hand with markers placed on each segment of the thumb and index finger. These markers were included to capture wrist and finger kinematics in bowling. This data was used in other studies and is not within the scope of this thesis.

Segment	Marker name	Description
Head	HD1, HD2, HD3, HD 4	Marker 1, Head cluster; Marker 2, Head cluster; Marker 3, Head cluster; Marker 4, Head cluster
Thorax	C7	7th cervical vertebra
	T8	8th thoracic verebra
	IJ	Incisura Jugularis
	PX	Xiphoid process
	RAC	Right Acromioclavicular joint
	LAC	Left Acromioclavicular joint
	MA	Manubrium
Scapula	ST1, ST2, ST3, ST 4	Marker 1, scapula tracker; Marker 2, scapula tracker; Marker 3, scapula tracker; Marker 4, scapula tracker
Right Humerus	RU1, RU2, RU3, RU4, RU5, RU6	Marker 1, UA cluster 1, Marker 2, UA cluster 1, Marker 3, UA cluster 1; Marker 4, UA cluster 2; Marker 5, UA cluster 2; Marker 6, UA cluster 2
	RHME	Medial epicondyle
	RHLE	Lateral epicondyle
Right Forearm	RF1, RF2, RF3 RF4, RF5, RF6	Marker 1, LA cluster 1; Marker 2, LA cluster 1; Marker 3, LA cluster 1; Marker 4, LA cluster 2; Marker 5, LA cluster 2; Marker 6, LA cluster 2
	RUS	Ulna styloid
	RRS	Radial styloid
Right Thigh	RT1, RT2, RT3	Marker 1, Thigh cluster; Marker 2, Thigh cluster; Marker 3, Thigh cluster
	RFME	Medial epicondyle
	RFLE	Lateral epicondyle
Right Shank	RS1, RS2, RS3	Marker 1, Shank cluster; Marker 2, Shank cluster; Marker 3, Shank cluster
	RMM	Medial malleolus
	RLM	Lateral malleolus
Right Foot	RCAL	Calcaneus
	RMT1	1st metatarsal bone
	RMT2	5th metatarsal bone
Left Humerus	LU1, LU2, LU3	Marker 1, UA cluster; Marker 2, UA cluster; Marker 3, UA cluster
	LHME	Medial epicondyle
	LHLE	Lateral epicondyle
Left Forearm	LF1, LF2, LF3	Marker 1, LA cluster; Marker 2, LA cluster; Marker 3, LA cluster
	RUS	Ulna styloid
	RRS	Radial styloid
Left Thigh	LT1, LT2, LT3	Marker 1, Thigh cluster; Marker 2, Thigh cluster; Marker 3, Thigh cluster
	LFME	Medial epicondyle
	LFLE	Lateral epicondyle
Left Shank	LS1, LS2, LS3	Marker 1, Shank cluster; Marker 2, Shank cluster; Marker 3, Shank cluster
	LMM	Medial malleolus
	LLM	Lateral malleolus
Left Foot	LCAL	Calcaneus
	LMT1	1st metatarsal bone
	LMT2	5th metatarsal bone
Pelvis	RPSIS	Right Posterior superior iliac spine
	RASIS	Right Anterior superior iliac spine
	LPSIS	Left Posterior superior iliac spine
	LASIS	Left Anterior superior iliac spine

Table 5-1 Markers used for motion capture of a right hand bowler where UA-upper arm, LA-lower arm

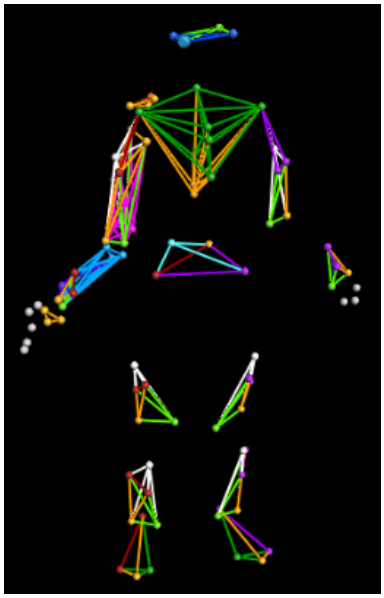

Figure 5.2 Static trial showing the marker model in nexus

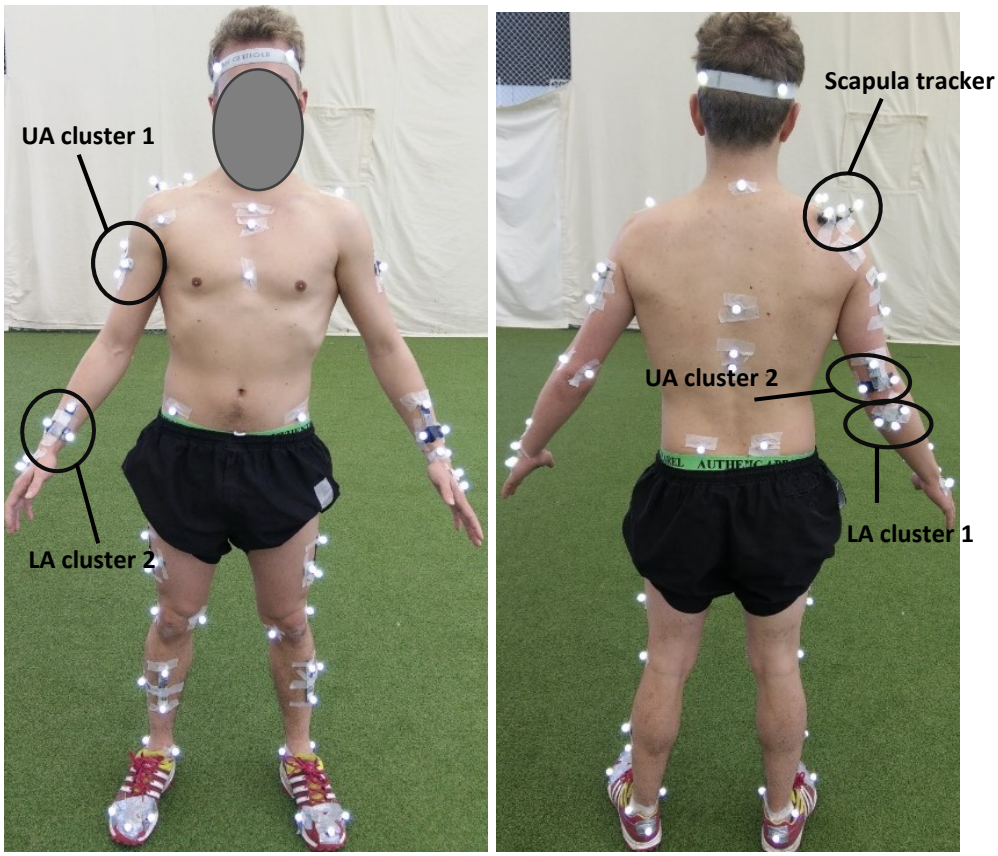

Figure 5.3 Image showing location of scapula, upper and lower arm clusters for a right hand bowler

5.2.4 Experimental protocol

The motion capture system was setup along a single training pitch, centred at the bowling crease and allowing for a 19-yard run up (Figure 5.4). Upon arrival, each bowler was asked to warm up after which two researchers would then attach the markers and clusters.

Figure 5.4 Cameras were setup centred at the bowling crease and allowed for normal run-up of bowlers.

Firstly, the following anatomical landmarks were digitised; sternoclavicular joint (SC), epicondyles of the humerus, ulna and radial styloid of the forearm on the bowling arm. This was done using a 5-marker T-shaped wand. A full description of the digitisation process is presented in Section 5.3.2. After digitisation of the landmarks on the bowling arm, markers were placed at these locations. These markers were used as backup in the case of marker occlusion. Next, a static trial was captured of the marker model with the subject standing, arms slightly elevated at the side and palms facing forward.

The scapula pose was digitised in two positions (Figure 5.9 b & c), first with the arm along the side of the body then with the arm elevated, at the top of the bowling arc, near ball release. Both calibration positions were used as inputs into the UKNSM (described in Chapter 6) while the

latter calibration position was used to recreate scapula kinematics during the dynamic trails. The use of digitised markers in dynamic trials is described in Section 5.3.2.

The next trial captured was used to find the subject's glenohumeral rotation centre (GHRC) (Figure 5.10a). The three anatomical landmarks of the scapula were palpated and the scapula locator (Johnson et al., 1993) was adjusted to meet these points. After demonstrating flexion/extension, abduction/adduction and internal/external rotation of the humerus to the subject, they were asked to sit on a stool in the centre of the capture volume and alternate among these rotations, keeping the elbow flexed at 90° and not exceeding 90° of humerus elevation. While this was done, the scapula locator was used to track the movement of the scapula. The duration of this trial was 25-30 seconds (Figure 5.10a).

The next two dynamic trials were conducted to determine the functional flexion/extension and pronation/supination axes of the elbow. Keeping the elbow joint steady, the subject performed 5 cycles of flexion/extension avoiding the terminal ranges and with the wrist in the neutral position. This was then followed by 5 cycles of pronation/supination with the elbow flexed at 90°. Throughout both trials the subject was asked to ensure the motion was smooth and at a constant velocity to allow accurate calculation of instantaneous helical axes (Section 5.3.4).

Lastly, the bowling trials were conducted. Bowlers were asked to bowl 12 deliveries (two overs) each, taking a break in between overs if necessary. One over consisted of their normal stock delivery while the second over was a variation from this stock delivery. Fast bowlers bowled six slower deliveries for their variation over while spin bowlers bowled six faster deliveries. Spin bowlers' stock delivery was either off spin or leg spin. After the markers were removed, the subjects were asked to fill out a questionnaire before they left (Figure 5.5).

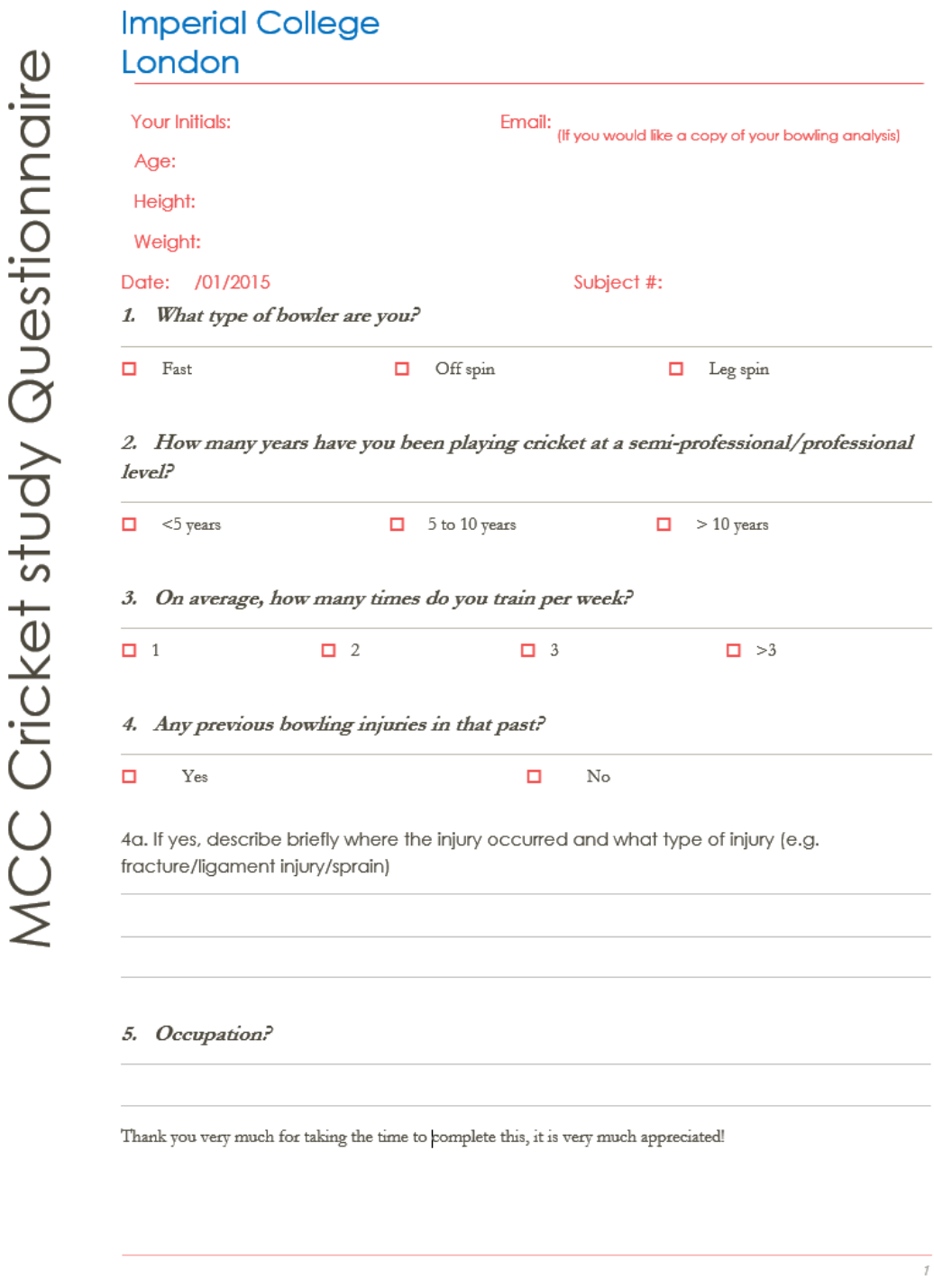

MCC Cricket study Questionnaire

Imperial College London

Your Initials: Email: (If you would like a copy of your bowling analysis)

Age:

Height:

Weight:

Date: /01/2015 Subject #:

1. *What type of bowler are you?*

☐ Fast ☐ Off spin ☐ Leg spin

2. *How many years have you been playing cricket at a semi-professional/professional level?*

☐ <5 years ☐ 5 to 10 years ☐ > 10 years

3. *On average, how many times do you train per week?*

☐ 1 ☐ 2 ☐ 3 ☐ >3

4. *Any previous bowling injuries in that past?*

☐ Yes ☐ No

4a. If yes, describe briefly where the injury occurred and what type of injury (e.g. fracture/ligament injury/sprain)

5. *Occupation?*

Thank you very much for taking the time to complete this, it is very much appreciated!

1

Figure 5.5 Questionnaire used to collect subject information

5.2.5 Hawk-eye system

The hawk-eye system was developed by Dr Paul Hawkins to track the ball in sports such as

tennis or cricket so that officials are provided with a quick and accurate system when making important decisions in real game situations. The system comprises six cameras placed around the field and incorporates both image analysis and radar technology to track the ball. In the case of cricket, it can track the ball's entire trajectory, from the point of release by the bowler until it reaches the batsman.

Due to limitations because of the proprietary nature of the system, the only data that was collected from the system was a PNG image showing the trajectory of each delivery viewed from the bowler's end (Figure 5.6) and the speed of each delivery. These images were then digitised using software (*GetData Graph Digitizer*) to identify the location the ball bounced relative to the middle stumps. The vertical and horizontal distances measured from the middle stump would indicate the line and length of each delivery (Figure 5.6).

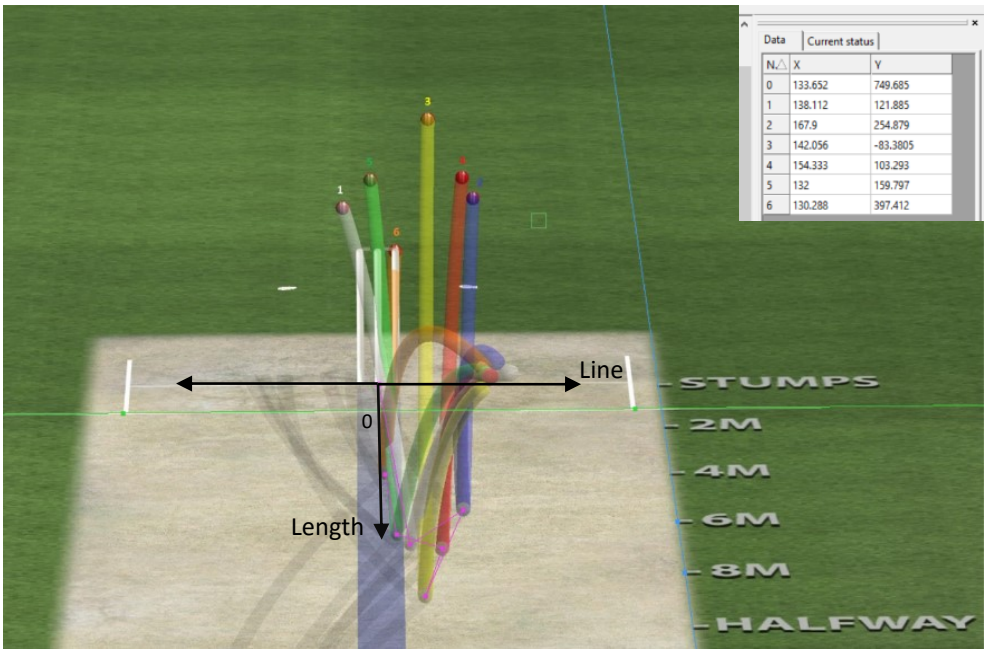

Figure 5.6 Hawkeye data showing trajectories and digitisations for one over of fast bowling

5.3 Development of the kinematic model for the upper limb

The rationale behind marker placement as well as the functional methods used in modelling is presented in this section. Anatomical landmarks for each segment were used to describe its anatomical coordinate frame following ISB standards (Wu et al., 2005). A full description of the anatomical frames of each segment and Euler sequences for each joint is given in Chapter 2. This is summarised in Table 5-2.

Scapulothoracic	YX'Z"
Glenohumeral joint	ZX'Y"
Humerothoracic	YX'Y"
Elbow	ZX'Y"
Hip	ZX'Y"
Thorax relative to pelvis	ZX'Y"
Knee	ZX'Y"
Ankle	ZX'Y"

Table 5-2 Euler sequences used

5.3.1 Soft tissue artefact and marker placement

One limitation of using markers attached to the skin is that they may move relative to the underlying bone causing errors in the pose estimation of the segment leading to underestimation or an overestimation of the actual bone movement (Meskers et al., 1998; Karduna et al., 2001). This error is known as soft tissue artefact (STA) (Cappozzo et al., 1996; Cutti et al., 2006) and while there exist methods that reduce the effect of the moving soft tissue on the markers, STA can never be totally removed. The errors due to STA have the same frequency content as the underlying bone making it impossible to remove using standard filtering techniques (Leardini et al., 2005). The effect of STA depends on the speed and nature of movement, physical characteristics of the individual, and marker placement (Cappello et al., 2005; Cappozzo et al., 1996; Cutti et al., 2005). Specifically for the upper arm, it was shown that markers or clusters used were greatly affected during humeral internal/external rotation (Cutti et al., 2005). Regardless of this, the use of skin fixed markers for capturing human movement has been shown to be suitable for fast dynamic movements (Lloyd et al., 2000a) when careful consideration is taken during marker placement.

Other than optimising placement of markers, techniques that have been investigated to minimise the effect of STA include adding joint constraints between segments (Cutti et al., 2008; Biryukova et al., 2000), double anatomical landmark calibration (Cappello et al., 1997) and the use of functional joint axes (Stokdijk et al., 1999).

Three markers attached to a rigid aluminium T-frame were used as technical clusters (Figure 5.3) to reduce STA (Cappozzo et al., 1996), where each cluster defines a technical frame on the segment. Clusters on the lower limbs and upper arm were placed so that two markers were parallel to the long bone of the segment avoiding the large muscles. The lower arm or forearm technical cluster was located just proximal to the wrist joint on the radius. This location was

also chosen since it was ideal for capturing pronation/supination rotation of the forearm (Chin et al., 2010; Anglin & Wyss, 2000). Additionally, two clusters were used proximal and distal to the elbow joint for both the lower and upper arm (Figure 5.3). Both of these clusters were used in calculating the glenohumeral joint centre and were shown to be better when digitising the humeral epicondyles for bowlers (Eftaxiopoulou, 2011). They could also be used as redundant markers in case of marker occlusion. Details of the placement of the scapula tracker are given in Chapter 4.

5.3.2 Digitisation method and post-processing

The digitisation or anatomical landmark calibration (Cappozzo et al., 1995) procedure is based on the concept that an anatomical point is palpated and its location defined using a 5 marker T-shaped wand or pointer. The position vector of this point is known since the distance of the tip to the origin of the wand coordinate frame is known (Figure 5.7). It is then transformed from the wand coordinate frame to the technical coordinate frame of the segment. The reason this is done is that there are large skin deformations observed at these anatomical landmarks, particularly at the elbow and wrist therefore, placement of markers at these locations is not recommended (Leardini et al., 2005; Cappozzo et al., 1995).

The point is considered digitised when its 3D position in the technical frame is known. From this information, the digitised point can then be replotted in the technical frame for each point in time in the dynamic trial (Cappozzo et al., 1995). This new point in the dynamic trial is then transformed to the global frame and is used to calculate the segment's anatomical frame. Details of this transformation are presented in Chapter 2.

The definition of the wand coordinate frame is shown in figure Figure 5.7.

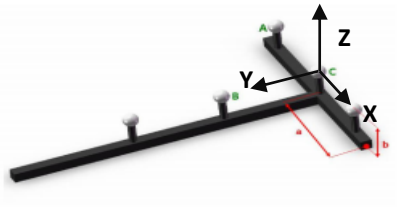

Origin	Marker C on the wand
X	Line pointing from C to A
Y	Line pointing from C to B
Z	Perpendicular to X and Y pointing upward

Figure 5.7 Coordinate frame of Wand (Shaheen, 2010)

Digitisation of the scapula position was also done using the same method where instead of using the wand, a scapula locator (Figure 5.8) is used. The three points on the locator were used to identify the acromion, inferior angle and root of the scapula spine. These points were then digitised relative to the scapula tracker and used in the definition of the scapula anatomical coordinate frame in dynamic trials.

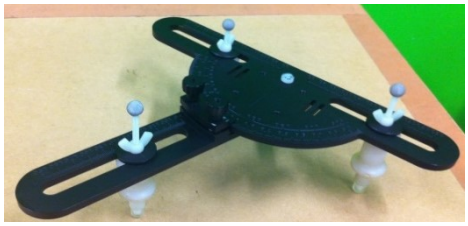

Figure 5.8 Scapula locator used to identify scapula landmarks

Due to time constraints, only the anatomical landmarks of the bowling arm were digitised using the wand. For the lower limbs and non-bowling arm, markers were placed at their anatomical landmark and using the static trial (Figure 5.2), their locations were digitised relative to the respective technical coordinate frame of the segment.

(a) (b) (c)

Figure 5.9 (a) digitisation of medial epicondyle on bowling upper arm, (b) scapula digitisation at rest, (c) scapula digitisation near ball release

5.3.3 Glenohumeral and hip joint centres

Chin et al. (2010) and Lloyd et al. (2000b) approximated the glenohumeral rotation centre (GHRC) in their cricket studies by placing two markers on the anterior and posterior aspect of

the humerus and a third marker on the acromion angle of the scapula. The GH centre was then approximated by a perpendicular bisector of the line joining the humeral markers. The validity of this method was assessed in a laboratory study using a simple marker setup and two subjects. The results showed that there was an average difference of 5° for FE between upper arm horizontal and ball release when comparing to a calculation using the GHRC using the spherical fitting method. The conclusion was that while this method offers a simple, quick way of identifying the GH centre, it would be highly susceptible to errors due to poor reproducibility since there were no guidelines in the literature on the exact placement of the markers.

The alternative method chosen was a least squares solution proposed by Gamage and Lasenby (2002) since it has been reported to perform better than other sphere-fitting functional methods (Lempereur et al., 2011; Camomilla et al., 2006). The GHRC was determined by considering the movement of three upper-arm technical markers relative to the scapula. The position vectors of these three markers in the scapula coordinate frame were assumed to be rotating about a fixed centre of rotation. Therefore, the three technical markers should lie on co-concentric spheres (Figure 5.10b). Upper arm cluster 2 was used in this calculation.

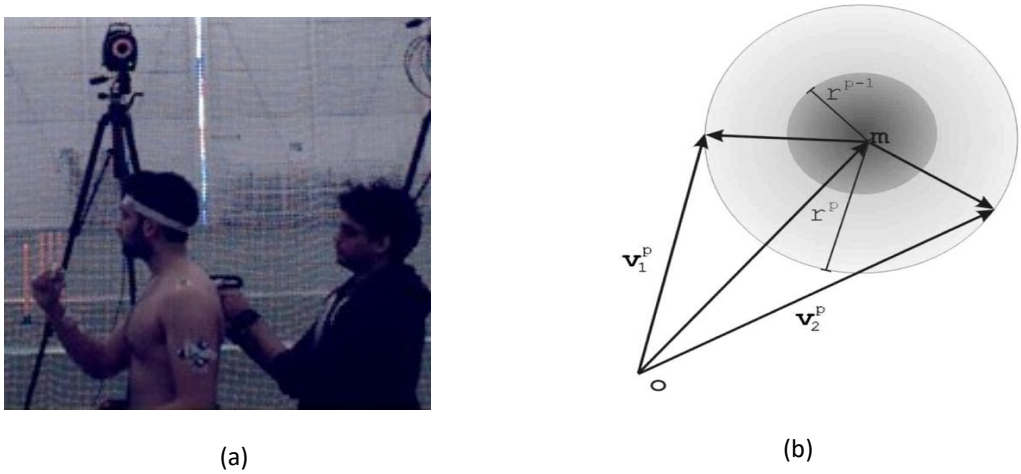

(a) (b)

Figure 5.10 (a) using the scapula locator while the subject performs the functional movement for calculating GHRC (b) the assumption of spherical marker movement for marker P. r^p is the radius of the P^{th} sphere (Gamage & Lasenby, 2002)

The following cost function was formulated for P markers and N time frame:

$$C = \sum_{p=1}^{P} \sum_{k=1}^{N} [\left(\boldsymbol{v}_k^p - \boldsymbol{m}\right)^2 - (r^p)^2]^2$$

Equation 5.1 cost function for estimating GHRC (Gamage & Lasenby, 2002)

Where $\boldsymbol{v}_k^p$ represents the *p*th vector in the *k*th time instance, $\boldsymbol{m}$ is the centre of rotation and r^p is the radius of the sphere for the *p*th vector. P in this case is equal to 3 and N is in the region of 9000 frames. To estimate r^p and $\boldsymbol{m}$ that minimize the cost function, the above equation is differentiated with respect to r^p, which can then be differentiated with respect to $\boldsymbol{m}$.

Algebraic manipulations then yield a solution in the following form.

$$\boldsymbol{m} = (A^{-1}) * \boldsymbol{b}$$

Equation 5.2 GHRC solution (Gamage & Lasenby, 2002)

Where A is a 3x3 matrix given by:

$$\mathrm{A} = 2 \sum_{p=1}^{P} \left[\left\{ \frac{1}{N} \sum_{k=1}^{N} \boldsymbol{v}_k^p \left(\boldsymbol{v}_k^p\right)^T \right\} - \overline{\boldsymbol{v}_k^p \left(\boldsymbol{v}_k^p\right)^T} \right]$$

Equation 5.3

$$\mathbf{b} = \sum_{p=1}^{P} \left[\overline{(\boldsymbol{v}^p)^3 - \boldsymbol{v}^p (\boldsymbol{v}^p)^2} \right]$$

Equation 5.4

Once the GHRC was determined for the bowling arm, it was calculated relative to the humerus technical coordinate frame for use in the dynamic trials. The GHRC for the non-bowling side was determined by first defining a vector from right side acromion marker RAC to the calculated GHJC in a thorax technical coordinate frame. This vector was then recreated relative the left side acromion marker and mirrored, to define the left side GHRC (Figure 5.11).

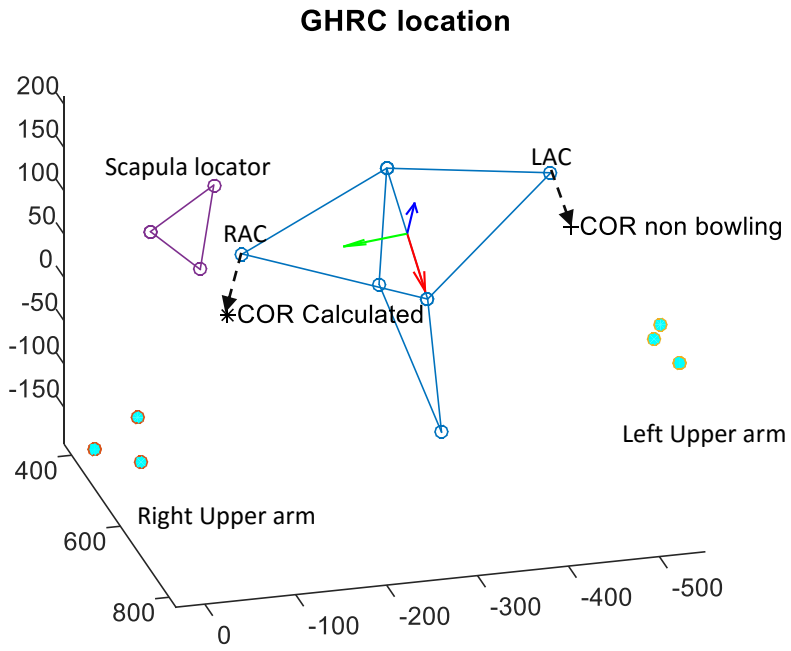

Figure 5.11 Anterior view of the thorax showing calculated GHRC (*) for a right arm bowler and approximated GHRC (+) on the left side.

The spherical fitting method was also used to calculate the rotation centre for the hip joint. In this case, the markers on the thigh cluster were assumed to lie on concentric spheres moving relative to the pelvis coordinate frame. This calculation was done for all 12 bowling trials and with the average values for both left and right sides being digitised relative to the left and right technical frames respectively (Appendix 2).

5.3.4 Instantaneous helical axis (IHA)

Helical axes were used to describe flexion/extension (FE) and pronation/supination (PS) at the elbow. Chin et al. (2010) showed that rotations about these functional axes more accurately describe movement occurring when compared to rotations about anatomical axes in cricket bowling. This is because flexion/extension of the elbow does not occur about the anatomical axis, which is defined as a vector between the humeral epicondyles. Therefore, use of the anatomical axis for measuring flexion/extension of the elbow would result in an underestimation or overestimation of the actual joint angle and part of the FE motion would be incorrectly registered as occurring about another axis when the Euler sequence decomposition was done. This is known as kinematic cross talk.

The functional FE axis of the elbow was found to deviate approximately 6° (±2.6°) from the anatomical axis (Chin et al., 2009; Duck et al., 2003). Similarly, the PS functional axis was found to pass through the radial head in a region near the lateral epicondyle of the humerus where it crosses the FE axis at an angle of 88.9° (±5.1°) (Veeger et al., 1997; Biryukova et al., 2000).

The instantaneous helical axis describes the angular velocity vector ω of a moving segment at a certain time (Figure 5.12). In this technique, a position vector and an orientation vector are defined. Movement is described in terms of a rotation about and a translation along a single axis called a helical or screw axis. One limitation of using this method is that it is highly dependent on experimental variability and the time increments chosen between axis calculation (Woltring et al., 1985).

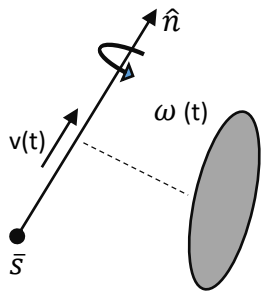

Figure 5.12 Instantaneous helical axis (Woltring et al., 1985)

In calculating the IHA for the elbow, the rotation matrices (R) of the elbow between a predefine number of frames intervals (t) were calculated throughout the trial. This angular interval was denoted by ϕ. Then using numerical differentiation, the linear velocity of the forearm markers were calculated. Each IHA was calculated in a least squares sense and described by a position vector ($\bar{s}$) and unit direction vector $\hat{n}$. The number of IHA's calculated per trial is dependent on the interval (t) chosen.

The angular velocity (ω), IHA vector ($\hat{n}$), the translation speed along the axis (v) and the pivot point ($\bar{s}$) are calculated based on algorithms created by Woltring et al. (1985).

$$\omega = \sqrt{\bar{\omega}^T \cdot \bar{\omega}} \qquad \text{Equation 5.5}$$

$$\hat{n} = \frac{\overline{\omega}}{\omega} \quad \text{Equation 5.6}$$

$$v = \dot{s}^T \cdot \hat{n} \quad \text{Equation 5.7}$$

$$\bar{s} = s + \frac{\overline{\omega} \cdot \dot{s}^T}{\omega^2} \quad \text{Equation 5.8}$$

Since $\hat{n}$ is extremely sensitive to disturbances if ϕ is small (Veldpaus et al., 1988), a trial and error process was used to determine an appropriate value for 't' as it is directly related to the rotation interval, ϕ. Small angular velocities associated at the terminal range of the movement where the segment decelerates to zero velocity and accelerates in the opposite direction, can lead to inaccurate calculations and cause outliers (Stokdijk et al., 1999). To exclude these outliers, the maximum angular velocity (ω_m) of all the IHAs were calculated and then a limit (ω_c) was calculated using the following equation.

$$\omega_c = \mathrm{k}\,\omega_m \quad \text{where, } 0 < \mathrm{k} < 1 \quad \text{Equation 5.9}$$

Therefore, only IHA with an angular velocity greater than or equal to ω_c were accepted. k was between 0.4 and 0.6 for the trials calculated as this range represented the best outlier rejection.

Finally, an optimal IHA $\hat{n}_{opt}$, as well as an optimal pivot point $s_{opt,}$ (and their respective error estimations $\hat{n}_e$ & s_e) were determined in a least squared sense by the following equations:

$$\bar{s}_{opt} = Q^{-1} \cdot \frac{1}{N} \sum_{i=1}^{N} Q_i \cdot \bar{s}_i \quad \text{Equation 5.10}$$

$$Q = \frac{1}{N} \sum_{i=1}^{N} Q_i \quad \text{Equation 5.11}$$

$$Q_i = I - n_i \cdot n_i^T \quad \text{Equation 5.12}$$

$$s_e = \frac{1}{N}\sum_{i=1}^{N} norm(s_{opt} - s_i) \qquad \text{Equation 5.13}$$

$$\hat{n}_e = \frac{1}{N}\sum_{i=1}^{N} \text{acos}(n_{opt} \cdot n_i)^T \qquad \text{Equation 5.14}$$

A pilot study with three bowlers was conducted in the motion laboratory at Imperial College London to calculate the functional flexion/extension and pronation/supination of the elbow joint and its feasibility for use in the kinematic model for bowlers. Eight bowling trials were captured for each bowler. A simple marker setup with clusters present on the upper and lower arm was used. The FE and PS trials captured were as described in Section 5.2.4. The results are as shown in Figure 5.13 and Figure 5.14 .

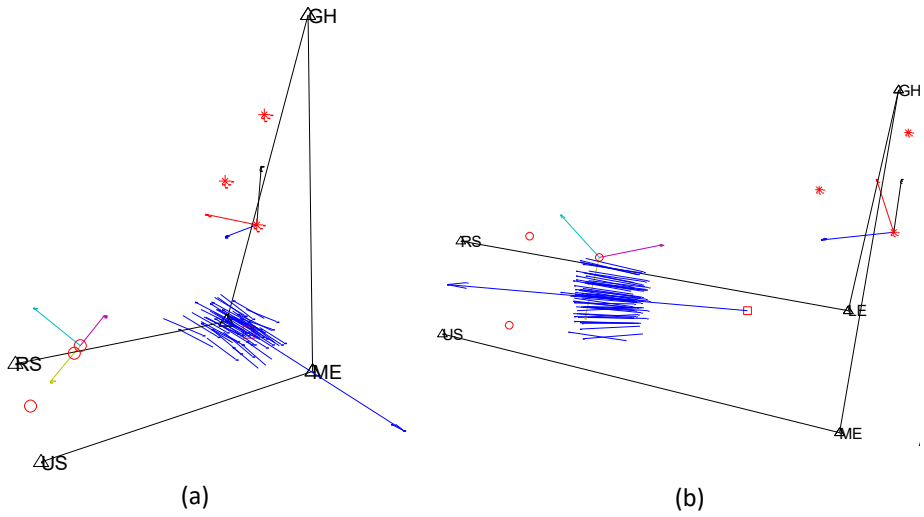

Figure 5.13 Elbow IHA calculation showing functional axis for (a) FE and (b) PS. Shorter blue vectors are the IHA calculated while the optimal axis and pivot point is shown as a red box and long blue arrow respectively. Anatomical landmarks of GH, ME, LE, US & RS are also shown.

The functional axes calculated are in agreement with literature (Chin et al., 2010). Elbow kinematics were calculated using the functional and anatomical axes and comparisons were made. For the functional axes, FE angles were determined using the position of **Forearm1** relative to **Humerus1** using sequence ZX'Y''. Pronation-supination was calculated using the

position of **Forearm3** relative to **Forearm2** using the sequence YX'Z''. Table 5-4 shows the anatomical and functional coordinate frames used.

	Elbow FE	Elbow PS
Pivot point error, S_e (cm)	1.66	12.10
Mean helical axis error, N_e (°)	1.57	1.55
Number of IHA calculated	30	286
Angle between mean helical axis and anatomical axis (°), (std)	4.33 (1.03)	89.9(2.14)

Table 5-3 Summary of calculated optimal IHA for FE and PS

Segment	Calculation of coordinate frame
Humerus Anatomical	Origin: midpoint (EC) between ME and LE. Y: unit vector from EC to GHRC (superior positive) X: cross-product of Y-axis and unit vector from LE to ME (anterior positive) Z: orthogonal to X-Y plane (positive left to right)
Humerus 1 Functional	Origin: pivot point of F-E Helical axis. Z: F-E helical axis (positive in lateral direction) X: cross-product of the unit vector from EC to GHRC and Z axis Y: orthogonal to X-Z plane (superior positive)
Forearm Anatomical	Origin : Wrist joint centre (WC) Y: Unit vector from WC to EC (superior positive) X: cross-product between Y-axis and unit vector from US to RS (anterior positive) Z: orthogonal to X-Y plane (positive right)
Forearm 1 Functional	Origin: Wrist joint centre (WC) Z: mean F-E helical axis X: cross-product of the unit vector from WC to EC and Z axis Y: orthogonal to X-Z plane (superior positive).
Forearm 2 Functional	Origin: Wrist joint centre (WC) Y: mean P-S helical axis (superior positive) X: cross-product of Y-axis and F-E helical axis (anterior positive) Z: orthogonal to X-Y plane (superior positive).
Forearm 3 Functional	Origin: Wrist joint centre (WC) Y: mean P-S helical axis (superior positive) X: cross-product Y-axis and unit vector from US to RS (positive to right) Z: orthogonal to X-Y plane (superior positive).

Table 5-4 Upper arm and forearm anatomical and functional coordinate frames

The eight bowling trials were used to determine the average and standard deviation. The averaged elbow rotations are plotted with respect to frames, where one frame is equivalent to 0.005 seconds. Positive rotations were assigned as flexion, adduction and pronation. The zero mark for each rotation occurs when the forearm is aligned with the upper arm in the anatomical position. In other words, when the forearm is fully extended and supinated.

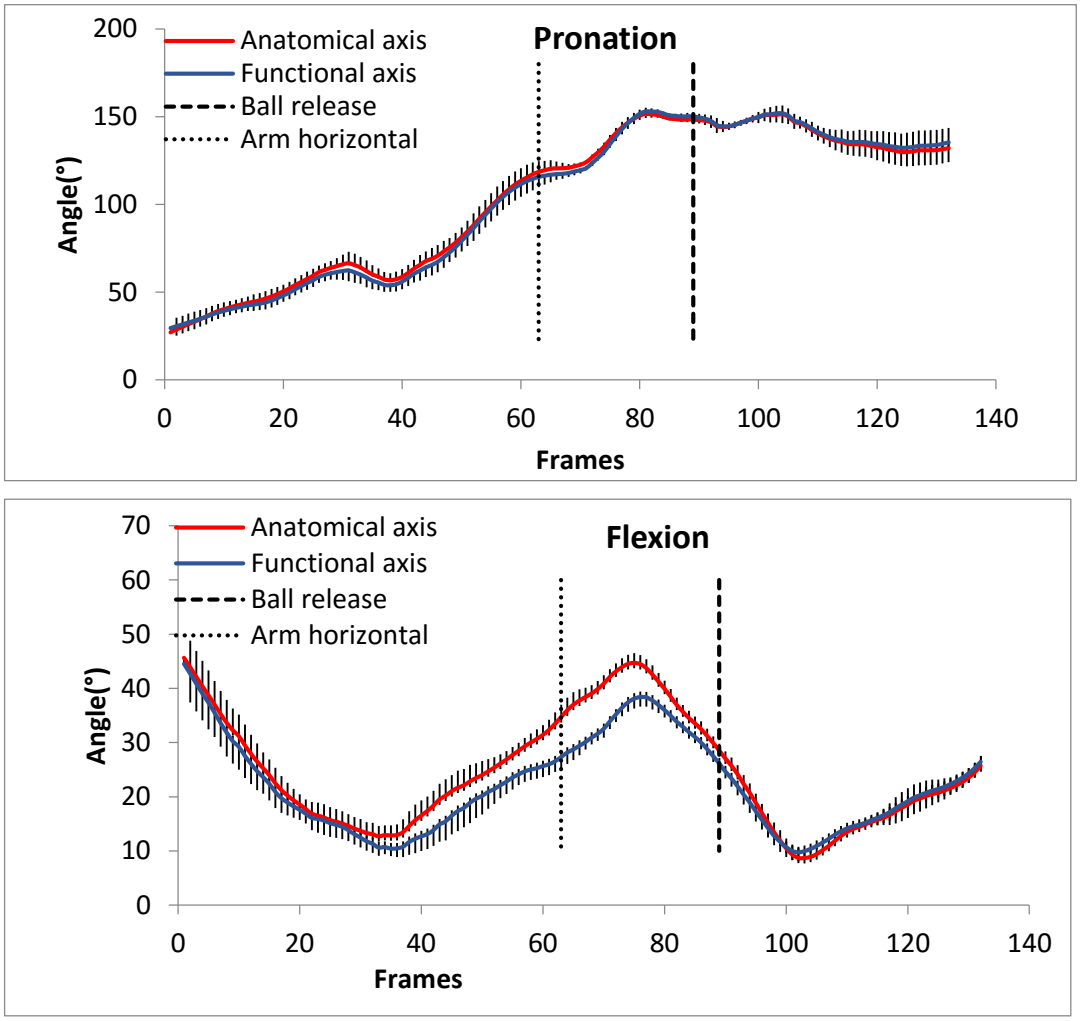

Figure 5.14 Elbow kinematics using anatomical and functional coordinate frames for a leg spin bowler

The use of the functional axis at the elbow showed that it made a difference in measuring elbow kinematics, if not at least similar to the anatomical axis method. The conclusion was that the functional axis method would be used to calculate elbow kinematics in bowlers.

5.3.5 Calculation of rotation matrices

Joint rotations were calculated using the method given by Soderkvist and Wedin (1993) where the numerical solution involves least-squares minimisation to ensure that measured data of markers from one position to another conforms to the rigid body assumption. This is done by solving the following two least-squares problems.

$$b_i = Ra_i + t \qquad \text{Equation 5.15}$$

$$min \sum_{i=1}^{m} \|Ra_i + t - b_i\|^2 \qquad \text{Equation 5.16}$$

Where, R is rotation matrix and is constrained to be orthogonal, a_i & b_i are the i^{th} marker coordinates in two positions, t is the translation vector relative to the global frame and m is the number of markers.

5.3.6 Solidification

For instances where there were significant marker occlusions and an occluded marker's trajectory could not be correctly predicted in nexus, the solidification procedure developed by Chèze et al. (1995) was used. The first step was to define a mean rigid shape for a cluster of markers that best represents the marker configuration with minimal errors due to STA or occlusion. Therefore, it was calculated from the static trial. Then the mean rigid shape was registered onto the cluster in the dynamic trial where a least-squares minimisation was used to replace the measured markers in the dynamic trial with those of the mean rigid shape. The method was also used to compensate for skin movement where it was reported to reduce kinematic errors by 20-25% when the maximum distances between markers was less than 15cm (Chèze et al., 1995).

This method was used for the scapula tracker cluster where there were four markers. The mean shape was calculated by first finding the angles between each vertex of every possible triangle that make up the cluster. Then the standard deviations for these angles are summed and the triangle with the least standard deviation indicates the best three markers, from which the mean rigid shape is calculated.

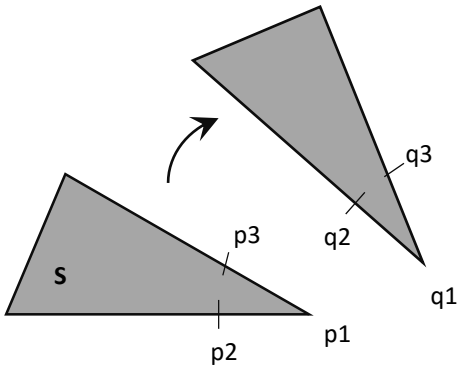

Figure 5.15 Mapping mean rigid shape (s) to measured shape in dynamic trial.

A similar calculation was done in the dynamic trial where the least deformed triangle from the measured markers found by comparing its vertices to that of the mean shape. Then the least deformed vertex of this triangle was used to define three points (q_1, q_2 & q_3); one defined at the vertex and two are a unit distance away, lying on the two adjacent sides of the vertex(Figure 5.15). Using these three points and the corresponding points on the mean shape, a transformation matrix was calculated in a least-squares sense (Soderkvist & Wedin, 1993). This was then used to transform all the markers that make up the mean rigid shape to the measured one in the dynamic trial.

5.3.7 Normalisation, interpolation and smoothing

Due to limitations imposed during the motion capture process where the capture volume was big enough to capture only part of the bowling action as well as time constraints involved in running the mathematical model for the entirety of the bowling action, a new, shorter definition of the bowling phases is used in this thesis (Figure 5.16). This includes the following key points in time within the bowling action:

1. When the upper arm is vertical (UAV) in the global frame
2. When the upper arm is horizontal (UAH) in the global frame
3. Ball release (BR)
4. When the upper arm returns to the vertical position culminating in a complete cycle

Other identifiers within the bowling action are back foot contact (BFC) and front foot contact (FFC) describing when the back and front foot is planted on the ground during the delivery phase. Identification of these points in the action was done in *Vicon nexus 1.8.5* (Vicon, Oxford,

UK) where video images were used to define these events. UAV was identified when the upper arm was horizontal in the global frame while BR occurred at the first frame the ball is not in contact with any part of the hand (Marshall & Ferdinands, 2003).

Kinematic curves were normalised based on the phase upper arm horizontal to ball release (0-100%). This phase was chosen, since it comprises the range where the risk of impingement is said to be greater and the range used to assess the legitimacy of a delivery. Kinematic data presented are plotted with additional data on either side of the 0-100% bowling motion. This represents approximately when the upper arm starts and ends near a vertical position relative to the global frame and varied for each bowler depending on how much of the pre and post-delivery action was captured.

A fourth order Butterworth filter was used to smooth the trajectories of each marker. The cut-off frequency of 15Hz was determined from a Fast Fourier Transform in Matlab 8.6 (The Mathworks Inc, Natick, USA). In addition, a cubic spline interpolation function was used to reduce each trial length to the same number of points in order to calculate the average curve and standard deviation at each point. Averages and standard deviations were calculated across six trials for each delivery type.

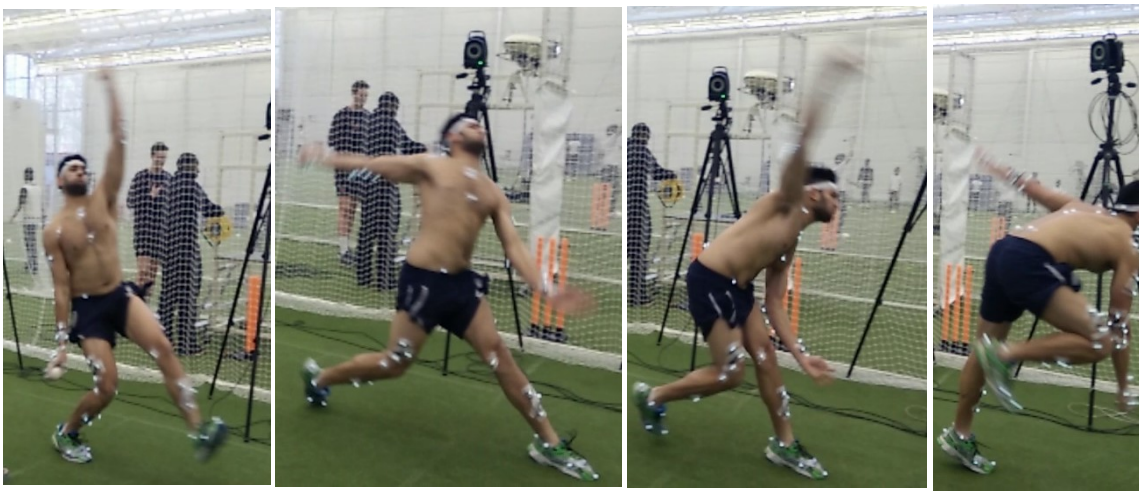

Figure 5.16 A key points in the bowling action cycle. 1-4 showing upper arm vertical, upper arm horizontal, ball release and finishing in upper arm vertical

5.3.8 Statistics

The coefficient of multiple correlation (CMC) (Kadaba et al., 1989) was used to measure the similarity between the kinematic waveforms calculated. This statistical measure has been used for scapula kinematics where its value ranges from 0 to 1 indicating dissimilar to similar waveforms respectively (Amasay & Karduna, 2009). The within-day variant of this calculation was used in this thesis and is as follows:

$$CMC = \sqrt{1 - \frac{\sum_{s=1}^{S}\sum_{i=1}^{W}\sum_{j=1}^{N}(Y_{sij} - \bar{Y}_{sj})^2 / SN(W-1)}{\sum_{s=1}^{S}\sum_{i=1}^{W}\sum_{j=1}^{N}(Y_{sij} - \bar{Y}_{s})^2 / S(NW-1)}} \qquad \text{Equation 5.17}$$

Where S is the number of the sessions, W is the number of waveforms used to calculate the average joint angle $\bar{Y}_s$, N is the number of points or frames that makeup the waveform, Y_{sij} is the joint angle at time j and $\bar{Y}_s$ is the total average joint angle. The CMC values were used to evaluate the repeatability kinematic data over six trials while a second CMC formulation (Ferrari et al., 2010) was used to measure similarity between waveforms acquired by different methods: scapula tracker and regression.

Interpretation of the CMC values follows the same levels of similarity or repeatability as described by Garofalo et al. (2009). These are; 0.65<CMC<0.75 are moderate, 0.75<CMC<0.85 are good, 0.85<CMC<0.95 are very good and 0.95<CMC<1 is excellent.

Two-way repeated measures ANOVA was used to test for significant differences in scapulothoracic range of motion. The two independent variables were phase of action (three levels: back foot contact to upper arm horizontal, upper arm horizontal to ball release and ball release to the end of captured motion) and over (two levels: stock and variation). Where significance was found, paired sample t-tests were used post hoc. A paired sample t-test was also used to test of significant differences in technique parameters between overs. The significance level was set at $p<0.05$ for all statistical test in this thesis. ANOVA and t-test were done in SPSS (v22, Chicago, USA).

5.3.9 Regression predicted scapula kinematics

Measured kinematics from the scapula tracker is presented and compared to two sets of regression equations. The set first regression equation (regression 1) used was developed from

the scapula study presented in Chapter 4 however, given the small sample size used, a more established set of equations used to predict scapula rotations was also chosen (regression 2). This was taken from the original UKNSM (Charlton & Johnson, 2006) which was developed based on scapula palpation experiments where scapula rotations are predicted using humerothoracic plane of elevation (PoE), elevation and internal/external rotation.

Average humerothoracic kinematics for each subject was used as the dependant variable in the regression equations. The predicted scapulothoracic rotations were then compared to the measured scapula kinematics for each subject using the new CMC formulation. The RMS difference between the methods and across subjects were calculated to give an indication of how closely to predicted kinematics were to the measured values.

5.4 Results

Fast and slow bowlers were analysed separately and given the smaller number of slow bowlers, the limited power of statistical test on such a small sample is acknowledged. General comparisons are made highlighting key differences in technique. Details of the eleven fast bowlers and four slow bowlers are presented in Table 5-5 and Table 5-6.

Bowler	Age	Height (m)	Weight(kg)	Training days per week	Bowler type
f1	23	1.78	72	3	Right arm fast
f2	19	1.83	65	3	Right arm fast
f3	22	1.85	84	2	Right arm fast
f4	19	1.88	83	>3	Right arm fast
f5	20	1.83	88	2	Right arm fast
f6	20	1.77	70	2	Right arm fast
f7	20	1.93	90	1	Left arm fast
f8	29	1.8	85	2	Right arm fast
f9	29	1.85	86	1 (summer only)	Right arm fast
f10	25	1.8	68	1	Right arm fast
f11	27	1.87	95	1	Right arm fast
s1	22	1.78	62	2	Left arm Off-spin
s2	20	1.73	64	>3	Right arm Off-spin
s3	34	1.84	108	3	Right arm Leg-spin
s4	25	1.75	72	1	Right arm Leg-spin

Table 5-5 Fast and slow bowlers included in the study

Kinematic data are presented in the following way: firstly, humerothoracic and scapulothoracic

rotations are presented. Then the use of regression equations to improve measured scapula kinematic data is assessed. Finally, bowling technique parameters are presented for all bowlers and their stock and variation overs. Kinematic data are presented graphically without standard deviations for clarity. Full details with standard deviations are shown in Appendix 1.

Bowler	Stock over	Variation over	Level of play*
f1	Normal fast delivery	Slower ball	University
f2	Normal fast delivery	Slower ball	University
f3	Normal fast delivery	Slower ball	University
f4	Normal fast delivery	-	University
f5	Normal fast delivery	Slower ball	University
f6	Normal fast delivery	Slower ball	Amateur
f7	Normal fast delivery	Slower ball	Amateur
f8	Normal fast delivery	Slower ball	Amateur
f9	Normal fast delivery	Slower ball	Amateur
f10	Normal fast delivery	-	Amateur
f11	Normal fast delivery	-	Amateur
s1	Off spin	Faster ball	University
s2	Off spin	Faster ball	University
s3	Leg spin	Faster ball	University
s4	Leg spin	Faster ball	Amateur

Table 5-6 Details of bowlers and who were able to bowl a variation. * University level of play indicates bowlers competed at a university level or higher.

5.4.1 Humerothoracic and scapulothoracic kinematics

5.4.1.a Fast bowlers

The CMC values for humerothoracic rotations for fast bowlers show a very good correlation with values above 0.91 except for one subject who had a good correlation with a value of 0.84 for axial rotations in their variation over (Table 5-7). Therefore, it was considered appropriate to use the mean data in further analysis.

	plane of elevation		elevation		axial rotation	
	stock	variation	stock	variation	stock	variation
f1	0.99	0.99	0.99	0.99	0.99	0.99
f2	0.99	1.00	0.95	0.99	0.91	0.98
f3	1.00	0.99	0.99	0.99	0.99	0.99
f4	1.00	-	0.98	-	0.97	-
f5	0.99	0.99	0.99	0.95	0.98	0.96
f6	1.00	0.99	0.99	0.98	0.95	0.96
f7	0.99	0.99	0.95	0.97	0.97	0.98
f8	0.99	1.00	0.98	0.99	0.94	0.97
f9	1.00	0.99	0.98	0.97	0.95	0.84
f10	1.00	-	0.97	-	0.90	-
f11	1.00	-	0.98	-	0.96	-

Table 5-7 Fast bowlers' within-subject CMC values for humerothoracic rotations across the six trials for each over

Figure 5.17 and Figure 5.18 shows the humerothoracic kinematics for fast bowlers. Humerothoracic elevation at ball release was between 98°-139° with an externally rotated arm ranging from 29°-100°. The trend shown by the graphs illustrate the varying levels of external rotation as the arm rotates to ball release which was then followed by internal rotation of the humerus. The inter-subjects correlation for the three rotations were 0.71, 0.94 and 0.56 for the stock over and 0.64, 0.91 and 0.62 for the variation over.

Comparing kinematic waveforms for both overs showed and excellent repeatability, with values of 0.99, 1 and 0.96 for the three humerothoracic rotations.

(a)

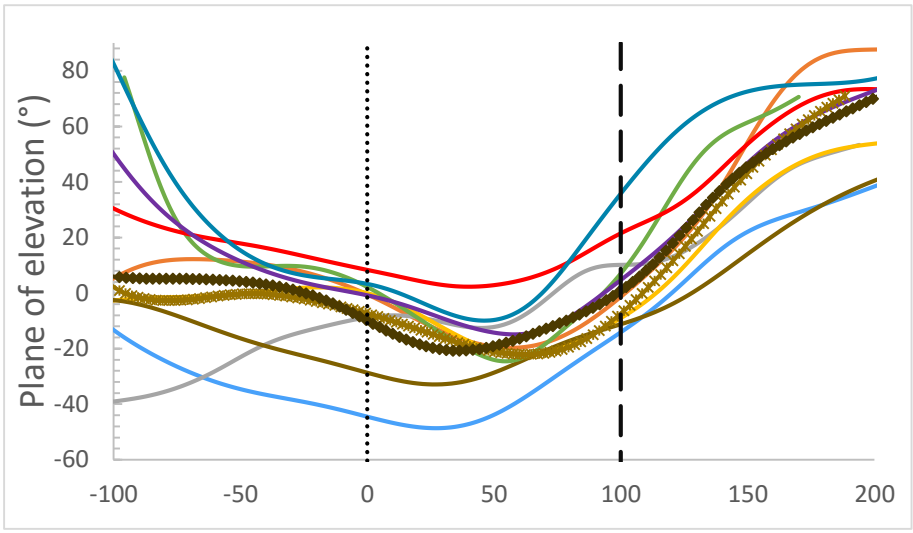

(b)

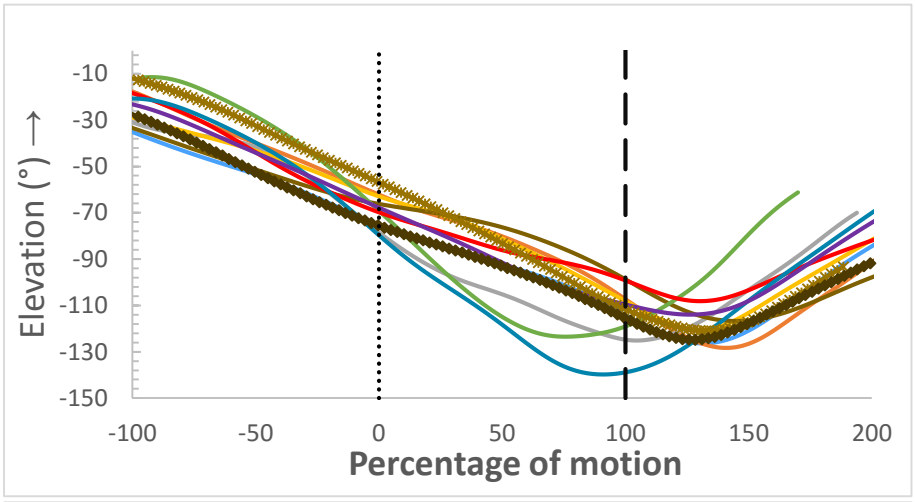

(c)

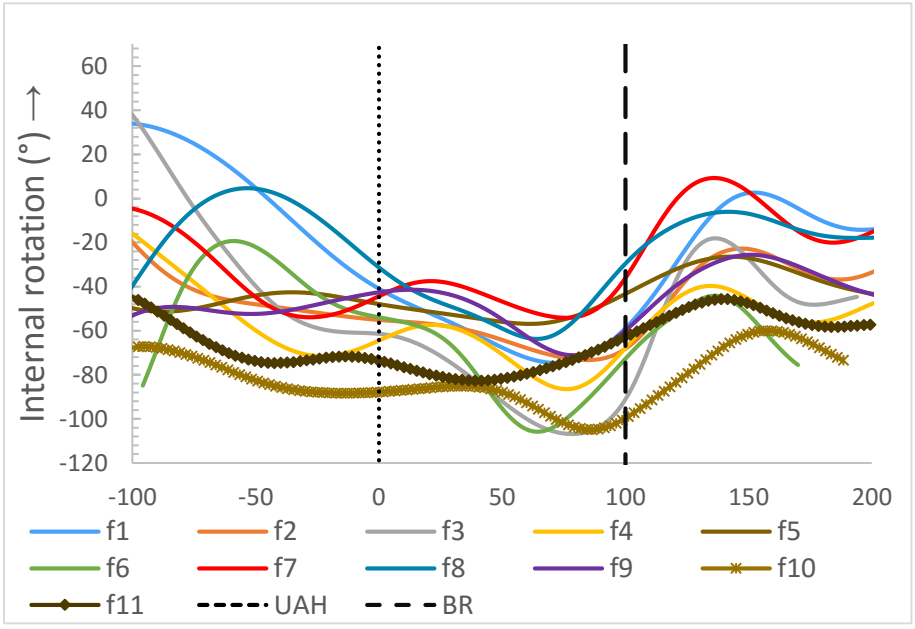

Figure 5.17 Mean humerothoracic kinematics for fast bowlers, stock over. (a) Plane of elevation (b) elevation/depression (c) internal/external rotations. UAH- upper arm horizontal, BR-ball release.

(a)

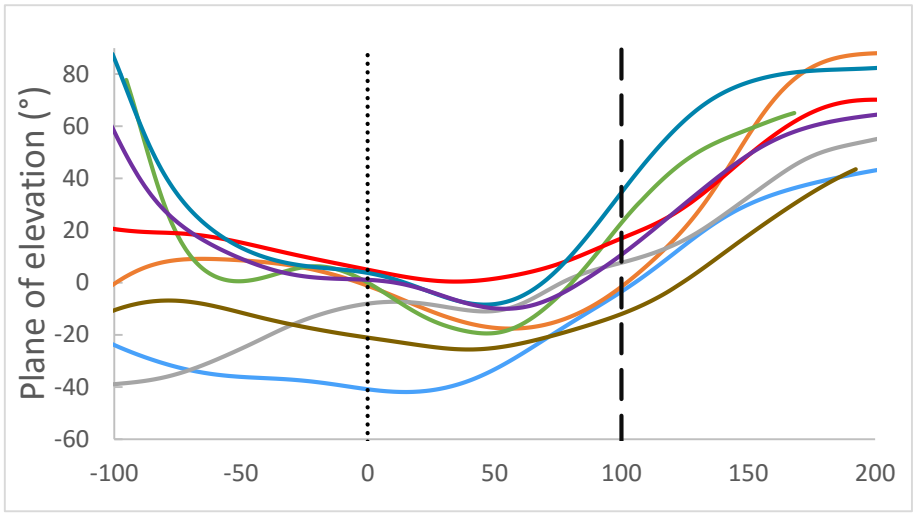

(b)

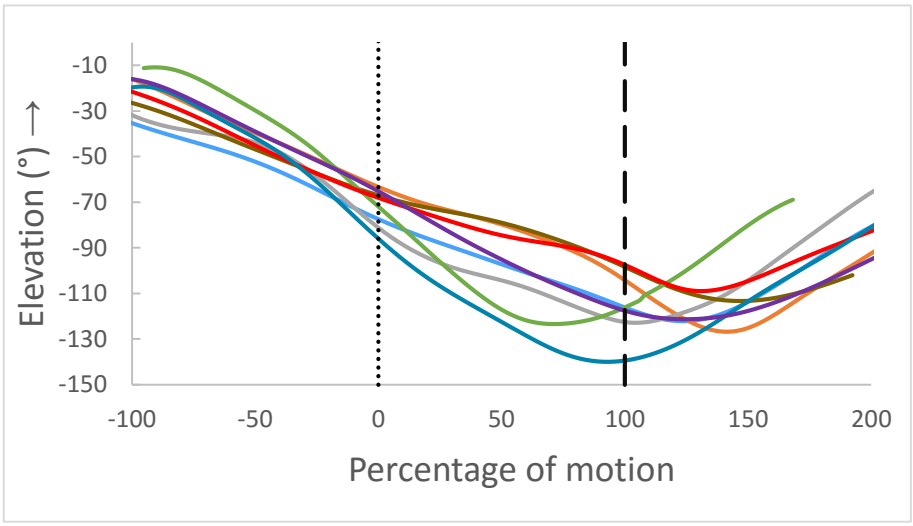

(c)

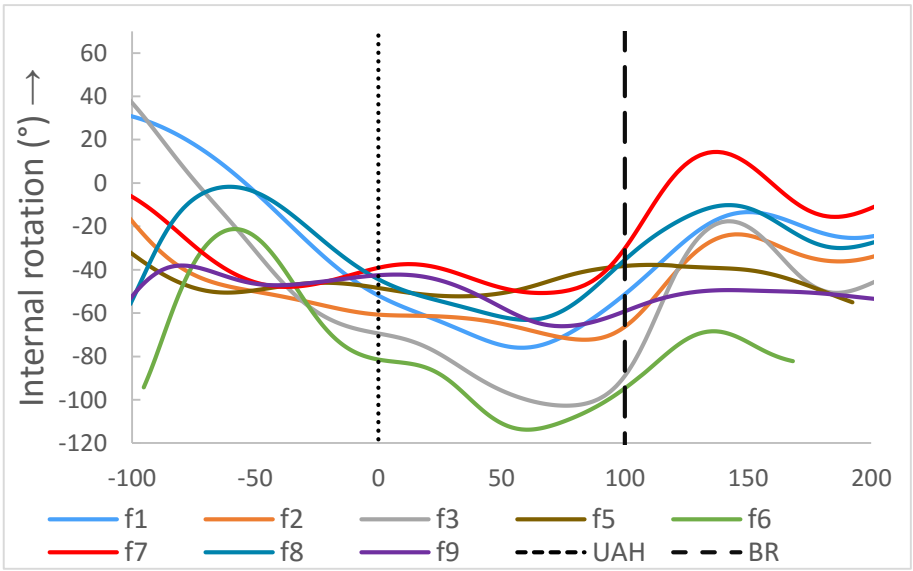

Figure 5.18 Mean humerothoracic kinematics for fast bowlers, variation over. (a) Plane of elevation (b) elevation/depression (c) internal/external rotations. UAH- upper arm horizontal, BR-ball release.

Waveform similarities were excellent with the exception of subject f1and posterior/anterior tilt for subject f9's variation over (Table 5-8). This poor repeatability is also confirmed when looking at the standard deviations for these specific curves (Appendix 1).

	internal/external		**up/down**		**posterior/anterior**	
	stock	variation	stock	variation	stock	variation
f1	0.76	0.69	0.93	0.50	0.33	0.00
f2	0.97	0.98	0.98	0.98	0.90	0.91
f3	0.99	0.96	0.99	0.99	0.98	0.97
f4	0.97	-	0.99	-	0.98	-
f5	0.98	0.97	0.96	0.96	0.95	0.94
f6	0.99	0.98	1.00	0.97	0.98	0.95
f7	0.99	0.99	0.97	0.98	0.91	0.95
f8	0.98	0.99	0.99	0.99	0.91	0.98
f9	0.97	0.98	0.96	0.96	0.96	0.86
f10	0.99	-	1.00	-	0.93	-
f11	0.99	-	0.98	-	0.95	-

Table 5-8 Fast bowlers' within-subject CMC values for scapulothoracic rotations across the six trials for each over

Figure 5.19 and Figure 5.20 show the scapulothoracic kinematics for stock and variation overs respectively. The inter subject correlation for the three scapulothoracic rotations were 0.64, 0.71 and 0.62 for the stock over and 0.82, 0.64 and 0.54 for the variation over. This indicates a poor to good correlation between the measured waveforms.

Comparing kinematic waveforms for both overs showed an excellent repeatability, with values of 0.98, 0.98 and 0.98 for the three scapulothoracic rotations.

(a)

(b)

(c)

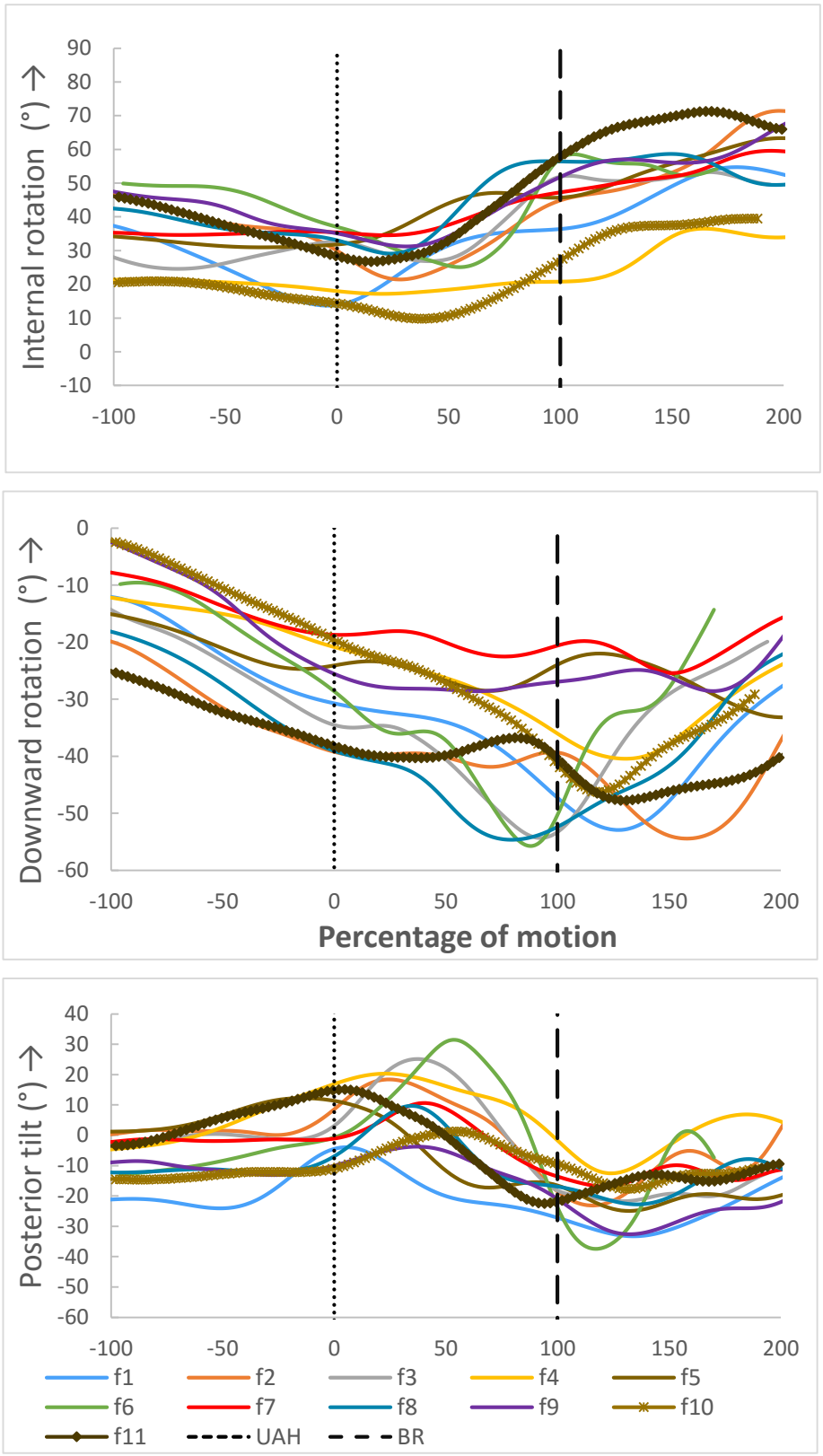

Figure 5.19 Mean measured scapulothoracic kinematics for fast bowlers, stock over.
(a) internal/external (b) up/downward (c) posterior/anterior rotations. UAH- upper arm horizontal, BR- ball release.

(a)

(b)

(c)

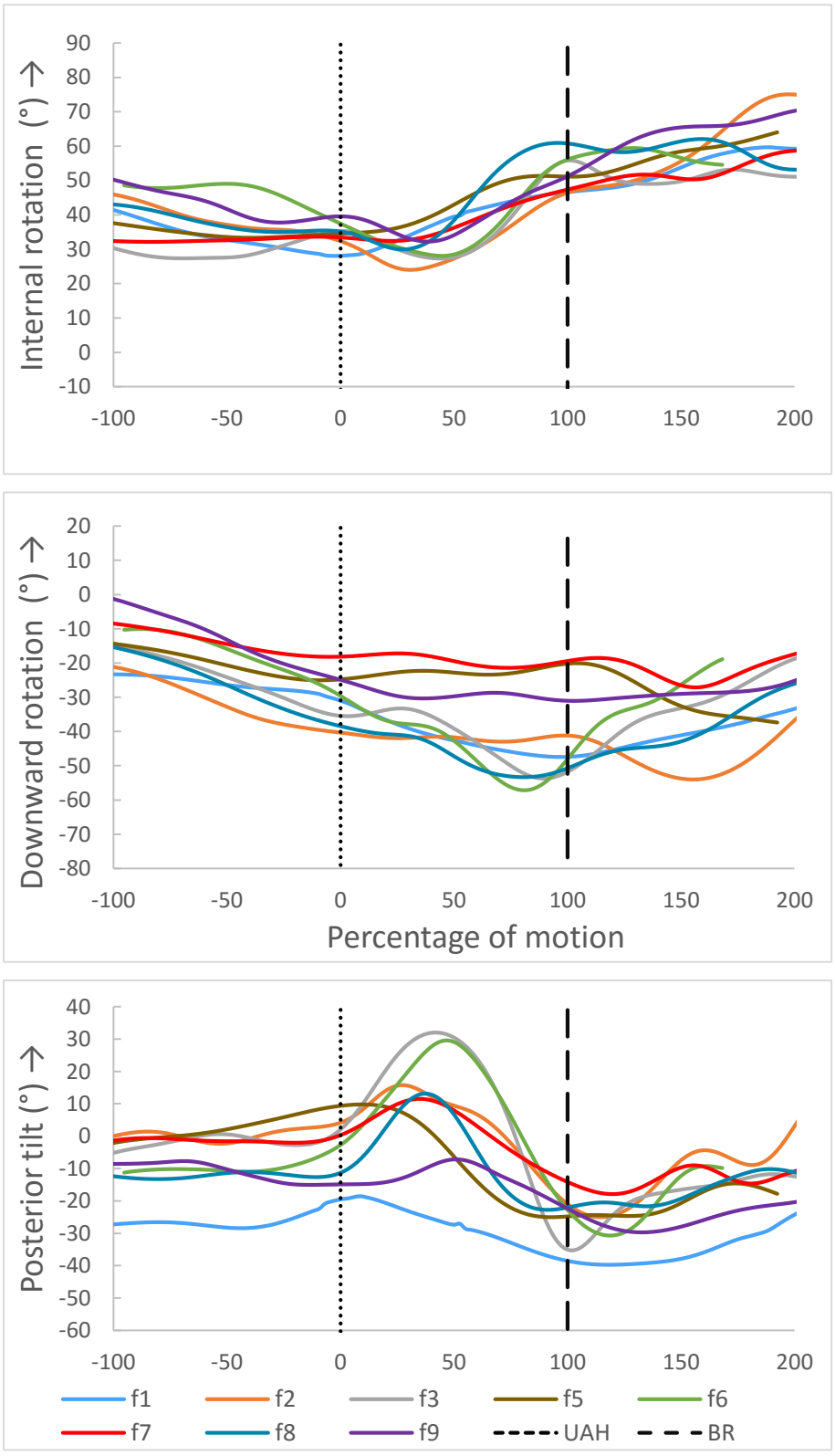

Figure 5.20 Mean measured scapulothoracic kinematics for fast bowlers, variation over. (a) internal/external (b) up/downward (c) posterior/anterior rotations. UAH- upper arm horizontal, BR-ball release.

5.4.1.b Slow bowlers

Given the inherent differences in bowling technique between off-spin and leg-spin bowlers, subject s1 and s2 were separated from s3 and s4 when considering inter-subject repeatability.

The CMC values generally show a very good to excellent correlation for humerothoracic rotations in slow bowlers (Table 5-9). Subject s4 was found to be the exception for axial rotation in their variation over.

	plane of elevation		**elevation**		**axial rotation**	
	stock	variation	stock	variation	stock	variation
s1	0.98	0.99	0.93	0.93	0.97	0.97
s2	0.98	0.99	0.94	0.99	0.93	0.89
s3	1.00	0.99	0.99	0.99	0.97	0.93
s4	0.99	0.98	0.98	0.97	0.80	0.65

Table 5-9 Slow bowlers' within-subject CMC values for humerothoracic rotations across the six trials for each over

The inter subject correlation for plane of elevation and axial rotation were moderate to poor with values of 0.65 and 0.28 respectively for their stock over. These values were reduced to 0.28 and 0.14 for their variation over. Values of 0.78 and 0.86 were calculated for humerothoracic elevation for stock and variation overs respectively.

Figure 5.21 and Figure 5.22 show the humerothoracic waveforms for slow bowlers' stock and variation overs respectively.

Comparing kinematic waveforms for both overs showed an excellent repeatability, with values of 0.99, 0.99 and 0.92 for the three humerothoracic rotations.

(a)

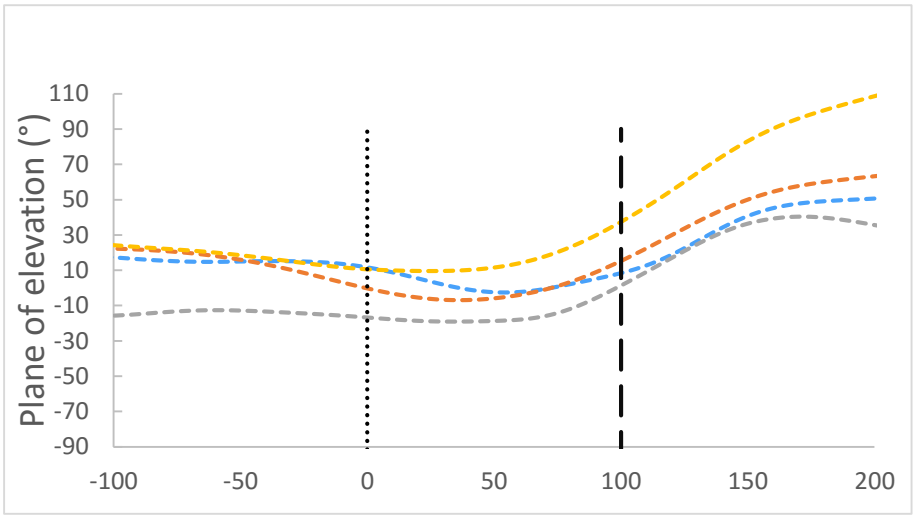

(b)

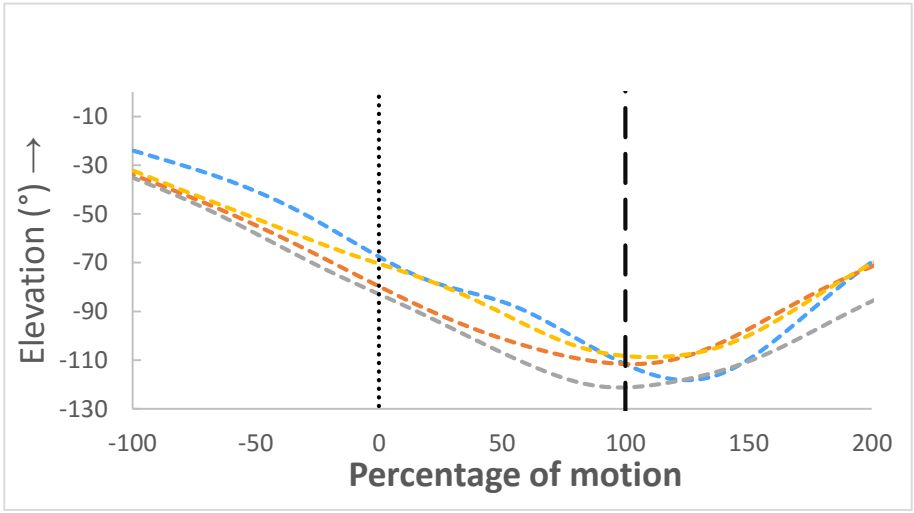

(c)

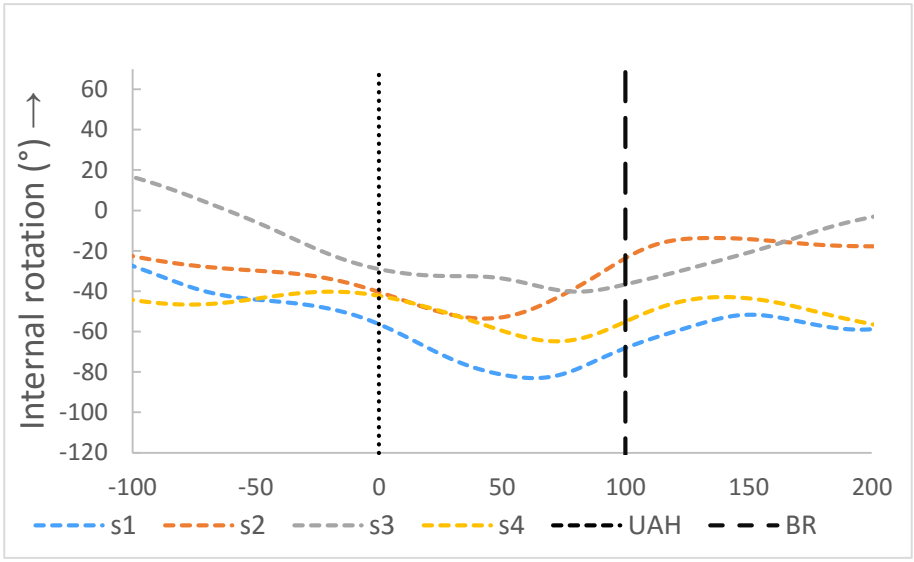

Figure 5.21 Mean humerothoracic kinematics for slow bowlers, stock over. (a) Plane of elevation (b) elevation/depression (c) internal/external rotations. UAH- upper arm horizontal, BR-ball release.

(a)

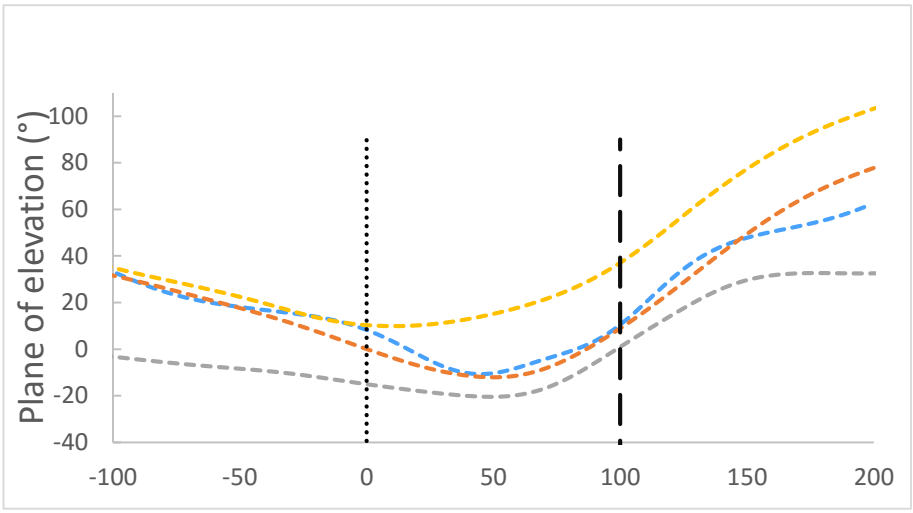

(b)

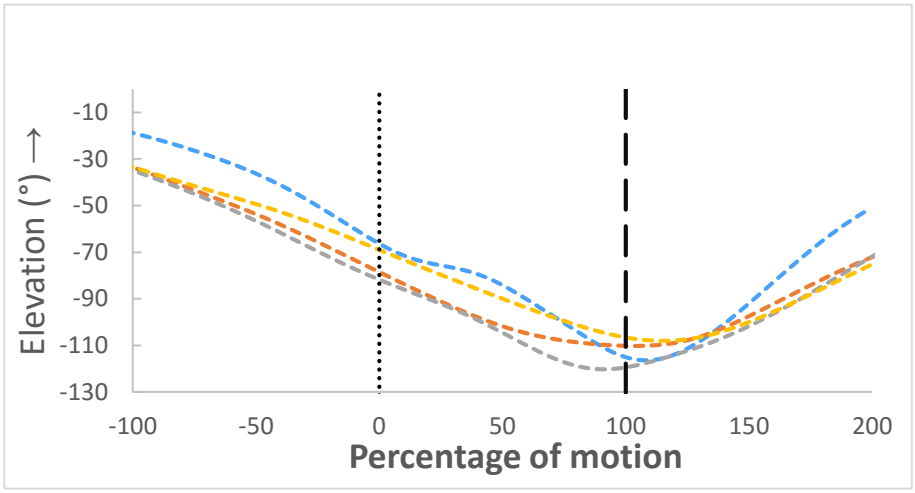

(c)

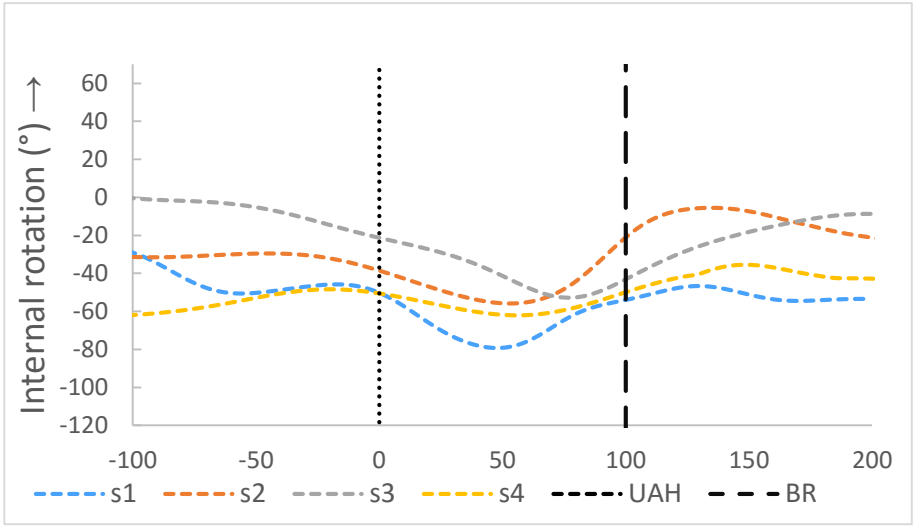

Figure 5.22 Mean humerothoracic kinematics for slow bowlers, variation over. (a) Plane of elevation (b) elevation/depression (c) internal/external rotations. UAH- upper arm horizontal, BR-ball release.

The CMC values for slow bowler's scapulothoracic rotations are shown in Table 5-10 where there was a very good to excellent repeatability.

	internal/external		**up/down**		**posterior/anterior**	
	stock	variation	stock	variation	stock	variation
s1	0.99	0.97	0.97	0.98	0.93	0.97
s2	0.95	0.98	0.95	0.99	0.91	0.92
s3	0.98	0.99	0.99	0.99	0.98	0.97
s4	0.99	0.97	0.94	0.94	0.89	0.85

Table 5-10 Slow bowlers' within-subject CMC values for scapulothoracic rotations across the six trials for each over

Figure 5.23 and Figure 5.24 show the scapulothoracic kinematics for slow bowler's stock and variation overs respectively.

The inter subject correlation for the three scapulothoracic rotations were 0.55, 0.57 and 0.32 for the stock over and 0.64, 0.63 and 0.55 for the variation over.

Comparing kinematic waveforms for both overs showed an excellent repeatability, with values of 0.99, 0.97 and 0.94 for the three scapulothoracic rotations.

(a)

(b)

(c)

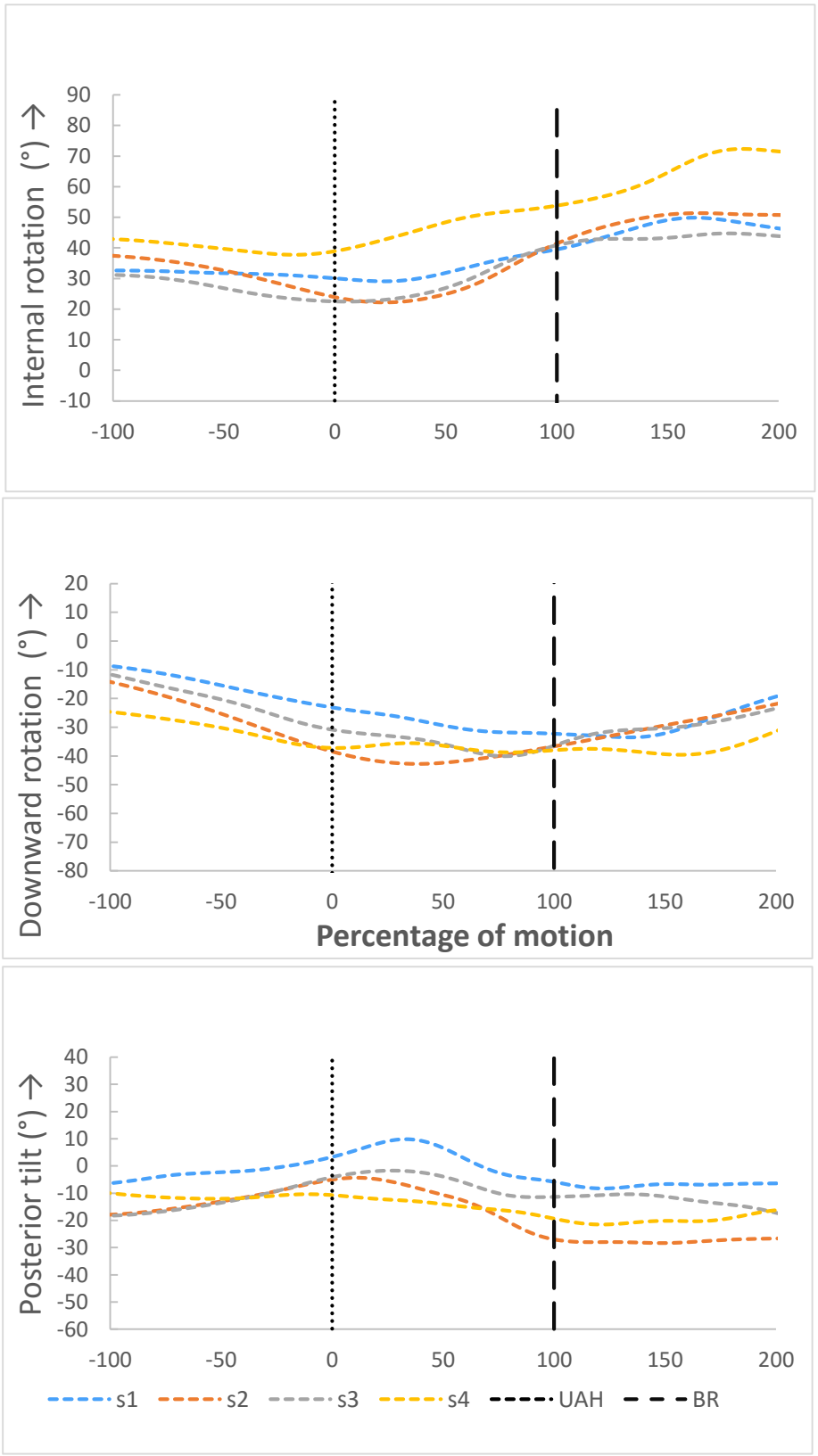

Figure 5.23 Mean measured scapulothoracic kinematics for slow bowlers, stock over. (a) internal/external (b) up/downward (c) posterior/anterior rotations. UAH- upper arm horizontal, BR-ball release.

(a)

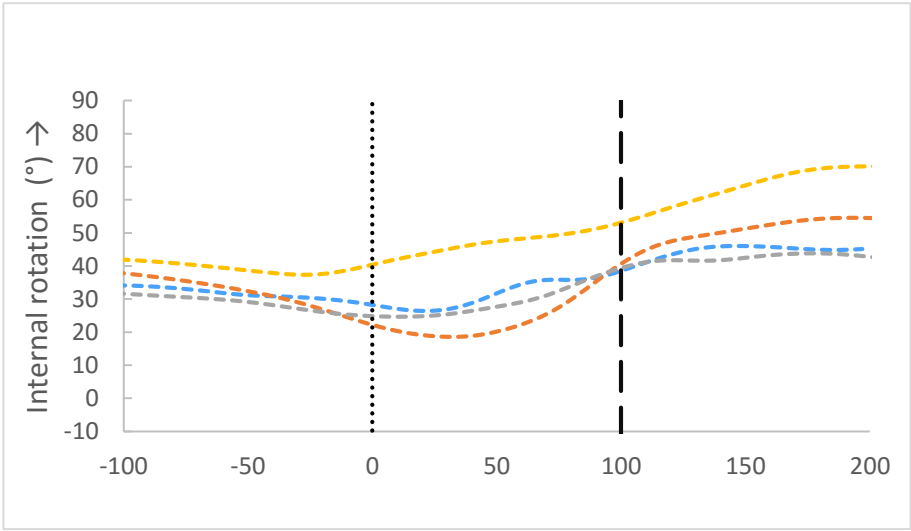

(b)

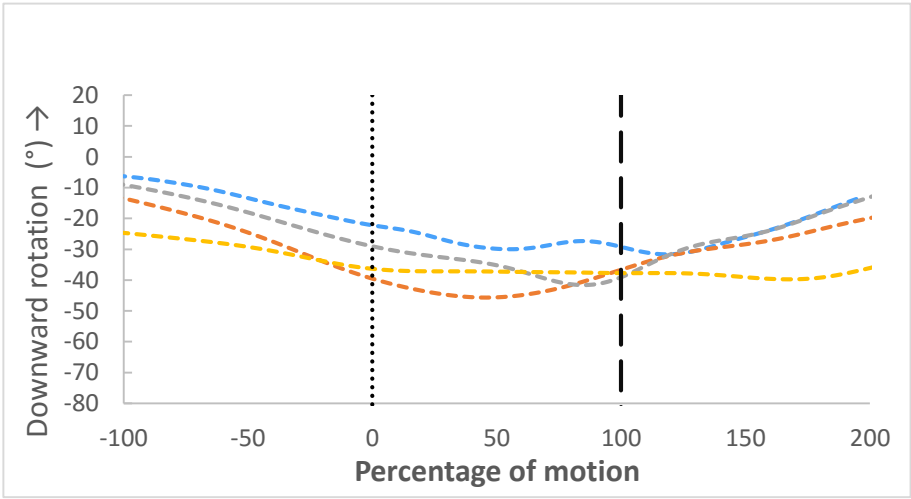

(c)

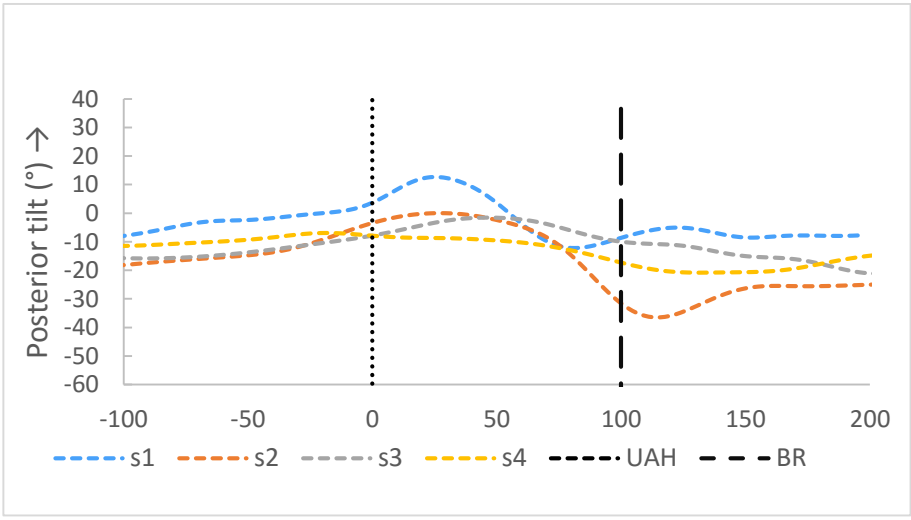

Figure 5.24 Mean measured scapulothoracic kinematics for slow bowlers, variation. (a) internal/external (b) up/downward (c) posterior/anterior rotations. UAH- upper arm horizontal, BR-ball release.

5.4.1.c Scapula kinematics predicted using regression equations

Scapulothoracic rotations predicted using the regression 1 and rotations predicted using regression equations from the UKNSM (regression 2) are presented in Figure 5.25 and Figure 5.26 for fast and slow bowlers respectively.

(a)

(b)

(c)

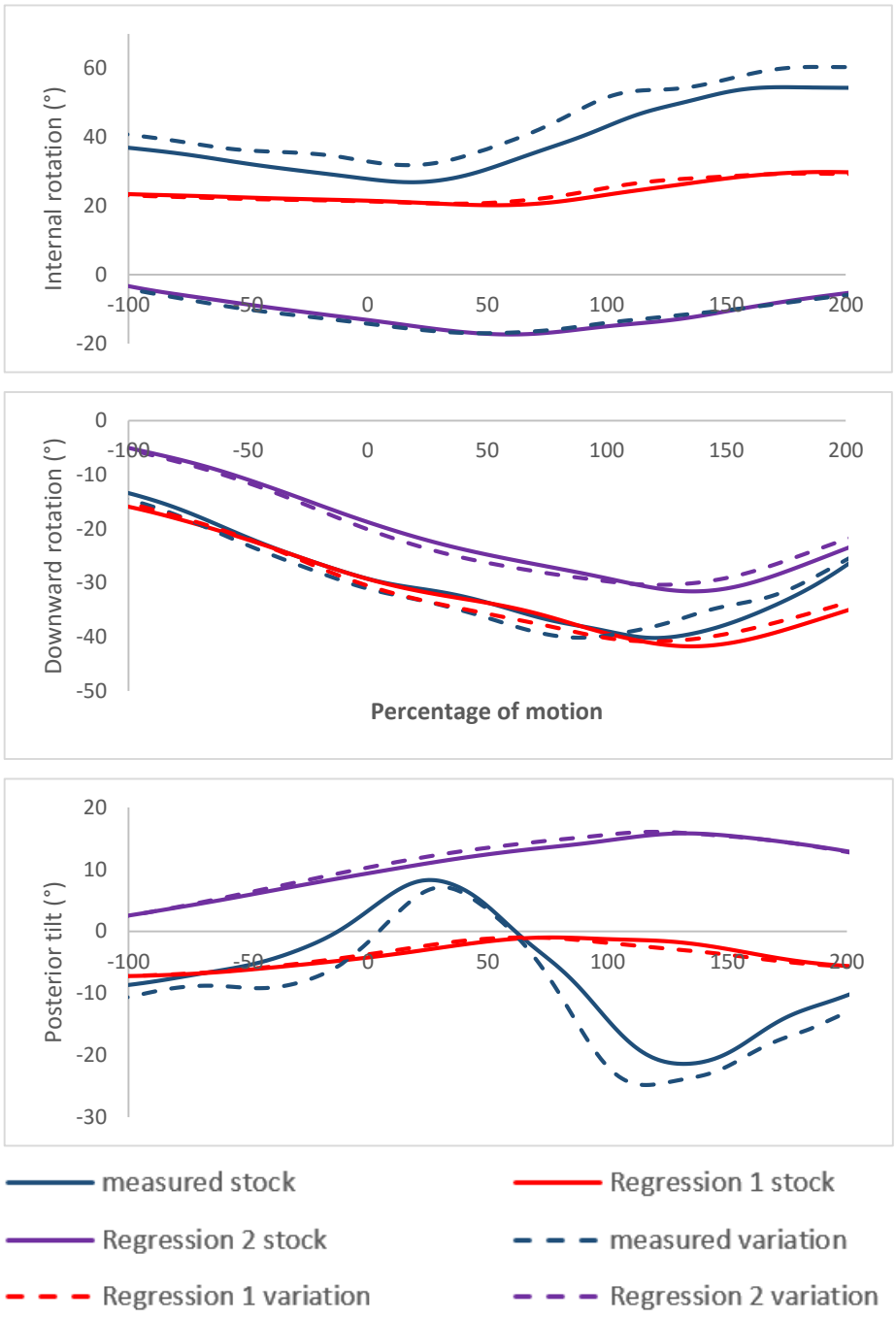

Figure 5.25 Mean scapulothoracic kinematics predicted using regression methods 1 and 2 for fast bowlers. (a) internal/external (b) up/downward (c) posterior/anterior rotations.

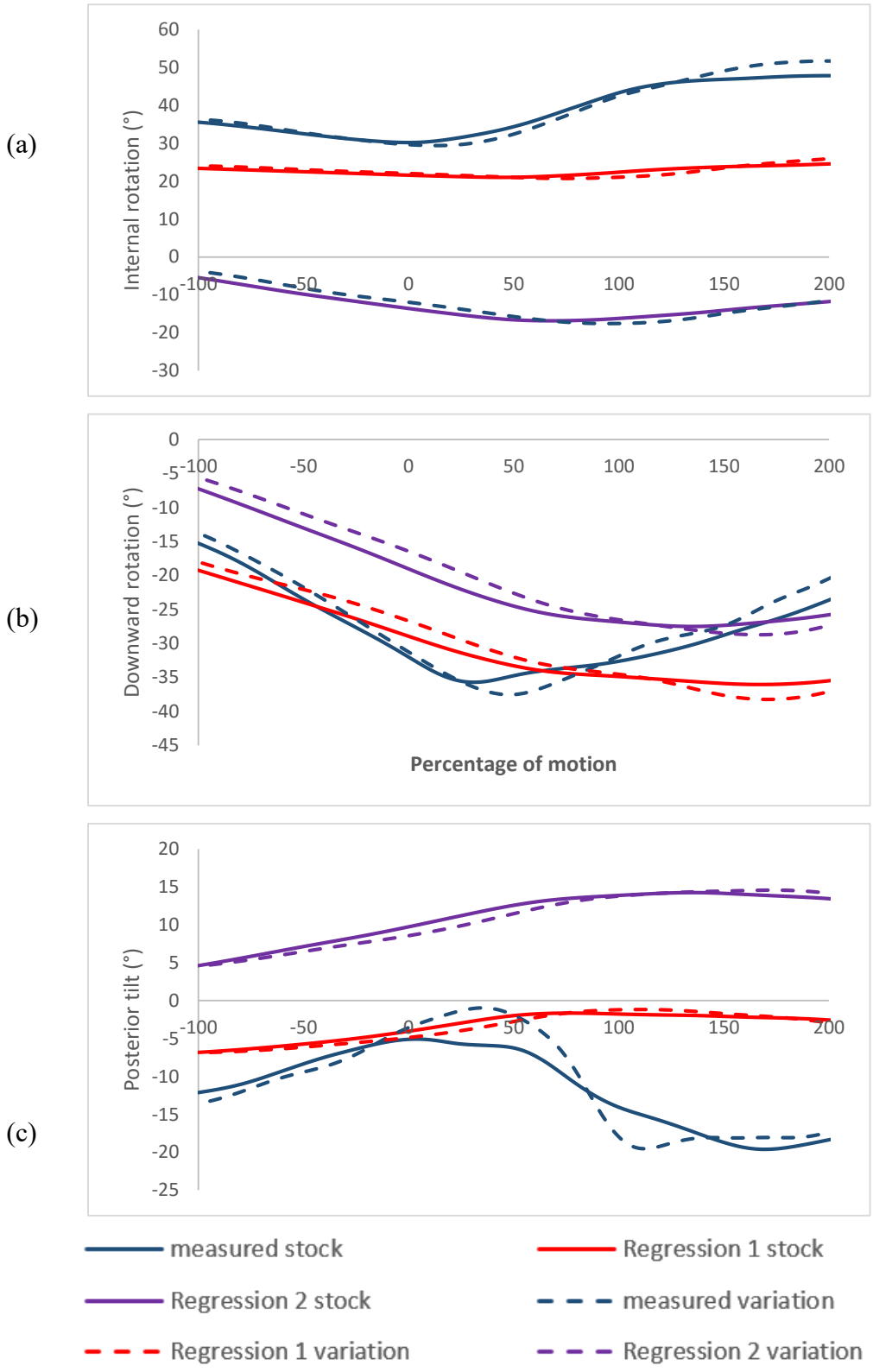

Figure 5.26 Mean scapulothoracic kinematics predicted using regression methods 1 and 2 for slow bowlers. (a) internal/external (b) up/downward (c) posterior/anterior rotations.

Scapula upward rotation predicted using both regression equations showed very good to excellent correlation with the measured waveform (Table 5-11 and Table 5-12). Regression 2 was worse in predicting internal/external scapula rotation indicated by the mean CMC values of 0.48 and 0.41 versus regression 1's 0.67 and 0.65 for stock and variation overs respectively. Both regression equations showed a very poor correlation with measured scapula posterior/anterior tilt.

	internal/external		**up/down**		**posterior/anterior**	
	stock	variation	stock	variation	stock	variation
f1	0.73	0.80	0.94	0.97	0.00	0.00
f2	0.76	0.76	0.97	0.97	0.00	0.00
f3	0.70	0.70	0.93	0.94	0.27	0.22
f4	0.87	-	0.99	-	0.29	-
f5	0.67	0.60	0.91	0.92	0.00	0.00
f6	0.69	0.71	0.94	0.94	0.44	0.48
f7	0.40	0.39	0.88	0.88	0.00	0.00
f8	0.82	0.81	0.95	0.97	0.47	0.44
f9	0.73	0.73	0.94	0.96	0.00	0.00
f10	0.77	-	0.97	-	0.61	-
f11	0.68	-	0.98	-	0.00	-
s1	0.00	0.00	0.96	0.96	0.45	0.37
s2	0.71	0.69	0.90	0.90	0.33	0.35
s3	0.78	0.78	0.90	0.85	0.70	0.79
s4	0.79	0.78	0.95	0.96	0.00	0.00

Table 5-11 Fast and slow bowlers' CMC between measured scapula kinematics and predicted using regression 1

	internal/external		up/down		posterior/anterior	
	stock	variation	stock	variation	stock	variation
f1	0.71	0.72	0.95	0.97	0.00	0.00
f2	0.65	0.60	0.97	0.97	0.00	0.00
f3	0.37	0.42	0.91	0.92	0.00	0.00
f4	0.55	-	0.99	-	0.35	-
f5	0.36	0.00	0.92	0.92	0.00	0.00
f6	0.76	0.72	0.96	0.95	0.32	0.33
f7	0.54	0.00	0.92	0.90	0.29	0.00
f8	0.38	0.42	0.96	0.97	0.00	0.00
f9	0.62	0.52	0.96	0.97	0.00	0.00
f10	0.16	-	0.99	-	0.43	-
f11	0.48	-	0.97	-	0.00	-
s1	0.00	0.00	0.98	0.98	0.42	0.36
s2	0.77	0.73	0.93	0.93	0.00	0.00
s3	0.57	0.70	0.94	0.92	0.78	0.76
s4	0.35	0.14	0.94	0.95	0.00	0.00

Table 5-12 Fast and slow bowlers' CMC between measured scapula kinematics and predicted using regression 2

Figure 5.27 shows the RMS difference between both regression methods and measured kinematics. Fast bowlers' stock and variation overs are represented by the red and green colours while purple and blue was used for slow bowlers. A dashed line meant that the kinematics was predicted using regression 2 while a '+' marker represented regression 1.

Regression 1 and 2 showed a consistent pattern for scapula internal/external rotations however, regression 2 had a much larger difference greater than 40°. Regression 1 was also found to be better to Up/down with a maximum difference of less than 11.7° compared to regression 1's maximum difference of 28.7°.

For posterior/anterior tilt, regression 1 showed the lowest difference for slow bowlers up to 50% of the motion which then increased to a maximum of 20°. The differences for fast bowlers were generally greater than 15° where regression 2 had the largest difference for both sets of bowlers.

(a)

(b)

(c)

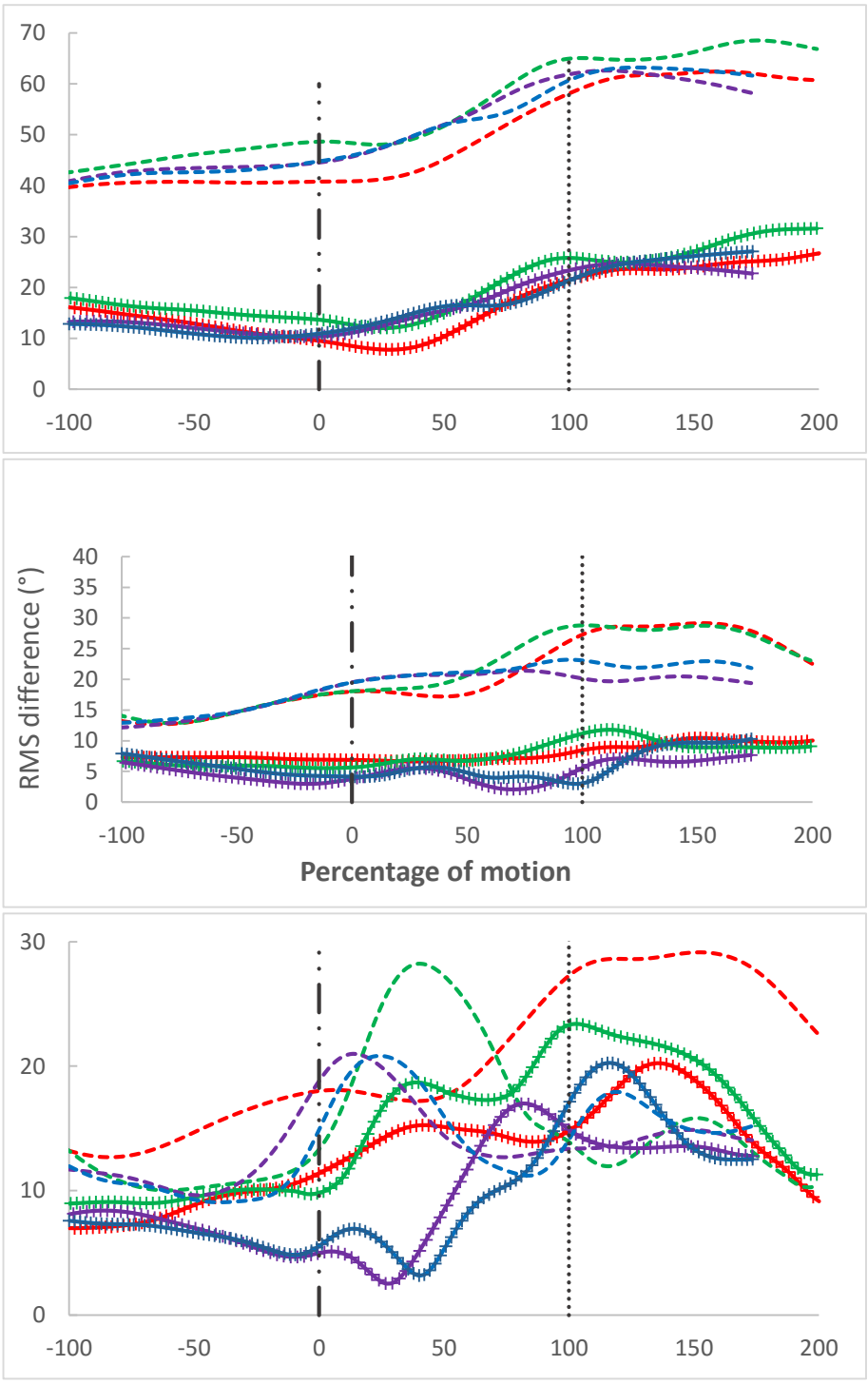

Figure 5.27 RMS difference between measured and both regression methods for Scapulothoracic rotations. (a) internal/external (b) up/downward (c) posterior/anterior RMS difference.

5.4.1.d Glenohumeral joint rotations

Figure 5.28 and Figure 5.29 shows the glenohumeral joint rotations for fast bowlers' stock and variation overs.

Inter-subject CMC values for fast bowlers stock over were 0.83, 0.90 and 0.77 and for variation over were 0.78 0.84 and 0.71 for the three glenohumeral rotations. Table 5-13 shows an excellent repeatability the three glenohumeral rotations.

	Flexion/extension		**Add/abduction**		**Internal/external rotation**	
	stock	variation	stock	variation	stock	variation
f1	0.91	0.91	0.92	0.97	0.96	0.87
f2	0.98	0.98	0.99	1.00	0.98	0.99
f3	0.98	0.98	1.00	0.99	1.00	0.99
f4	0.98	-	0.99	-	0.99	-
f5	0.96	0.98	0.99	0.99	0.98	0.98
f6	1.00	0.97	1.00	0.99	0.99	0.96
f7	0.98	0.97	0.99	0.99	0.99	0.98
f8	0.98	0.99	0.99	0.99	0.97	0.99
f9	0.94	0.92	0.97	0.98	0.95	0.93
f10	0.98		0.99	-	0.98	-
f11	0.98	-	0.99	-	0.98	-

Table 5-13 Fast bowlers' within-subject CMC values for glenohumeral rotations across the six trials for each over

(a)

(b)

(c)

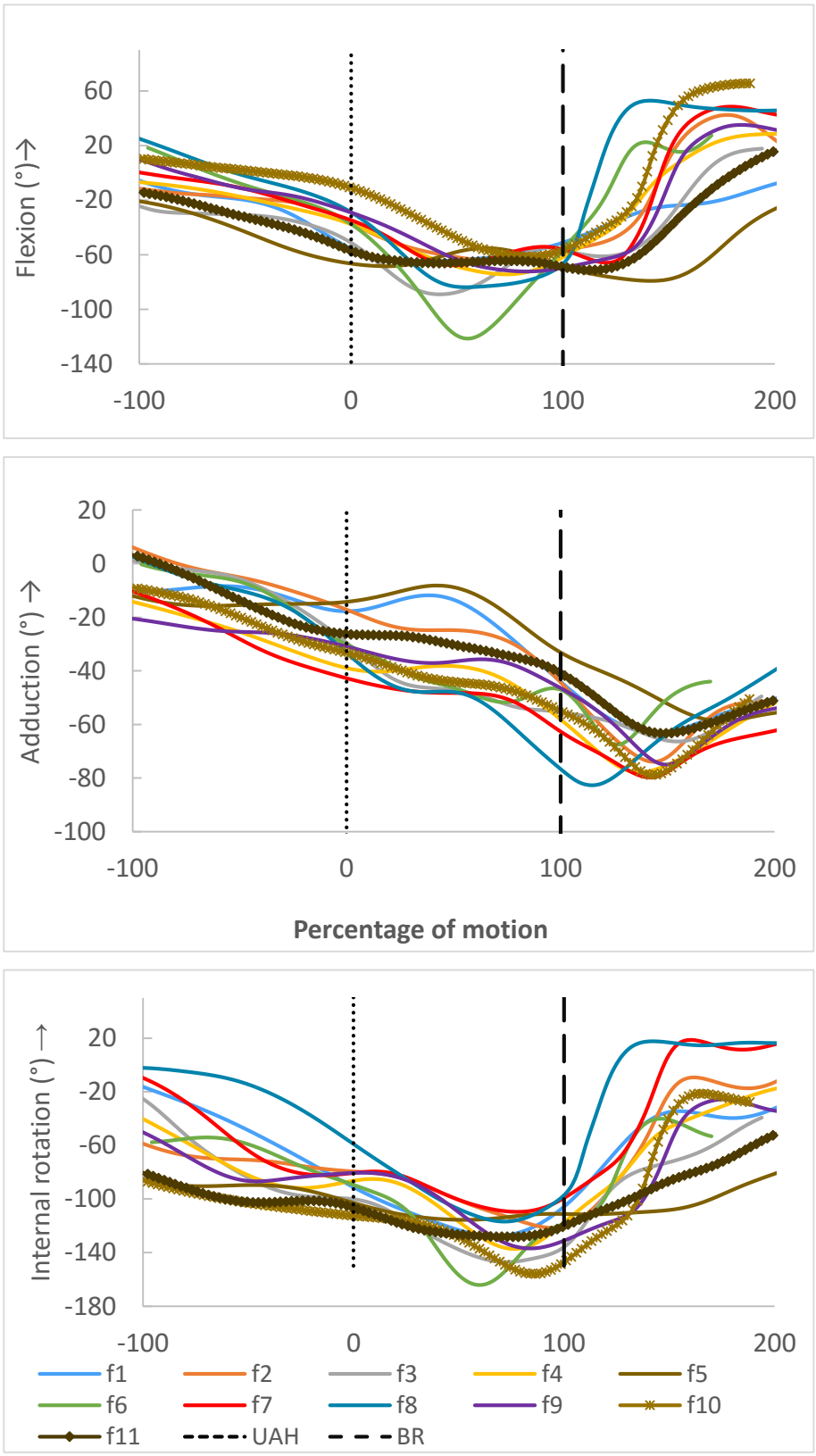

Figure 5.28 Mean glenohumeral rotations for fast bowlers, stock over. (a) Flexion/extension (b) abduction/adduction (c) internal/external rotations. UAH- upper arm horizontal, BR-ball release.

(a)

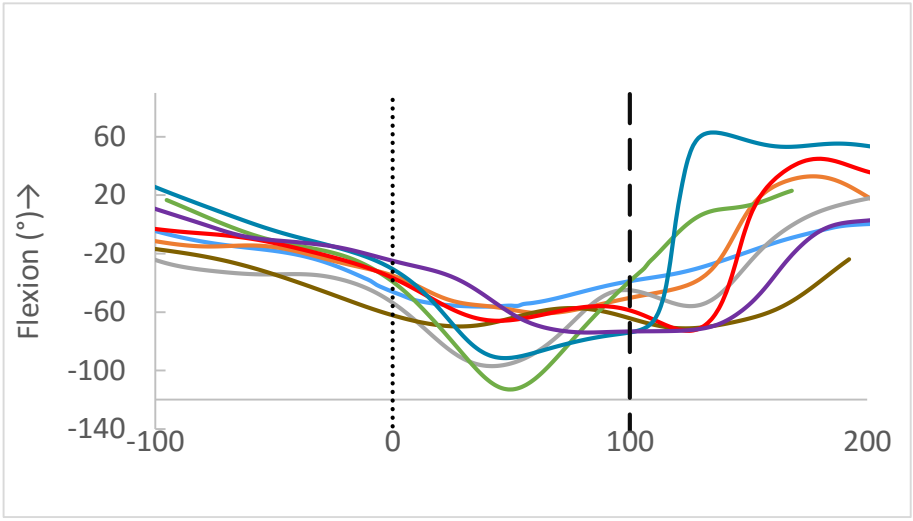

(b)

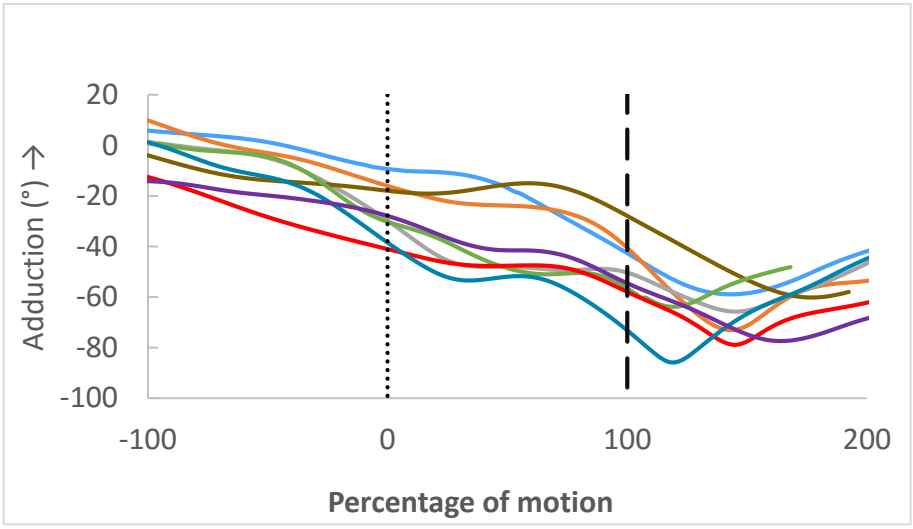

(c)

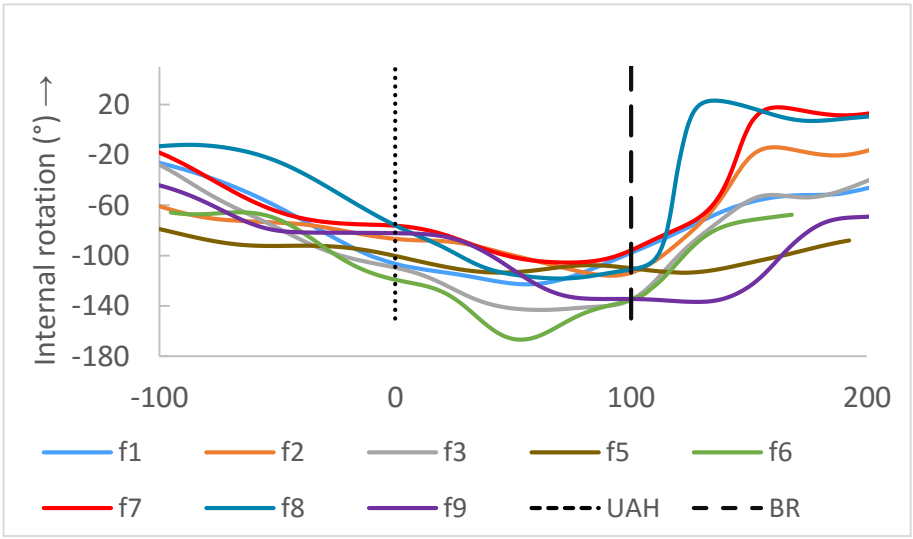

Figure 5.29 Mean glenohumeral rotations for fast bowlers, variation over. (a) Flexion/extension (b) abduction/adduction (c) internal/external rotations. UAH- upper arm horizontal, BR-ball release

Figure 5.30 and Figure 5.31 show the glenohumeral joint rotations for slow bowlers' stock and variation overs.

Inter-subject CMC values of 0.62, 0.82 and 0.55 were calculated for their stock over which improved in their variation over to 0.78, 0.90 and 0.76.

The CMC values show an excellent repeatability for glenohumeral rotations for all subjects and across both over.

	Flexion/extension		**Add/abduction**		**Internal/external rotation**	
	stock	variation	stock	variation	stock	variation
s1	0.97	0.98	0.97	0.99	0.96	0.98
s2	0.94	0.97	0.97	0.97	0.96	0.97
s3	0.96	0.97	0.98	0.96	0.96	0.96
s4	0.99	0.96	0.99	0.97	0.98	0.91

Table 5-14 Slow bowlers' within-subject CMC values for glenohumeral rotations across the six trials for each over

(a)

(b)

(c)

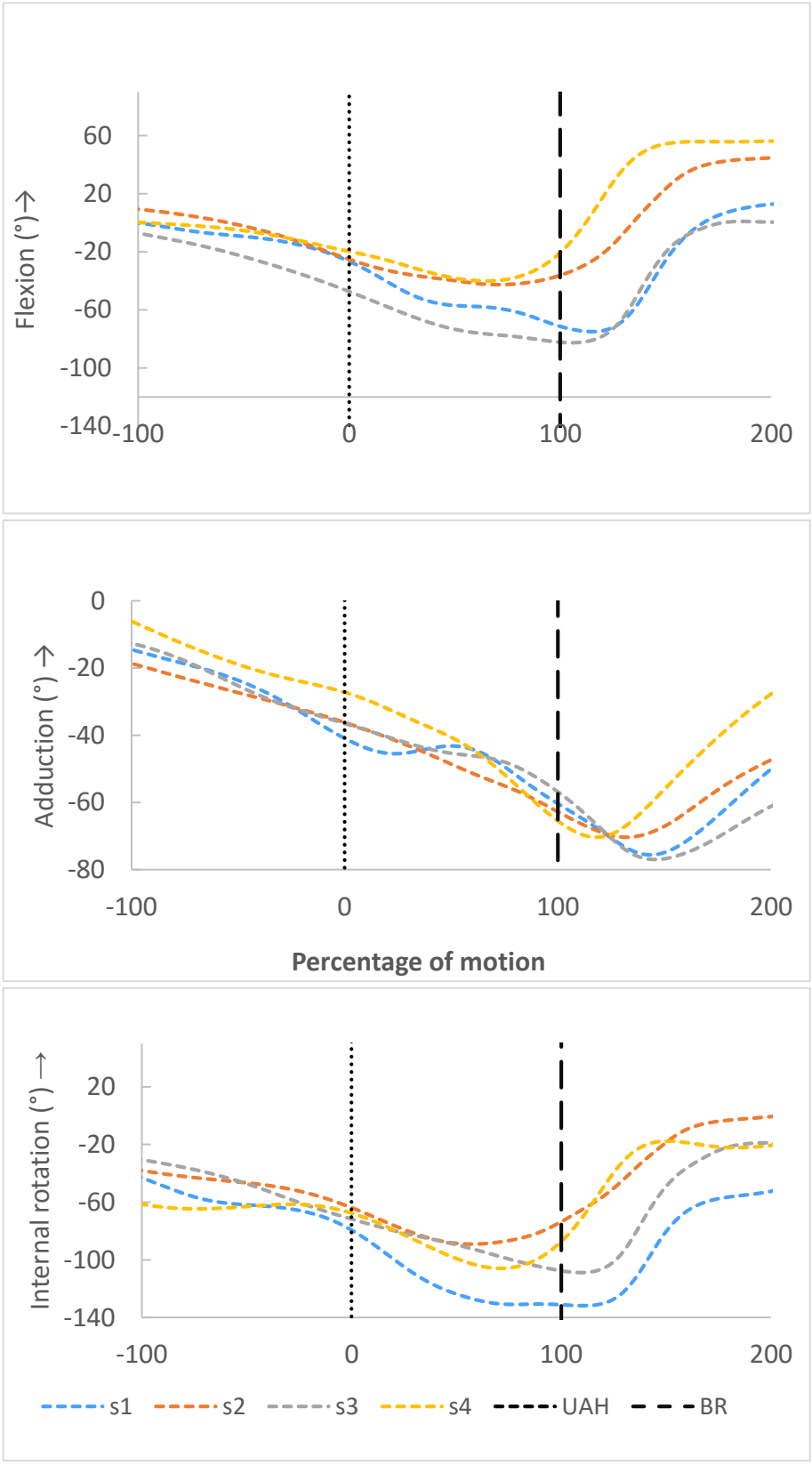

Figure 5.30 Mean glenohumeral rotations for slow bowlers, stock over. (a) Flexion/extension (b) abduction/adduction (c) internal/external rotations. UAH- upper arm horizontal, BR-ball release

(a)

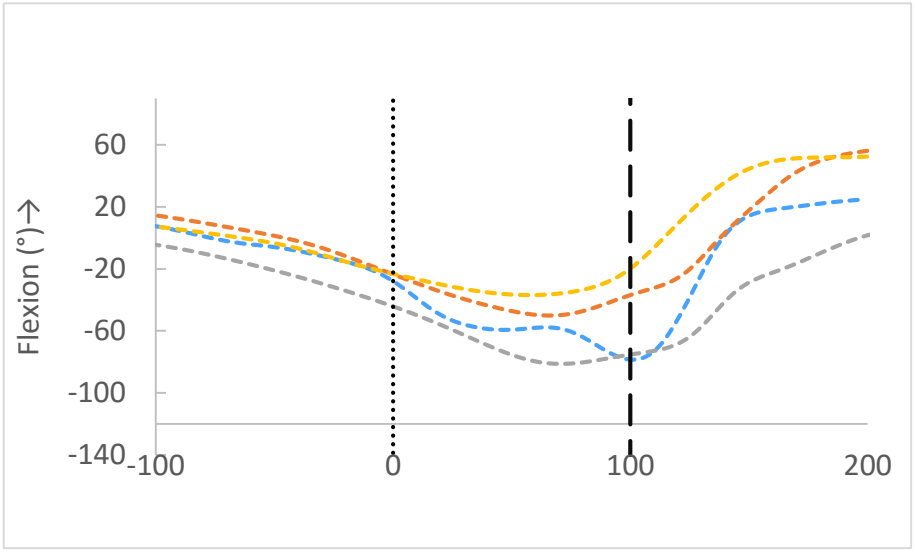

(b)

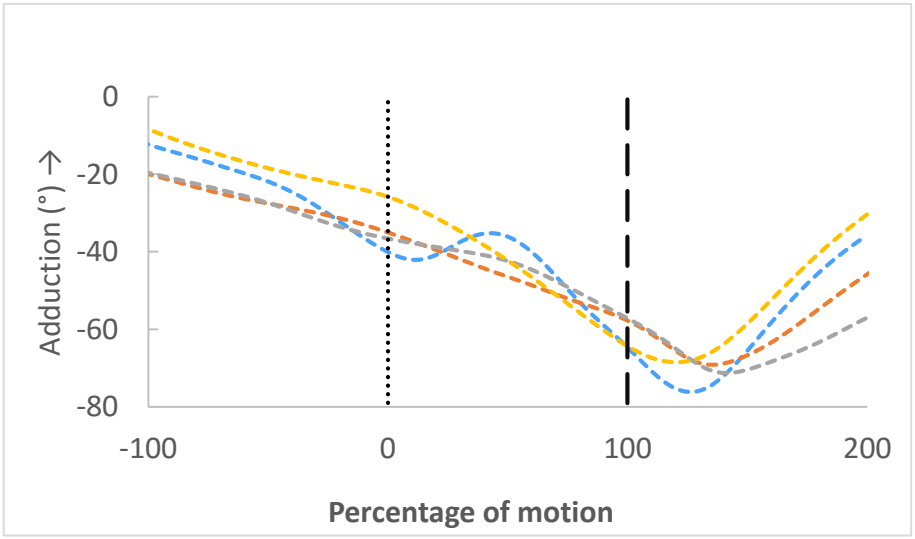

(c)

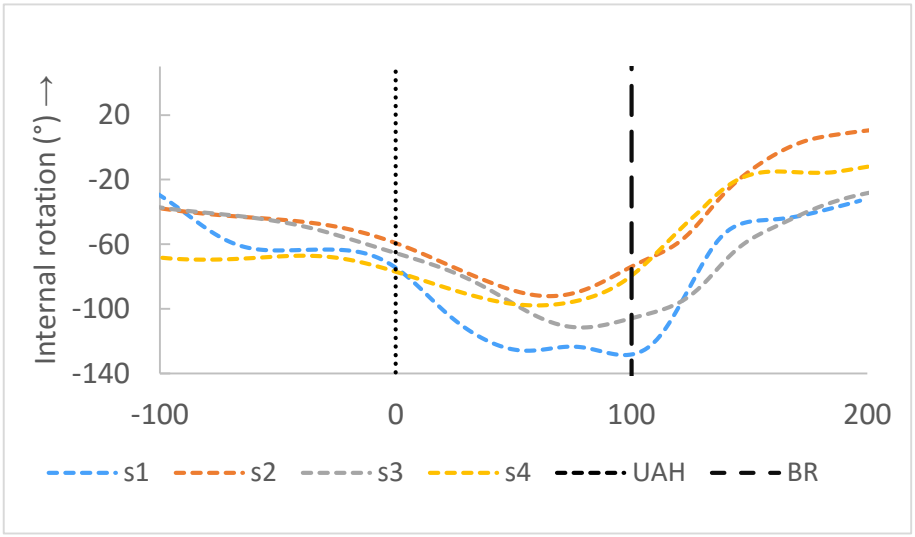

Figure 5.31 Mean glenohumeral rotations for slow bowlers, variation over. (a) Flexion/extension (b) abduction/adduction (c) internal/external rotations. UAH- upper arm horizontal, BR-ball release

5.4.1.e Discussion

One of the hypothesis under investigation in this thesis is the link between internal rotation of the upper arm during ball release and the risk of impingement. The importance of the scapula and its kinematics in preventing impingement have been discussed in previous chapters. Measured scapula kinematics is therefore an important factor in assessing the risk of impingement in bowlers. As such, one of the aims of this analysis was to look at measured scapula kinematics in bowlers and performance of a scapula-tracking device.

5.4.1.e.1 Humerothoracic rotations-Fast bowlers

Excellent humerothoracic CMC values were reported, showing a very high repeatability for measured humerothoracic rotations.

The positive plane of elevation at the start of the motion for subject f6, f8 and f9 in both Figure 5.17 and Figure 5.18 could be explained by the differences in thorax flexion at the designated starting point even though the upper arm was vertical in the global coordinate frame. The positive value indicates that the arm was slightly ahead of the thorax.

The humerus was found to be significantly ($p<0.05$) more externally rotated at upper arm horizontal for fast bowlers' variation over. This is illustrated in Table 5-15 which shows a summary of humerothoracic angles for fast bowlers. There was the trend, particularly in the more experienced bowlers, of greater external rotation at around 75% of the motion in the stock over which was then followed by internal rotation as arm moves to the ball release point (Figure 5.17). This effect is summarised in Figure 5.34 showing the range of external rotation between 0-100% and the subsequent range of internal rotation during the follow through phase. On average, there was an external rotation change of 32° and 24° for the stock and variation overs respectively within this period. The larger external range of motion in the stock over, prior to ball release was found to be statistically significant. The average internal rotation range of motion was 41° and 38° for stock and variation overs respectively in the follow through phase. Therefore, the effect of bowling a slower delivery slightly reduced the amount of internal rotation after ball release. This observation is in agreement with literature (Marshall & Ferdinands, 2003; Zhang, 2011) which showed that one of the mechanism of generating ball speed was rapid internal rotation of the upper arm. Therefore, the delayed external rotation that occurred in the stock over in order to facilitate rapid internal rotation could be explained by this.

The range of humerothoracic elevation for the fast bowlers was between 57° and 86° at upper arm horizontal and between 98° and 139° at ball release across both overs (Table 5-15). There were no significant differences between these angles for both overs. These angles are of great importance for both bowlers as the risk of impingement is greater due to the combined effect of humerus axial rotation at high elevation angles, as discussed in Chapter 3. The disparity between these elevation angles may be explained by differences in technique where some bowlers ultilise greater lateral trunk flexion (Table 5-20) rather than shoulder elevation in contributing to the height at which ball release occurs.

It is interesting to note that the actual humerus axial rotation angle for fast bowlers between both overs was dependant on each subject where some had a more internally rotated arm for the slower ball while others had a more externally rotated arm (Table 5-15), highlighting differences in techniques. This is also indicated for the poor inter-subject correlations particularly for axial rotations with values of 0.56 and 0.62 within stock and variation overs respectively.

	Stock over				Variation over			
	Humerothoracic elevation angle (°)		**Humerothoracic external rotation angle (°)**		**Humerothoracic elevation angle (°)**		**Humerothoracic external rotation angle (°)**	
	UAH	**BR**	**UAH**	**BR**	**UAH**	**BR**	**UAH**	**BR**
f1	-75 (3)	-114 (5)	-40 (3)	-59 (2)	-78 (3)	-116 (2)	-52 (5)	-52 (4)
f2	-62 (2)	-107 (5)	-55 (2)	-68 (3)	-63 (1)	-104 (3)	-61 (1)	-66 (4)
f3	-78 (1)	-125 (1)	-61 (1)	-92 (2)	-81 (2)	-123 (2)	-69 (2)	-89 (3)
f4	-63 (2)	-108 (3)	-65 (3)	-67 (7)	-	-	-	-
f5	-66 (3)	-98 (2)	-49 (3)	-43 (3)	-67 (2)	-98 (3)	-48 (2)	-38 (2)
f6	-69 (4)	-119 (4)	-54 (5)	-72 (8)	-72 (5)	-117 (2)	-81 (2)	-95 (4)
f7	-70 (2)	-99 (1)	-82 (2)	-68 (1)	-68 (1)	-97 (3)	-85 (1)	-73 (2)
f8	-80 (5)	-139 (2)	-31 (7)	-29 (10)	-86 (2)	-139 (1)	-44 (2)	-35 (2)
f9	-68 (2)	-110 (3)	-43 (2)	-60 (3)	-65 (2)	-118 (3)	-43 (2)	-59 (3)
f10	-57 (2)	-111 (2)	-88 (3)	-100 (4)	-	-	-	-
f11	-75 (3)	-115 (3)	-74 (1)	-63 (3)	-	-	-	-

Table 5-15 Average fast bowler humerothoracic elevation and axial rotation angles at upper arm horizontal (UAH) and ball release (BR) for both stock over and variation over (slower ball). Standard deviations are in parenthesis.

5.4.1.e.2 Humerothoracic rotations-Slow bowlers

Excellent humerothoracic CMC values were reported. The effect of bowling a faster delivery slightly reduced the repeatability for humerothoracic axial rotation. This meant that quality of measured GH kinematics would depend on the performance of the scapula tracker.

The only significant difference observed was a lower humerothoracic elevation angle at upper

arm horizontal (Table 5-17). Given that the upper arm horizontal is identified in the global frame, the lower elevation angle was most likely due to the larger trunk flexion that occurred when bowling the faster delivery. The act of delaying arm elevation as the trunk flexes was also highlighted in the literature (Worthington et al., 2013) as a means of generating ball speed.

The range of humerothoracic elevation for the slow bowlers was between 108° and 121° at ball release across both overs (Table 5-17). The elevation angle was similar for the variation over except for s3 who had a much greater elevation angle when bowling their faster ball.

All the slow bowlers showed a greater amount of internal rotation after ball release for their stock over (Figure 5.34). There was a clear pattern of humerus axial rotation for s1 and s2 in their stock over (Figure 5.21c). Off spin bowlers s1 and s2 had slightly earlier internal rotation prior to ball release when compared to s3 and s4 (Figure 5.21). The amount of internal rotation after ball release for leg-spin bowlers was 55° and 15° for s3 and s4 respectively. There was no clear trend for upper arm internal rotation after ball release when the slower bowlers bowled their faster delivery. The difference in technique between both types of spin bowlers is also highlighted by the pronation angle at the elbow shown in Appendix 1.

A distinctly different pattern of axial rotation is highlighted by the low inter-subject CMC values, showing the variation in technique within the group.

5.4.1.e.3 Scapulothoracic rotations

No statistically significant differences were found for measured scapula kinematics between stock and variation over for any bowler. This indicated that any technique changes that occurred did not happen at the shoulder, assuming that scapula kinematics was reliably measured.

For fast bowlers, there was an excellent repeatability for measured scapula kinematics with f1 being the exception. The trend of the scapulothoracic waveforms (Figure 5.19 and Figure 5.20) show there was an initial external rotation and posterior tilting at upper arm horizontal transitioning to internal rotation (range 15°-60°) and anterior tilting at ball release. The scapulothoracic upward rotation at ball release was between 19° and 56°. Scapula posterior/anterior tilt was found to be overestimated where the average change in rotation angle between 0-100% was 32° and 39° for both overs with the highest change of 68° recorded for subject f3 (Figure 5.33) with a posterior tilt angle of 29° in their variation over. Subject f6 had a maximum posterior tilt angle of 31° in their stock over. This overestimation is also confirmed in the motion capture data showing how the digitised points of the scapula penetrating the

thorax during posterior tilting and showing considerable anterior tilting. Both these instances highlight the effect of speed on measuring scapula kinematics using the tracker. This behaviour is expected given the results of the study in Chapter 4.

For slow bowlers, the trend of scapulothoracic rotations was observed to be similar to that of the fast bowlers where there was external rotation and posterior tilt during elevation to ball release which transitioned into internal rotation and anterior tilting. The internal rotation angle at ball release was between 40° to 55° while the upward rotation angle was between 31° and 37°. There was a maximum posterior tilt between upper arm horizontal and ball release of 10° recorded for subject s1, which increased to 12° in their variation over. Therefore, there was less exaggerated posterior tilt when compared to the fast bowlers. Subject s4 did not show this trend of posterior tilting before ball release in their stock over.

The CMC values for scapulothoracic rotations provides an assessment of the performance of the scapula tracker device in dynamically measuring scapula kinematics during bowling. Scapulothoracic CMC values for both sets of bowlers show a very good to excellent correlation with f1 being the exception (Table 5-8 and Table 5-10). The isolated instance of subject f1 poor correlation could have been due to poor placement of the scapula tracker, where the bulge of the posterior deltoid may influence the movement of the tracker. There was an excellent correlation for scapula up/down rotation, however this was significantly reduced in their variation over as well as for the other rotations indicating that the tracker was not firmly fixed during their second over. For the other subjects, the high CMC values indicate that the measured scapula kinematics was highly repeatable. This however is not an indication of accuracy.

Scapula up/down rotations for all bowlers were within a feasible range compared to what is reported in other studies during humerothoracic elevation (Chu et al., 2012; McClure et al., 2001; Shaheen et al., 2011a). Table 5-16 shows a comparison of measured scapula range of motion for each degree of freedom. In this comparison, measured scapula internal/external rotation was found to be greater than what is reported the literature, indicating that this measurement was also over estimated. One key difference in this case is that there was a greater internal rotation measured after ball release in the follow through while for scapula tilt, the over estimation occurred within 0-100% of the motion. Given that the errors in scapula tilt occurred in a shorter period of time, it is of greater concern rather than the gradually increasing internal rotation (Figure 5.25).

Study	Motion	Measurement method	Scapula ROM		
			IE (°)	UD(°)	PA(°)
Shaheen et al. (2011a)	Scapula plane elevation to 140	Scapula palpator with pressure feedback	2	45	2
McClure et al. (2001)	Sagittal plane flexion to 140	Bone pins	14	44	23
	Scapula plane abduction to 140		15	42	22
	Humerothoracic external rotation to 60° with the arm abducted to 90°		15	15	14
Chu et al. (2012)	Abduction in frontal plane (ROM 128°)	Dynamic stereo X-ray	10.6	45.7	14.7
	Scaption (ROM 121.7°)		12	48.5	14
	Internal/external rotation at 90° abduction (ROM 111.3°)		7.1	14.9	14.8
Scapula study presented in Chapter 4	Slow circumduction	Scapula palpator	13	31	6
		Scapula tracker	14	28	15
Fast bowlers stock	Full speed bowling	scapula tracker	29	27	29
Fast bowlers variation			29	27	32
Slow bowlers stock			25	23	14
Slow bowlers variation			25	24	18

Table 5-16 Measured scapula range of motion (ROM) compared with other studies.

One limitation of this comparison however, is that humeral kinematics are different and researchers typically do not investigate the range of motion that is involved in cricket bowling as evident by a review done by Lempereur et al. (2014) on 17 key papers that described both invasive and non invasise methods for measuring in vivo scapula kinematics. Therefore measured scapula kinematics is also compared to values reported in Chapter 4 during slow circumduction of the arm, where the performance of the scapula tracker was worse in full speed bowling trials with a similar conclusion as reported above.

Slow bowlers had less of an issue for scapula posterior/anterior tilt showing a similar range of motion that was reported in Chapter 4. This may indicate the influence of speed of motion on the scapula tracker for measures this degree of freedom.

The issue of poor measurement of posterior/anterior tilt using a scapula tracker device during high elevation angles was also illustrated in literature (Karduna et al., 2001). Regardless of these shortcomings, the value of the scapula tracker is still high given that it reliably measured up/down rotation and the errors with internal/external rotations may be less crucial when considering it occurred later in the follow through. Scapula upward rotation is important in athletic motion as it elevates the acromion during humerothoracic elevation, clearing the acromion from the rotator cuff and decreasing the risk of impingement (Kibler, 1998). In contrast to this, impingement subjects were found to have increase anterior tilt (Lukasiewicz et al., 1999) and increased internal rotation (Ludewig & Cook, 2000). Furthermore, delayed posterior tilting or early anterior tilting would theoretically decrease the subacromial space increasing the risk of impingement. So total scapula kinematics is important in preventing impingement. The exact application of these findings to cricket bowling is unknown especially when trying to quantify the rank of scapula rotations in preventing impinging positions. Nevertheless, the issue of poorly measured posterior/anterior tilting was catered for with the adaptations made to the upper limb model. This is presented in Chapter 6.

Figure 5.32 and Figure 5.33 summarise the range of scapula rotations within three defined phases. The graphs show a clear pattern among all bowlers that majority of the rotational changes that occurred for internal/external and posterior/anterior, occurred between 0-100%. While there was minimum scapula up/down rotational changes in this region. Scapula posterior/anterior tilting overestimation is also highlighted by these figures. It is therefore plausible that errors in scapula posterior/anterior and internal/external would also affect scapula upward/downward rotations.

	Stock over				Variation over			
	Humerothoracic elevation angle (°)		**Humerothoracic internal/external angle (°)**		**Humerothoracic elevation angle (°)**		**Humerothoracic internal/external angle (°)**	
	UAH	**BR**	**UAH**	**BR**	**UAH**	**BR**	**UAH**	**BR**
s1	-68 (1)	-112 (2)	-78 (1)	-82 (3)	-66 (4)	-114 (6)	-82 (2)	-77 (8)
s2	-80 (2)	-114 (1)	-39 (2)	-19 (3)	-79 (1)	-111 (1)	-38 (2)	-21 (3)
s3	-83 (2)	-112 (1)	-29 (2)	-38 (2)	-82 (3)	-121 (2)	-21 (2)	-44 (7)
s4	-71 (3)	-108 (3)	-42 (3)	-55 (5)	-69 (4)	-106 (3)	-51 (3)	-49 (6)

Table 5-17 Average slow bowler humerothoracic elevation and axial rotation angles at upper arm horizontal (UAH) and ball release (BR) for both overs. Standard deviations are in parenthesis.

5.4.1.e.4 Regression predicted scapula kinematics

Regression predicted kinematics were compared to the measured kinematics to determine whether they could reliably be used. The criteria for a good regression prediction was dependant on a minimum error with respect to the measured kinematics for scapula internal/external and up/down rotations only and that the predicted curves followed the same trends shown by the scapula tracker. These two criteria was judged using the new CMC formulation to measure the similarities between waveforms and calculation of the RMS difference.

Regression 1 and 2 show an equally excellent similarity with measured up/down rotations. Regression 1 was better for internal/external rotations with an average value of 0.67 and 0.65 for both overs (Table 5-11) compared to regression 2's values of 0.48 and 0.41(Table 5-12) across all subjects. Both regression methods showed a very poor similarity with measured scapula posterior/anterior tilt. Knowing the high measurement errors associated with this scapula rotation, these results might prove to be acceptable however upon further investigation, the regression predicted kinematics did not match where posterior and anterior rotations occurred (Figure 5.25 and Figure 5.26). The RMS difference between the methods showed that regression 1 predicted kinematics was closer to the measured kinematics with a maximum error of 26° compared to a regression 2's maximum of 65° for internal/external rotation at ball release. There was a similar trend for up/down rotations where regression 1 showed a

consistently lower error across all subjects and overs.

The idea for using both of these regression equations was to provide an alternative for the predictably poorly measured posterior/anterior scapula rotation. Regression 2 was found to be worse. This was expected since these equations were formulated with low humerothoracic elevation angles compared the regression 1. While regression 1 did attenuate the overestimation (Figure 5.27) it was concluded that its potential is limited, considering that it did not follow the same trend and the RMS difference increased to a maximum at ball release, where the errors in measured kinematics might not be as large. Furthermore, at the start of the motion there were angular offsets as much as 17° and 8° for internal/external and up/down rotations respectively (Figure 5.26 and Figure 5.27).

5.4.1.e.5 Glenohumeral joint rotations

No significant differences were found between the measured kinematics of both overs for any bowler. The errors of measured scapula kinematics would also be manifested in glenohumeral kinematics.

For fast bowlers, GH abduction angle was between 36° to 80° at the point of ball release across both overs for fast bowlers. The humerus was externally rotated within a range of 90° to 140° at ball release. All the subjects showed some degree of GH internal rotation after ball release where subject f6 and f10 had an unusually high maximum external rotation of 164° and 154° respectively prior to ball release. Subject f11 had the least amount of internal rotation while subject f8 had the greatest change in internal rotation just after ball release. These trends were true for both overs.

Glenohumeral rotations were found to have a very high repeatability similar to (Table 5-13 and Table 5-14). For both overs, subjects f3 and f6 showed much earlier maximum extension and external rotation (Figure 5.28 and Figure 5.29). This occurred at the same instant in the motion where both of these subjects showed the greatest posterior tilting, indicating that both the events were related. Another effect due to errors in measured scapula kinematics was demonstrated in the degree of external rotation for f6 and f10 of greater than 150° (Figure 5.28). The maximum glenohumeral external rotation in professional baseball pitchers was reported as 124° (Freehill et al., 2011) and 136.9° ± 14.7° (Wilk et al., 2009) when passively assessed at 90° abduction. Given that these overhead athletes show the greatest amount of external rotation during their sporting task the GH external rotation for both these subjects may have been overestimated due

to errors associated with soft tissue artefact, especially considering the GH abduction of 45° and 56° respectively. A recent study (Yeadon & King, 2015) showed that using marker positions at the elbow for cricket bowling rather than digitised points showed a better accuracy for measuring elbow extension. This may also be true for axial rotations of the humerus and might explain why such large external rotations were observed in some subjects especially when considering that humerus axial rotation has been shown to be susceptible to soft tissue artefacts (Cutti et al., 2005). An attempt was made to correct for this problem by including the lateral epicondyle marker together with the three markers of the cluster in calculating the least squares rotation matrix (Soderkvist & Wedin, 1993). Only the lateral epicondyle was chosen since it was observed during the labelling process that the medial epicondyle suffered from marker occlusion and for a significant amount of time during external rotation of the humerus to upper arm horizontal.

For bowler f5, their GH abduction angle at ball release was approximately 30° in both overs and given the fact that their humerothoracic elevation angle was within comparable range to the other fast bowlers, such a low abduction angle could only be explained by measurement errors in measured scapula kinematics.

GH abduction for the slow bowlers was between 66° to 59° at ball release. The humerus was externally rotated within a range of 71° to 131° at ball release for all slow bowlers. The results for axial rotation show that for the stock over, off-spinners s1 and s2 showed a different amount of external rotation prior to ball release. All slow bowlers demonstrated GH internal rotation after ball release where s4 had the greatest change in internal rotation of 85° in the moments prior to and just after ball release.

The range of internal rotation for off spin bowlers increase from an average value of 63° to 80.5° when delivering their faster delivery. This again highlighted the use of internal rotation in increasing ball speed. On the other hand, only s4 showed a slight increase in the range of internal rotation from 69° to 77°, while bowler s3 had a decrease from 81° to 55° indicating that they did not rely on internal rotation for their faster delivery.

The range of internal rotation prior to ball release as well as the axial rotation angle that were observed was similar regardless of the type of bowler. This appears to contradict Gregory et al. (2002) who postulated that spin bowlers were at great risk of injury due to greater internal rotation when compared to fast bowlers. The graphs however show that the slow bowlers show a much more consistent internal rotation in the early period prior to ball release (Figure 5.30)

indicating that it may not necessarily be the amount of internal rotation that is important but velocity at which this internal rotation occurs or the internal rotation torque at the GH joint. This new hypothesis is later investigated.

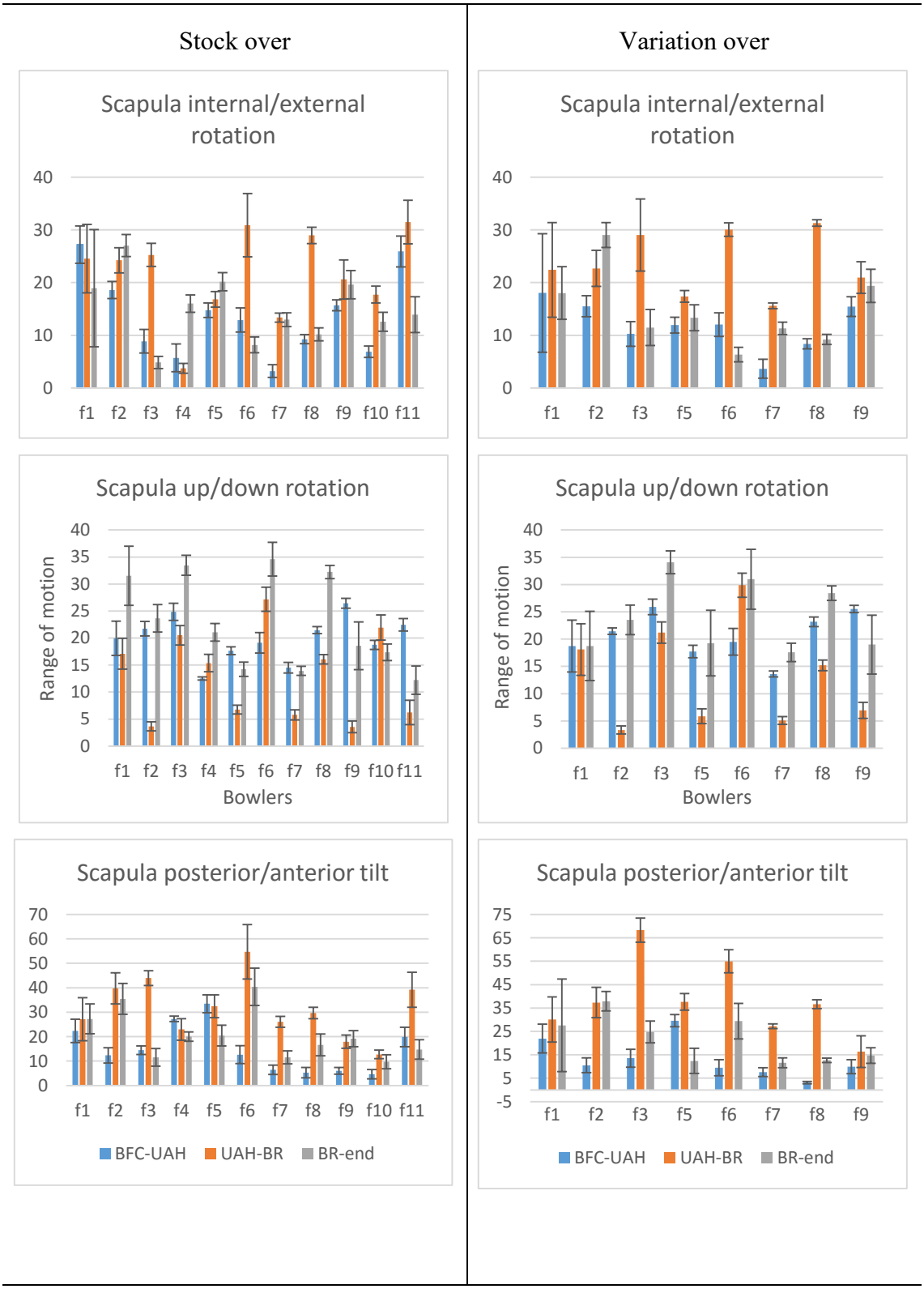

Figure 5.32 Fast bowlers' scapulothoracic range of motion for both overs, measured within three phases of the bowling action, BFC- back foot contact, UAH- upper arm horizontal and BR- ball release

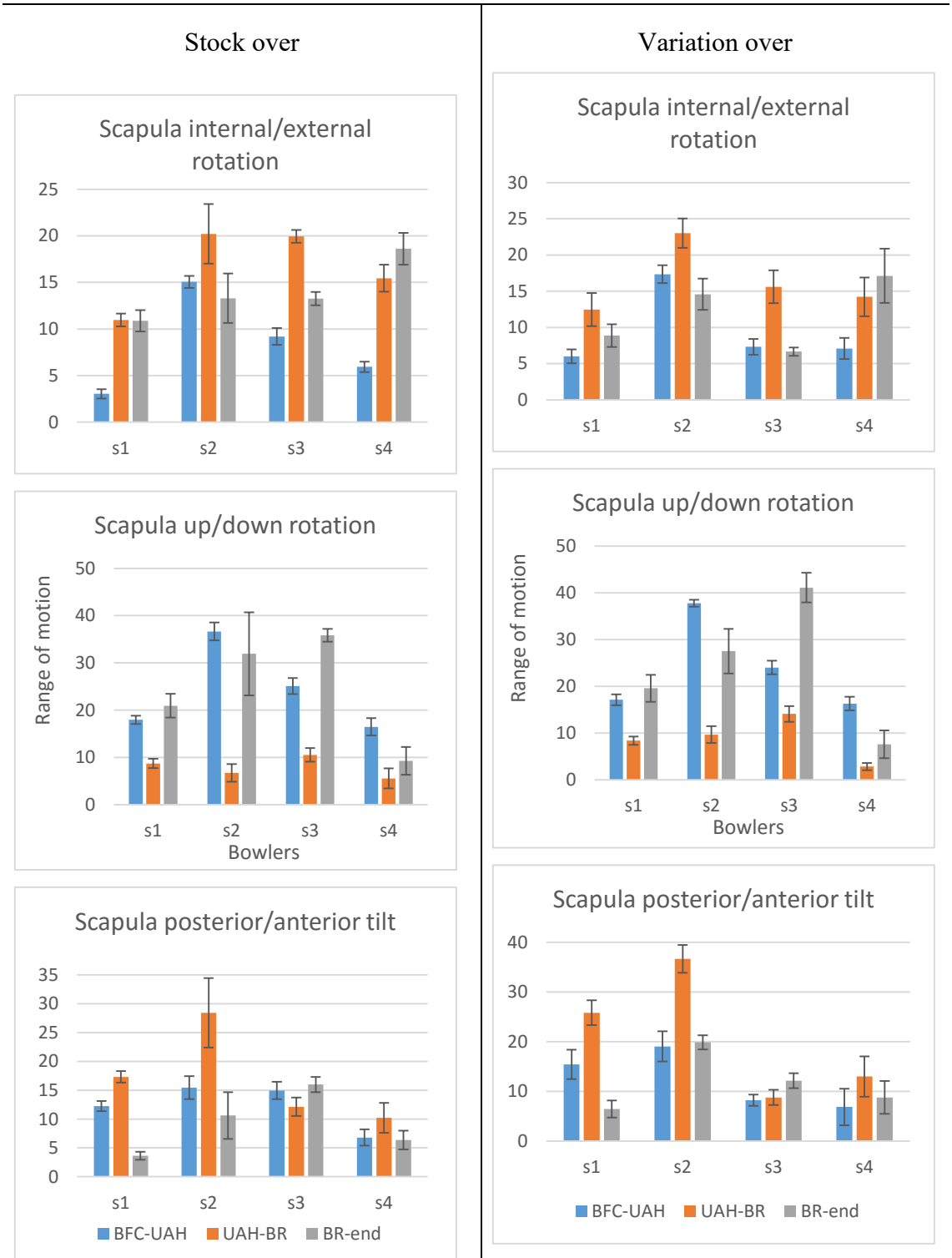

Figure 5.33 Slow bowlers' scapulothoracic range of motion for both overs, measured within three phases of the bowling action, BFC- back foot contact, UAH- upper arm horizontal and BR- ball release

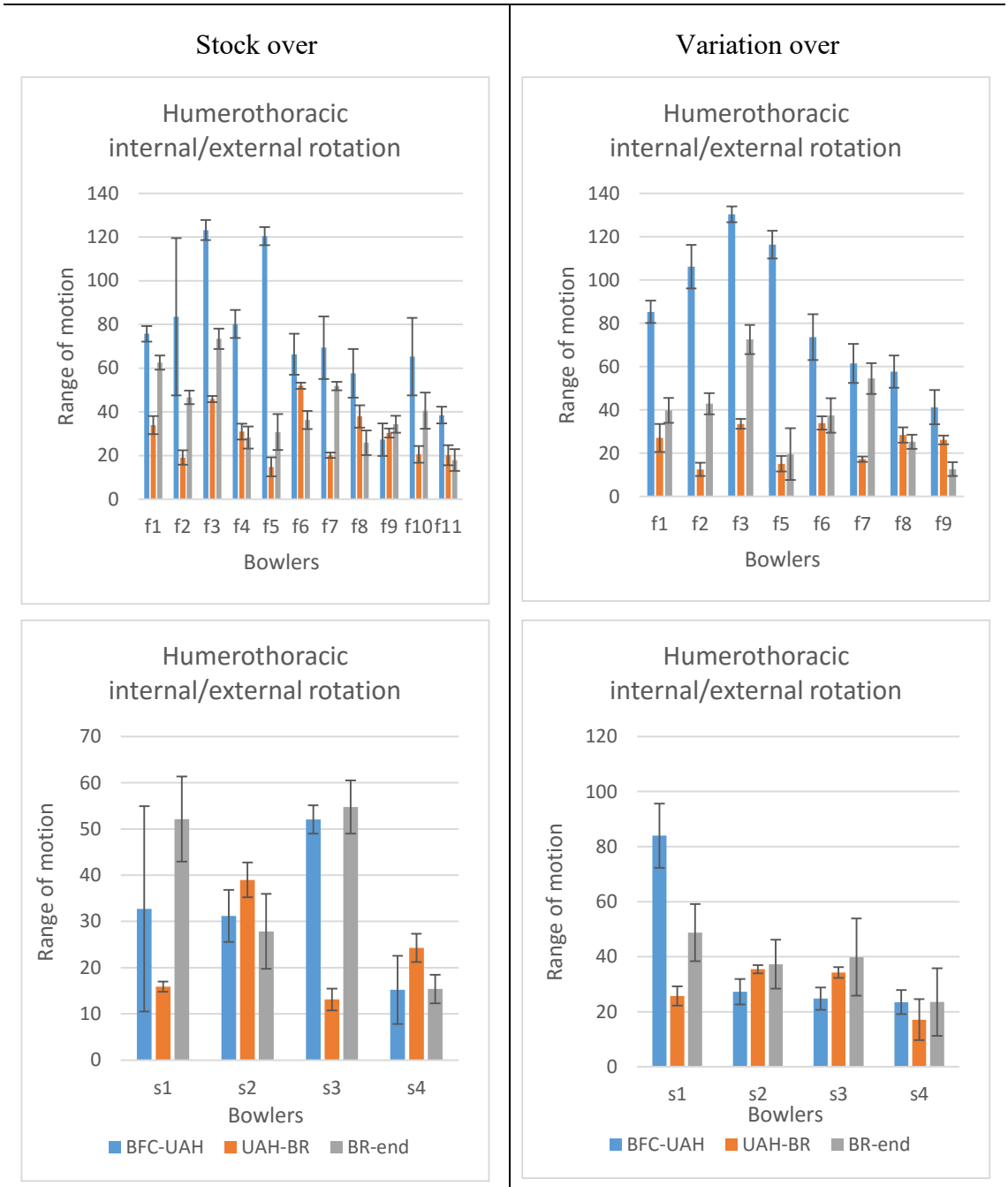

Figure 5.34 Fast and slow bowlers' humerothoracic range of axial rotation for both overs, measured within three phases of the bowling action, BFC- back foot contact, UAH- upper arm horizontal and BR- ball release, mainly internal rotation occurs from BR-end.

5.4.2 Bowling technique parameters

A review of the literature (Ranson et al., 2008; Glazier et al., 2000; Ferdinands et al., 2010; Burnett et al., 1998) identified variables used to classify cricket bowling techniques. These are as follows;

- Humerus angle relative to trunk in the sagittal plane- this was a measure of the anti-clockwise angle between the negative Y-axes of both the thorax and bowling arm. Standing up right with the thorax Y-axis pointing vertically down and the upper arm at UAH, this angle would be 270°.
- Shoulder alignment- this was the angle calculated in the transverse plane, between a vector connecting both left and right glenohumeral joint centres and the global axis parallel along the length of cricket pitch. 180° at back foot contact indicated a side-on action with the bowling shoulder pointing away from the batsman while 270° indicated a front-on action with the shoulder alignment parallel to the bowling crease.
- Shoulder counter rotation (SCR) - this is the change in shoulder alignment angle from back foot contact to the most side-on or minimum shoulder alignment. A value greater than 30° indicated a mixed action.
- Pelvic-shoulder separation (PSS) angle- this is an angle in the transverse plane, between a vector connecting both left and right GH joint centres and the Z-axis (mediolateral) of the pelvis. A value greater than 30° at back foot contact indicated a mixed action.
- Back foot angle- this is an angle in the transverse plane between the X-axis (anteroposterior) of the foot and the global axis along the length of the pitch. An angle of 270° indicated the foot was parallel to the bowling crease.

A shoulder alignment angle of greater than 210° with less than 30° of both SCR and PSS at back foot contact indicated a front-on action. While a side-on action was indicated by a shoulder angle of less than 210° instead with the other two conditions unchanged. If there was greater than 30° of SCR and PSS at back foot contact, this indicated a mixed action (Portus et al., 2004).

A summary of these calculated variables is presented in Table 5-19 while the corresponding standard deviations is shown in Table 5-20.

Other important variables that complete the description of the bowling technique and quality of over is presented in Table 5-20 while Table 5-21 shows the corresponding standard deviations

	Humerus angle relative to trunk in sagittal plane (°)				Shoulder alignment (°)		Shoulder counter rotation (°)		Pelvic-shoulder separation angle (°)				Back foot angle (°)		Bowling action
	Stock		Variation		Stock	Variation	Stock	Variation	Stock		Variation		Stock	Variation	
	UAH	BR	UAH	BR	BFC	BFC	BFC to min	BFC to min	BFC	BR	BFC	BR	BFC	BFC	
f1	283	216	279	206	230	230	12	13	20	52	16	42	308	310	**front-on**
f2	289	217	290	221	210	210	13	13	-17	33	-16	36	332	337	**front-on**
f3	269	173	268	180	226	227	16	18	21	28	24	17	284	283	**front-on**
f4	294	222	-	-	196	-	9	-	16	36	-	-	293	-	**side-on**
f5	286	221	285	227	226	230	39	37	4	8	4	12	332	332	**mixed**
f6	277	152	276	150	223	219	26	26	2	63	0	65	314	315	**front-on**
f7	287	217	289	221	206	214	28	35	5	11	9	7	281	282	**side-on**
f8	273	171	267	176	202	200	5	4	16	15	15	13	265	258	**side-on**
f9	286	192	287	197	199	203	1	5	4	25	9	21	287	282	**side-on**
f10	296	210	-	-	240	-	33	-	17	55	-	-	312	-	**mixed**
f11	276	204	-	-	203	-	4	-	-8	20	-	-	292	-	**side-on**
s1	287	217	289	203	194	196	16	16	-2	42	-3	41	301	303	**side-on**
s2	269	190	272	190	189	185	19	19	6	14	1	29	258	269	**side-on**
s3	280	216	280	207	198	196	13	12	25	7	34	21	233	229	**side-on**
s4	284	186	286	180	188	183	8	7	22	29	20	35	219	221	**side-on**

Table 5-18 Average bowling technique variables calculated for both groups of bowlers and both overs. UAH-upper arm horizontal, BFC-back foot contact

	Humerus angle relative to trunk in sagittal (°)				Shoulder alignment (°)		Shoulder counter rotation (°)		Pelvic-shoulder separation angle (°)				Back foot angle (°)	
	Stock		Variation		Stock	Variation	Stock	Variation	Stock		Variation		Stock	Variation
	UAH	BR	UAH	BR	BFC	BFC	BFC to min	BFC to min	BFC	BR	BFC	BR	BFC	BFC
f1	3	8	4	4	2	2	2	2	1	2	4	4	3	3
f2	3	6	2	4	2	1	1	2	3	5	2	1	3	2
f3	2	3	2	3	3	2	1	2	2	3	3	2	5	7
f4	2	6	-	-	4	-	3	-	2	3	-	-	2	-
f5	4	2	2	8	4	5	4	5	3	3	5	6	3	3
f6	4	8	6	4	1	2	1	1	2	4	1	7	2	3
f7	2	2	2	3	7	7	7	8	3	3	4	1	4	4
f8	5	4	2	3	3	2	2	1	3	3	2	3	4	3
f9	2	5	3	7	2	2	1	2	2	2	2	5	2	3
f10	3	10	-	-	3	-	3	-	4	9	-	-	5	-
f11	3	9	-	-	2	-	2	-	4	3	-	-	7	-
s1	2	5	5	14	4	3	4	3	3	4	1	4	5	3
s2	3	3	2	2	4	2	4	2	2	3	3	2	2	4
s3	2	2	3	6	3	4	4	3	9	4	4	2	4	5
s4	4	15	4	8	3	4	2	3	3	6	3	7	3	7

Table 5-19 Corresponding standard deviations for variables calculated in

	Upper trunk Flexion ROM (°)		Upper trunk lateral ROM (°)		Upper trunk axial ROM (°)		Elbow FE ROM (°)		Ball speed (ms^{-1})		Line (cm)		Length (cm)		Upper arm horizontal to ball release time (s)	
	Stock UAH-BR	Variation UAH-BR	Stock UAH-BR	Variation UAH-BR	Stock UAH-BR	Variation UAH-BR	Stock UAH-BR	Variation UAH-BR	Stock	Variation	Stock	Variation	Stock	Variation	Stock	Variation
f1	42	34	27	25	14	12	6	7	31.81	26.29	33.17	42.69	569.31	722.28	0.0829	0.0875
f2	45	45	35	38	6	5	9	7	26.99	25.47	43.50	39.72	353.66	215.02	0.0983	0.1000
f3	43	41	30	32	35	36	30	29	30.26	27.23	33.09	40.80	766.28	853.72	0.1163	0.1133
f4	42	-	32	-	20	-	6	-	28.15		44.82	-	393.97	-	0.0950	-
f5	34	30	14	14	22	19	12	13	33.60	26.58	59.43	70.19	474.99	685.98	0.0788	0.0900
f6	31	25	32	37	48	50	6	4	29.56	23.34	52.18	21.88	430.89	558.86	0.1179	0.1221
f7	34	33	27	24	7	5	11	10	25.53	24.24	12.13	21.24	590.70	332.62	0.1133	0.1100
f8	31	33	31	30	17	21	10	10	26.67	23.83	57.35	12.34	452.07	377.52	0.1067	0.1079
f9	24	20	28	23	24	17	12	14	27.44	20.20	39.25	60.95	444.78	372.73	0.0921	0.1083
f10	28	-	28	-	18	-	4	-	21.76	-	32.84	-	522.30	-	0.1117	-
f11	62	-	30	-	12	-	10	-	26.58	-	58.77	-	900.21	-	0.1067	-
s1	37	42	38	36	9	10	6	17	18.81	23.02	17.81	37.51	698.33	393.10	0.1133	0.1229
s2	8	12	25	28	35	39	8	6	19.08	24.78	59.91	43.93	397.57	213.04	0.0950	0.0900
s3	2	3	10	19	13	13	11	6	15.86	19.83	28.16	50.45	353.30	721.89	0.1017	0.1050
s4	13	14	26	28	13	19	19	21	19.01	25.44	23.26	46.24	700.03	239.39	0.0933	0.0892

Table 5-20 Other key bowling variables calculated. UAH-upper arm horizontal, BFC-back foot contact. Light green highlights- full deliveries, light blue-good length

	Upper trunk Flexion ROM (°)		Upper trunk lateral ROM (°)		Upper trunk axial ROM (°)		Elbow FE ROM (°)		Ball speed m/s		Line (cm)		Length (cm)		Upper arm horizontal to ball release time (s)	
	Stock UAH-BR	Variation UAH-BR	Stock UAH-BR	Variation UAH-BR	Stock UAH-BR	Variation UAH-BR	Stock UAH-BR	Variation UAH-BR	Stock	Variation	Stock	Variation	Stock	Variation	Stock	Variation
f1	3	5	4	6	2	3	1	1	0.89	0.86	19.27	8.84	233.58	47.68	0.0078	0.0071
f2	3	2	2	1	1	1	2	2	0.72	0.35	14.96	22.99	163.54	158.19	0.0041	0.0000
f3	3	1	4	2	5	4	2	2	0.73	0.68	21.72	18.49	148.32	87.23	0.0041	0.0052
f4	2	-	2	-	3	-	1	-	0.91	-	9.50	-	190.13	-	0.0055	-
f5	2	3	2	5	4	6	3	2	0.51	1.08	19.02	14.64	138.33	44.16	0.0031	0.0063
f6	3	3	2	3	4	6	1	1	1.06	3.41	12.13	21.64	188.47	165.84	0.0060	0.0083
f7	2	1	2	2	2	1	1	1	0.35	0.36	12.82	12.30	160.79	205.53	0.0052	0.0045
f8	3	2	5	5	4	3	2	1	1.18	0.72	14.66	6.57	211.33	162.73	0.0082	0.0040
f9	2	3	2	1	3	3	2	2	1.14	0.59	19.76	26.83	171.56	194.93	0.0075	0.0075
f10	5	-	5	-	4	-	1	-	0.63	-	21.93	-	227.12	-	0.0117	-
f11	2	-	3	-	3	-	1	-	0.66	-	10.09	-	170.72	-	0.0082	-
s1	2	3	1	2	1	1	1	6	0.53	1.76	9.54	35.54	135.74	185.49	0.0052	0.0120
s2	1	2	2	1	2	2	3	2	0.45	0.21	17.84	12.00	70.00	95.63	0.0055	0.0000
s3	1	1	4	1	3	1	1	1	0.52	0.54	16.82	25.56	87.53	330.33	0.0041	0.0055
s4	2	2	4	2	2	3	1	4	0.26	0.45	14.43	24.04	210.41	171.05	0.0106	0.0047

Table 5-21 Corresponding standard deviations for variables calculated in Table 5-20

5.4.2.a Discussion

A second hypothesis brought forward from a review of the literature was that a front-on action with rotator cuff imbalances predisposes a bowler to impingement. As such technique parameters that are commonly used to classify bowling action were calculated and the bowlers were classified as either front-on, side-on or mixed bowling action.

Shoulder alignment, shoulder counter rotation and pelvic-separation angles at back foot contact were used to determine the bowling action. The back foot angle was used as an additional variable if there were any inconsistencies.

In Table 5-18 factors that are attributed to a front on action is highlighted in green while those of a mixed action is highlighted in red. Instances of differing bowling technique between overs were noted however, the bowler was classified based on their stock delivery especially if the values had a high standard deviation. An example of this is subject f7 who was more front-on (214°) and had 35° of SCR in their variation over. However, these were found to be within a margin of error given a standard deviation of greater than 7° (Table 5-19). Back foot angle was generally found to be in agreement with the other variables where a more forward pointing back foot (>290°) was observed in front-on bowlers.

Two fast bowlers were found to have a mixed action showing a significant amount of shoulder counter rotation. All the slow bowlers were found to be side-on with the off-spinners showing a greater counter rotation where s1 showed a much larger trunk flexion and lateral rotation again highlighting the differences in bowling technique for slower bowlers.

The range of motion for upper trunk rotations is shown in Table 5-20. There was a trend where the more experienced fast bowlers displayed greater trunk flexion from an extended position at BFC. There was significantly ($p<0.05$) less upper trunk flexion for the fast bowlers in the period of upper arm horizontal to ball release in their variation over, while the slow bowlers showed greater trunk flexion when bowling their variation over. This illustrates the point that for both sets of bowlers, greater trunk flexion was used to bowl a faster delivery. Also, there was a significantly ($p<0.05$) smaller pelvic-shoulder separation angle at ball release for fast bowlers in their variation over, meaning that both segments were more aligned when bowling a slower delivery. It should be noted that trunk kinematics measured here is not the same as lumbar spine kinematics measured in the literature investigating lower back injuries in fast bowlers. This upper trunk kinematic measure is used as an approximation to allow for comparison between

bowling conditions.

One fast bowler (f3) and two slow bowlers (s1 and s4) exceeded the allowable 15° change in elbow flexion/extension (FE) thereby, making their bowling action illegal (Table 5-20). Subject f3 was one of the fastest bowlers tested and as previously discussed showed a pattern of external rotation followed by rapid internal rotation in the transition to ball release. In addition, their elbow angle was found to be approximately 52° (Appendix 1 and Figure 5.35) and extended their arm by 30° at ball release showing a coupled effect of upper arm internal rotation and elbow extension in bowling their stock delivery. Subject s1's action was illegal for their faster delivery while s4 was illegal for both overs.

(a) (b)

Figure 5.35 Bowler f3 showing significant elbow extension where (a) is 0.04 seconds before ball release and (b) is at ball release.

The ball speeds observed for the fast bowlers show that using a strict classification of fast bowlers (Albernethy, 1981), they could be described as fast-medium bowlers with subject f10 being slow-medium. There was a significant difference ($p<0.05$) observed in ball speed between both overs for all bowlers.

The results of ball length and line shows that all of the balls delivered bounced within the pitch where there was a greater amount of variability in the line compared to length. The values highlighted in light green in Table 5-20 indicated the average length was full at less than 6 meters away from the batting middle stump. Those values highlighted in dark blue indicated a good length while those not highlighted indicated a short length of greater than 8 meters away from the batting stump.

These calculated variables confirm the nature of the bowlers tested, particularly the fast

bowlers, where differences in techniques for bowling their variation is noted. One important consideration that is left to be discussed is the difference between front-on and side-on actions at the shoulder. There is very little empirical evidence in the literature that describes this difference. Anecdotally it is said that front-on bowlers rely more on the rotation of the upper arm at the shoulder in generating speed while side-on bowlers also use the kinematics of the trunk to increase the linear velocity of the shoulder joint and thereby increase the ball release speed. Therefore, it is conceivable that front-on bowlers would put a greater load at the GH joint.

5.5 Conclusion

A description of the methods used to calculated bowling kinematics where the results of the scapula tracker in full speed bowling is presented given the importance of scapula kinematics in upper arm motion. There was a very good repeatability for humerothoracic and scapulothoracic kinematics for all bowlers with only a few exceptions. Analysis of the glenohumeral rotations specifically abduction and axial rotations showed that even though the measured scapula kinematics showed a good repeatability, inconsistencies of low GH abduction angles at ball release and high GH external rotations prior to ball release for a few subjects indicated that scapula kinematics may not have been accurately measured for f5, f6 and f10. The measured scapula kinematics for other subjects was found to be acceptable except for scapula up/down rotations where, measured posterior/anterior tilt was poor especially between 0-100% of the motion and internal/external rotations also over estimated late in the follow through. Regression methods were investigated to predict posterior/anterior tilt but given the limitations of the regression method there is an unwillingness to use it.

For fast bowlers, a greater internal rotation for their faster delivery was not significant, instead the amount of external rotation prior to ball release was the significant technique change. While for slow bowlers, a lower humerus elevation angle at ball release was found to be significant. The GH abduction angle for fast bowlers was between 36° to 80° at the point of ball release with the humerus externally rotated within a range of 90° to 140° at ball release. The GH abduction angle for the slow bowlers was between 66° to 59° at ball release with the humerus externally rotated within a range of 71° to 131° at ball. Due to variability in internal rotation range of motion between bowlers, it was hypothesised that a greater internal rotation torque at the GH joint may explain why slow bowlers are reported as having greater risk of shoulder injuries.

Finally, the classification of bowling technique parameters was done and other useful bowling variables presented to provide a clear picture of the nature of bowlers tested.

The next chapter describes the musculoskeletal modelling process for bowling, detailing the adaptations made to the model.

Chapter 6

Upper limb musculoskeletal modelling of cricket bowling using the UKNSM

This chapter describes the upper limb biomechanical model that was used to predict muscle forces and glenohumeral joint load during bowling. Adaptations to the model and the rationale for doing so are also presented.

6.1 Introduction

Musculoskeletal (MS) models are used to analyse strategies for preventing pathology caused by overuse (van Drongelen et al., 2011), developing ergonomic designs (Arnet et al., 2012) or optimal treatment techniques such as surgery and implant design. Using measured subject specific kinematic and anthropometric parameters as input, MS models can predict muscle and joint forces within the body during movement to study the effect of different parameters such as loading conditions or altered kinematics. In this manner, musculoskeletal models examine the effect of different variables for simulating real life scenarios or simulating phenomena that would be otherwise difficult to carry out experimentally.

In vivo measurement of biomechanical factors are technically and ethically challenging where it is usually limited to measurement of specific muscle forces restricted to a laboratory setting. Musculoskeletal models address many of these issues. They offer a fast and convenient method for testing hypotheses on the behaviour of the musculoskeletal system. However, approximations or simplifications are usually made which tend to limit the power of these models. These limitations include;

- Maximum active muscle stress is limited to a constant value, but studies have shown that it can vary.
- Muscles are modelled as frictionless elements between attachment sites where larger muscles are represented by more than one element or line of action. Simplified muscle force prediction models may not consider muscle co-contraction and proper muscle dynamics.
- Body segment parameters are taken from regression. In addition, Muscle attachments and segment lengths are taken from cadaveric studies where they are scaled based on a linear ratio between the subject and cadaver segment lengths.
- Errors in measured kinematics can significantly affect the model outputs.

For this thesis, the UK National Shoulder Model (UKNSM) was used as it has been previously validated for extreme upper limb activities in addition to being the preference of researchers at Imperial College London. This chapter presents the technical details of the model and adaptations that had to be made in order to use the model for cricket bowling.

The focus of this chapter is to present a technical review of the UKNSM and methods used to overcome various modelling issues in simulating musculoskeletal dynamics of cricket bowling.

6.2 United Kingdom National Shoulder Model

The UK National Shoulder model is a comprehensive 3D inverse dynamic model of the upper limb consisting of six segments, 17 degrees of freedom, 87 muscles and 3 ligament lines of action (Figure 6.1, Table 6-2). The model was developed using segment geometry taken from the Visible Human (VH) male dataset (Spitzer & Whitlock, 1998), muscle data and morphology were taken from Van der Helm et al. (1992) and Johnson et al. (1996) and body segment parameters of mass, centre of mass and moment of inertia were taken from De Leva (1996) regression equations. This validated (Johnson & Pandyan, 2005) MS model has previously been used to look at the shoulder musculoskeletal load for activities of daily living (Pandis, 2013; Charlton, 2003) and pull-ups (Prinold, 2012). All modelling work is done in Matlab v8.6 (The Mathworks Inc., Natick, USA).

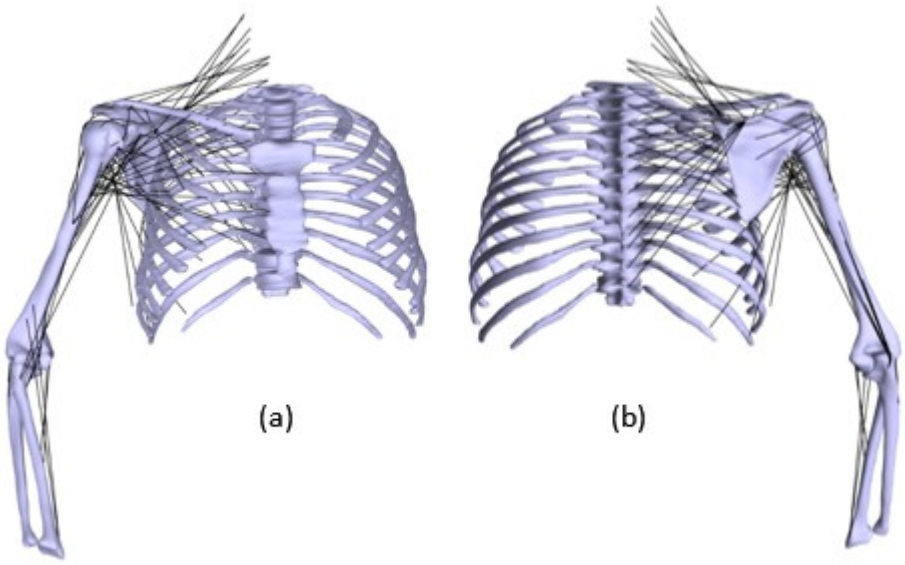

Figure 6.1 Anterior and posterior view of muscle lines of action in the UKNSM

The model has as its input, kinematic data in the form of marker trajectories from the motion capture trials as well as subject specific anthropometrics such as upper segment lengths. An overview of the subsequent steps involved in the calculation is shown in Figure 6.2.

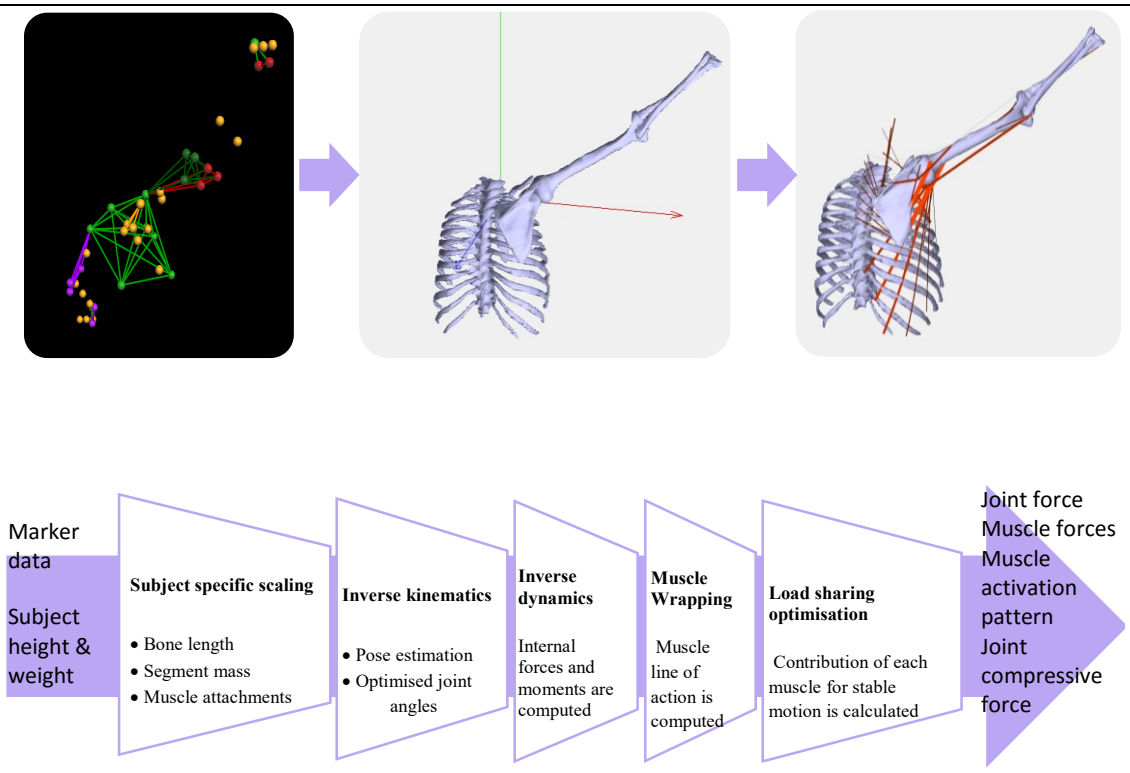

Figure 6.2 Calculation steps involved in the UKNSM. Each step is a separate matlab function where the output is used as the input in the next stage in the calculation.

6.2.1 Scaling

Scaling of segments is important since it has been shown to affect the calculated musculoskeletal load. For instance, the length of the clavicle has been shown to greatly affect kinematics (Charlton, 2003) since it constrains the movement of the scapula and the fact there is an inherent link between clavicle elevation, protraction and scapula kinematics (Karduna et al., 2001). In addition, scapula scaling would also play a major role given the large number of muscle attachments and shape variability across subjects.

Segments are linearly scaled in three dimensions based on the ratio of length with that of the VH dataset. The lengths used for the clavicle, humerus and forearm are simply the lengths between the joint centres along the long axis of each segment. The scapula is scaled based on the length between inferior angle (AI) and acromioclavicular (AC) anatomical landmarks. The thorax is scaled using marker locations to define its length in the orthogonal directions representing height (h), width (w) and depth (d) of the thorax (Figure 6.3) and unlike the other segments is scaled in a non-homogeneous way.

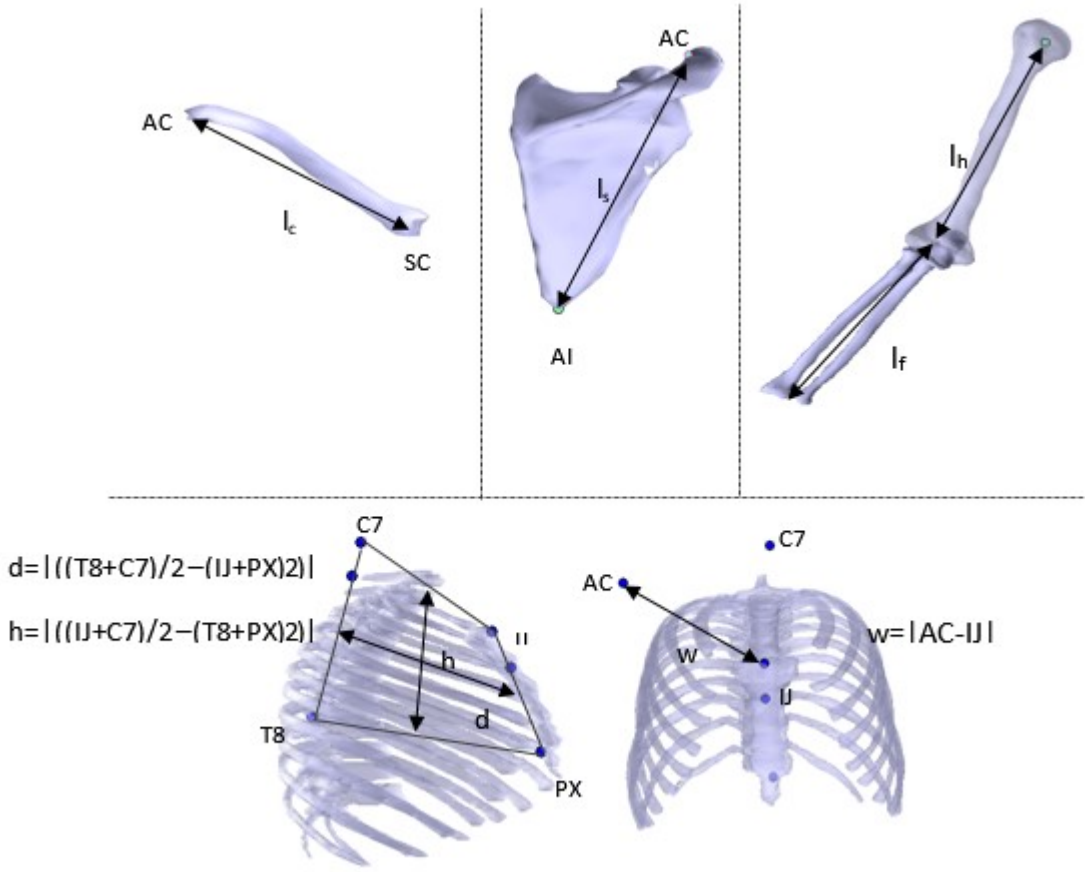

Figure 6.3 Segment lengths used in scaling lc – clavicle length, ls-scapula length, lh-humerus length, lf –forearm length, d-thorax depth, h-thorax height and w-thorax width

6.2.2 Inverse Kinematics

Measured marker trajectories are used as input for defining anatomical coordinate frames and calculating joint kinematics. Included in this input is marker data obtained from a scapula tracker device (Prinold et al., 2011) (Figure 6.4). The glenohumeral joint centre was calculated using a spherical fitting method described by Gamage and Lasenby (2002). A scaled offset from the scapula defined the GH joint centre in the model. This was done to ensure the scaled humerus and scapula formed a coherent joint since this is not guaranteed if the measured GH joint centre was used.

Calculation of joint kinematics was done using the Euler sequences in Table 6-1. Segment coordinate frames are defined as the superior pointing Y, lateral pointing X and posterior pointing Z axes (Figure 6.5).

Figure 6.4 Tracker used to record scapula kinematics during cricket bowling

Articulation	Abbreviation	Sequence used by model
Sternoclavicular	SC	y-z'-x"
Acromioclavicular	AC	y-z'-x"
Glenohumeral	GH	x-z'-y"
Elbow	Elbow	x-z'-y"
Scapulothoracic	ST	y-z'-x"
Humerothoracic polar	SHDpol	y-z'-y"

Table 6-1 Euler sequence for upper limb joint kinematics in the UKNSM

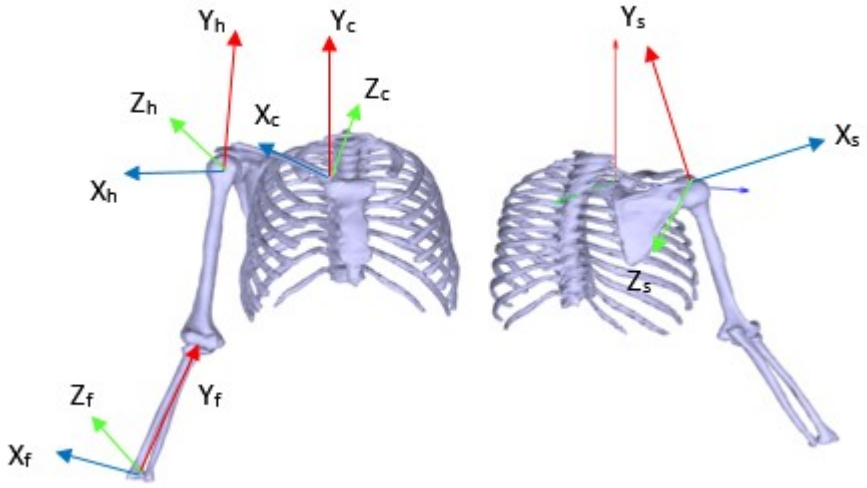

Figure 6.5 Anterior and posterior view of the upper limb segment coordinate frames in the UKNSM (c-clavicle, s-scapula, h-humerus, f-forearm)

There are 17 degrees of freedom (DOF) in the model, namely 6 at the thorax, 3 at the SC joint,

3 at the AC joint, 3 at the GH joint and 2 at the elbow. The spherical GH joint means that translations of the humeral head on the glenoid is not considered in this model.

Elbow kinematics about the x and y-axes, representing flexion/extension and pronation/supination are used for the two DOF joint where these angles are applied to the respective function axis of the elbow (Figure 6.6) to build a rotation matrix that represents the rotation between the forearm and humerus.

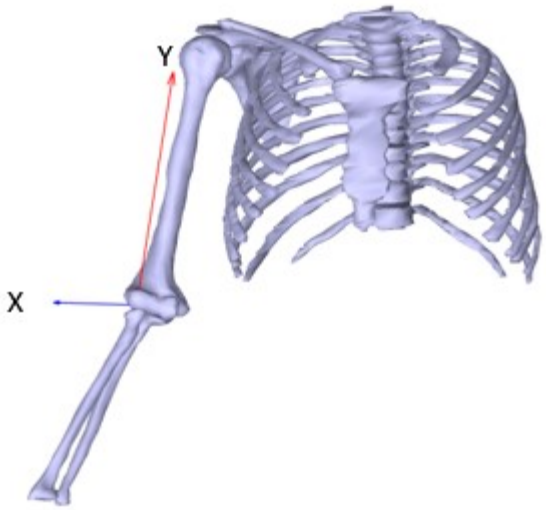

Figure 6.6 Functional X and Y axis for the elbow in the UKNSM for flexion/extension and pronation/supination respectively

Musculoskeletal models are very sensitive to kinematic input (Nikooyan et al., 2010; Charlton & Johnson, 2006) where scapula kinematics have been shown to significantly affect the output (Charlton, 2003; Masjedi & Johnson, 2011). Furthermore, the combination of the SC and AC joint rotations are dependent on the shape of the thorax, clavicle and scapula (Bolsterlee et al., 2014). For these reasons, kinematic optimisation is done to find the best compromise between measured segments kinematics and preventing none physiological positions and orientations. The optimisation routine used was the constrained minimisation function *fmincon* in Matlab v8.6 (Mathworks, Natick, USA) using a sequential quadratic programming algorithm.

The first step in the kinematic optimisation is minimisation of the clavicle axial rotations at the AC joint. A regression equation was used to initially determine the axial rotation of the clavicle depending on the position of the humerus (Barnett et al., 1999). This was then used in the minimisation of rotations at the AC joint as described by van der Helm and Pronk (1995) where

the minimised clavicle axial rotation was then paired with its two other measured rotations. This is done since only two landmarks could be placed to identify the clavicle and therefore its axial rotation is unknown. Once the six total rotations of the sternoclavicular (SC) and scapulothoracic (ST) joints are calculated they are used as direct input into the next step in the optimisation routine. Initially, this combination of six rotations is slightly varied to give 500 unique combinations. This is then used as input into the optimisation routine where it runs for each of the 500 combinations. The combination that resulted in smallest value for the minimised cost functions is then used as input for the time frame. This is done to ensure a global minimum is found in the optimisation. The output of the optimised angles for the 1st frame is then used as input into the 2nd time frame and so on.

There are three methods for kinematic optimisation routines available in the UKNSM all of which use the scapulothoracic gliding plane (STGP) as a major constraint in the optimisation. The STGP is approximated using an ellipsoid fitted to the right side of the rib cage (Figure 6.7) where the interaction between the scapula's medial border and STGP forms the fundamental differences between each optimisation method. The separation of the scapula from the rib cage has been theorised to play an important role since the scapula tilts backwards during overhead activities to avoid impingement of the rotator cuff as well as positioning the scapula to allow stronger moment arms in certain muscles. The ellipsoid STGP is scaled with the thorax for each subject.

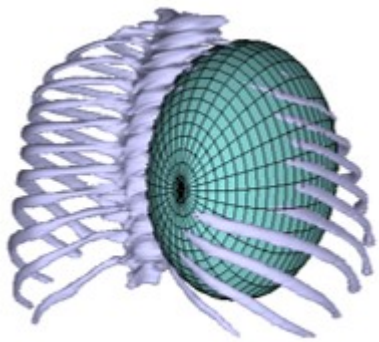

Figure 6.7 Scapulothoracic gliding plane (STGP) ellipsoid

The first method assumes a fixed-closed chain mechanism (Nikooyan et al., 2011; Pronk et al., 1993) where two scapula landmarks; trigonum spinae (TS) and inferior angle (AI) are constrained to lie on the surface of the STGP. In addition, the length of the conoid ligament

calculated at rest is constrained to be constant throughout the motion while the difference between measured and optimised rotations are minimised. Studies have shown that this leads to highly constrained system (Charlton, 2003) in addition to the fact that modelling the STGP as a purely translational joint may be inappropriate due to changes in muscle thickness (Charlton, 2003). This fixed STGP constraint also results in a high model sensitivity to scaling of the thorax and clavicle due to its link to the scapula (Charlton, 2003). The conoid constraint tethers the scapula to the clavicle at the AC joint where both segments move together in clavicle axial rotation. The use of this constraint was found to negatively affect the solution optimisation during pullups (Prinold & Bull, 2014) and coupled with the fact that there is evidence the conoid length increases with greater arm elevation (Seo et al., 2012) makes the use of this constraint inaccurate. The cost function (Equation 6.1) and constraints (Equation 6.2) used in this method are shown below.

$$J_\theta = w_1\left((dC_x^2)\right) + \left(dC_y^2\right) + (dC_z^2) + w_2\left((dS_x^2) + \left(dS_y^2\right) + (dS_z^2)\right) \qquad \text{Equation 6.1}$$

$$AI_{constr} \quad \left\{\left(\frac{AI_x - M_x}{A_x}\right)^2 + \left(\frac{AI_y - M_y}{A_y}\right)^2 + \left(\frac{AI_z - M_z}{A_z}\right)^2 - 1 = 0\right\}$$

$$TS_{constr} \quad \left\{\left(\frac{TS_x - M_x}{A_x}\right)^2 + \left(\frac{TS_y - M_y}{A_y}\right)^2 + \left(\frac{TS_z - M_z}{A_z}\right)^2 - 1 = 0\right\} \qquad \text{Equation 6.2}$$

$$l_{con,constr} \quad \{l_{con,0} - l_{con,sim} = 0\}$$

Where,

dC – difference between measured and optimised acromioclavicular (AC) joint angles,

dS – difference between measured and optimised scapulothoracic joint angles

w_1 & w_2 are weighting factors with values of 1 and 2 respectively.

$l_{con,0}$ & $l_{con,sim}$ are the rest and simulated conoid ligament length.

A & M are semi principal axes lengths and the origin of the STGP ellipsoid respectively.

The second kinematic optimisation method relaxes the constraint on AI and TS. Instead of fixing these points to the STGP they are constrained to lie outside the STGP thereby, preventing the scapula from penetrating the thorax but are unmodified if these points are already outside the STGP ellipsoid. This method does not consider the length of the conoid ligament but uses

the same cost function as the first method for minimisation. The cost function (Equation 6.3) and constraints (Equation 6.4) are shown below.

$$J_\theta = w_1\left((dC_x^2)\right) + \left(dC_y^2\right) + (dC_z^2) + w_2\left((dS_x^2) + \left(dS_y^2\right) + (dS_z^2)\right) \quad \text{Equation 6.3}$$

$$AI_{constr} \quad \left\{\left(\frac{AI_x - M_x}{A_x}\right)^2 + \left(\frac{AI_y - M_y}{A_y}\right)^2 + \left(\frac{AI_z - M_z}{A_z}\right)^2 - 1 > 0\right\}$$

$$TS_{constr} \quad \left\{\left(\frac{TS_x - M_x}{A_x}\right)^2 + \left(\frac{TS_y - M_y}{A_y}\right)^2 + \left(\frac{TS_z - M_z}{A_z}\right)^2 - 1 > 0\right\} \quad \text{Equation 6.4}$$

Where, w_1 & w_2 in this case is set to 0.75 and 2 respectively.

The last optimisation method involves defining the midpoints of AC to AI and AC to TS. Both these midpoints are then constrained to lie outside the STGP. The radial distance between the surface of the STGP ellipsoid to both AI and TS are minimised together with minimisation of the six joint angles and conoid ligament length (Bolsterlee et al., 2014). The cost function and constraints are given by Equation 6.5 and Equation 6.6.

$$\min(J_\theta + wf * J_{con}) \quad \text{Equation 6.5}$$

$$Midpt1_{constr} \quad \left\{\left(\frac{Midpt1_x - M_x}{A_x}\right)^2 + \left(\frac{Midpt1_y - M_y}{A_y}\right)^2 + \left(\frac{Midpt1_z - M_z}{A_z}\right)^2 - 1 > 0\right\}$$

$$Midpt2_{constr} \quad \left\{\left(\frac{Midpt2_x - M_x}{A_x}\right)^2 + \left(\frac{Midpt2_y - M_y}{A_y}\right)^2 + \left(\frac{Midpt2_z - M_z}{A_z}\right)^2 - 1 > 0\right\} \quad \text{Equation 6.6}$$

Where,

$$J_{con} = (dTS_{sim} - dTS_0)^2 + (dTAI_{sim} - dAI_0)^2 + (l_{con,sim} - l_{con,0})^2 \quad \text{Equation 6.7}$$

J_θ is the same as previous methods, $Midpt1$& $Midpt2$ are the midpoints, from AC to AI and AC to TS, wf=0.03, dTS_{sim} & dAI_{sim} are the simulated radial lengths from the STGP surface.

dTS_0 and dAI_0 are reference values of 0.17 cm and 0.67 cm. $l_{con,0}$ was the calculated resting length of the conoid ligament.

6.2.3 Inverse dynamics

The intersegmental joint forces and moments are calculated based on Newton's equations of motion. Once this is done muscle wrapping and load sharing were computed to get the final model outputs.

6.2.3.a Muscle wrapping

After the inter-segmental joint moments have been calculated the next step involves calculating the lines of action and moment arms of each muscle.

Muscles were simulated to wrap around bony segments of the upper limb that were fitted with a geometric wrapping object between its origin and insertion. The geometry of these objects includes an ellipsoid, sphere and cylinder. The muscle wrapping algorithm works by calculating the shortest path from origin to insertion around the wrapping object with the assumption that there is no friction interaction between the muscle and other structures. From its origin (O), the tangential point at which the muscle meets and leaves the wrapping object is known as the effective origin (EO) and effective insertion (EI) respectively (Figure 6.8). The wrapping path is defined by the straight line from origin to EO where it then wraps around on the surface, leaving the surface of the wrapping object at EI to its insertion (I) forming a final straight-line segment. Muscle wrapping only occurs if direct line of sight between the origin and insertion is obstructed by the wrapping object. In this way, muscle paths are calculated for each frame only wrapping if necessary.

Via points (Klein Horsman et al., 2007) were used for the anterior and posterior deltoid as well as the long head of the biceps. Via points are defined by a fix point relative to a segment and is used to constrain a muscle's path (Figure 6.8) as well as to increase the moment arm of the muscle.

A limitation of using wrapping objects in this way is that it leads to unrealistic muscle line of action predications especially when a large range of motion is involved.

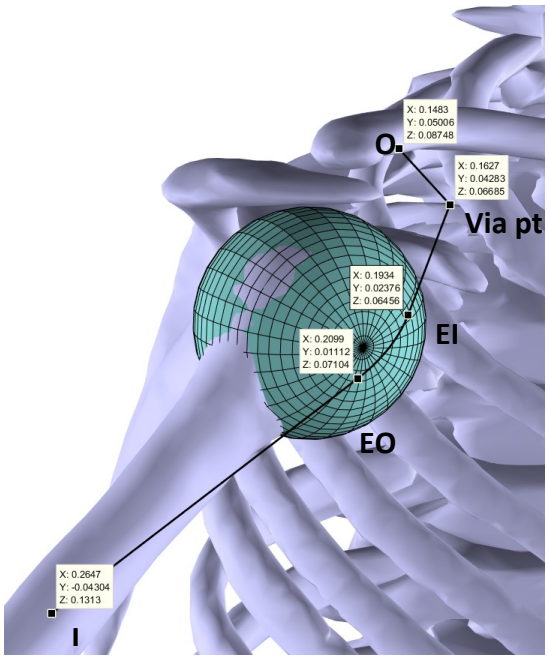

Figure 6.8 Anterior deltoid 2 muscle path around the humeral spherical wrapping object. **O**- muscle origin, **EI**-effective insertion, **EO**-effective origin, **I**-muscle insertion.

There are 16 total wrapping objects in the UKNSM. Three are ellipsoid, two are spherical and the rest are cylindrical objects. Ellipsoids are fitted to the rib cage, spherical objects are fitted to the humeral head and cylindrical objects are fitted to the long axis of the humerus, ulna and radius as well as across the elbow. One additional feature of cylindrical wrapping objects is that the wrapping path can be constrained to wrap in a clockwise or anti-clockwise manner therefore, these objects have been utilised in preventing muscle-flipping issues, particularly at the GH joint.

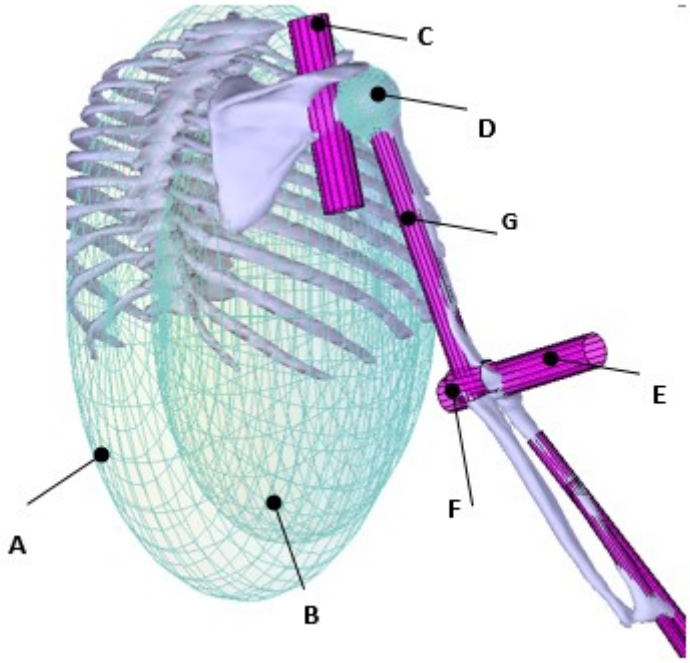

Figure 6.9 Key muscle wrapping objects in the UKNSM. **A**-ellipsoid fitted to entire rib cage, **B**-ellipsoid fitted to right side of rib cage, **C**- cylinder used to prevent flipping of infraspinatus wrapping, **D**-Sphere fitted to humeral head for wrapping rotator cuff, and deltoid, **E**-cylinder across anterior aspect of elbow joint for wrapping biceps, **F**- cylinder across posterior aspect of elbow joint for wrapping triceps and **G**-cylinder fitted along length of humerus.

A combination of wrapping objects are used to better match in vivo muscle paths. In the case of the latissimus dorsi, three wrapping objects (A, D and G shown in Figure 6.9) are used to determine its path. Other muscles that originate proximal to the humerus and insert along its length wrap around a combination of D and G. A summary of the muscles of the UKNSM and wrapping objects is presented in Table 6-2 where a zero indicates that there is no wrapping.

Muscle	Number of divisions	PCSA Cm^2	Primary Wrapping object	Wrapping object segment
Trapeziuz clavicle	3	3.3	0	-
Trapezius scapula	13	9.7	E	Scapula
Levetator Scapulae	4	2.3	E	Scapula
Rhomboid minor	2	1.3	0	-
Rhomboid major	5	4.4	0	-
Serattus Anterior	9	10.5	E	Scapula
Pectoralis minor	3	3.3	0	-
Latissimus Dorsi	5	6.6	E	Thorax
Pectoralis major	10	19	E	Thorax
Deltoid	5	12.2	S	Humerus
Supraspinatus	1	3	S	Humerus
Infraspinatus	3	6	S	Humerus
Subscapularis	3	7.8	S	Humerus
Teres minor	1	2.1	S	Humerus
Teres major	1	4.1	S	Humerus
Coracobrachialis	2	2.04	0	-
Biceps short	1	2.83	C	Ulna
Biceps long	1	2.97	S	Humerus
Triceps long	6	13.42	C	Radius
Brachialis	2	5.24	C	Radius
Anconeous	2	1.6	0	-
Brachioradialis	2	2.14	C	Ulna
Supinator humerus	1	1.51	C	Ulna
Pronator humerus	2	1.04	0	-
Costoclavicular ligament	1	0.205	0	-
Conoid ligament	1	0.495	0	-
Trapezoid ligament	1	1.705	0	-

Table 6-2 Muscle elements and associated wrapping objects and the segments they are fitted to. E-ellipsoid, S-sphere, C-cylinder, 0-no wrapping

Although there is no clear theory that defines the minimum or maximum number of lines of action for each muscle (Van der Helm et al., 1992), the UKNSM derives multiple lines of action muscles (Table 6-2) depending on the fascicular anatomy of the muscle. This discretisation of the muscles has been shown to affect muscle outputs depending on the load-sharing conditions used. Furthermore, the moment arm of a muscle is linked to the force generation capability of that muscle and is dependent on the wrapping path. Therefore, the muscle wrapping calculation plays an important role in muscle load-sharing optimisation.

6.2.3.b Muscle load-sharing optimisation

The final step in the inverse dynamics calculation is distribution of the muscle forces so that moments exerted by the muscles are in equilibrium with the intersegmental joint moments. This is done using muscle load-sharing optimisation that involves solving the indeterminate system ensuring a unique solution of muscle contribution for maintaining stability. In finding a solution, the sum of the squared muscle stresses are minimised (Charlton & Johnson, 2006) (Equation 6.8). In addition, the net GH joint reaction vector is constrained to point within the glenoid rim to avoid dislocation. This was implemented by fitting an ellipse to the glenoid (Figure 6.10) and constraining the force vector within the ellipse. This constraint ensured that the stability of the joint is maintained throughout the motion, where the joint reaction force locus that is plotted is one of the outputs of the model.

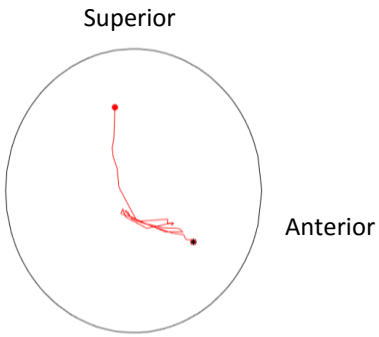

Figure 6.10 Lateral view of the ellipse representing the glenoid rim. The red line shows the locus of GH joint force.

The use of muscle force upper bounds is frequently used in literature but has rarely been investigated during dynamic activity. Musculoskeletal models have been shown to be sensitive if the upper limit of their allowable force is reached (Southgate et al., 2012). The maximum allowable stress for all muscles was set to $100Ncm^{-2}$ therefore, the muscles' PCSA determines the maximum force for each muscle in the load-sharing optimisation. Table 6-2 shows the PCSA of all the muscles in the UKNSM. These values are used for all subjects since PCSA is not scaled.

$$\sum_{i=1}^{i=87} \left(\frac{F_i}{PCSA_i}\right)^2$$

Equation 6.8 Load-sharing optimisation cost function in UKNSM. F_i-force of ith muscle

The conoid ligament was assumed to have a constant strain of 10% since its length was not calculated based on scapula and clavicle kinematics due to the high sensitivity to scaling and measured kinematics of these segments in the kinematic optimisation.

Muscles are modelled as frictionless, massless elements with a uniform tension throughout. The use of a muscle model that incorporates the effects of muscle activation dynamics, velocity-force and force-length relationships is outside the scope of this thesis. Furthermore, high speed and extreme range of motion are sensitive to these parameters (Winters & Stark, 1985) and as such would add even more complexity to the model.

6.2.4 Ball weight implementation

The ball was added to the model by constraining the centre of mass of the ball a fixed distance away from the wrist, and effectively adding the mass of the ball to the forearm. The distance used was half the original length of the hand. The mass was then removed at the point of ball release. The reason for this implementation was that the wrist joint and hand was not modelled. A mass of 163 grams was used for the ball.

6.3 Modifications to the UKNSM

The importance of subject specific MS models is clear, however there is currently a lack of coherent scaling method and robust calculation of kinematics representative of subject measured kinematics. For this reason, the UKNSM in its current form was found to be unsuitable for modelling the cricket bowling action where these limitations in scaling and kinematics optimisation also manifest in muscle wrapping errors and therefore affecting the output of the model. This section presents changes made to the model, mainly focused on kinematic optimisation and muscle wrapping.

6.3.1 Kinematic optimisation changes

The motivation behind changing the kinematic optimisation was because none of the methods currently implemented provided a robust solution where the scapula was in an acceptable physiological position and there were minimum unsolved frames. To highlight the problems of

each method, six trials of a fast bowler (f4) were used.

The first method was shown to be unsuitable for less extreme motions where it was found to too constraining as discussed in section 6.2.2. Therefore, it is expected to be unsuitable for bowling. This method was found to be the least robust resulting in the most unsolved frames in load-sharing and poor scapula position. The implication of using such constraints means that the scapula kinematics would be greatly altered since its movement is influenced by the shape of the STGP and the conoid length constraint. This is confirmed by Figure 6.11, which shows the poor scapula position on the STGP.

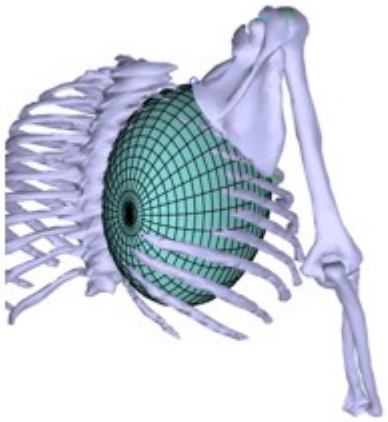

Figure 6.11 Improper scapula position when using kinematic optimisation using method 1 for bowler f4. This occurs when the constraints are satisfied and optimisation successfully ran therefor showing method 1 is unsuitable.

The inconsistency of this kinematic optimisation method is illustrated in Table 6-3 showing the average RMS difference for sternoclavicular and scapulothoracic joint rotations for six trials of fast bowling where the difference was greater than 20° for measured scapula kinematics.

	$SC_X(°)$	$SC_Y(°)$	$SC_Z(°)$	$ST_X(°)$	$ST_Y(°)$	$ST_Z(°)$
RMS difference	79.33	9.10	21.93	20.18	36.42	30.13

Table 6-3 Average RMS difference for sternoclavicular (SC) and scapulothoracic (ST) joint rotations for bowler f4 between optimised and none optimised joint angles using kinematic optimisation method 1

The second method showed that softer constraints did indeed result in a better output. However, one of the limitations of the scapula tracker that was discussed was that it was over estimated anterior/posterior tilt. So in the event of exaggerated anterior tilt, no optimisation occurred since the constraints of AI and TS being outside the STGP are satisfied. This results in a sizable gap

between AI and STGP. Conversely, when optimisation was required it resulted in a poor scapula position due to an increase in clavicle retraction and depression when trying to satisfy the constraints (Figure 6.12). This poor scapula position consistently occurred when the arm was near upper arm horizontal and when the clavicle was already retracted. As the arm moves to ball release, it eventually corrected itself to a physiological position.

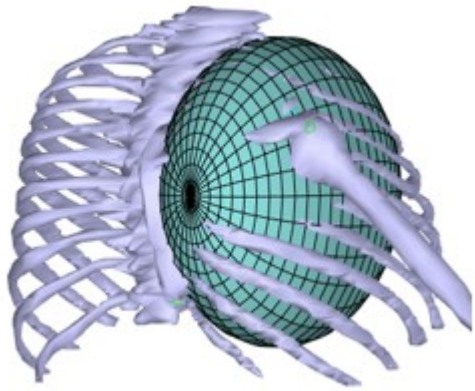

Figure 6.12 Poor scapula position due to excessive changes in clavicle kinematics when using optimisation method 2 for bowler f4. The optimisation ran successfully with the constraints satisfied.

The average RMS difference between optimised and none optimised kinematics show moderate changes consistency (Table 6-4) however, the changes in clavicle kinematics were found to unacceptable.

	$SC_X(°)$	$SC_Y(°)$	$SC_Z(°)$	$ST_X(°)$	$ST_Y(°)$	$ST_Z(°)$
RMS difference	0.00	19.28	11.53	8.53	9.94	3.89

Table 6-4 Average RMS difference for sternoclavicular (SC) and scapulothoracic (ST) joint rotations for bowler f4 between optimised and none optimised joint angles using kinematic optimisation method 2

The third method also resulted in poor scapula positions. Since the medial border was not constrained to lie outside the STGP but rather its distance to the surface of the STGP was minimised, it resulted in the medial border clipping into the rib cage while the midpoints constraints were satisfied (Figure 6.13).

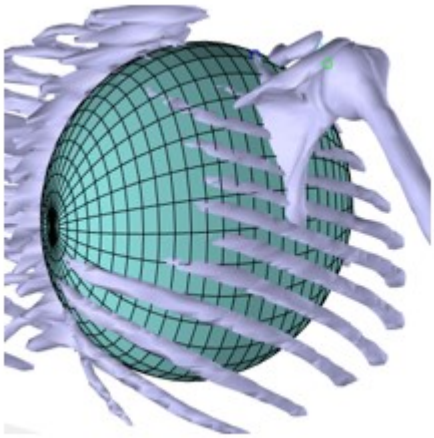

Figure 6.13 Optimised kinematics for bowler f4 using method 3. The scapula medial boarder clips into rib cage even though optimisation was successful.

The RMS differences show a good consistency across the trials where the maximum difference between optimised and none optimised joint angles was 1.68° recorded for scapula protraction/retraction (Table 6-5). The small differences in this method meant that there was very little changes made to calculated joint kinematics and is representative if no optimisation is used. Therefore, the problems experienced in this method further highlight the need for a proper kinematic optimisation solution.

	SC_X(°)	SC_Y(°)	SC_Z(°)	ST_X(°)	ST_Y(°)	ST_Z(°)
RMS difference	0.11	1.44	0.21	0.15	0.15	0.61

Table 6-5 Average RMS difference for sternoclavicular (SC) and scapulothoracic (ST) joint rotations for bowler f4 between optimised and none optimised joint angles using kinematic optimisation method 3

The process of finding an acceptable solution started with adjusting the weighting factors in the cost functions of methods 2 and 3. This was found to have very little effect on the major problems of both methods. Then the upper and lower bounds for each of the six angles were limited to prevent excessive changes to the kinematics. This was found to work with limit effect however, there was occasionally the case when the optimised angles would reach the upper or lower bounds, plateauing resulting in a static scapula during humerothoracic rotations. These minor changes were found to be unacceptable since the underlying problem of both methods stems from the constraint definition. The new optimisation method would need to strike a balance between methods 2 and 3 where the optimised angles are close to the measured ones with an acceptable scapula position. In addition, the method would have to attenuate the

exaggerated anterior/posterior tilting in the measured scapula kinematics.

For the new kinematic optimisation, AI was constrained to move between the original STGP ellipsoid and another concentric ellipsoid where there was 3cm between their surfaces (Equation 6.10). In addition, the acromioclavicular (AC) joint was constrained so that it did not go into the STGP thereby preventing excessive clavicle depression. The original constraint for TS was not changed. The cost function (Equation 6.9) was also adjusted to reduce the weighting on scapula posterior/anterior tilt and increase the weighting on scapula pro/retraction and elevation. These optimisation parameters showed good potential however there were cases when the optimised scapula internal/external rotation deviated from the measured value by more than 21° in favour of internal rotation. Further investigation identified the major issue was the non-homogeneous scaling of the thorax. This scaling sometimes resulted in a stretched ellipsoid in the anterior-posterior direction and relatively shorter in the width in the medial-lateral direction. This effectively reduced the STGP surface at the back of the rib cage causing excessive internal rotation in the phase of upper arm horizontal to ball release. A solution that was investigated involved taking the width of the thorax (w in Figure 6.3) to homogeneously scale the thorax thereby ensuring a good STGP shape however it was found that this had a limited impact on the much larger issues in the model and therefore the default thorax scaling was used.

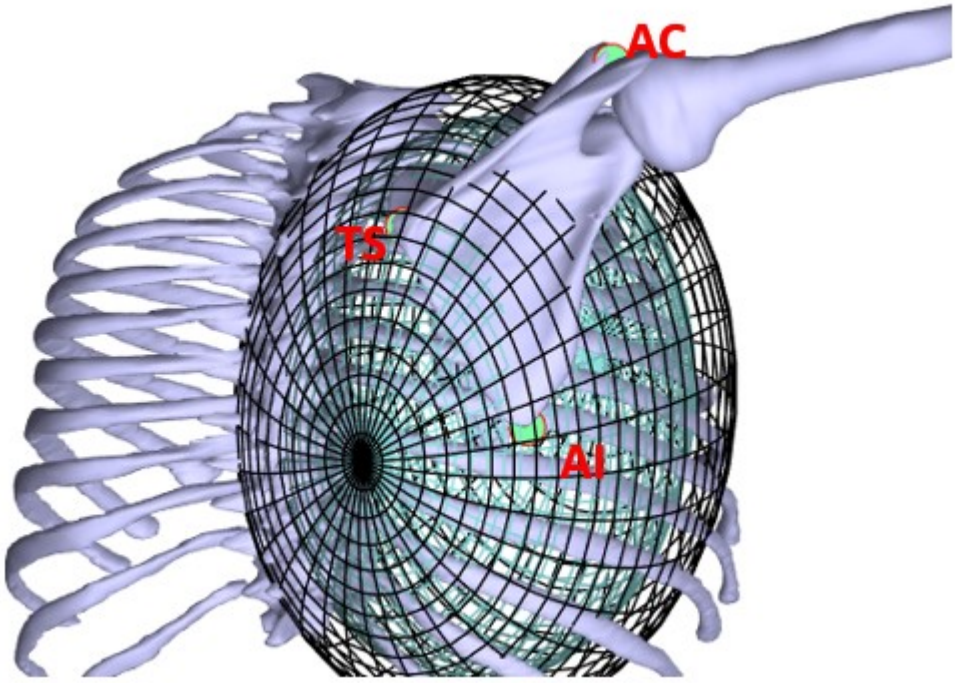

Figure 6.14 Posterior view of the shoulder showing new constraints used. AI constrained between both ellipsoids, TS and AC constrained to be outside the original STGP ellipsoid.

An ellipse fitted to the rib cage with TS and AI digitised in a cadaver study showed that the separation of these points to the STGP was 3.32cm and 2.42cm respectively. For this reason, a value of 3cm separation between both concentric ellipsoids was chosen so that they were within physiological bounds. Intuitively, the occasion where the scapula separation may be greater than this would involve heavily loaded activates as oppose to the case of a freely rotating arm in bowling. Therefore, these values may be acceptable. There is no published work on this separation during dynamic activities. Given this limitation and together with limitations in scapula scaling where, the homogeneously scaled scapula may not match the subject's scapula and the curvature of the rib cage, the separation value chosen was found to be a good compromise based on the improvements in the optimisation routine.

$$J_\theta = w_1\left((dC_x^2)\right) + 2 * \left(dC_y^2\right) + 2 * (dC_z^2) + w_2\left(0.5 * (dS_x^2) + \left(dS_y^2\right) + (dS_z^2)\right) \quad \text{Equation 6.9}$$

$$AI_{constr1} \quad \left\{\left(\frac{AI_x - M_x}{A_x}\right)^2 + \left(\frac{AI_y - M_y}{A_y}\right)^2 + \left(\frac{AI_z - M_z}{A_z}\right)^2 - 1 > 0\right\}$$

$$TS_{constr1} \quad \left\{\left(\frac{TS_x - M_x}{A_x}\right)^2 + \left(\frac{TS_y - M_y}{A_y}\right)^2 + \left(\frac{TS_z - M_z}{A_z}\right)^2 - 1 > 0\right\}$$

Equation 6.10

$$AC_{constr2} \quad \left\{\left(\frac{AI_x - M_x}{A_x}\right)^2 + \left(\frac{AI_y - M_y}{A_y}\right)^2 + \left(\frac{AI_z - M_z}{A_z}\right)^2 - 1 > 0\right\}$$

$$TS_{constr2} \quad \left\{\left(\frac{TS_x - M_x}{A_x + k}\right)^2 + \left(\frac{TS_y - M_y}{A_y + k}\right)^2 + \left(\frac{TS_z - M_z}{A_z + k}\right)^2 - 1 < 0\right\}$$

where k=3cm

The new optimisation avoided problems associated with the other methods showing an acceptable scapula position over the range of motion (Figure 6.15).The RMS difference was found to be greatest for scapula posterior/anterior tilt (Table 6-6). This is expected given the measurement errors for this rotation. There was also an increase in internal rotation of 13.97° which was the largest value recorded for all the subjects. This is also expected since AI on the scapula is constrained to move between the two ellipsoids and must conform to the shape of these scaled objects. On the other hand, there was little change to scapula up/down rotations and clavicle rotations. Given that scapula internal/external and anterior/posterior rotations are small compared to up/down rotation, it is expected that the measurement error associated with these two rotations will be greater hence, the larger changes due to optimisation may not be that inappropriate. In addition to improved agreement with measured rotations, there was a better continuity of the optimised rotations with fewer jumps in the rotations angles.

	$SC_X(°)$	$SC_Y(°)$	$SC_Z(°)$	$ST_X(°)$	$ST_Y(°)$	$ST_Z(°)$
RMS difference	0.00	4.05	13.91	23.11	13.97	2.49

Table 6-6 Average RMS difference for sternoclavicular (SC) and scapulothoracic (ST) joint rotations for bowler f4 between optimised and none optimised joint angles using new the kinematic optimisation

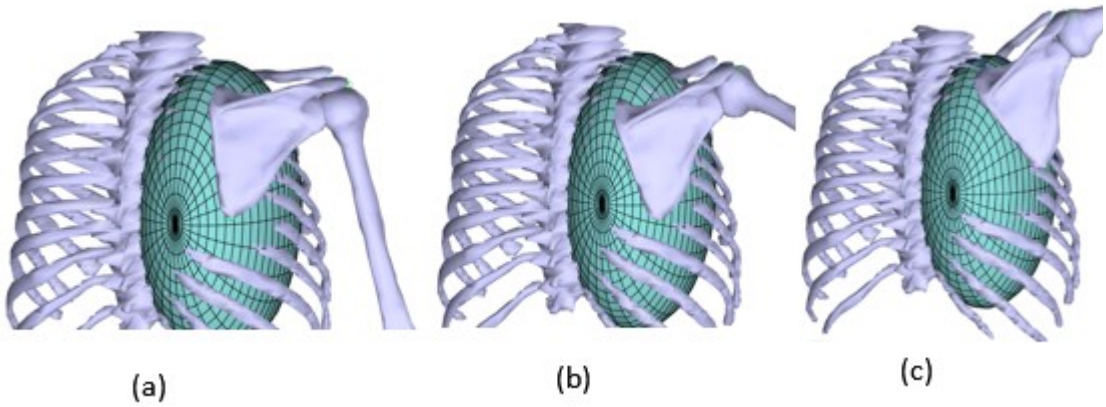

Figure 6.15 Scapula position using new kinematic optimisation for bowler f4 at the point of (a) upper arm vertical (b) upper arm horizontal (c) near ball release.

6.3.2 Muscle wrapping changes

Muscle wrapping issues arise when the muscle path drastically changes, often flipping to the other side of the joint during motion. As a result of this there is a sign change in the muscle's applied moment, effectively changing the function of the muscle to one that is not physiological. This muscle wrapping problem is one of the limitations of using a wrapping method that defines the muscle path to be the shortest distance between the origin and insertion around the wrapping object. For cricket bowling, this was found to be a major issue at the GH joint where muscles anterior to the joint would flip to the posterior side when the arm was extended and externally rotated near upper arm horizontal. The problematic muscles are presented using data from fast bowler f1. Included in this data is the muscle's moment arm about the GH joint in the humerus coordinate frame. Moment arms are compared to the literature. One limition of this is that the motion reported in this thesis are near terminal ranges of GH extension and external rotations while the relavent studiest report moment arms during axial rotation of the humerus and abduction in the sagittal plane or flexion in the coronal plane.

6.3.2.a Subscapularis

The subscapularis wraps around a spherical wrapping object centred on the humeral head to maintain its line of action during motion. Via points were also used. They were computed as the midpoint between the EI and EO and defined before glenohumeral elevation falls below 30°. These points were then used to constrain the muscle path throughout the motion.

Figure 6.16 shows where the three subscapularis elements for fast bowler f1 slides to the

posterior side of the GH joint despite the use of via points. This occurs during extension and external rotation of the humerus in the period before and after upper arm horizontal. As the arm continues to rotate and is anterior to the scapula, a normal line of action is restored as the elements slide forward.

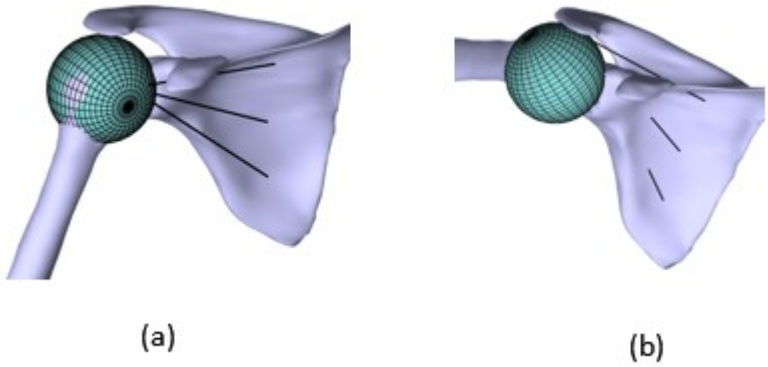

Figure 6.16 Anterior view of the GH joint showing (a) good subscapularis wrapping at the start of the bowling action (b) the subscapularis flipping to the posterior side when the arm is at upper arm horizontal.

The moment arm change due to this flipping is shown in Figure 6.17. The function of the subscapularis changes from an internal rotator of the humerus to an external rotator. Moment arms shown are averaged over the six trials for bowler f1 showing that it occurred consistently.

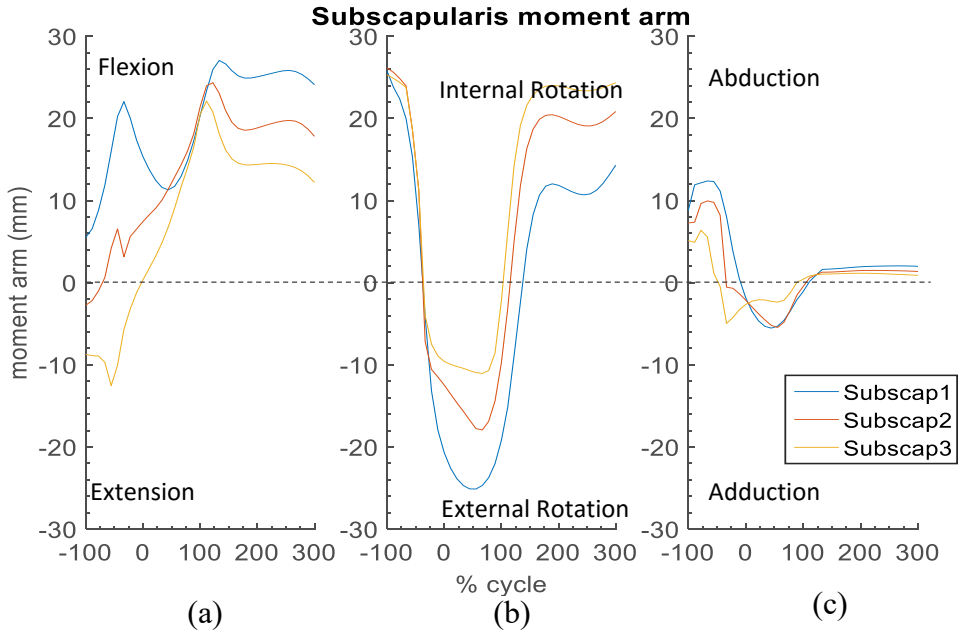

Figure 6.17 Subscapularis moment arm changes from internal rotation to external rotation before upper arm horizontal. Average moment arms are plotted for bowler f1 where 0-100% represents upper arm horizontal to ball release. (a) flexion/extension (b) internal/external (c) abduction/adduction moment arms

This problem was solved using a cylinder centred at the GH joint that is tethered to the scapula. The diameter of the cylinder was the same as the humeral head and was also parallel the Y axis of the scapula. This newly implemented wrapping object managed to keep the subscapularis wrapping around the anterior aspect of the GH joint (Figure 6.18) over the range of motion in cricket bowling.

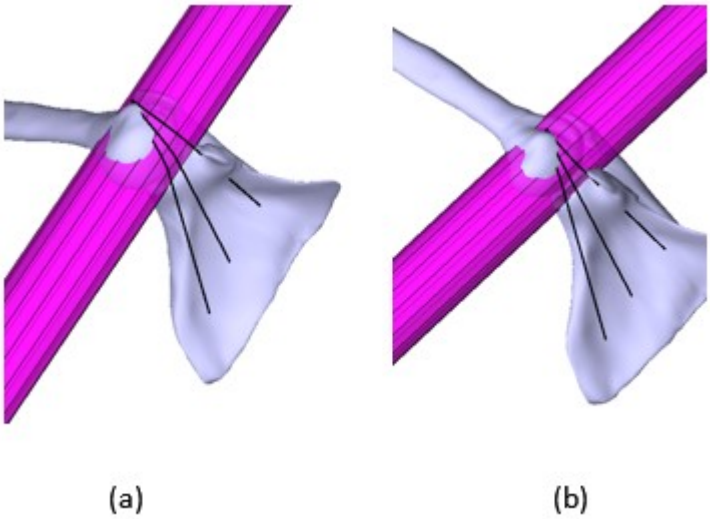

Figure 6.18 Anterior view of the GH joint showing successful subscapularis wrapping at (a) upper arm horizontal and (b) ball release.

Changes to the moment arm in this muscle is presented in Figure 6.19. In addition to avoiding the drastic change from an internal to external moment, there was an increase in the muscle's flexion and adduction moments in the phase of upper arm horizontal to ball release. The results show a good agreement with the literature where Ackland and Pandy (2011) showed that at 90° of external rotation when the arm was abducted to 120°, the internal rotation moment was reduced near to zero where subscap1 element began to have a small external rotation moment. The larger external rotation moment seen here maybe due to more externally rotated humerus prior to ball release and small sliding movements of the subscapularis elements relative to each other. The reduction in the internal moment arm of the subscapularis coincided with large a flexion and adduction moment arm showing that the action of the muscle was mainly used to keep humerus tethered to the scapula when the humerus was elevated.

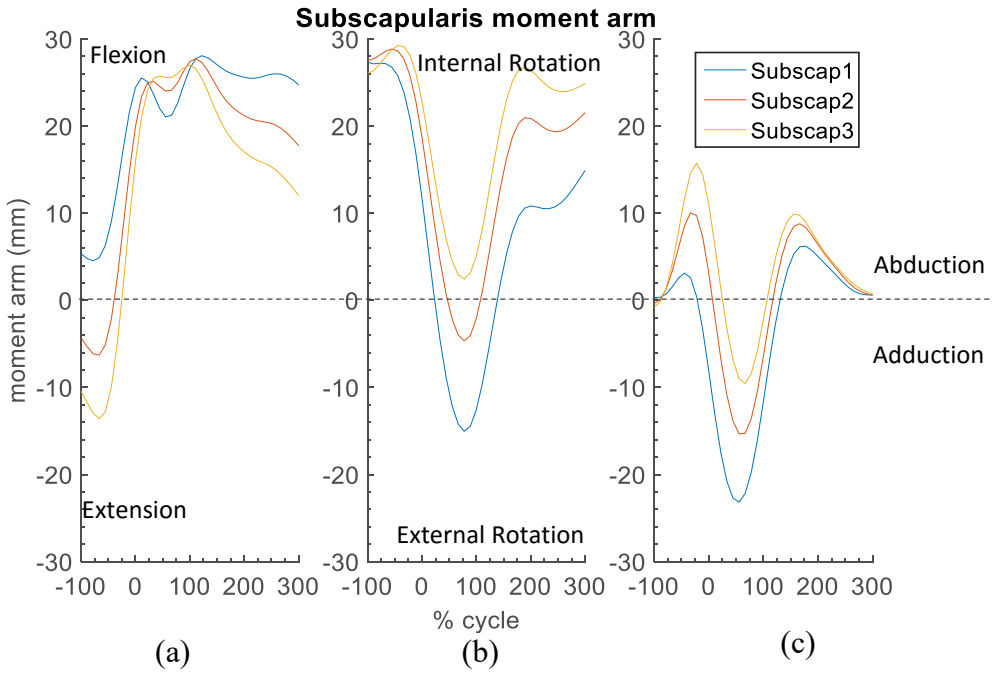

Figure 6.19 Subscapularis moment arm using new wrapping object. The sudden change from an internal moment to external one before upper arm horizontal did not occur. Subscap1-3 are the superior, middle and inferior elements. Average moment arms are plotted for bowler f1 where 0-100% represents upper arm horizontal to ball release. (a) flexion/extension (b) internal/external (c) abduction/adduction moment arms

6.3.2.b Anterior deltoid

The two anterior elements of the deltoid also suffered muscle-flipping issues. In this case, there were measures in place to prevent flipping however, they were found to be ineffective for the bowling action. These measures included the use of a cylindrical wrapping object and a via point. Figure 6.20 Shows how these were implemented. Under normal circumstances, the anterior deltoid would wrap around the humeral head unless it began to flip and came into contact with the wrapping cylinder. The wrapping cylinder was used to prevent flipping in only the lateral anterior deltoid element.

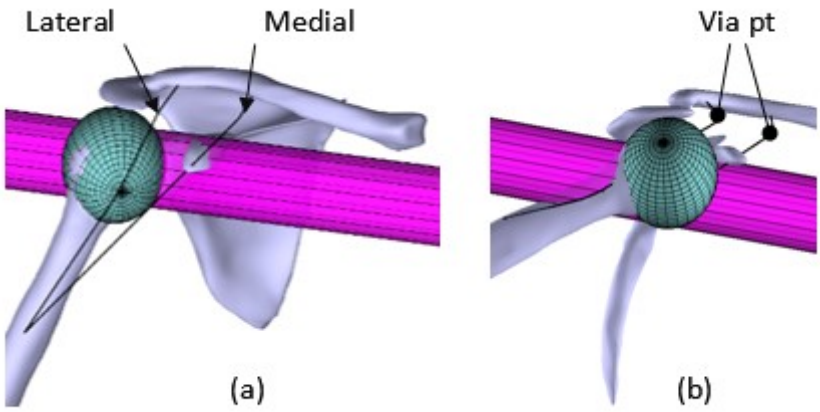

Figure 6.20 (a) Anterior view of both anterior deltoid at the start of motion (b) lateral view showing the lateral deltoid element wrapping around the cylinder however passing through the humerus while the medial element wraps around the sphere but flips inferior to the GH joint.

The resulting moment arm of this change in muscle path is shown in Figure 6.21, where there was a change from flexion to extension moments just before upper arm horizontal. The cylinder used to prevent flipping did have an effect since the extension moment arm would be larger if there was a complete flip to the posterior side of the joint.

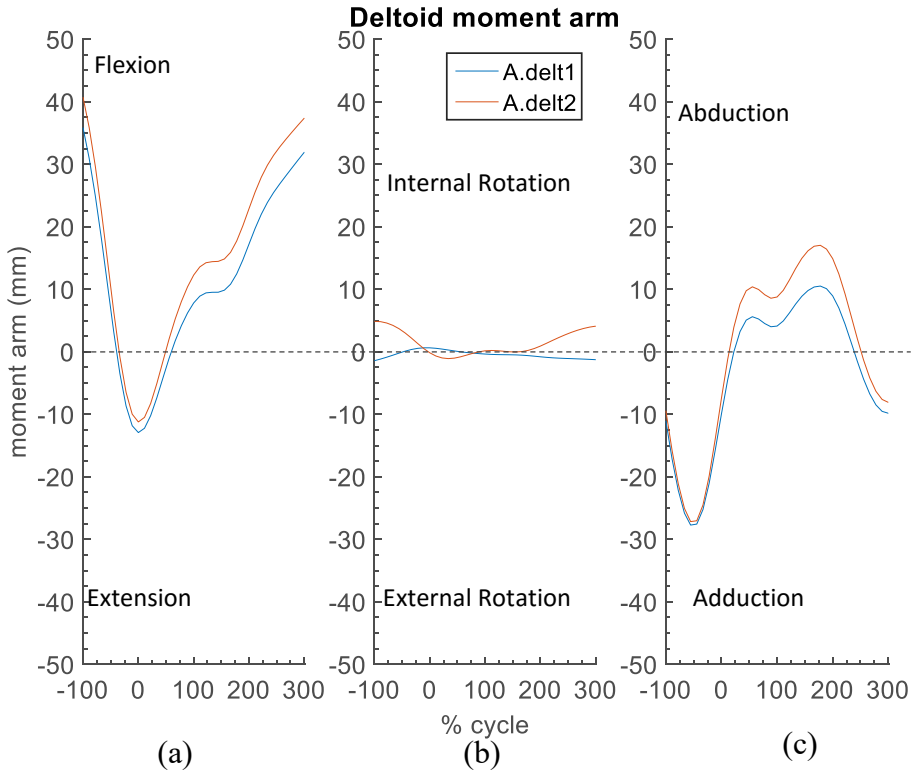

Figure 6.21 Average anterior deltoid moment arm for bowler f1.Both elements show an extension moment arm before upper arm horizontal where the muscle flipping was observed. A.delt1-medial sting, A.delt2- lateral element. 0-100% represent upper arm horizontal to ball release. (a) flexion/extension (b) internal/external (c) abduction/adduction moment arms

A second wrapping cylinder was designed to address this problem. This cylinder was also located at the GH joint centre, had the same diameter as the humeral head and was tethered to the movement of the scapula. In this case however, the cylinder was titled 10° anteriorly and 30° of adduction relative to the scapula. This was done to keep the muscles wrapping on the anterior aspect of the joint. In addition, the idea behind tilting the cylinder in the anterior direction was to cater for posterior tilting of the scapula. If the object was not tilted this way, then the wrapping object move ahead of the humerus during posterior tilting of the scapula giving a poor approximation of the humeral head. The performance of this wrapping object was found to be much better (Figure 6.22) when compared to the current implementation.

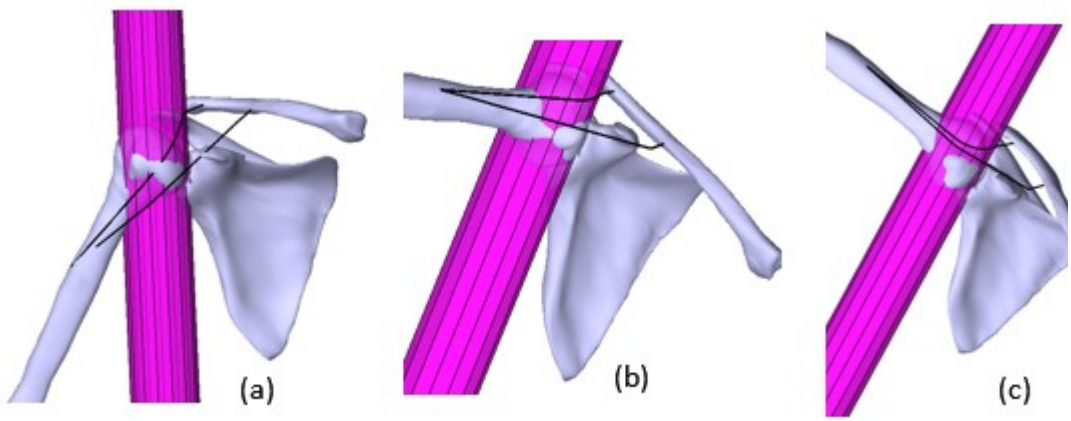

Figure 6.22 Anterior view of the GH joint showing new anterior deltoid muscle wrapping at (a) start of the bowling (b) upper arm horizontal (c) ball release. The muscle paths constrained by this new wrapping object was found to be better than the currently implemented one.

Together with a reduction in the flexion moment before upper arm horizontal, there was a greater adduction and abduction moment in the period before upper arm horizontal and ball release respectively (Figure 6.23).

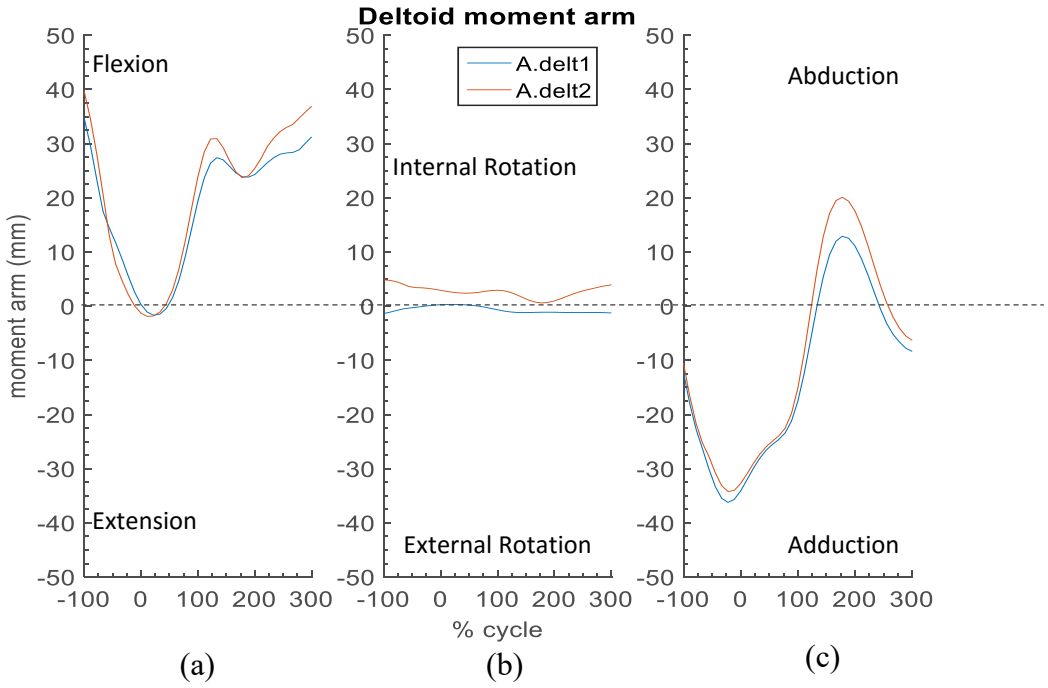

Figure 6.23 Improved anterior deltoid moment arms using the new wrapping object. A noticeable decrease in the extension moment as well as an increase in both abduction and adduction moment were observed. (a) flexion/extension (b) internal/external (c) abduction/adduction moment arms

6.3.2.c No muscle wrapping

Another major issue in the current muscle wrapping was that there was no wrapping for the anterior muscles around the humeral head. This resulted in the muscle paths passing through the humeral head close to the GH joint centre (Figure 6.24). This meant that the moment arm for these muscles would be small, thus effectively reducing the mechanical advantage of these muscles and their force producing capability in the load-sharing optimisation. Another issue is highlighted by the pectoralis major that originate from the clavicle. The function of this muscle is reversed since the line of action is posterior to the GH joint centre when the humerus is extended. Therefore, these muscle elements would incorrectly have an extension moment arm that is calculated within the model. Similar to the muscle flipping issues, this problem was worse when the arm was extended and externally rotated during the bowling action. A summary of affected muscles is shown in Figure 6.24.

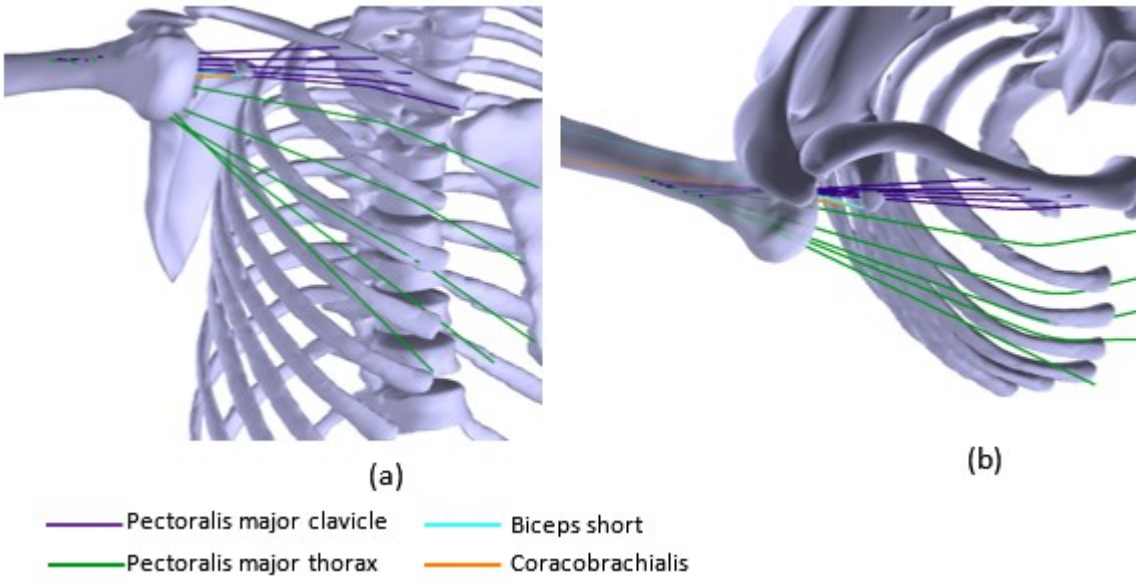

Figure 6.24 Muscles that have no wrapping at the GH joint shown from (a) anterior view (b) superior view at upper arm horizontal

The cylindrical wrapping object used for correcting the anterior deltoid was used for these muscles. Figure 6.25 shows the improvement that the new wrapping makes. Moment arms of these muscles are shown in Appendix 3.

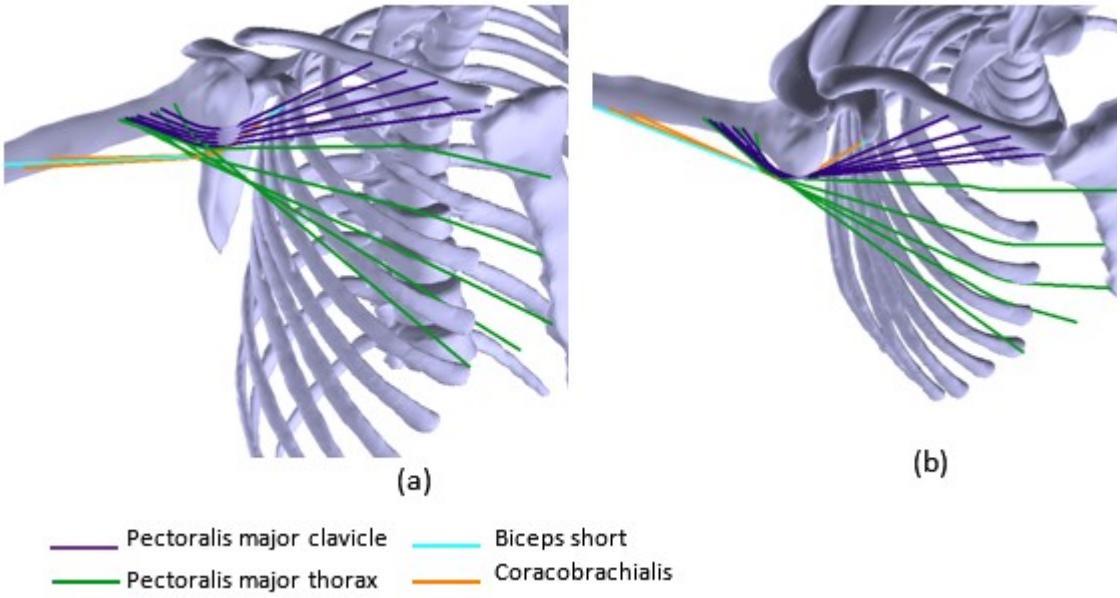

Figure 6.25 Muscles with no previous wrapping are shown here to wrap around the humeral head after using the new wrapping object. (a) anterior view (b) superior view

6.3.3 Other changes

The cost function in the muscle load sharing was changed so that the sum of the cubed muscle stresses is minimised (Equation 6.11). This was done to lower the high muscle force output of the model where higher powers have been shown to have a more significant effect on muscle forces (Cleather & Bull, 2010). In many cases, it was not possible to find a solution given the original muscle bounds in the model. Instead of arbitrarily adjusting the force bounds by increments for each subject, a base value of five was used and compared to an upper bound of 10,000 times the original value. The results of this is presented in the next section. Given the cost function used the upper bound will only influence muscle recruitment when this limit is reached and the smaller PCSA values used in the UKNSM compared to other upper limb models might also help justify (Prinold, 2012) the increase in muscle upper bounds.

$$\sum_{i=1}^{i=87} \left(\frac{F_i}{PCSA_i}\right)^3$$

Equation 6.11 Altered Load-sharing optimisation cost function in UKNSM. F_i- force of ith muscle

In addition to the technical changes made, various improvements to the model visualisation were made where a GUI was built to quickly load processed trials with an included playback

feature (Figure 6.26).

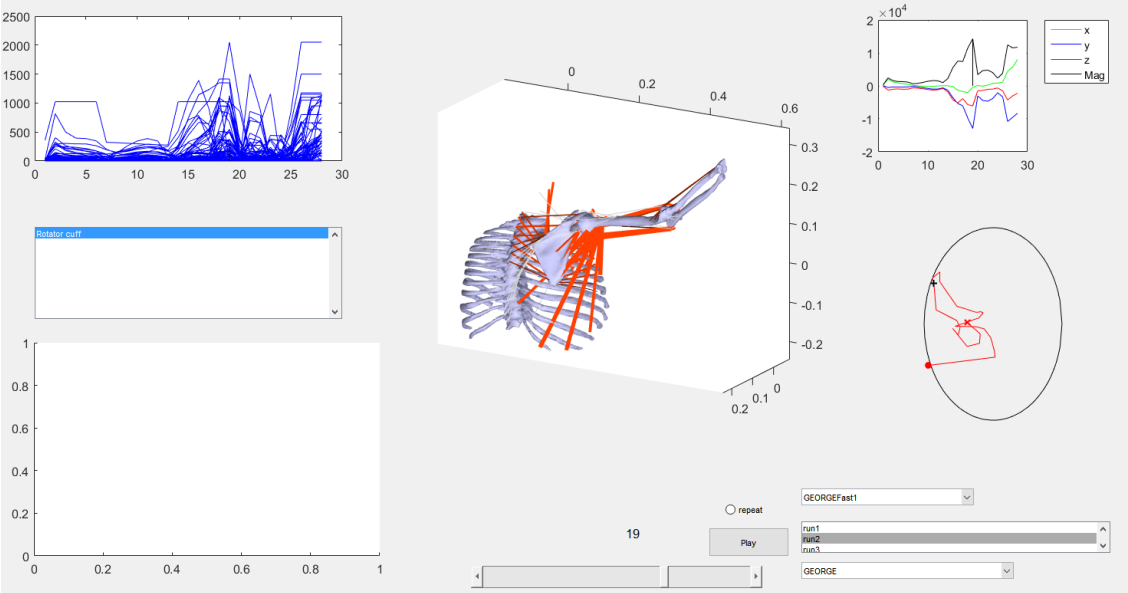

Figure 6.26 Matlab GUI built to aid in visualisation of model outputs.

6.4 Model sensitivity to new changes

The adaptations made to the model were found to be inadequate for all subjects as such, results of the kinematic optimisation and other changes made to the model for all bowlers and stock over is presented here. One of the major factors used to judge the improvement was a reduction in the amount of unsolved frames which mostly occurred in the arc between upper arm horizontal before and after ball release. The inability of the model to find a solution was either because the GH joint force violated the glenoid ellipse constraint or the muscle forces exceed their maximum set limit and no dynamic equilibrium could have been found. The range of motion for each bowler was interpolated to 50 frames resulting in 4500 frames among the 15 subjects.

Model sensitivity to certain parameters is presented and the improvement of the model in simulating the bowling action is assessed for each subject. The idea of doing this is to give an indication of how robust were the newly implemented changes. The maximum muscle forces were set to 5 times their original maximum values (Table 6-7) and was used throughout each iteration when modelling parameters were changed. This increase was necessary given the athletic nature of bowling and the fact that muscle PCSA values were derived from relatively

elderly cadavers (Veeger et al., 1997; Johnson et al., 1996). Only changes that were specified were made.

Muscle	Force
Latissimus Dorsi	3300
Anterior Deltoid	1900
Middle deltoid	1950
Posterior Deltoid	2250
Suprasinatus	1500
Infraspinatus	3000
Subscapularis	3900
Teres minor	1050
Teres major	2050

Table 6-7 Key muscles in the UKNSM showing the values of 5 times their maximum force.

The GH joint force locus on the glenoid and key muscles is presented to allow comparison among each change to the model. To indicate where these unsolved frames occurred, two phases in the motion are highlighted. These are;

- Phase 1- From the point between upper arm horizontal and ball release, to ball release. Using the same percentage of motion in this thesis, this would be 50-100% of the motion.
- Phase 2- From ball release to the point between ball release and the end of the trial. This would be 100-150% of the motion.

These smaller phases are used since the risk of impingement is more likely to occur within these phases as discussed previously. Therefore, it is crucial that the model finds a solution within these phases. Front-on fast bowlers and spin bowlers are labelled in their respective colours used throughout this thesis. These bowlers were given a higher priority when trying to find a robust model solution. All other fast bowlers are shown in black.

6.4.1 Default model

Firstly, the model was set to run with none of the new changes to give an idea of its baseline performance in simulating bowling. Kinematic optimisation method 2 was used as it was found to be the best among the three original optimisation methods. The results showed that there were 951 (21%) unsolved frames.

Figure 6.27a shows the impact of the unsolved frames where the glenoid ellipse constraint was

broken and occurred more often in the moments before ball release (phase 1). The resulting muscle forces were found to be higher when compared to muscle forces after the new changes were made (Figure 6.28). This trend was also noticed in the scapula stabiliser muscles such as the trapezius scapula, serratus anterior and rhomboid major. In contrast, the rotator cuff muscles were less active prior to ball release (Figure 6.29), particularly the supraspinatus, infraspinatus and teres minor muscles. This might explain why the other muscles contributed much larger forces in trying to satisfy the constraints.

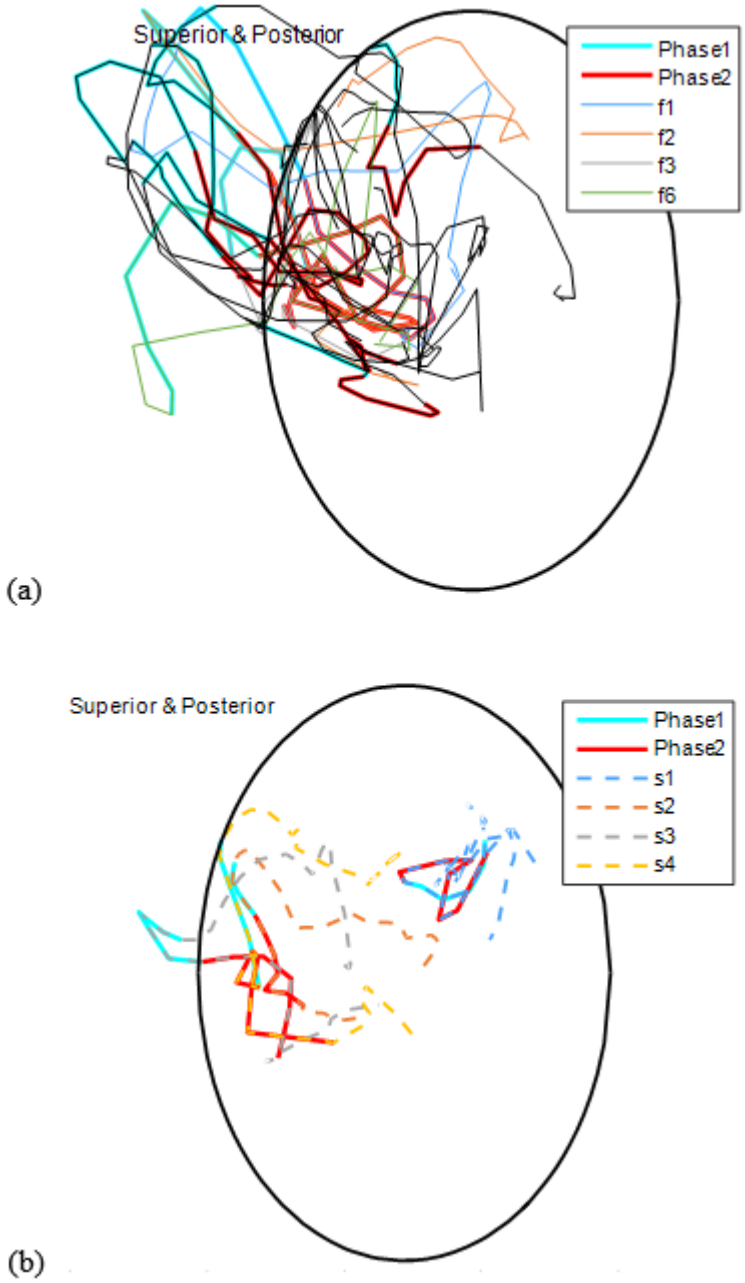

Figure 6.27 (a) Fast bowlers' average GH joint force locus (b) slow bowler's GH joint force locus on a plane parallel to the glenoid ellipse. The region of two important phases in the bowling action highlighted. Model run with its default kinematic optimistaion and muscle wrapping.

Slow bowlers exhibited the same problems although to a much lesser extent. These results show just a sample of the output data. It should be noted that problems discussed in the previous section still hold true, where the scapula was badly positioned at the back of the thorax.

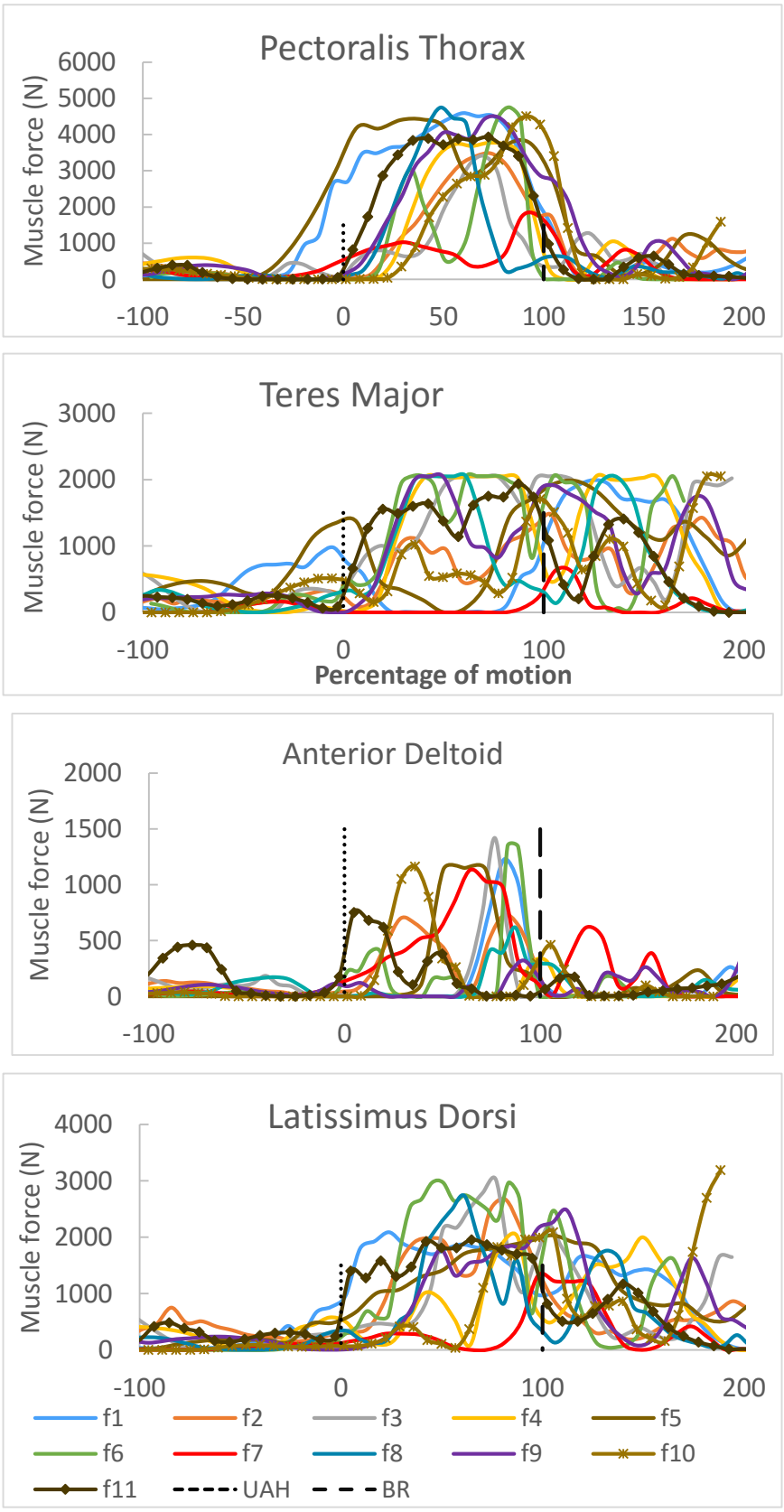

Figure 6.28 Key muscles attached to the humerus showing their force output when the model was used with its default kinematic optimisation and muscle wrapping

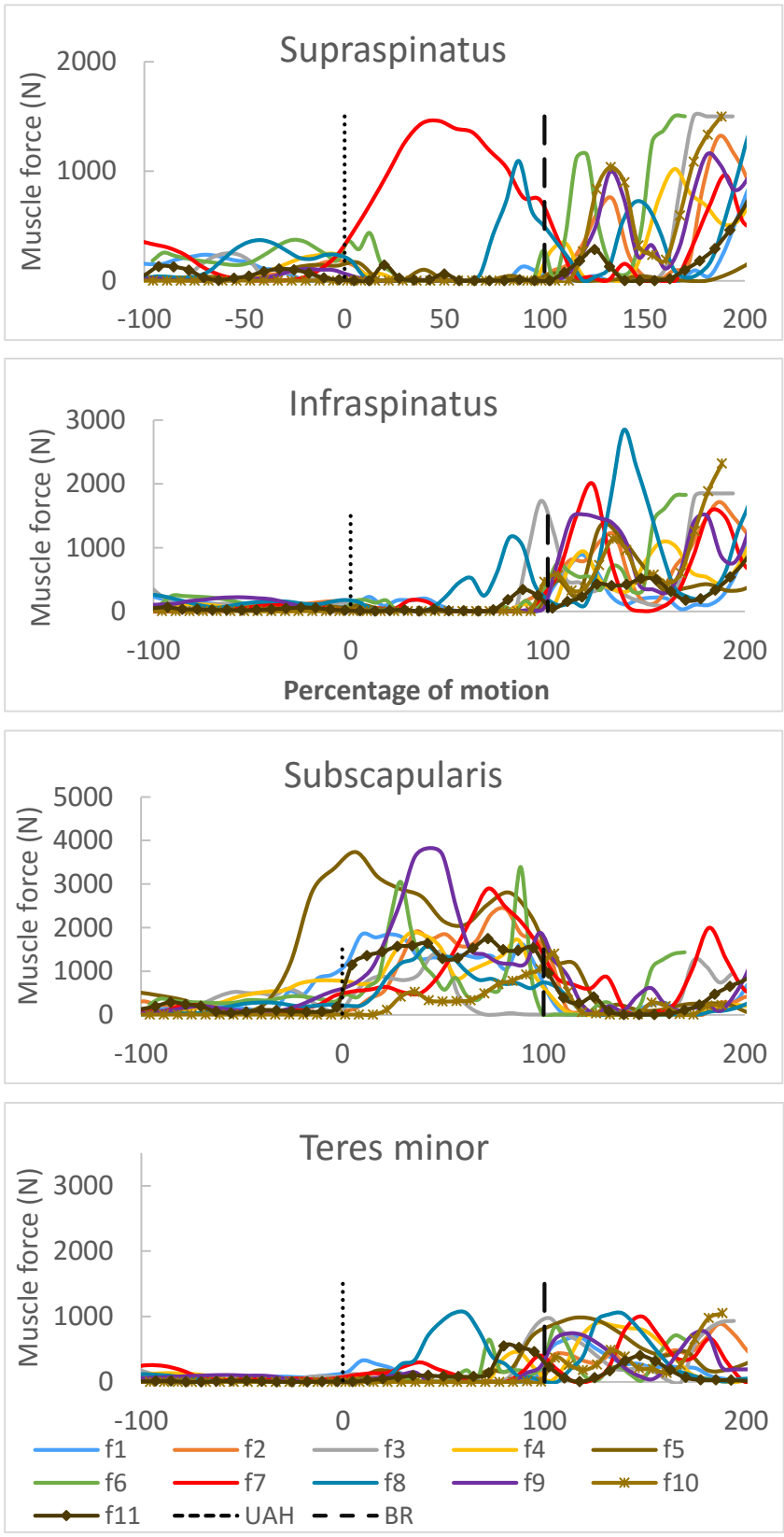

Figure 6.29 Rotator cuff muscle forces for the original UKNSM.

The RMS difference for scapula posterior/anterior (PA) and internal/external (IE) rotations were within 10°. While scapula up/down (UD) rotations was less with an average difference of less than 5° (Figure 6.30).

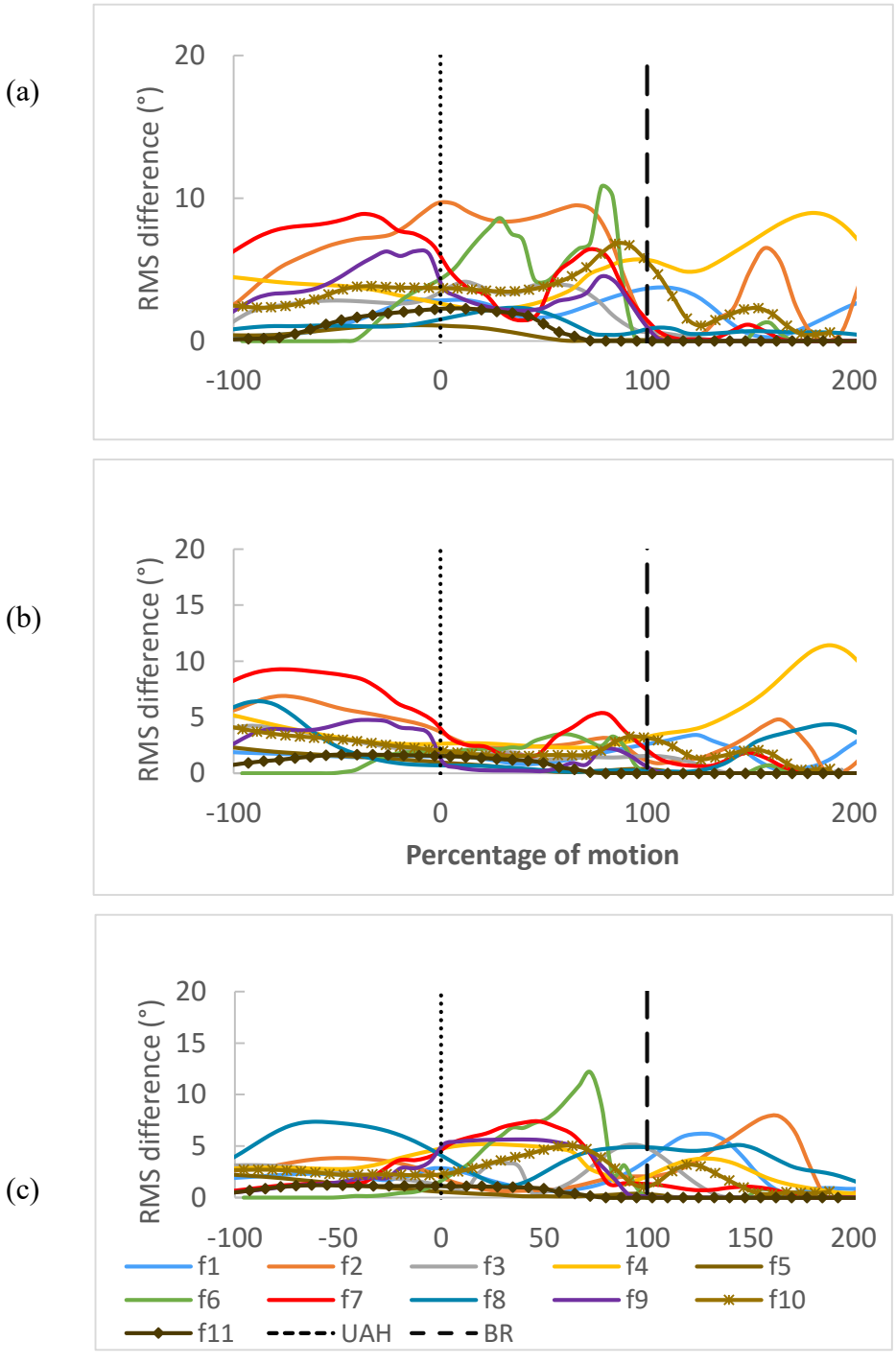

Figure 6.30 RMS difference between measured and optimised scapulothoracic kinematics for the original kinematic optimisation. (a) posterior/anterior (b) internal/external (c) up/downward rotations.

Finally, the resultant glenohumeral joint reaction force (GHJRF) shows a trend of increasing up to 7,000N -10,000N from upper arm horizontal (Figure 6.31). For the slow bowlers, s2 and s3 their GHJRF approached 8000N.

(a)

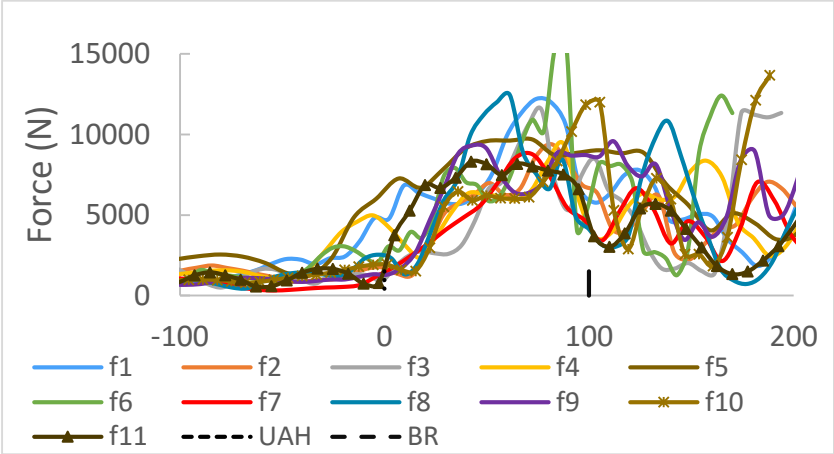

(b)

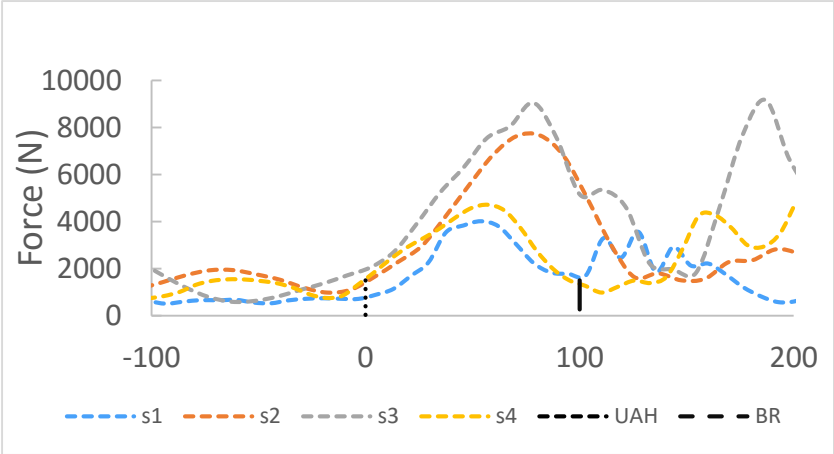

Figure 6.31 Glenohumeral joint reaction force (GHJRF) when using original model for (a) fast bowlers (b) slow bowlers

6.4.2 New kinematic and muscle wrapping changes implemented

The new changes for kinematic optimisation and muscle wrapping were turned on. There was a total of 612 (14%) unsolved frames which mostly occurred in phase 2, just after ball release. For the slow bowlers only s3 was found to have a number of unsolved frames in phase 1 (Figure 6.32). Figure 6.33 and Figure 6.34 show the muscle forces where there was greater muscle activity in the rotator cuff and a corresponding decrease in maximum force in the larger muscles attached to the humerus when compared to the original model. Teres major in both cases showed a similar pattern of reaching its maximum value. This is expected since scapula upward rotations show an RMS difference within the same range.

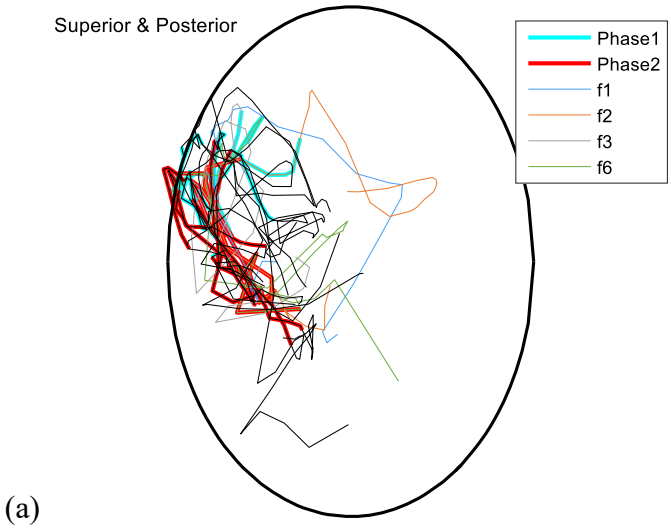

(a)

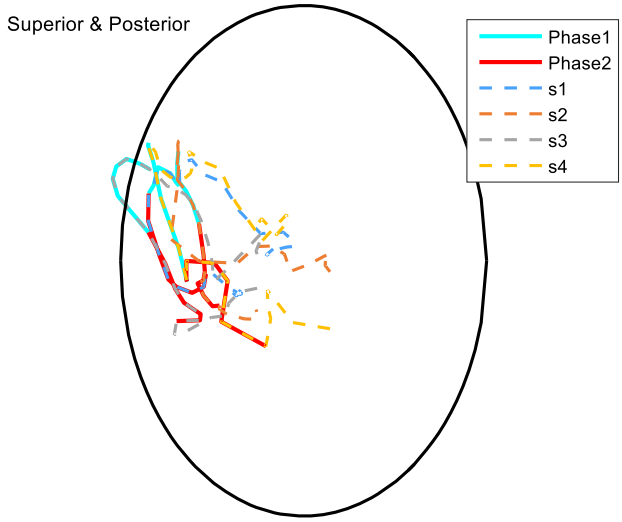

(b)

Figure 6.32 (a) Fast bowlers' average GH joint force locus (b) Slow bowlers' GH joint force locus on a plane parallel to the glenoid ellipse. The region of two important phases in the bowling action is highlighted. Model run using new changes to kinematics and muscle wrapping.

The RMS difference for scapulothoracic kinematics for both sets of bowlers is presented in Figure 6.35 and Figure 6.36. There was a much greater difference for scapula PA and IE for the optimised kinematics, when compared to the original model (Figure 6.30) however, the differences for scapula UD were within the same range. Bowler f1 and f6 showed larger change in scapula UD compared to other bowlers in both cases.

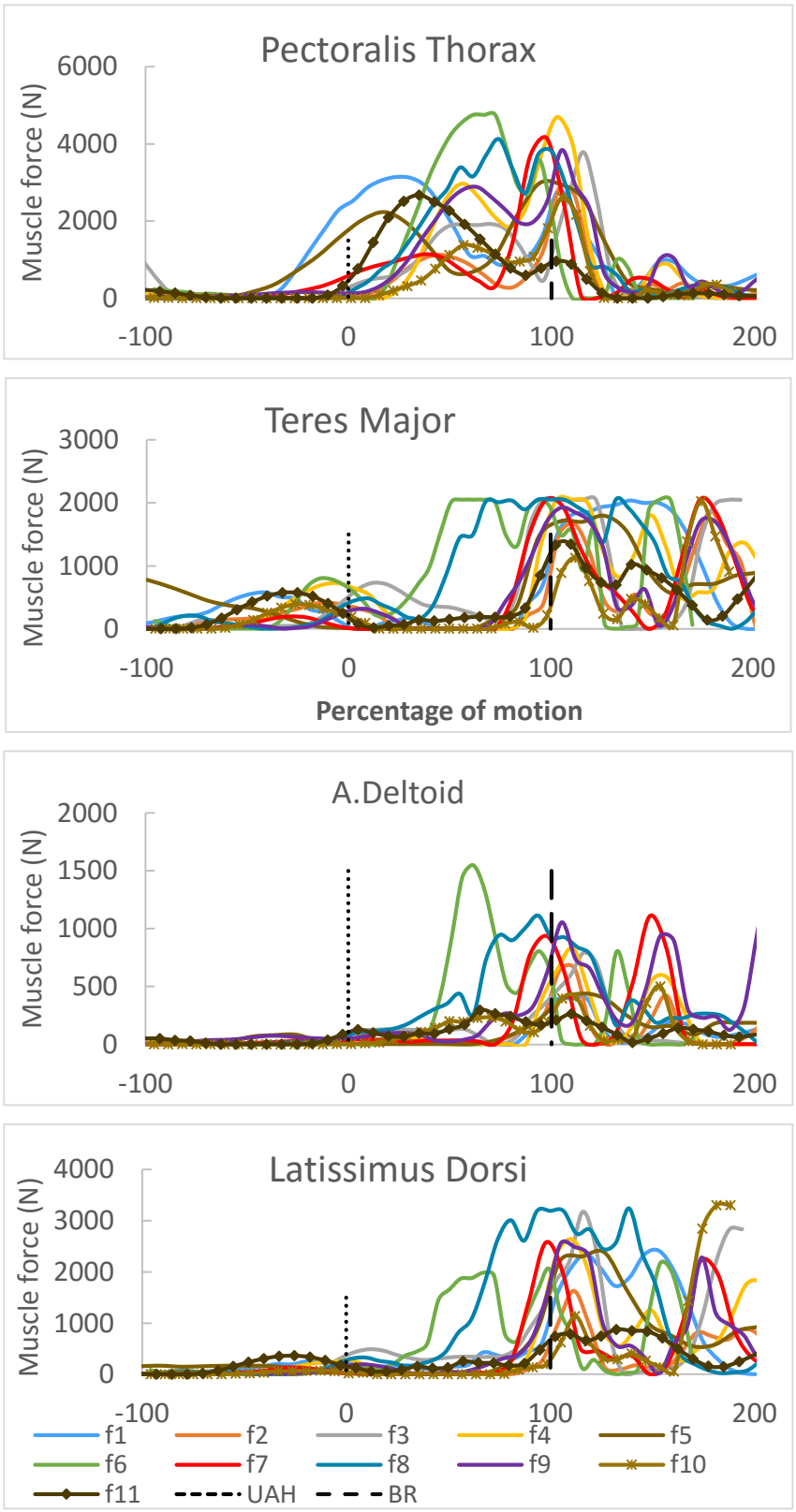

Figure 6.33 Key muscles attached to the humerus showing their force output when changes were made to the model

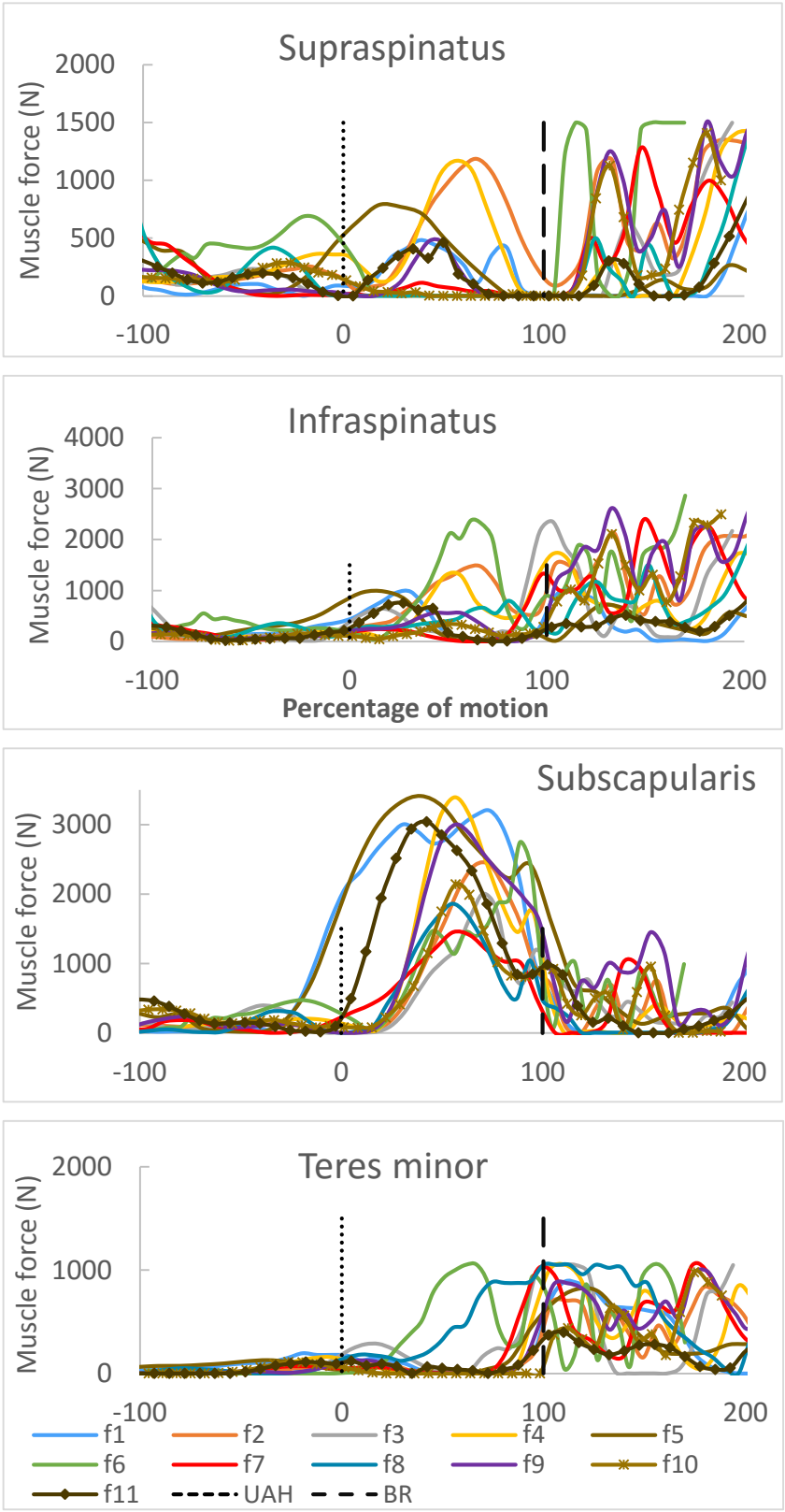

Figure 6.34 Rotator cuff muscle forces when new model changes were implemented

(a)

(b)

(c)

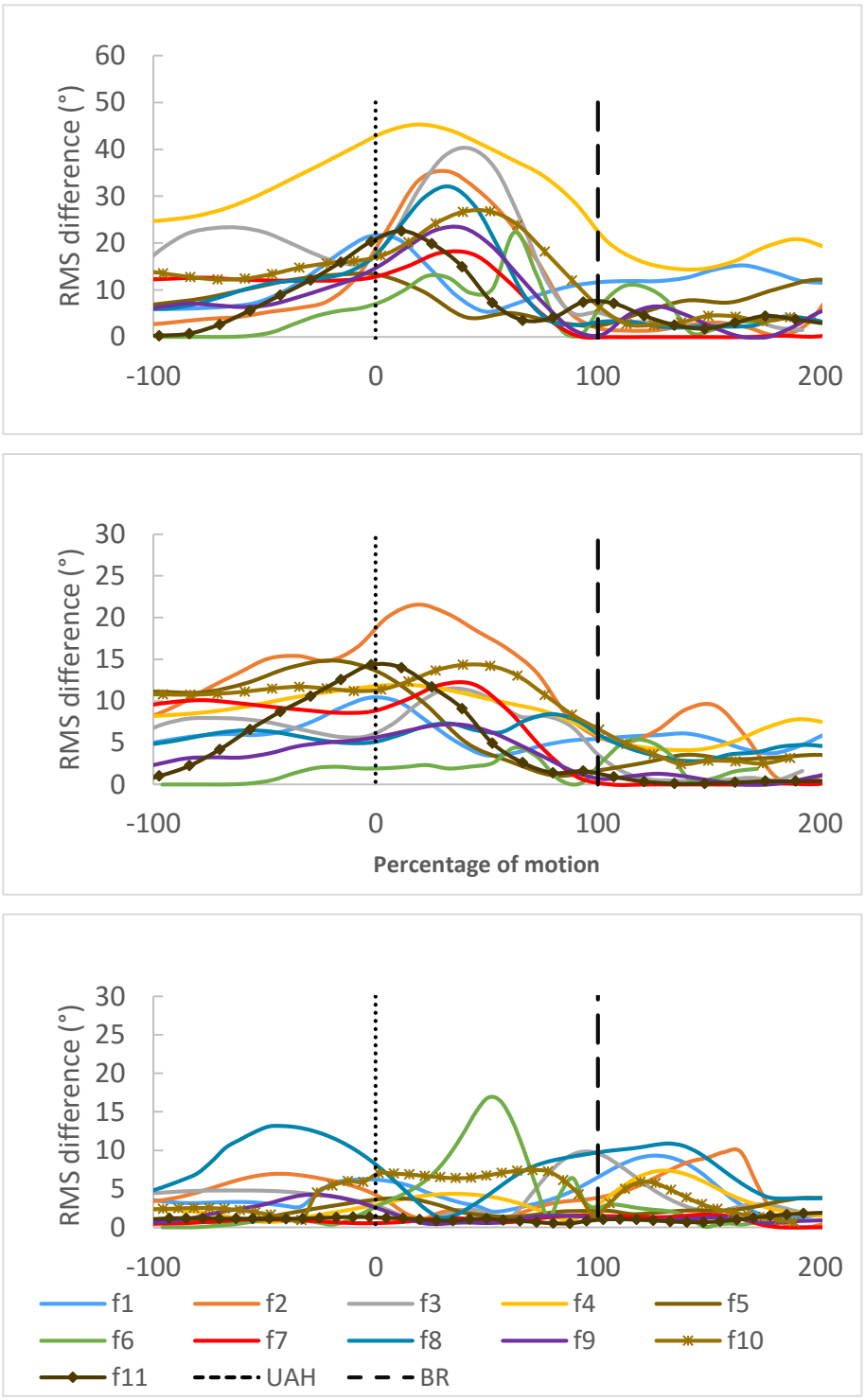

Figure 6.35 RMS difference between measured and optimised scapulothoracic kinematics over the range of the bowling action for fast bowlers. (a) posterior/anterior (b) internal/external (c) up/downward rotations.

(a)

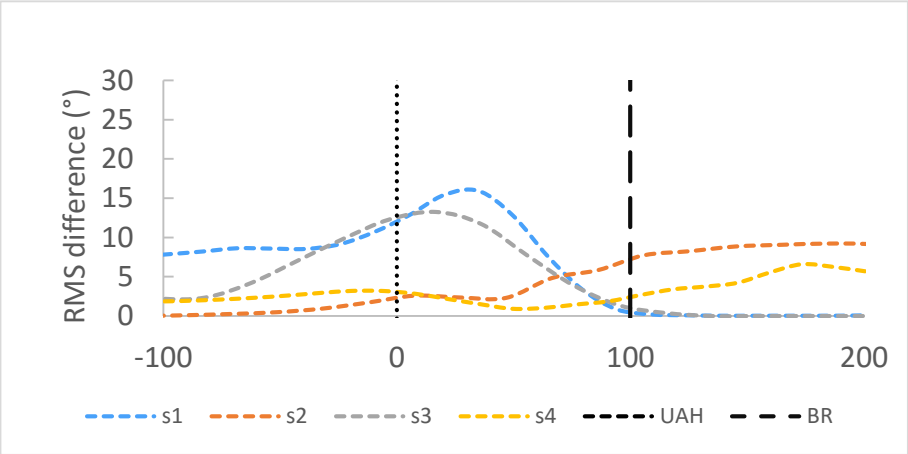

(b)

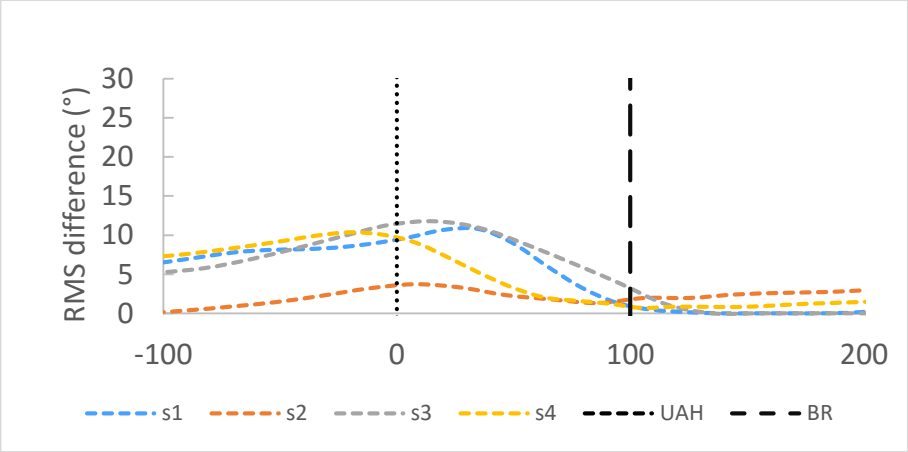

(c)

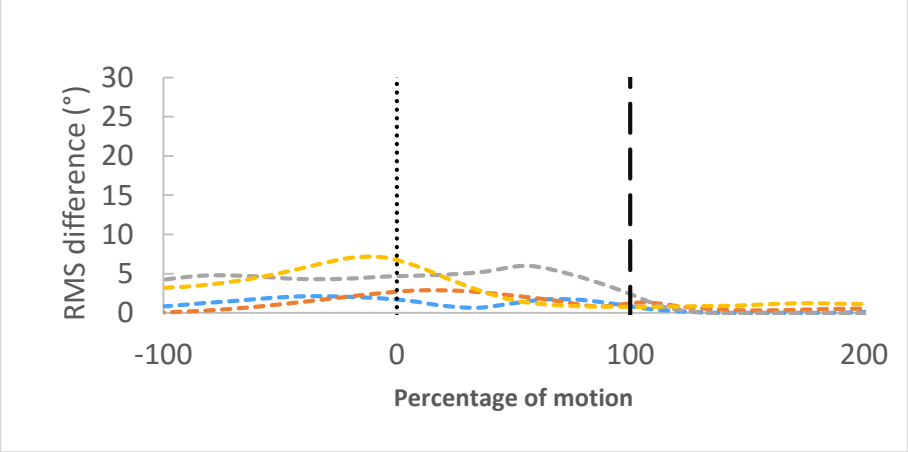

Figure 6.36 RMS difference between measured and optimised scapulothoracic kinematics over the range of the bowling action for slow bowlers. (a) posterior/anterior (b) internal/external (c) up/downward rotations.

The GHJRF (Figure 6.37) showed lower forces prior to ball release, however there was a less distinctive trend when compared to Figure 6.31. There was a reduction in this force for the slow bowlers except for s3.

(a)

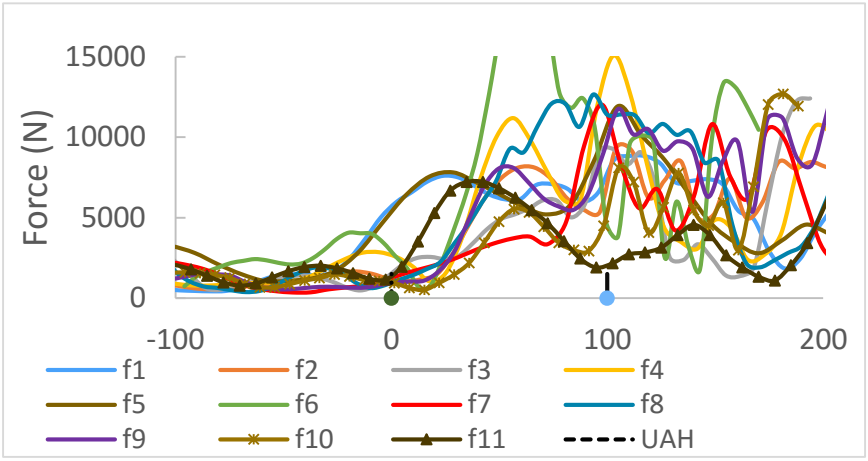

(b)

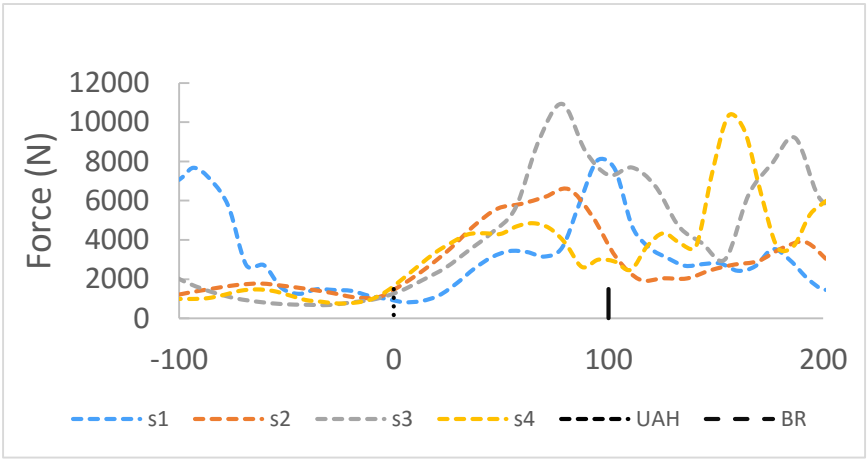

Figure 6.37 Resultant Glenohumeral Joint Reaction Force (GHJRF) for (a) fast and (b) slow bowlers when the new changes are used

6.4.2.a Regression scapula kinematics

The regression equations that were identified in Chapter 5 were used for scapula PA rotation as input into the optimisation. While there was a lower average RMS difference (Table 6-8) the optimised joint angles were found to be less consistent with jumps in the waveforms. Furthermore, there was as slight increase in the number of unsolved frames to 642 (14% overall).

	Scapula PA	Scapula IE	Scapula UD
f1	12.27	6.52	4.05
f2	12.39	7.17	4.29
f3	11.95	7.52	3.89
f4	17.34	10.68	3.56
f5	7.70	5.59	1.78
f6	7.21	2.70	1.89
f7	8.26	6.10	0.76
f8	12.26	8.38	7.39
f9	13.49	7.86	1.55
f10	13.79	7.26	3.55
f11	5.49	2.45	0.88
s1	7.08	4.32	0.79
s2	2.67	1.50	0.45
s3	7.32	5.26	1.42
s4	3.75	5.59	3.11

Table 6-8 Average RMS difference between measured and optimised scapulothoracic and AC joint kinematics

Changes in the GH joint force locus due to using the regression predicted scapula PA are shown in Figure 6.38 where the increase in unsolved frames is also indicated by a greater portion of the trace outside the ellipse.

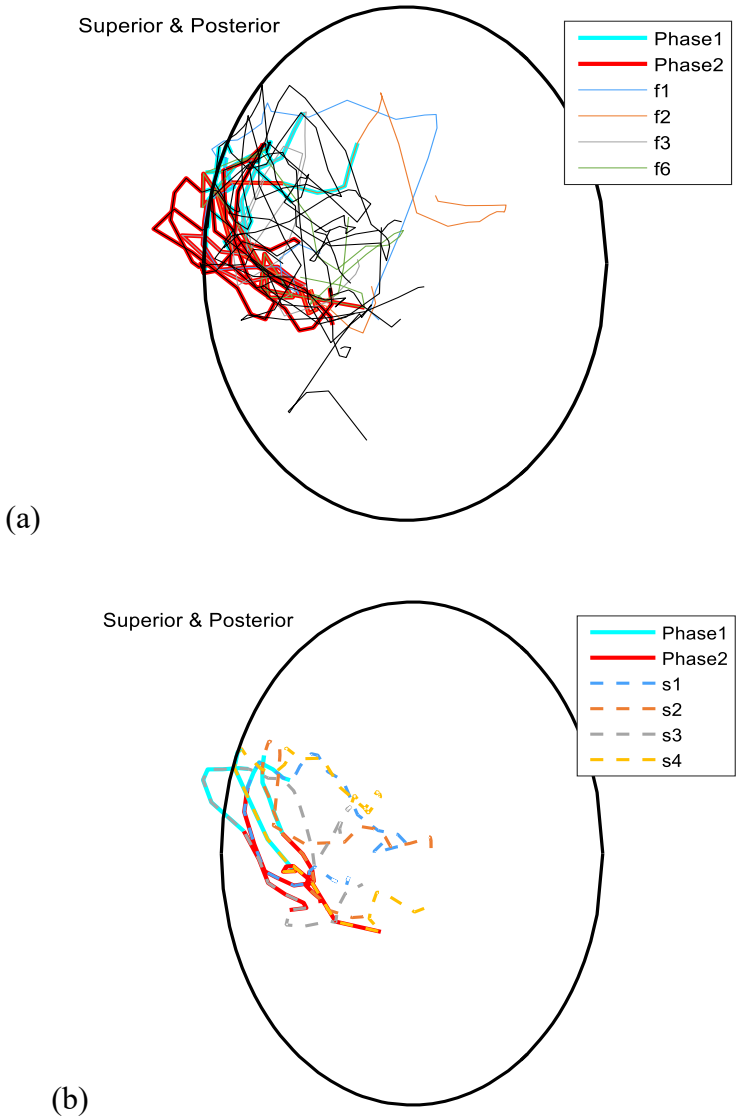

Figure 6.38 (a) Fast bowlers' average GH joint force locus (b) Slow bowlers' GH joint force locus on a plane parallel to the glenoid ellipse. The region of two important phases in the bowling action is highlighted. Model run using new changes to kinematics and muscle wrapping and regression kinematics for scapula PA.

6.4.3 New changes and unbounding force limit

The maximum muscle forces were set to 1000 times their initial maximum value to determine how many of the unsolved frames were caused by the force limit. The number of unsolved frames was reduced to 166 (4%). It should be noted that the trace of the GH joint force plotted in Figure 6.39 is averaged for the six trials of each bowler and given the close proximity of the force locus to the glenoid ellipse, it would cross the ellipse as it was within the margin of standard deviation. Therefore, the averages masked this small effect.

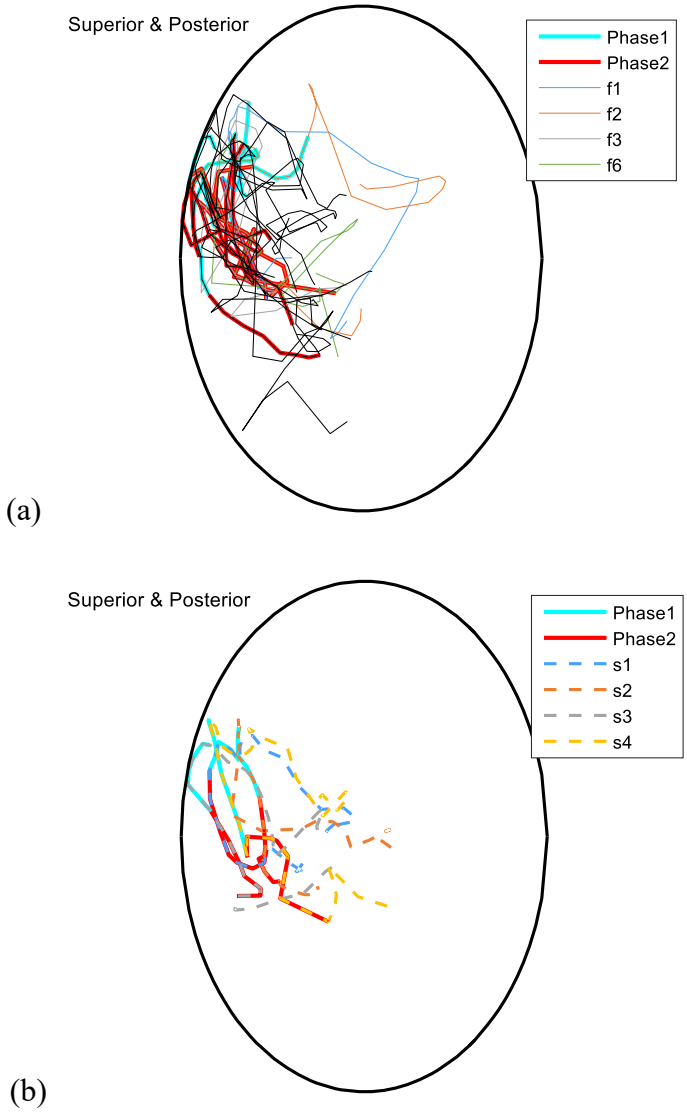

Figure 6.39 (a) Fast bowlers' average GH joint force locus (b) Slow bowlers' GH joint force locus on a plane parallel to the glenoid ellipse. The region of two important phases in the bowling action is highlighted. Model run using new changes to kinematics and muscle wrapping and effectively unbounded muscle forces.

The major issue with increasing the muscle forces was that there were extremely high forces in the teres major, latissimus dorsi and rotator cuff muscles for subjects f6, f8 and f10 (Figure 6.41 and Figure 6.42). A similar trend was noticed for the posterior deltoid and scapula stabilising muscles such as the trapezius scapula, serratus anterior and rhomboid major.The effect of these high forces meant that the resultant GH joint reaction force was found to be in excess of 15000N (Figure 6.40) for these subjects particularly in the region of phase 1 and 2.

(a)

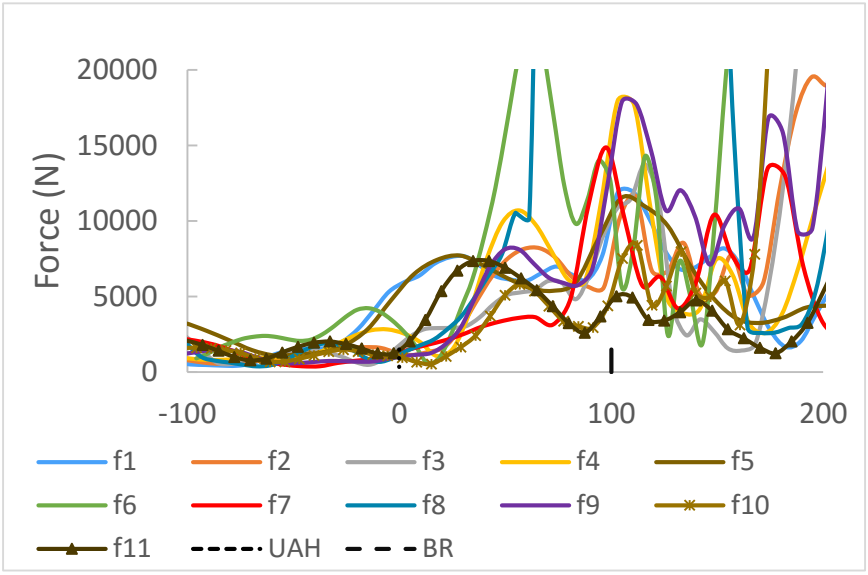

(b)

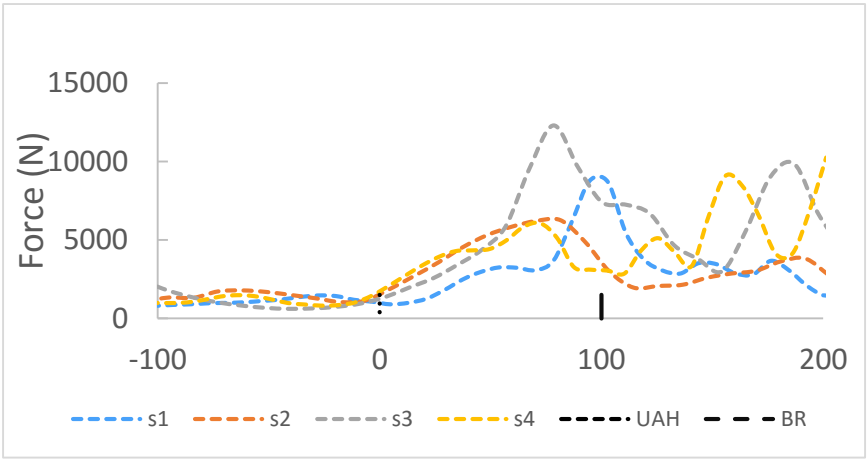

Figure 6.40 GHJRF for (a) fast and (b) slow bowlers when muscle forces are 1000 times their maximum and using the new kinematic and muscle wrapping changes.

The GHJRF for slow bowlers also presented also showing extremely high forces being calculated, specifically for s3 s1 and s4.

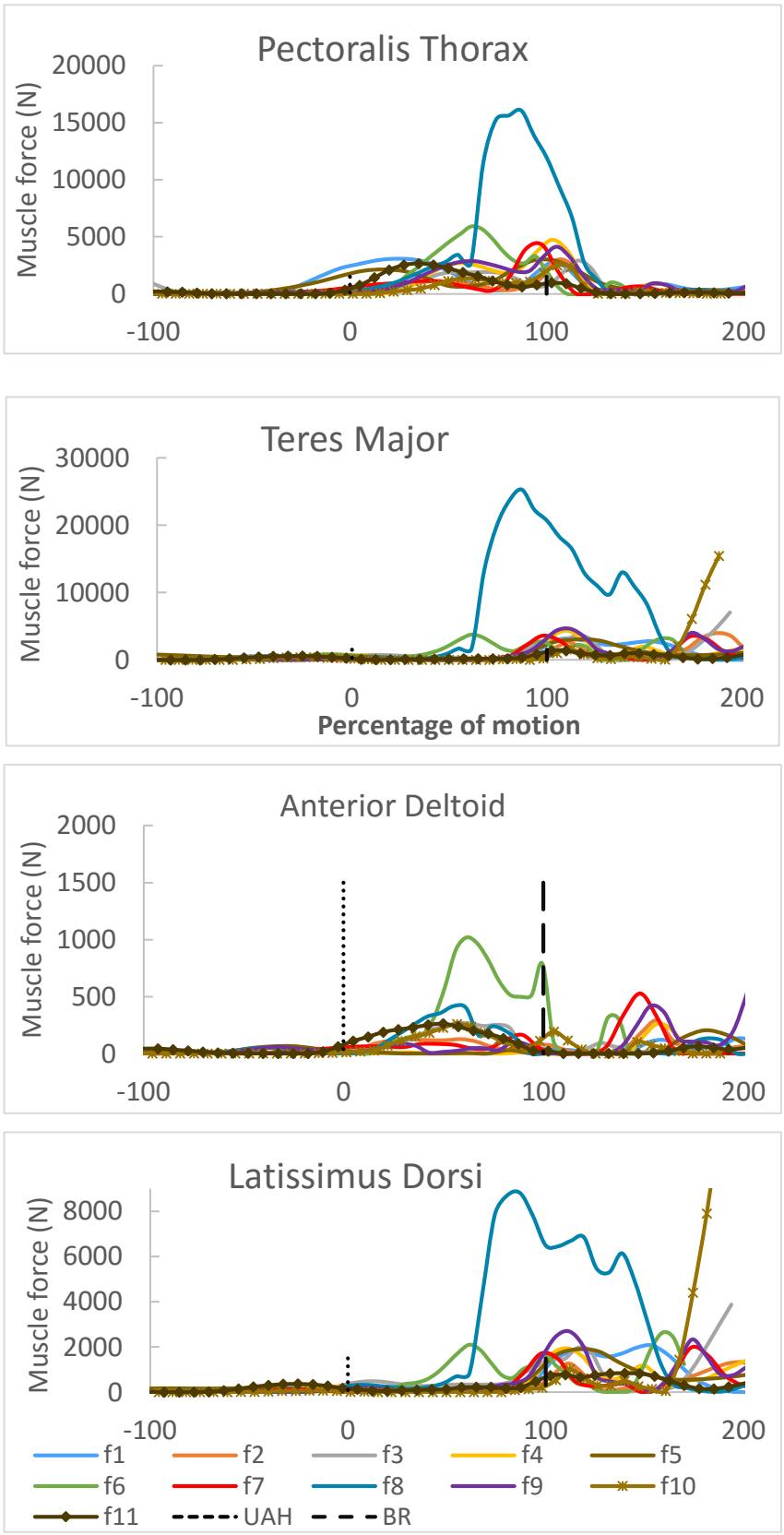

Figure 6.41 Key muscles attached to the humerus showing extremely high muscle forces.

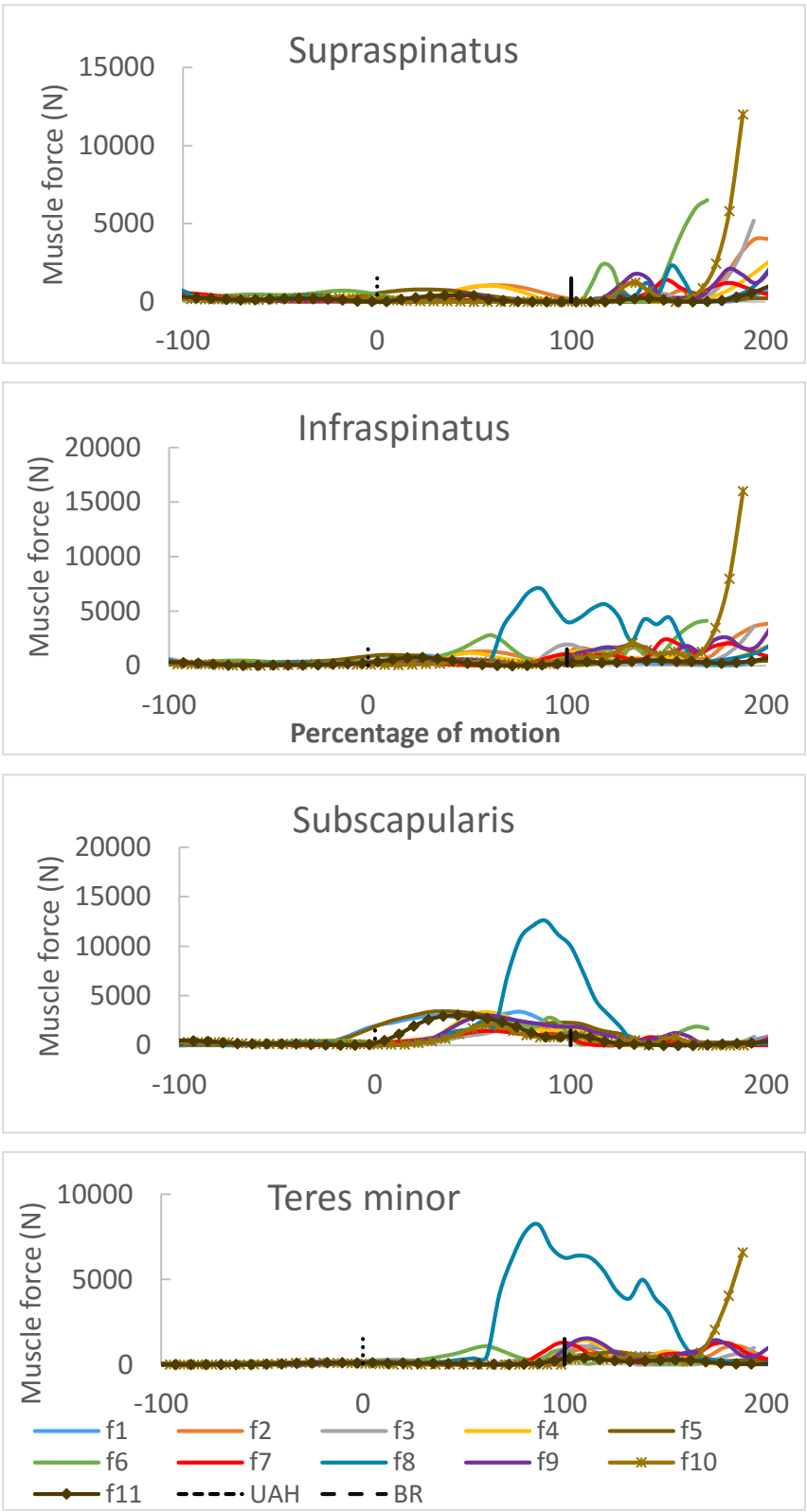

Figure 6.42 Rotator cuff muscle forces when unbounded.

One of the limitations of the minimisation function in Matlab is that it tends to max out a single muscle in satisfying the constraints before moving to another muscle. One way this has been addressed in literature is the use of min/max optimisation (Rasmussen et al., 2001), which effectively increases the force for all the muscles while preventing any one muscle from reaching maximum force output. This was also tested using the same cost function (Equation 6.11) to the power of one. This did not improve the solution significantly indicating that the problems with the model were elsewhere.

A number of other modelling parameters were investigated to identify a definitive factor or group of variables that could greatly improve the performance of the model in simulating cricket bowling. These include;

- Aligning the scapula and humerus frames at the start of the motion to reduce the amount of GH external rotation seen in subjects like f10.
- Increasing the amount of filtering on the raw marker data.
- Using digitised landmarks or actual marker positions when calculating humerus and forearm anatomical coordinate frames.
- Homogeneously scaling the thorax and the STGP ellipsoid.
- Resampling the raw data.

Combinations of these changes were made with five times the upper force limit and the new kinematic optimisation and muscle wrapping being used. Eventually, it was discovered that the model outputs were very sensitive to the time step between frames. The default interpolation to 50 frames meant that the raw data was resampled within the region of 140 to 170 Hz from 400Hz however, the model showed a reduction in unsolved frames when the data was resampled to 100Hz. Mathematically, the time step was used in the inverse dynamics in calculating joint angular velocities and accelerations. Therefore, the numerical differentiation methods employed in the model would only be valid for a certain range of sample frequency and explained why no solution could be found when changing any of the above variables, particularly in the fastest part of the bowling action.

It should be noted when the data was resampled, the results for the first two cases presented before (Section 6.4.1 and Section 6.4.2) where the same, where the default model configuration performed the worse with 18% unsolved frames compared to 9%. Similar problems for bowler f6 and f8 were observed when the muscle force limited was increase by a factor of 1000.

The resulting GH kinematics based on the optimised clavicle and scapula rotations may explain the problems with f6 and f8 (Figure 6.43). Subject f6 GH abduction was almost constant from 50% of the motion. This meant that during humerothoracic elevation the scapula was also upwardly rotating resulting in a near constant GH abduction angle. This is confirmed when looking at the RMS difference between measured and optimised kinematics for scapula UD rotations (Figure 6.35) where there was a difference of 16° at 50% of the motion. In addition to this, bowler f8 had significantly greater GH extension at ball release, where internal rotation of the scapula may further increase this angle. In addition f8 was reported as having the greatest measured GH internal rotation (Chapter 5) and this is also true after the kinematic optimisation. These issues shows that the model was sensitive to scapula kinematics particularly at an extreme range of motion and fast motion. The root of this sensitivity may be due to the muscle wrapping where these extreme ranges result in more muscle element sliding issues.

Efforts to correct both these issues included increasing the weighting of both scapula IE and UD in the cost function (Equation 6.9) however, it resulted in a greater change in the other optimised rotations which also let to other problems that negatively affected the solution. Given that these subjects would greatly affect the output of the fast bowlers' group with significantly higher muscle forces, they were left out.

Kinematic optimisation affects the final GH kinematics since the position of the humerus relative to the thorax is unchanged while kinematics of the scapula and clavicle are optimisted to based on the constraints. This is one of the limitations of the kinematic routine thus, future work should include adjustments to the humerothoracic angles so that GH kinematics are closer to what is measured.

(a)

(b)

(c)

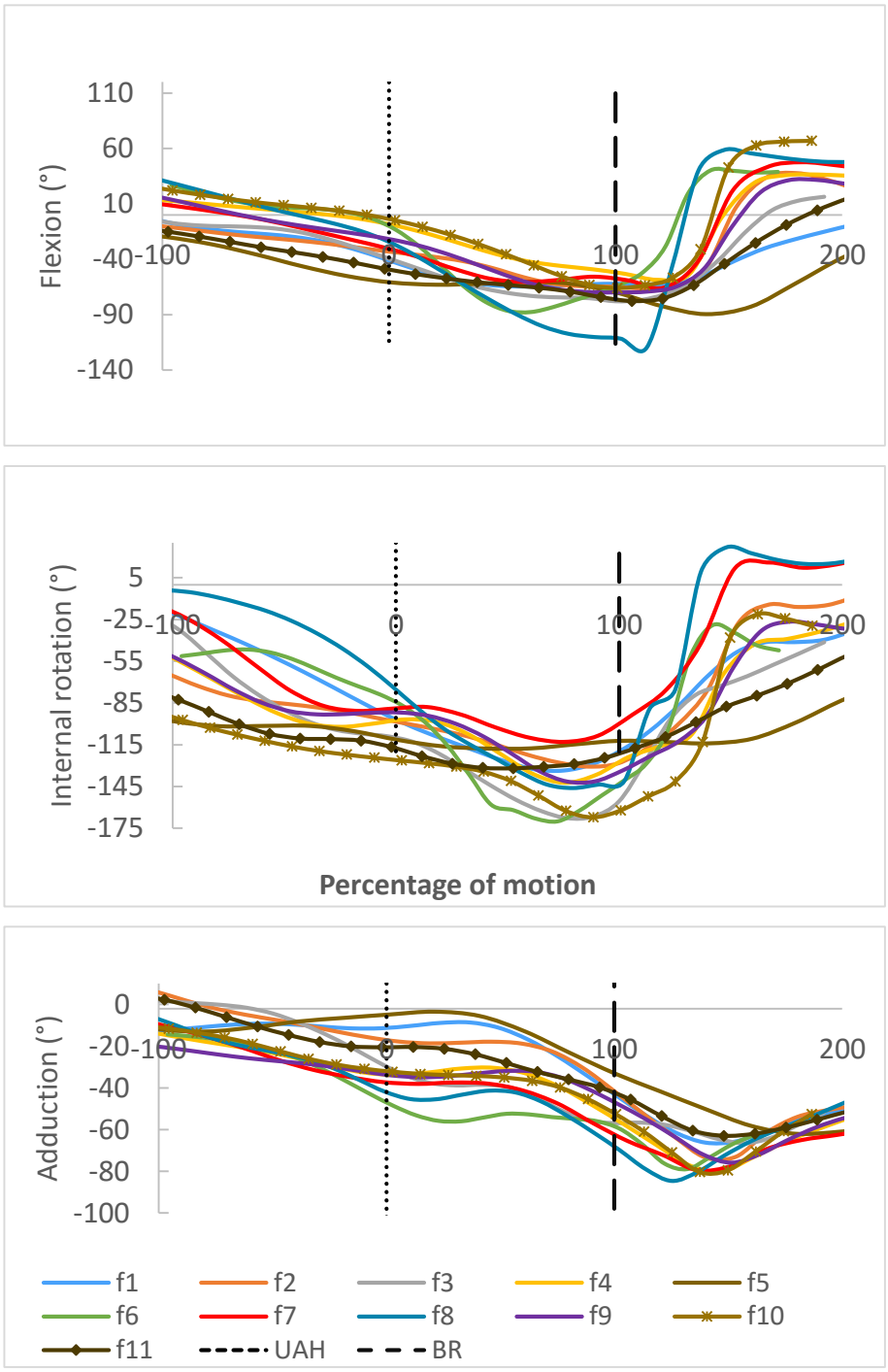

Figure 6.43 Glenohumeral kinematics for fast bowlers after the new changes were implemented. (a) flexion/extension (b) internal/external (c) abduction/adduction rotations.

In summary, the adaptations made to the model improved the models ability to find a solution within the more important phases of the bowling action. Even though the muscles forces were within the same range for the larger muscle groups, there was a different activation pattern and improved rotator cuff activity when the adaptations were implemented.

The use of regression predicted scapula PA negatively affected the models' output. The increase of the maximum force output of each muscle from a factor of 5 times to 1000 times, resulted in a large GH joint forces where the resultant was in excess of 10,000N for subjects f4 to f9 and s4, where subjects f8,f6 and f10 showed extremely high muscle forces. Later it was uncovered that these high forces may have been due to model sensitivity to one variable. An exercise looking at variables that greatly affected the quality of model outputs revealed that of all the variables that were changed, the model was most sensitive to the time step used. As such, the raw marker data was resampled to 100Hz.

Given the inability of the model to be used for all the subjects, a reduction in the number of subjects was necessary to proceed with the analysis. The modified UKNSM was to analyse the remaining subjects, the results of which are presented in Chapter 7.

6.5 Conclusion

The final kinematic optimisation improved the rotations of the clavicle and scapula while maintaining a close agreement with the measured scapula upward rotation. The use of ligament length constraints was discussed and found not to be appropriate.

Some limitations of the model that remained was the simple segment scaling that was used which would affect the kinematic optimisation and muscle wrapping, thus has a large impact on the final solution. The simple linear scaling of the segments may break the cohesive relationship that exist within the subject and may not accurately represent the athlete. A clearer understanding of how segments scale and variation in muscle attachments is important for improving the model. A more robust, non-homogeneous scaling method and a better fit or shape of the STGP were identified as improvements that could be made to the model (Prinold & Bull, 2014). The results of modelling work found this to be true.

Muscle wrapping issues were fixed using two new cylindrical wrapping objects, thus improving the functional accuracy of a number of muscles. The use of these new wrapping objects demonstrated an improved muscle wrapping path and moment arm for the affected muscles. Given the complex action being analysed, the use of literature to validate the moment arms is limited even though there were some observed agreement in the trend. The implementation of the two new wrapping objects was a temporary fix as there are more suitable strategies available in the literature (Marsden et al., 2008) for multi-object wrapping.

Final changes to the model, while not a perfect solution were deemed satisfactory and robust enough, striking a balance between reduced complexity and functional accuracy. There was a significant reduction in unsolved frames and erratic model outputs in most of the subjects. The results for two subjects seem to indicate that the model was sensitive to the amount of scapulothoracic internal and upward rotations however investigations were inconclusive. These subjects that showed unrealistic muscle and joint forces had to be eliminated from the analysis.

The next chapter presents the result of muscle forces during bowling using this modified UKNSM.

Chapter 7

Musculoskeletal forces at the shoulder during bowling

This chapter presents the results obtained from the modified UKNSM. Contrast in muscle recruitment strategies and glenohumeral joint stability are discussed as well as predisposition to impingement injury.

7.1 Introduction

The results and discussion that follow are based on data from Chapter 5 and the modified upper limb model described in Chapter 6. Understanding the contribution of the surrounding musculature to joint stability is important when analysing the pathomechanics of injuries. Factors that were analysed include the stability of GH joint at high elevations and loading of the shoulder muscles in vulnerable positions.

Impingement and rotator cuff damage have been described to be the most common problems in overhead athletes (Page, 2011) including cricket bowlers (Bell-Jenje & Gray, 2005). Kinematic factors that have been identified as key in assessing the risk of impingement include high humeral elevation and internal rotations and scapulothoracic factors like reduced upward rotation, posterior tilt and increase internal rotation. These factors are discussed within the context of cricket bowling together with muscle activation and high loading in vulnerable positions, are key to understanding the risk of injury

The aim of this chapter is to present the musculoskeletal shoulder loads in cricket bowlers and compare these results with literature to validate if they are physiologically reasonable predictions. After which individual areas of interest are focused on. This includes investigating the risk of impingement in bowlers.

7.2 Data analysis

All moments, moment arm and GH joint forces are described in the local, distal coordinate segment frame except when stated otherwise. Coordinate frames of the scapula and humerus are defined in Table 7-1. Multiple elements of a muscle have been grouped for clarity. Table 7-2 shows the number of elements for each muscle presented.

Muscle forces are presented as is, and are normalised to body weight when stated. Mean values are quantified over the six trials. Average values are the mean of the subject means.

Segment	Axis	Motion (+/-)
Scapula	X	Posterior/anterior
	Y	Internal/external
	Z	Upward/downward
Humerus	X	Flexion/extension
	Y	Internal/external
	Z	Abduction/adduction

Table 7-1 Description of the moments about the scapula and humerus orthogonal coordinate frames

Muscle	Abbreviation	number of elements
Trapezius Superior	Trap.S	3
Trapezius Middle	Trap.M	2
Trapezius Inferior	Trap.I	11
Rhomboid major	Rmaj	5
Rhomboid minor	Rmin	2
Serratus anterior	SA	9
Anterior deltoid	Delt.A	2
Middle deltoid	Delt.M	1
Posterior deltoid	Delt.P	2
Supraspinatus	SS	1
Infraspinatus	IS	3
Subscapularis	SBS	3
Teres Minor	T.Min	1
Teres Major	T. Maj	1
Pectoralis major thorax	Pec.MT	5
Pectoralis major clavicle	Pec.MC	5
Latissimus dorsi	LD	5
Biceps Long Head	Bic.L	1
Biceps Short Head	Bic.S	1
Coracobrachialis	CB	2
Tricep long	TRI.long	2
Triceps medial	TRI.med	2
Triceps lateral	TRI.lat	2

Table 7-2 Muscles included in the analysis with their abbreviation and number of elements

To avoid violations of statistical assumptions, comparison between slow bowlers is limited to descriptive statistics.

7.3 Results

7.3.1 Kinematics

A summary of glenohumeral elevation and internal/external rotation is presented (Table 7-3) since the optimisation routine in the model would have slightly changed these values. Humerothoracic elevation angle is also presented for reference. Values are quote for 50%, 100% and 150% of the motion where 100% is ball release.

	Humerothoracic elevation (°)			**Glenohumeral elevation (°)**			**Glenohumeral external rotation (°)**		
	50%	100%	150%	50%	100%	150%	50%	100%	150%
f1	94	114	116	65	70	69	-131	-127	-57
f2	84	109	123	57	72	72	-122	-131	-58
f3	107	125	96	76	83	67	-155	-160	-71
f4	85	114	112	49	74	78	-138	-136	-90
f5	77	104	118	60	77	90	-117	-111	-115
f7	88	103	103	68	79	79	-109	-101	-19
f9	94	112	105	63	78	72	-127	-134	-76
f10	89	112	114	53	76	82	-148	-166	-84
f11	95	119	116	67	81	69	-131	-122	-92
s1	88	116	108	63	83	75	-133	-132	-97
s2	104	114	96	63	73	69	-96	-81	-16
s3	110	121	106	82	86	77	-100	-110	-51
s4	94	108	97	57	68	66	-105	-87	-26

Table 7-3 Summary of Glenohumeral elevation and axial rotation angles for all bowlers, stock over at 50%, 100% and 150% of the motion

	Humerothoracic elevation (°)			Glenohumeral elevation (°)			Glenohumeral axial rotation (°)		
	50%	100%	150%	50%	100%	150%	50%	100%	150%
f1	2	6	7	6	15	19	5	7	13
f2	4	7	4	6	7	23	3	3	17
f3	3	1	2	3	2	10	4	7	5
f4	3	3	3	4	5	20	5	3	16
f5	2	4	2	4	5	7	3	2	3
f7	2	1	3	3	5	8	3	2	7
f9	2	3	5	3	6	38	3	5	31
f10	5	2	5	6	5	14	5	4	16
f11	6	3	7	7	6	22	3	5	12
s1	2	3	5	3	5	23	1	3	17
s2	2	1	6	4	4	14	2	5	11
s3	2	1	4	2	4	10	2	2	11
s4	7	3	6	8	19	18	7	19	13

Table 7-4 Corresponding standard deviations for Table 7-4

	Humerothoracic elevation (°)			Glenohumeral elevation (°)			Glenohumeral external rotation (°)		
	50%	100%	150%	50%	100%	150%	50%	100%	150%
f1	99	121	109	67	75	68	-131	-113	-72
f2	83	104	124	56	67	72	-120	-127	-65
f3	106	123	101	77	80	67	-159	-161	-67
f5	80	100	113	65	75	81	-115	-110	-113
f7	86	101	105	66	77	77	-109	-100	-34
f9	98	121	118	65	84	83	-128	-137	-140
s1	87	116	85	63	85	61	-131	-129	-52
s2	104	111	92	65	72	69	-95	-77	-5
s3	109	118	100	83	82	74	-110	-112	-69
s4	91	108	95	56	69	66	-104	-87	-18

Table 7-5 Summary of Glenohumeral elevation and axial rotation angles for all bowlers, variation over at 50%, 100% and 150% of the motion

	Humerothoracic elevation (°)			Glenohumeral elevation (°)			Glenohumeral axial rotation (°)		
	50%	100%	150%	50%	100%	150%	50%	100%	150%
f1	2	2	7	8	4	15	7	12	22
f2	2	2	2	3	3	18	2	1	11
f3	2	2	4	2	5	20	3	10	11
f5	4	3	5	6	4	10	4	2	4
f7	2	3	2	4	5	36	2	6	28
f9	3	2	4	5	5	15	5	2	13
s1	5	3	12	6	9	16	2	7	12
s2	2	1	2	4	4	8	2	6	12
s3	5	3	7	5	7	18	5	7	14
s4	6	2	7	8	10	9	10	9	8

Table 7-6 Corresponding standard deviations for Table 7-5

7.3.2 Glenohumeral joint reaction forces

The average GH joint forces for fast and slow bowlers (Figure 7.1) show large distraction (along the Y-axis) forces for both sets of bowlers of up 6000N and 4000N respectively.

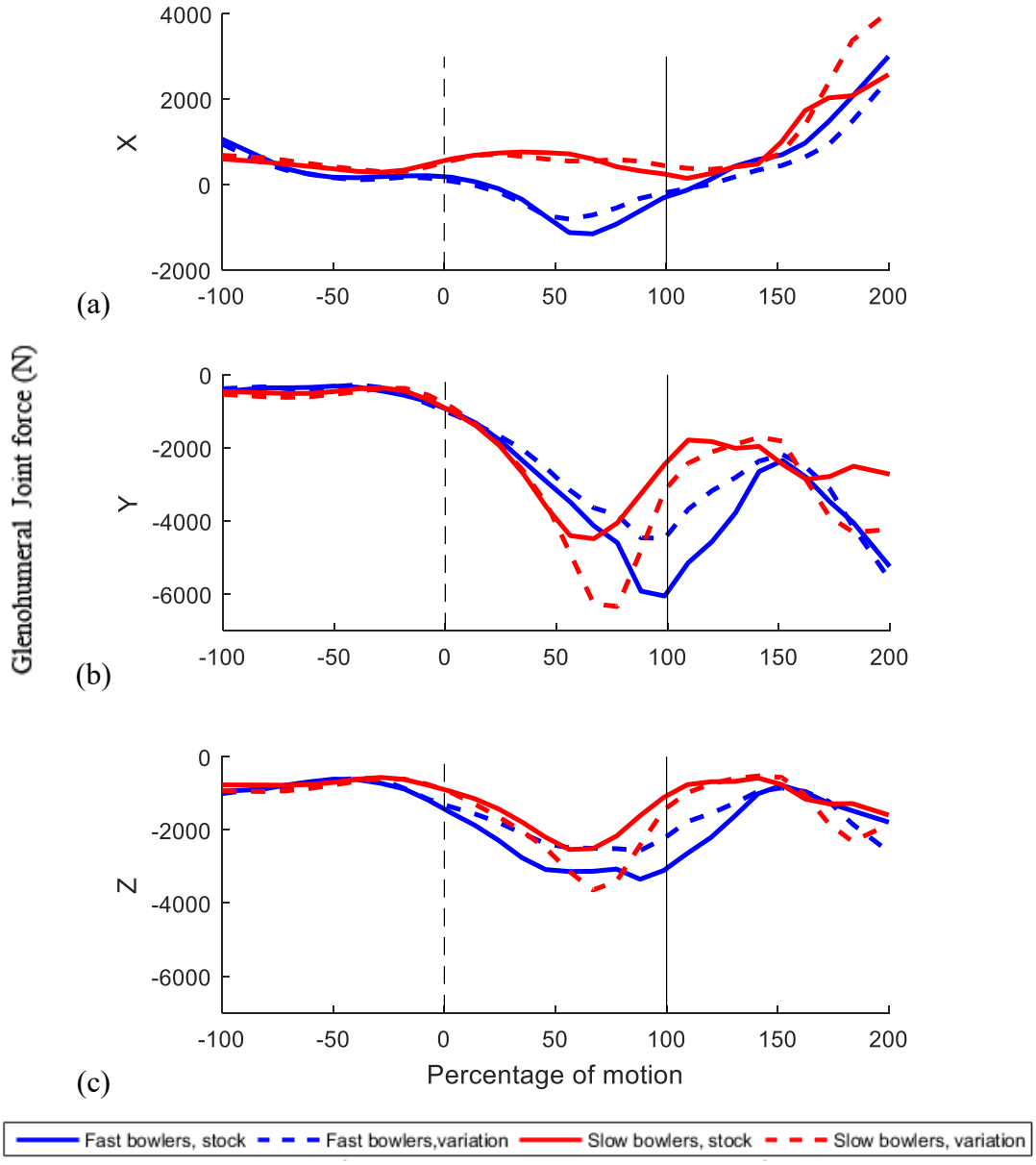

Figure 7.1 Mean glenohumeral joint reaction forces in the humerus coordinate frame for all bowlers.

Mean GH joint forces are plotted separately for each over showing the standard deviations in Figure 7.2.

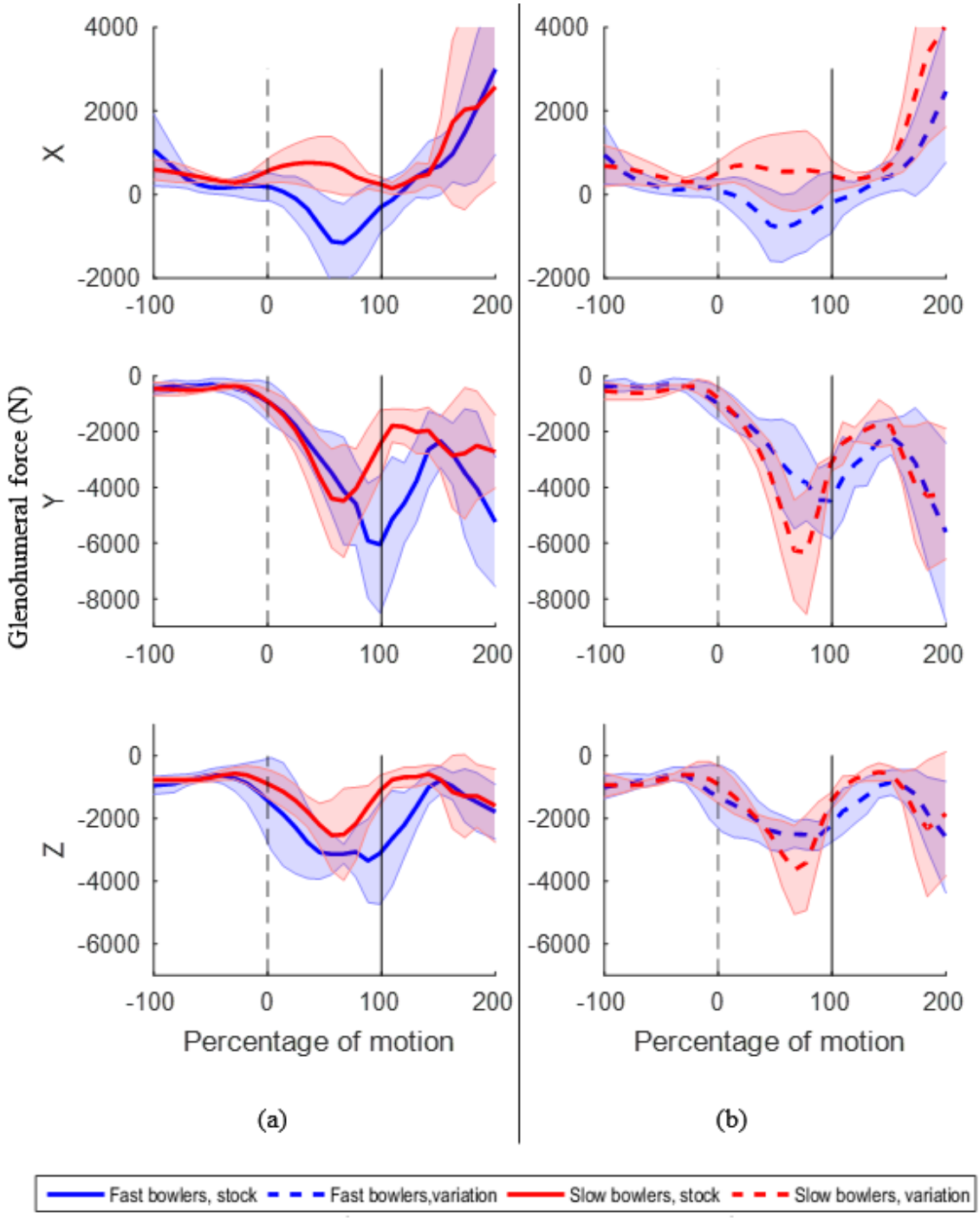

Figure 7.2 Mean glenohumeral joint reaction forces showing standard deviations for (a) stock over (b) variation over.

Figure 7.3 and Figure 7.4 show a summary of the peak GH joint force for two important phases; 50% to 100% and 100% to 150% of the motion. Values were normalised to ball speed. Slower bowlers were found to have peak forces between 50% to 100% of the motion in their variation over, comparable to fast bowlers' stock over.

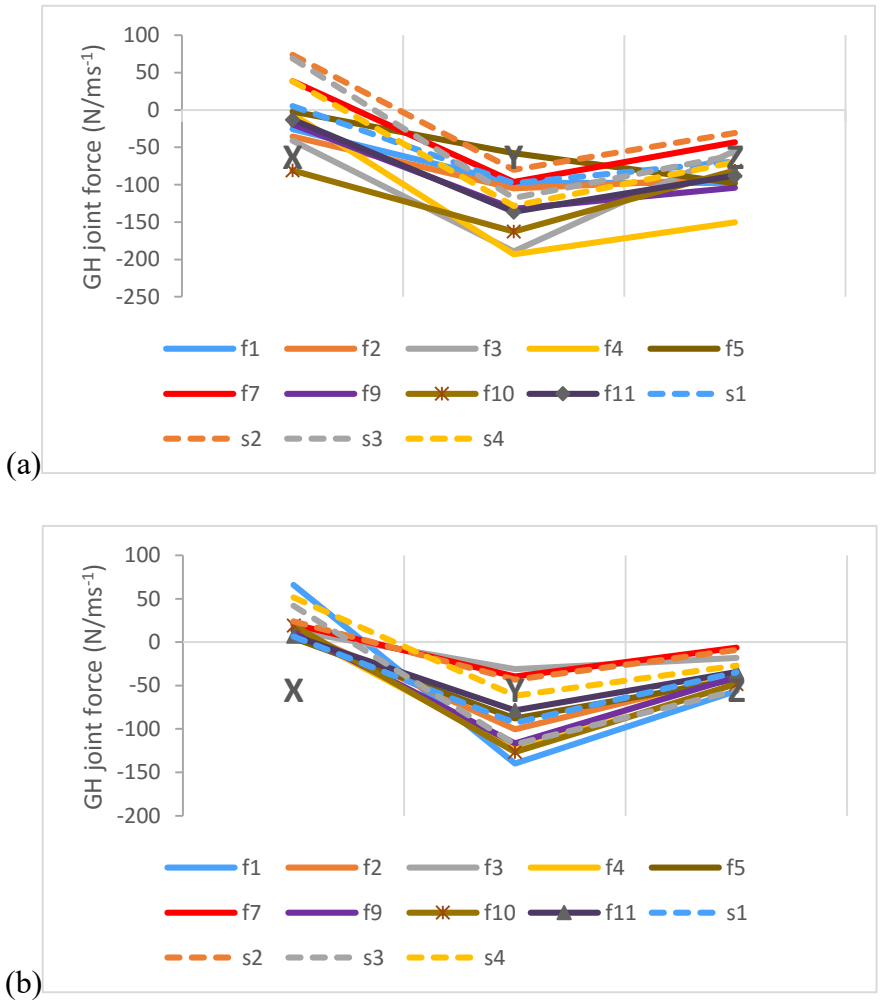

Figure 7.3 Peak glenohumeral joint force for all bowlers normalised to ball speed for stock over between (a) 50% to 100% and (b) 100% to 150% of the motion

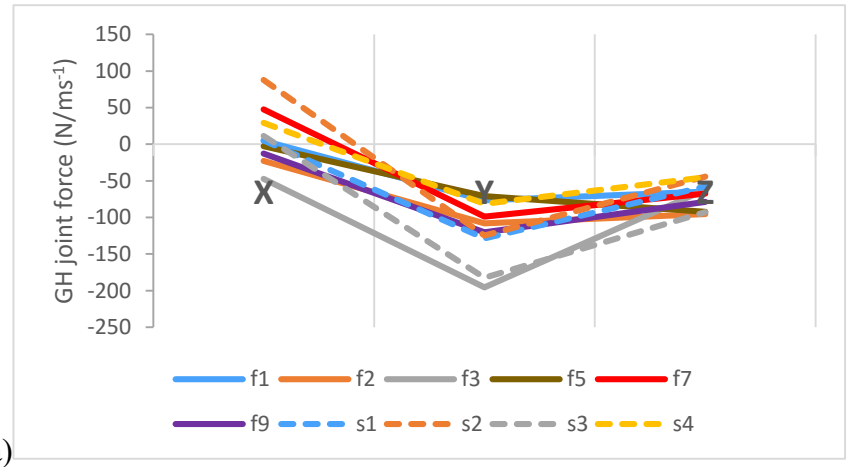

(a)

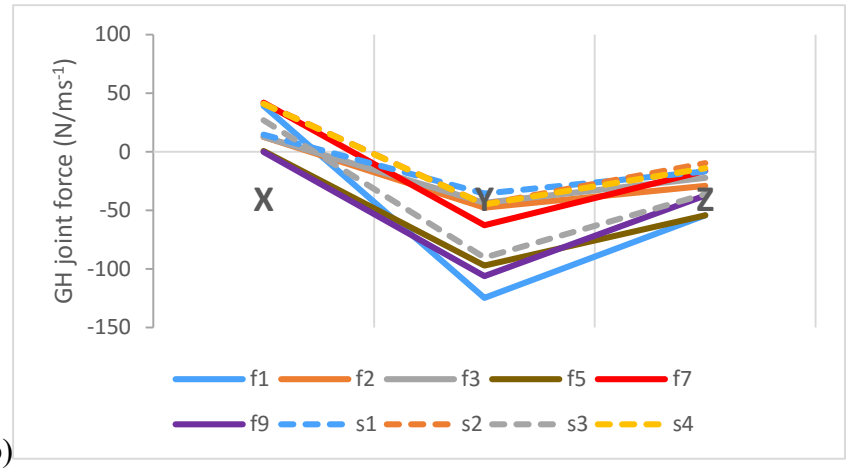

(b)

Figure 7.4 Peak glenohumeral joint force for all bowlers normalised to ball speed, variation over between (a) 50% to 100% and (b) 100% to 150% of the motion

The mean GH joint force is also plotted in the scapula frame to show the superior/inferior (Y axis) and posterior/anterior (Z axis) shear forces for bowlers.

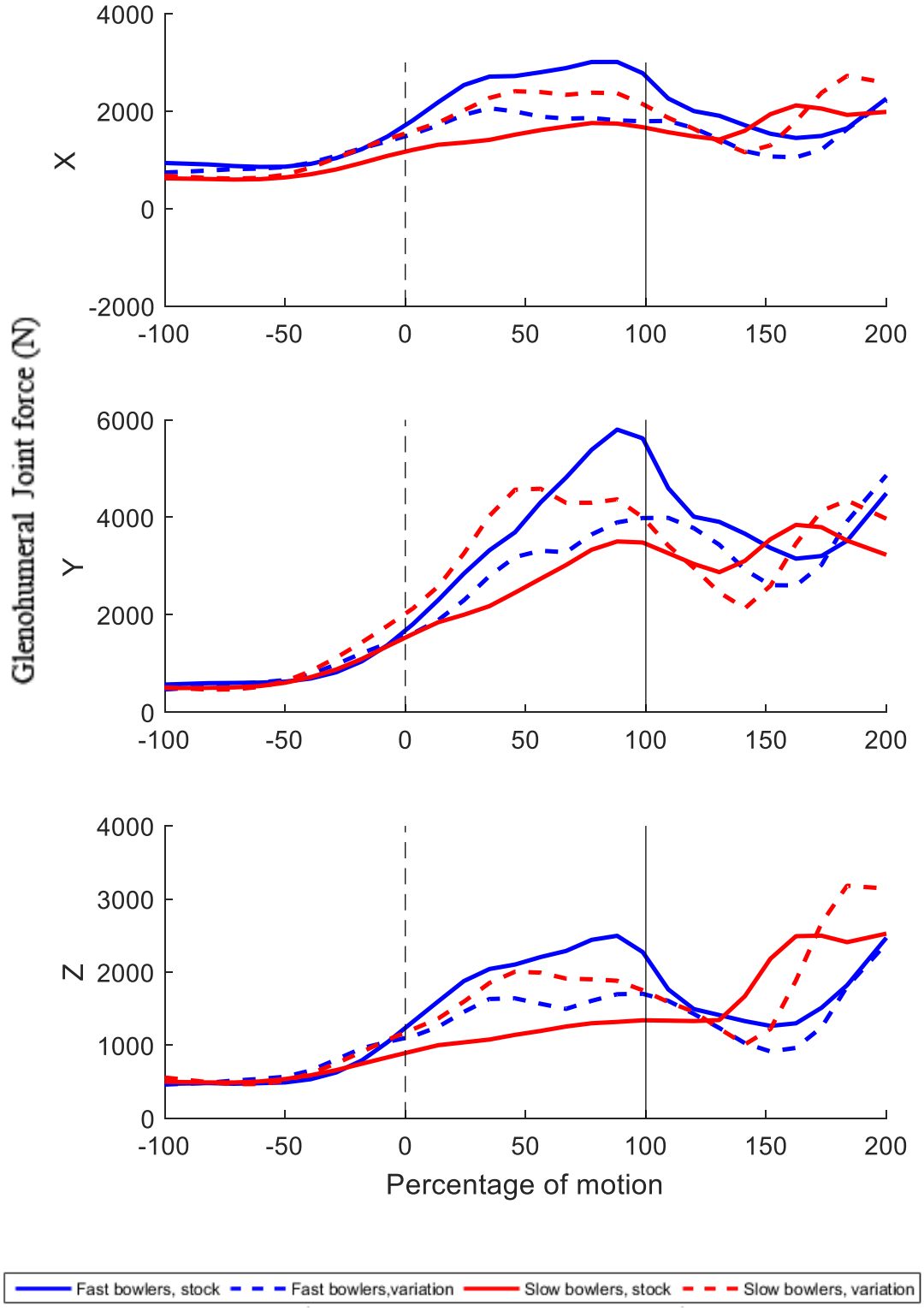

Figure 7.5 Mean glenohumeral joint reaction forces in the scapula coordinate frame for all bowlers.

7.3.3 GH joint stability

The stability of the GH joint is linked to the direction of the reaction force at the joint. A GH force locus that passes close to the glenoid rim indicates an increasingly unstable position. An important factor in assessing high-risk positions of GH joint instability is the magnitude of the joint reaction force and the location of this force on the glenoid. Figure 7.6 show the locus of the force for both sets of bowlers in their stock over while Figure 7.7 shows the same for their variation over. Key phases of the bowling action are highlighted where phase 1 shows motion from 50% to 100% while phase 2 shows 100% to 150%.

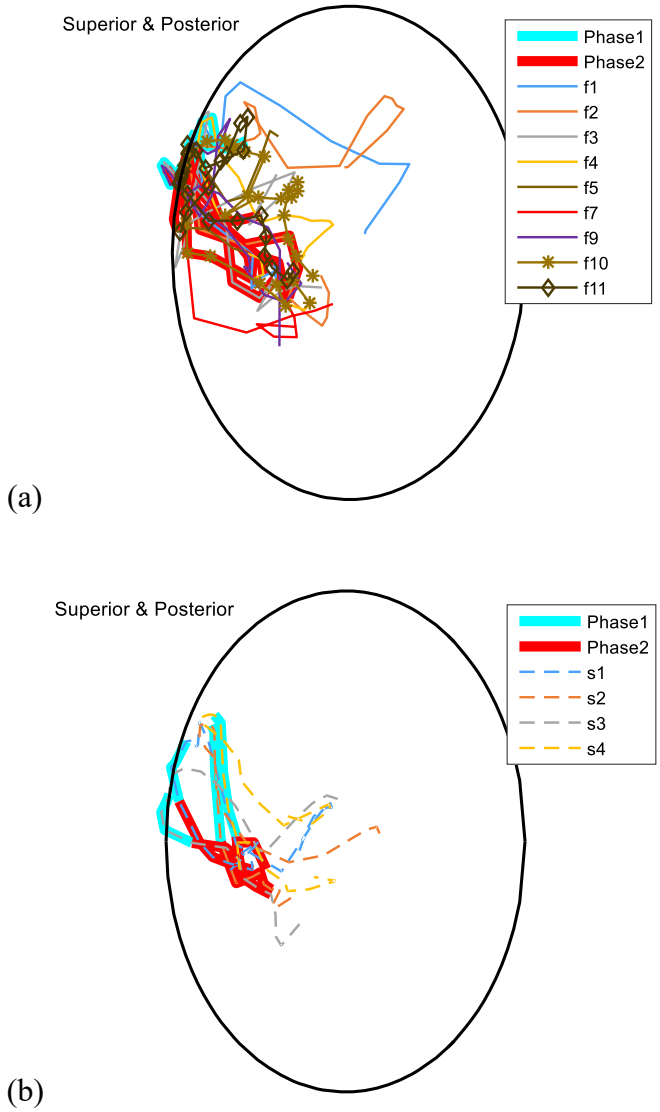

Figure 7.6 Mean and individual GH joint force locus for (a) fast bowlers and (b) slow bowlers, stock over. Phase1 is 50% to 100% of the motion and Phase2 is 100% to 150% of the motion

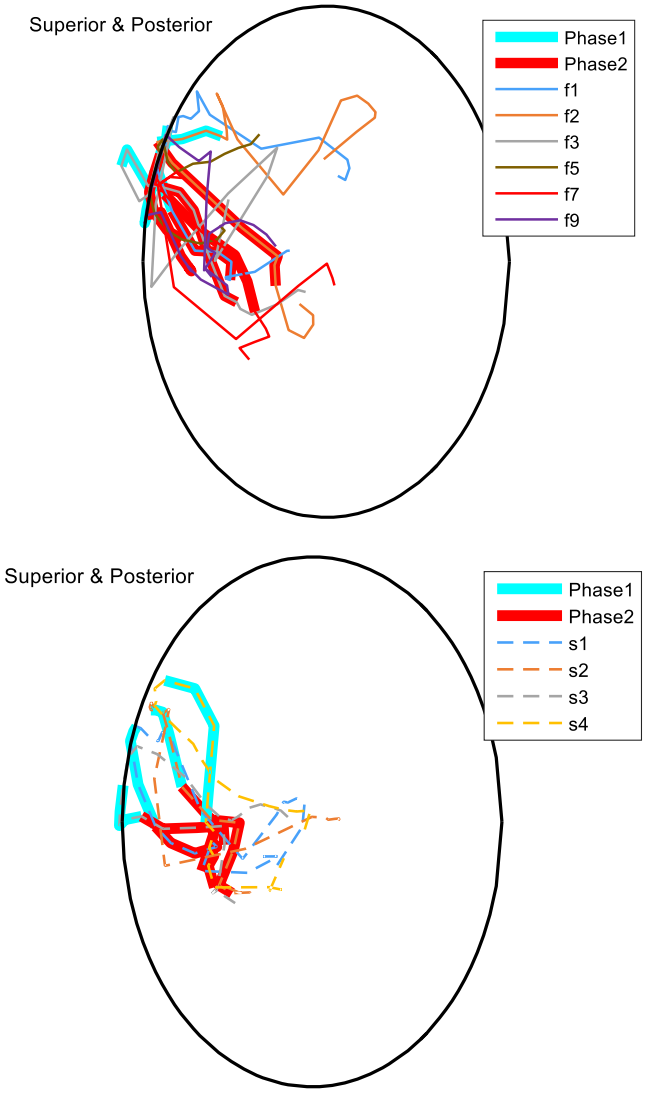

Figure 7.7 Mean and individual GH joint force locus for (a) fast bowlers and (b) slow bowlers, variation over. Phase1 is 50% to 100% of the motion and Phase2 is 100% to 150% of the motion

7.3.4 Average muscle forces

The average maximum muscle force for fast and slow bowlers in both overs is presented in Figure 7.8. The highest forces were seen in the pectoralis major and subscapularis with a value of just over 3 body weight while slow bowlers had an average maximum in the pectoralis major of 3.4 body weight.

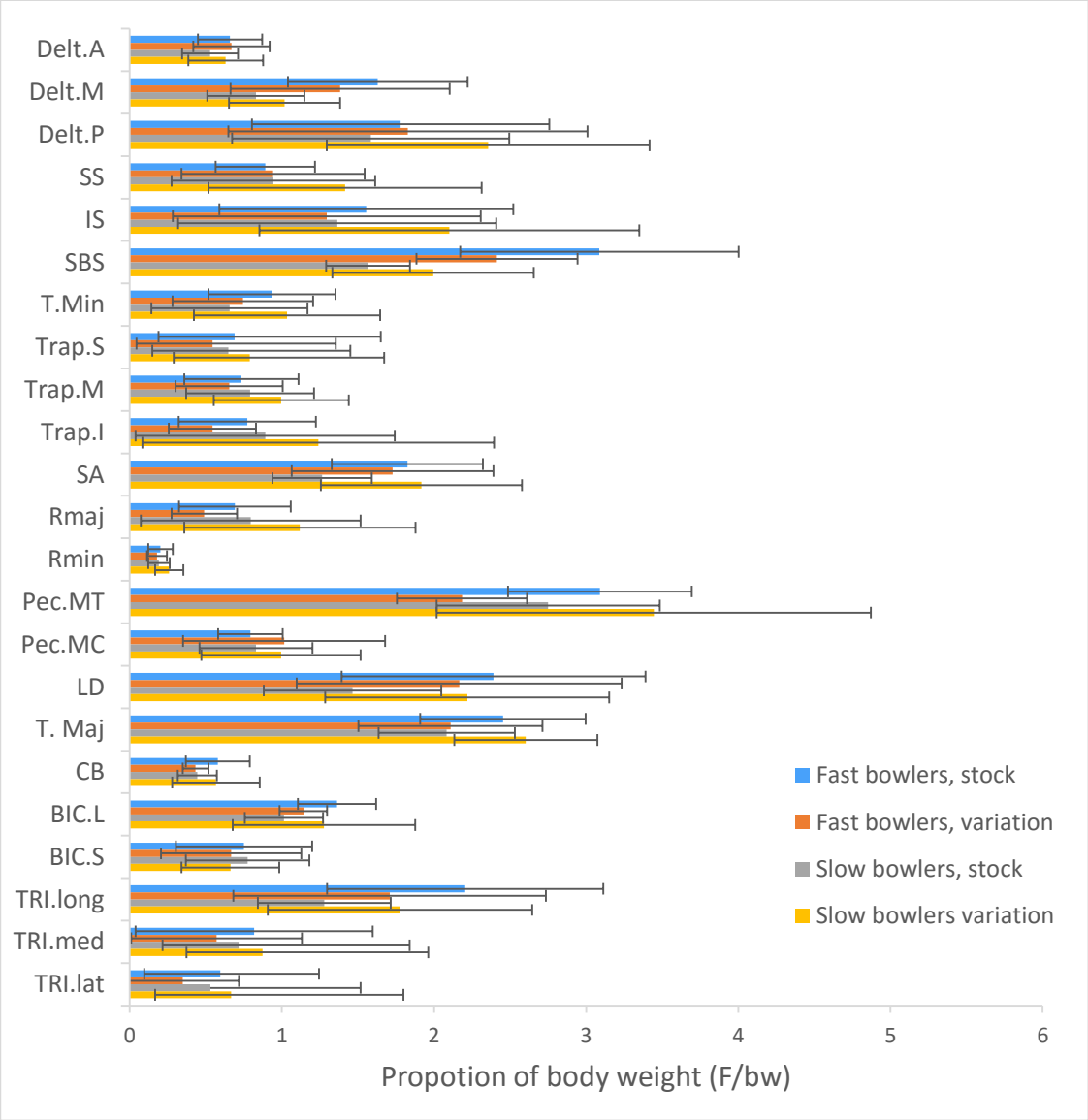

Figure 7.8 Average maximum normalised muscle forces for both sets of bowlers and both overs.

A summary of the muscle forces for each bowler is presented in Figure 7.9 and Figure 7.10 in the form of mean peak muscle forces in the two important phases of motion.

(a)

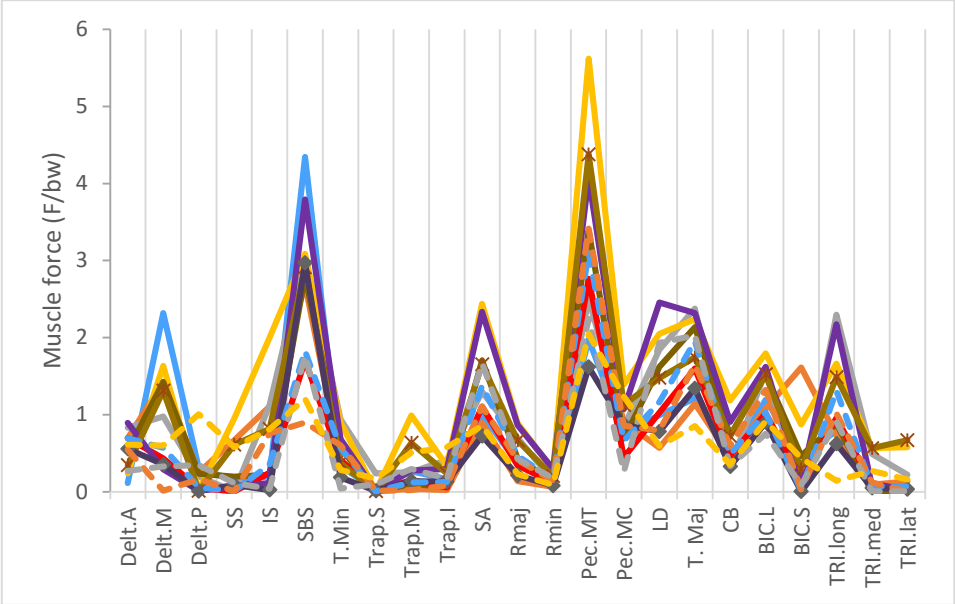

(b)

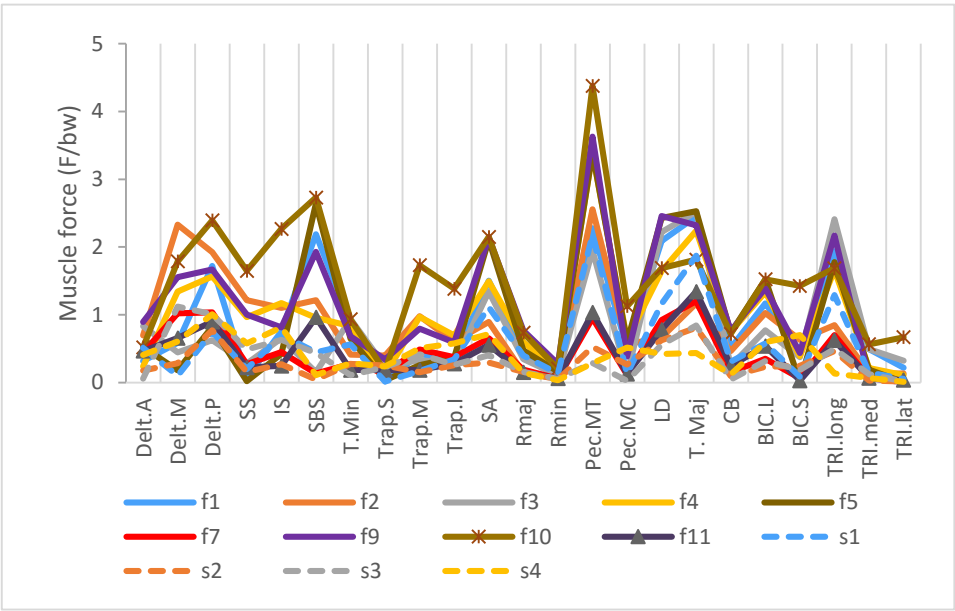

Figure 7.9 Mean peak muscle forces for all bowlers, stock over between (a) 50% to 100% and (b) 100% to 150% of the motion

(a)

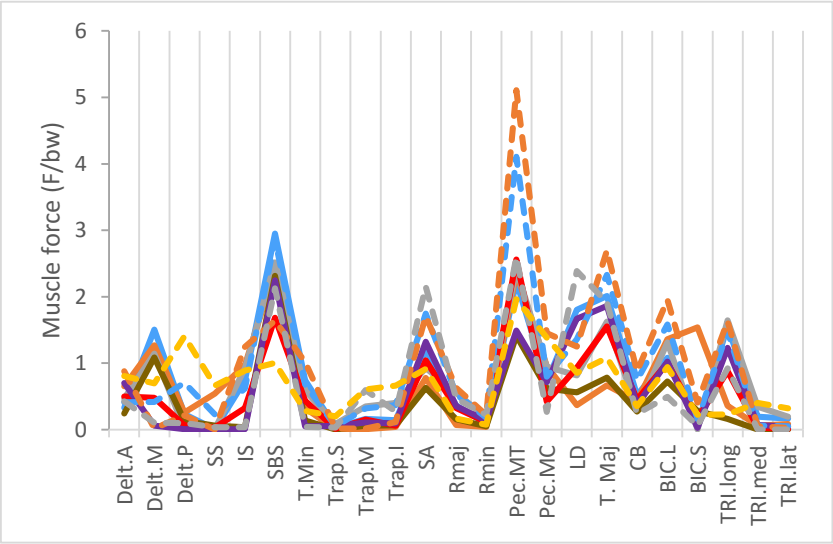

(b)

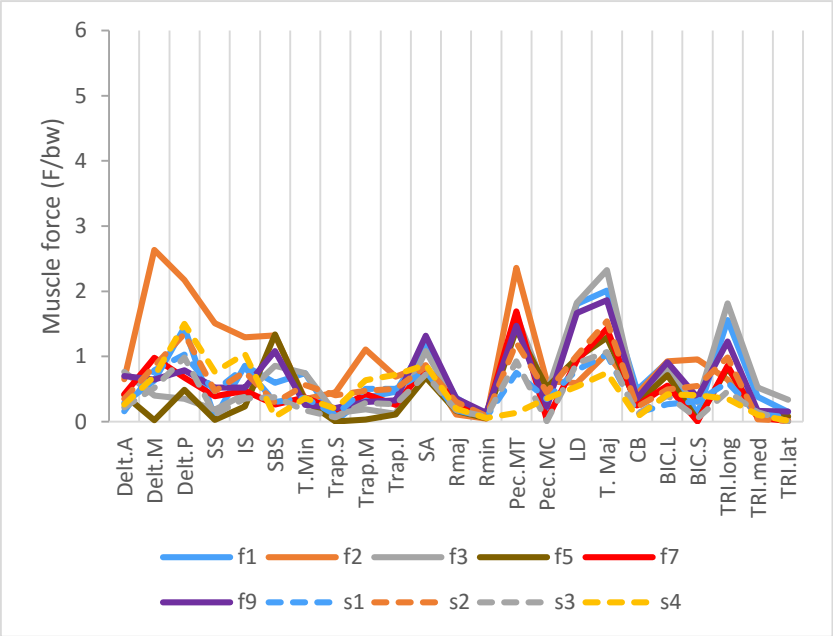

Figure 7.10 Mean peak muscle forces for all bowlers, variation over between (a) 50% to 100% and (b) 100% to 150% of the motion

7.3.5 Muscle activation

Muscle activation is present for bowlers and their stock over. These activation levels would help identify where maximum forces presented in Figure 7.8 occurred.

Figure 7.11 to Figure 7.16 shows that the most active muscles before ball release were subscapularis, middle deltoid, serratus anterior and teres major, biceps long and pectoralis major with the infraspinatus, teres minor, posterior deltoid, latissimus dorsi and scapula

stabilizer muscles being active in the follow through.

7.3.5.a Rotator cuff and deltoid muscles

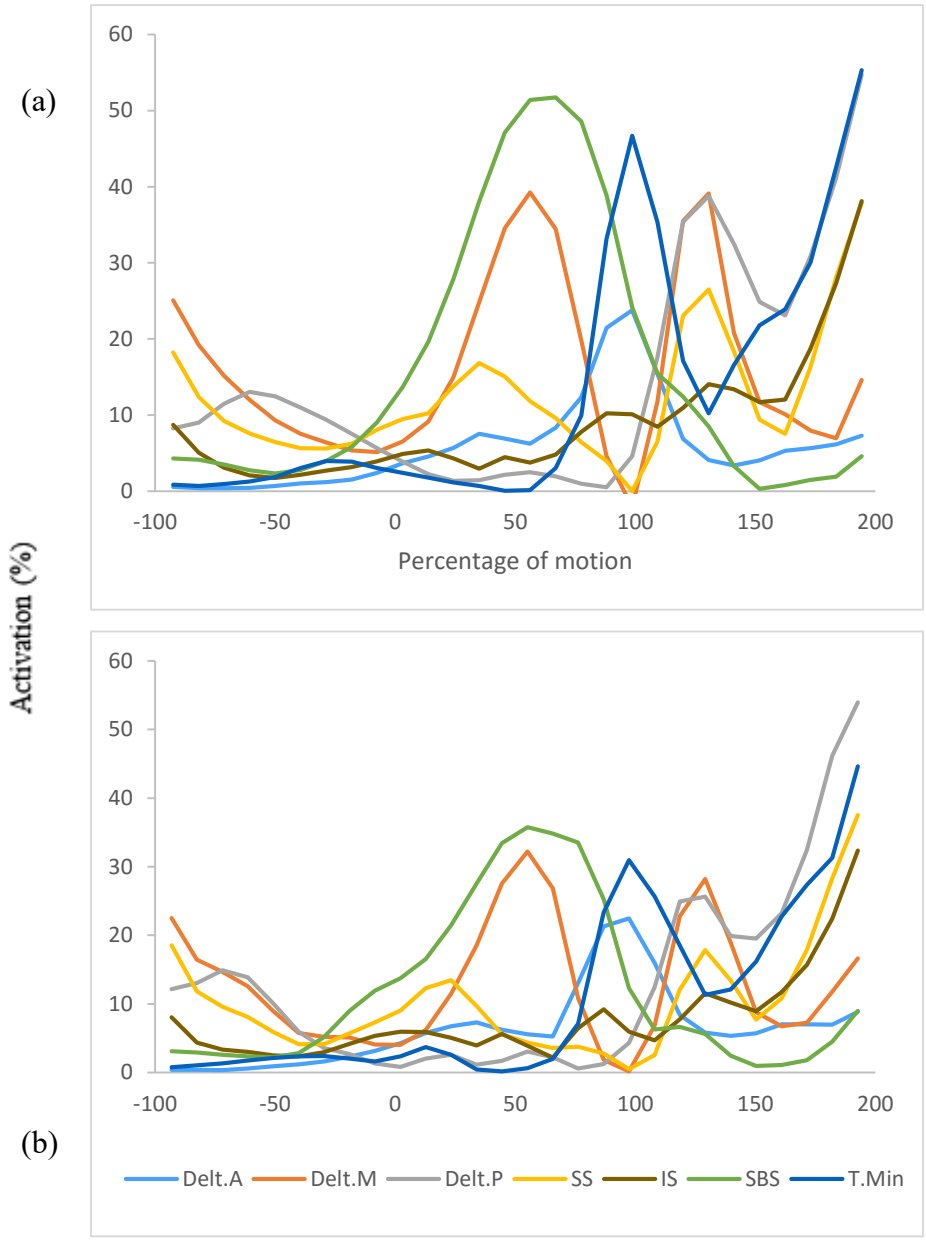

Figure 7.11 Average activation for rotator cuff and deltoid muscles for fast bowlers (a) stock and (b) variation over

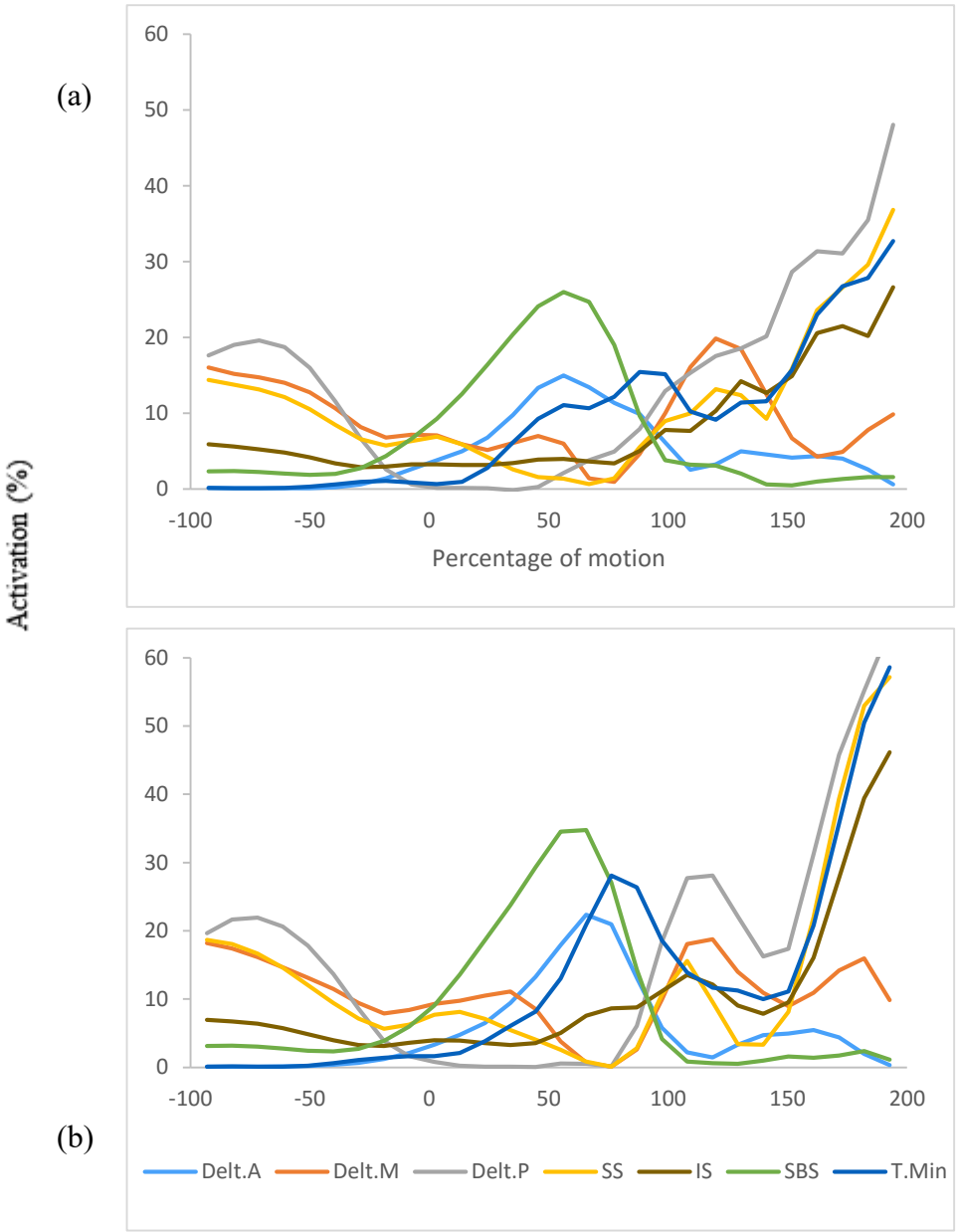

Figure 7.12 Average activation for rotator cuff and deltoid muscles for slow bowlers (a) stock and (b) variation over

7.3.5.b Scapula stabilisers

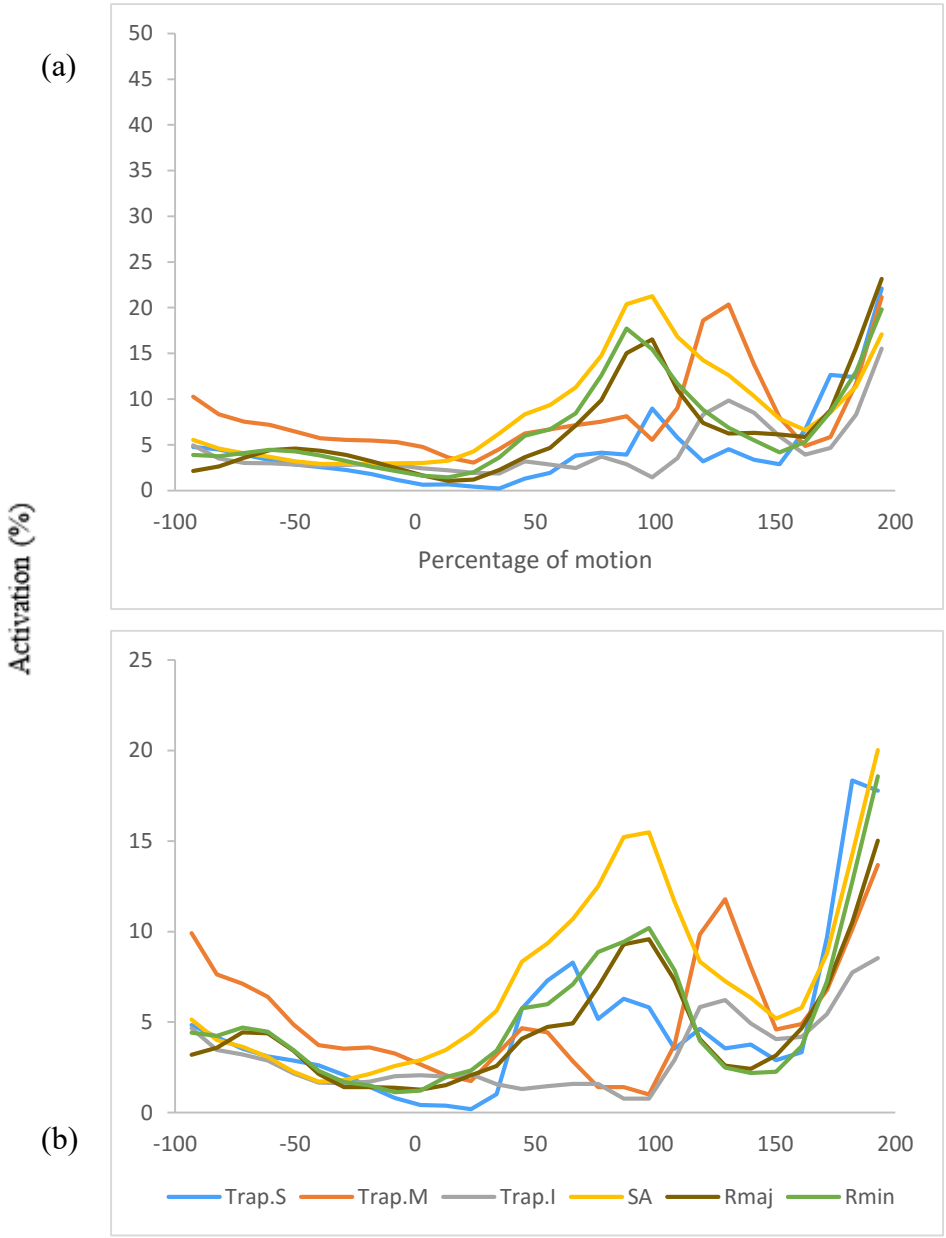

Figure 7.13 Average activation for scapula stabilizers for fast bowlers (a) stock and (b) variation over

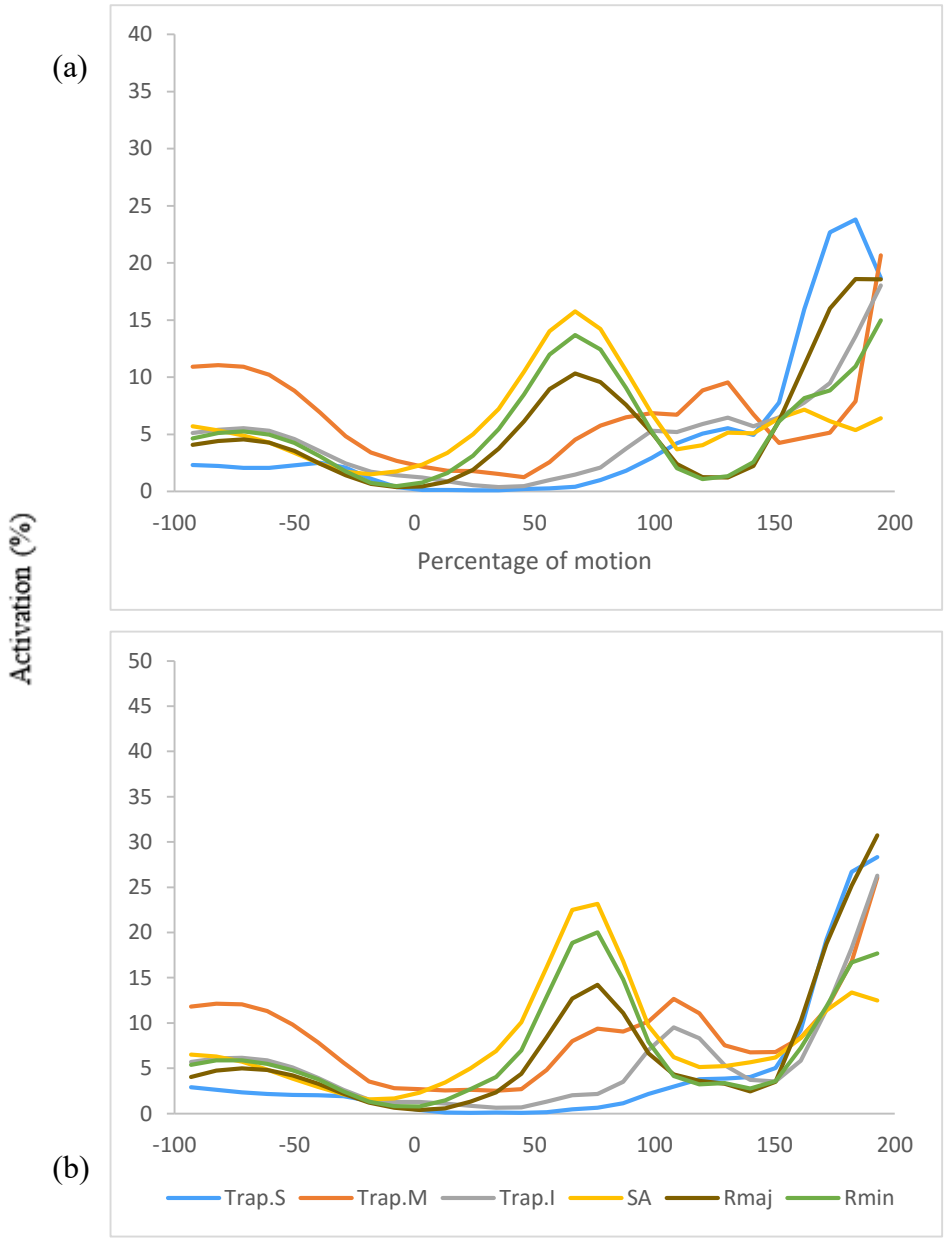

Figure 7.14 Average activation for scapula stabilizers for slow bowlers (a) stock and (b) variation over

7.3.5.c Rotators of the humerus

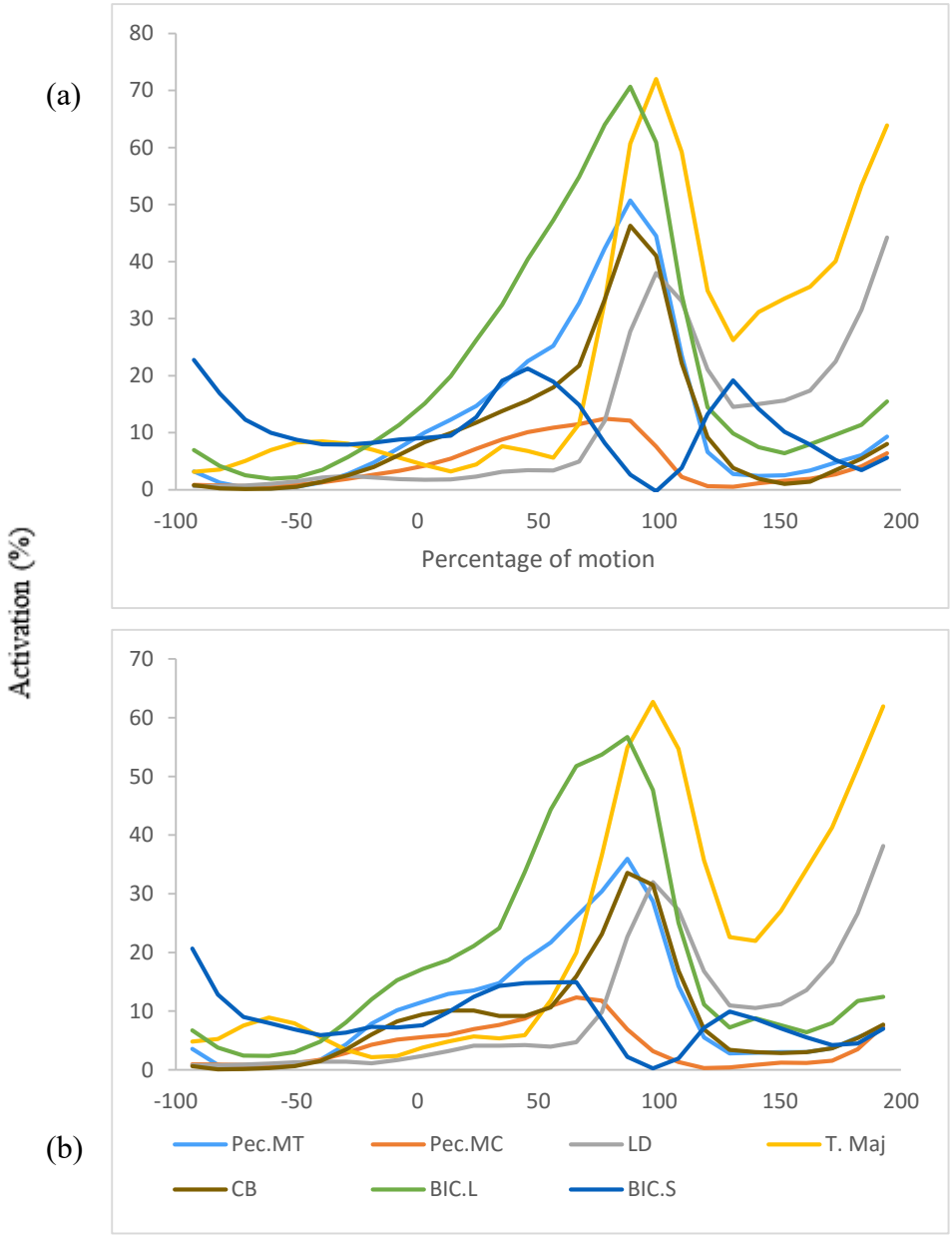

Figure 7.15 Average activation for key movers of the humerus for fast bowlers (a) stock and (b) variation over

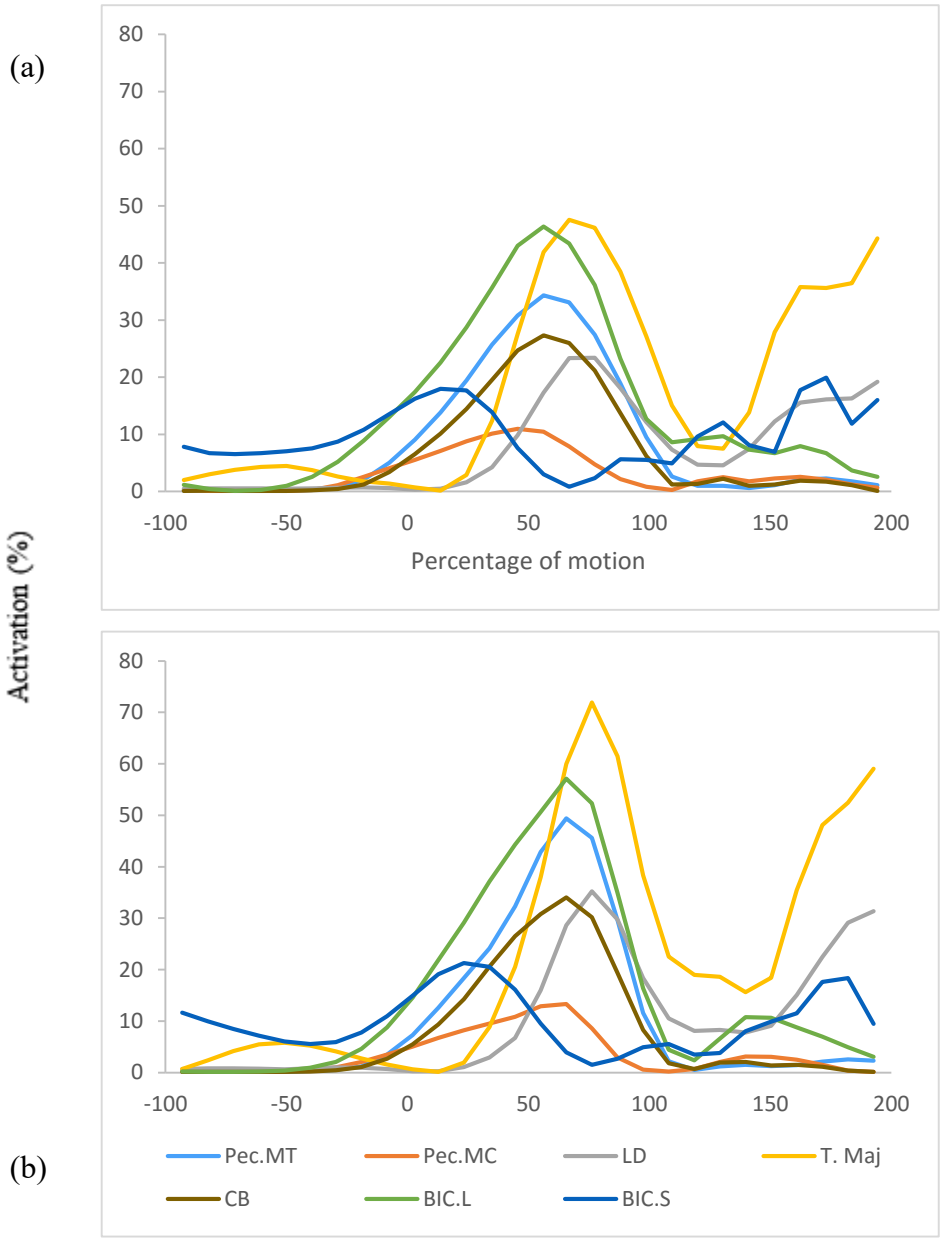

Figure 7.16 Average activation for key movers of the humerus for slow bowlers (a) stock and (b) variation over

7.4 Discussion

Firstly, the results presented are compared to the literature also including discussion on the risk of injuries. Important observations between subjects that might have been masked in the overall averages will also be presented. Finally, the issue of high joint and muscle forces is discussed where conclusions on the suitability of the UKNSM for simulating cricket bowling are made.

7.4.1 GH joint forces and stability

High circumduction velocity of the bowling arm particularly in fast bowling makes the shoulder vulnerable to distraction forces. This, coupled with the fact that the elbow is usually near full extension, as dictated by the laws of the game, necessitates a greater centripetal force to prevent distraction (Stuelcken et al., 2010).

The peak glenohumeral joint distraction forces of 6052N± 2463 and 6338N ±2221N for fast and spin bowlers (Figure 7.1) were significantly higher than those reported by Stuelcken et al. (2010) . These researchers found that in a study of 18 female fast bowlers where the GH force was calculated using a three-segment inverse solution model of the bowling arm, a peak distraction force of 599N ±111N was observed in the early stages of the follow through phase. Different GH joint forces is expected given the differences in the gender of subjects tested and differences in mean ball speed of 26 ms^{-1} ±1 for their fast bowlers versus 28.01ms^{-1} ±3.52 and 23.27ms^{-1} ±2.52 for fast and spin bowlers' faster delivery in this study. However, the much higher GH joint forces could be attributed to the sensitivity of the model to fast motion, which was highlighted in Chapter 6.

Figure 7.1b shows that the peak distraction forces between both sets of bowlers for their faster delivery were within comparable range while the same was observed for their slower delivery. A mean peak force of 7.9 body weight and 8.7 body weight for fast and spin bowlers occurred between 50% to 100% of the motion. The peak force for fast bowlers occurred closer to ball release contrary to what was observed by Stuelcken et al. (2010). Lower values of 5.6 body weight and 5.8 body weight were found for the slower delivery of the two tested, for fast and slow bowlers respectively.

Figure 7.3 and Figure 7.4 show a summary of the peak GH joint forces within the phase 1 and phase 2 when normalised to ball speed. Of note, subjects f4 and s3 showed the largest distraction forces when bowling the faster of the two deliveries. Subject f4 was ranked the 4th fastest bowler

which indicates that the joint forces at the shoulder did not scale with ball speed but depended on bowling technique. This was also true for the slow bowlers, where s3 had the slowest ball speed in the group when they bowled their faster ball.

An important consideration in investigating pathomechanics of the shoulder, particularly involving large range of motion, is the glenoid shear forces. The superior shear forces at the GH joint for both group of bowlers was greater than the posterior shear forces (Figure 7.5). Peak superior shear forces followed a similar trend to the distraction force, occurring closer to ball release for fast bowlers and occurring earlier for slow bowlers. The peak superior shear force values were 5800N ±1935N and 4584N ±2187N for fast and slow bowlers respectively, while peak posterior shear force values were 2496N ±894N and 2004N ±952N. For fast bowlers, the peak superior shear force were within range of the peak compressive force, highlighting the risk of translation of humeral head if these shear forces were to exceed the compressive force as described in the literature (Yanagawa et al., 2008). This risk was found for both overs of fast bowlers and stock over for slow bowlers. These findings support the claim that bowlers would be at risk of impingement especially during the follow through phase as acknowledged in the literature (Bell-Jenje & Gray, 2005; Stuelcken et al., 2010). The importance of shear forces is highlighted in the literature where it is attributed to GH joint capsular adaptations, manifested by increased external rotation and decreased internal rotations (Aginsky et al., 2004; Bell-Jenje & Gray, 2005; Giles & Musa, 2008). Normalising the shear forces also showed that it did not scale well with ball speed.

For both sets of bowlers, the faster of the two deliveries resulted in a larger GH distraction and shear force.

The GH joint stability plots (Figure 7.6 and Figure 7.7) show the same trend of an increasingly unstable position as the arm rotates into phase 1 of the motion followed by an increase in stability in the follow through. During rotation into phase 1 (50-100%) the GH joint reaction force moved posteriorly and superiorly towards the edge of the glenoid rim. As the arm continues to rotate into phase 2, there was an anterior and inferior migration of the force towards the centre. It was observed that for slow bowlers the phase 1 of the bowling action presented a greater risk of instability at the joint. In contrast, the GH joint force for fast bowlers was at the glenoid edge during the ball release and early follow through. These positions coupled with the large GH joint reaction force in these regions of the bowling action, make them high compromising positions.

There were no major changes between overs in the locus of the GH joint force, except for bowler f3 who could not satisfy the glenoid constraint for two frames within phase 1.

7.4.1.a Muscles that contribute to GH joint stability

Figure 7.17 and Figure 7.18 summarise the maximum moments contributed by muscles of the GH joint within 50%-100% and 100%-150% of the motion.

For phase 1, the subscapularis was the greatest contributor of the rotator cuff muscles. There were significant contributions from this muscle in GH flexion for all bowlers and for GH adduction for fast bowlers. Latissimus dorsi and pectoralis major thorax had the greatest internal rotation moments within this phase. There was little contribution by the middle deltoid with the arm in this elevated position.

In phase 2, there was again significant contribution by the subscapularis for fast bowlers with minor contributions from anterior and middle deltoids. The pectoralis major thorax and latissimus dorsi demonstrated significant internal rotation. The infraspinatus, posterior deltoid and teres minor contribute an external rotation moment, particularly for slow bowlers' faster delivery. The posterior deltoid, supraspinatus, infraspinatus and teres minor showed significant contributions to GH abduction during this follow through phase.

The major contributors to GH joint stability is an important consideration in injury analysis as it can point to key muscles that are at risk due to overuse. For the rotator cuff muscles, the subscapularis was found to offer the greatest stabilising potential in the joint followed by the infraspinatus during the follow through phase. The supraspinatus only contributed to joint stability in the follow through phase, indicating that the extended and externally rotated humerus in this phase did not allow for effective use of this muscle. Both the supraspinatus and infraspinatus are in eccentric loading in the follow through phase. These findings highlight the reliance on these muscles to provide joint stability that could lead to a high incidence of pathology due to repetitive loading. Typically when speaking in terms of injury risk at the shoulder, the supraspinatus is often mentioned however, these findings indicated that for cricket bowling, the subscapularis is at higher risk of overuse, particularly in the delivery phase. This may lead to weakening of the subscapularis, leading to superior and anterior translation of the humeral head and greater risk of impingement of the supraspinatus, similar to what is described in the literature for overhead athletes (Anderson & Alford, 2010). The injury mechanism warrants further investigation.

(a)

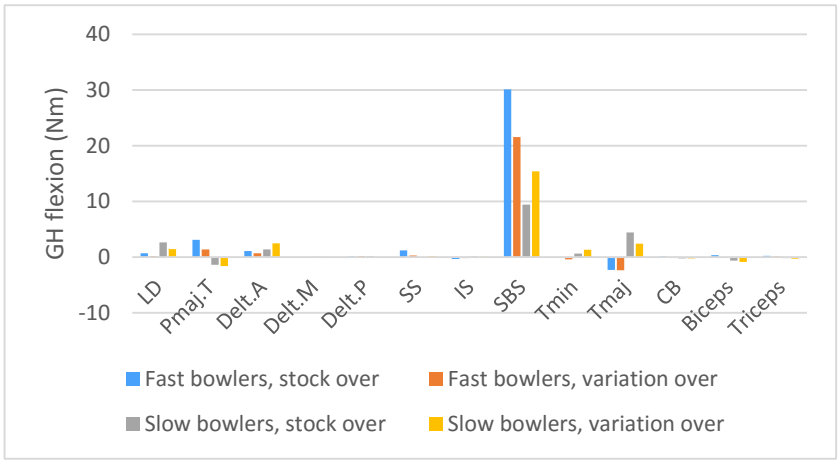

(b)

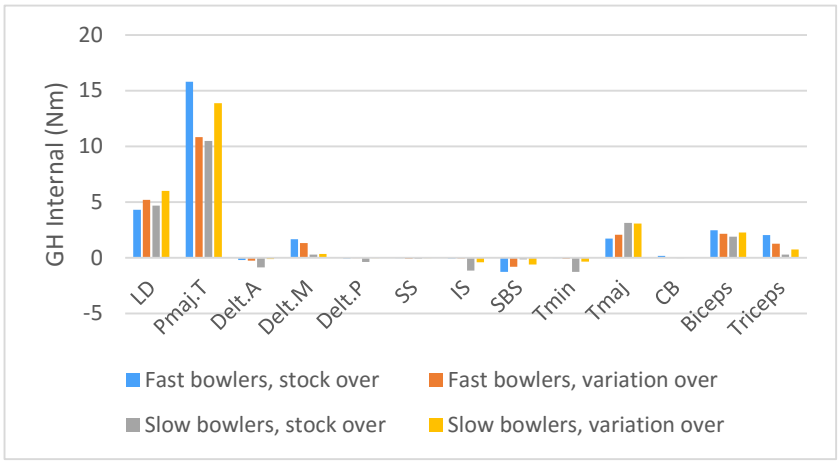

(c)

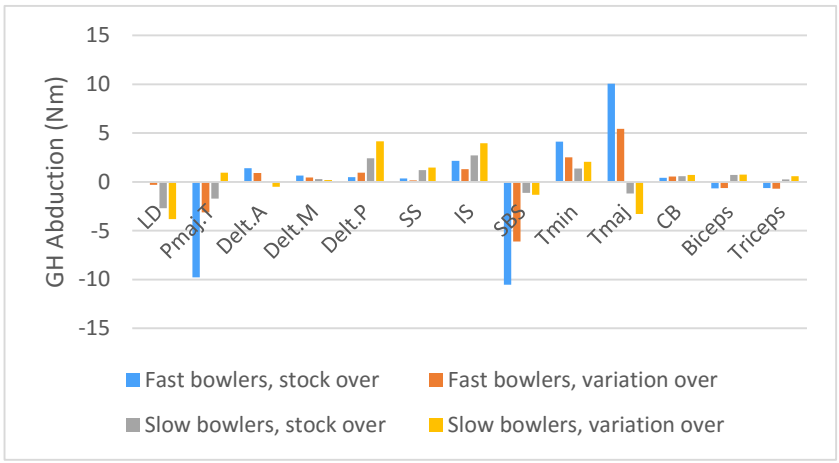

Figure 7.17 Moment of muscles about the GH joint in the humerus coordinate frame for phase 1 of the motion

(a)

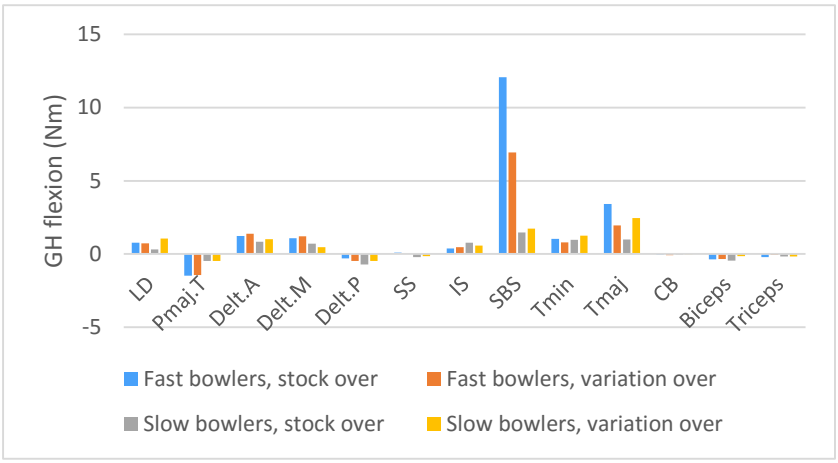

(b)

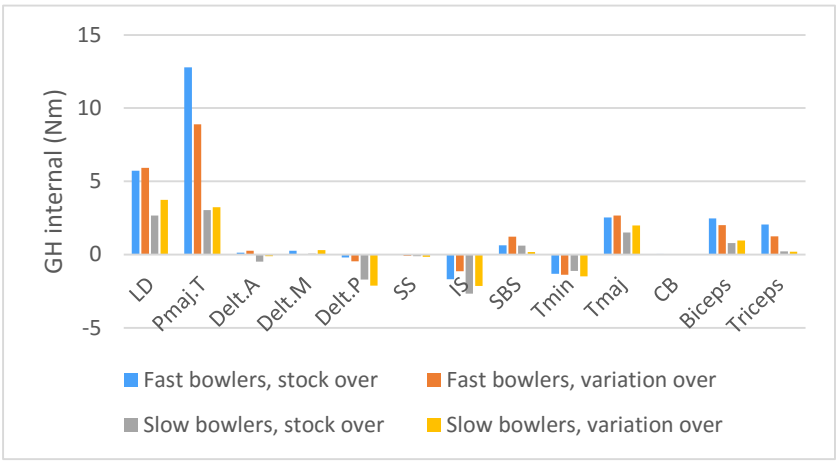

(c)

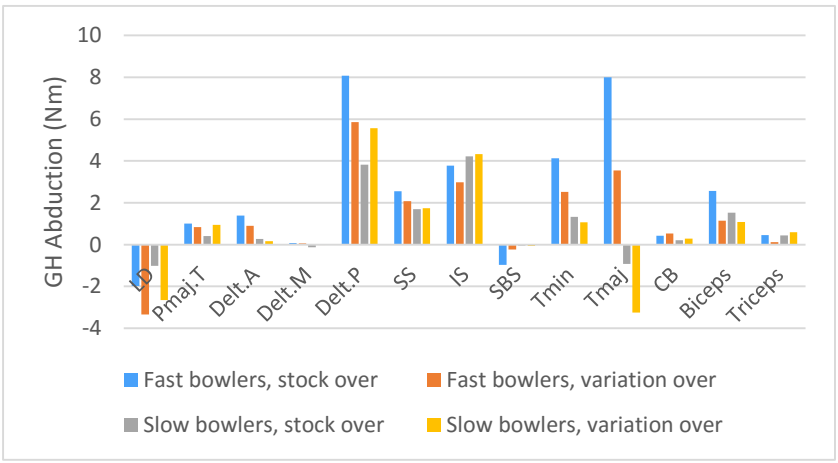

Figure 7.18 Moment of muscles about the GH joint in the humerus coordinate frame for phase 2 of the motion

Variations in the glenohumeral joint torques between both sets of bowlers and delivery types are presented in Figure 7.19 to Figure 7.24. During the phase of upper arm vertical to ball release, a peak adduction torque for fast bowlers occurred just before ball release whereas for slow bowlers it occurred just after 50% of the motion. During this phase where the shoulder circumducts backward in adduction and extension, the peak adduction torque values of -136 Nm and -111 Nm were observed for fast and slow bowlers respectively, while the peak extension values were 62 Nm and 40 Nm respectively for the stock over. For both groups bowlers a peak flexion torque (fast bowlers: 90 Nm, slow bowlers: 21 Nm) was observed following the peak extension torque as the arm rapidly increases its elevation angle to ball release.

Values of peak abduction/adduction and flexion/extension was observed to be dependent on the variation being bowled where, the faster delivery produced greater peak values. The largest changes being an increased peak adduction for slow bowlers to 146 Nm and a decrease in the peak flexion torque for fast bowlers to 66 Nm.

It was hypothesised in Chapter 5 that the GH internal rotation torque may provide a clearer distinction for bowlers who were at greater risk of injury. Figure 7.20 and Figure 7.23 present this data for stock and variation overs respectively. There was little variation between overs for both sets of bowlers as indicated by the mean GH internal rotation torque. Even though the mean internal rotation torque for slow bowlers was greater after ball release when compared to fast bowlers, due to a small sample size conlcusions on the greater risk of injury for spin bowlers could not be made.

Subject f3 and s3 had a noticeably greater internal rotation torque near 50% when compared to others in the group. The unique action of f3 that was described in Chapter 5, is highlighted in Figure 7.20a with a drastic external rotation torque prior to ball release. Interestingly, this was observed for both overs indicating that it may not be related to increasing ball speed but is closely tied to the technique of the bowler regardless of the delivery they bowl. Given these results, the proposed hypothesis is not supported.

It is interesting to note that the torque for both sets of bowlers and overs, show a consistent internal rotation torque near 50%. This is consistent to what is reported by Aginsky et al. (2004) who reported a functional deficiency of the external rotators and attributed injuries to muscle imbalance where the external rotators cannot oppose the large internal rotations at the GH during bowling. These results show the internal rotation torque at 50% thus highlighting another

key phase where there is risk of injury in the case of imbalances between internal and external rotators of the shoulder.

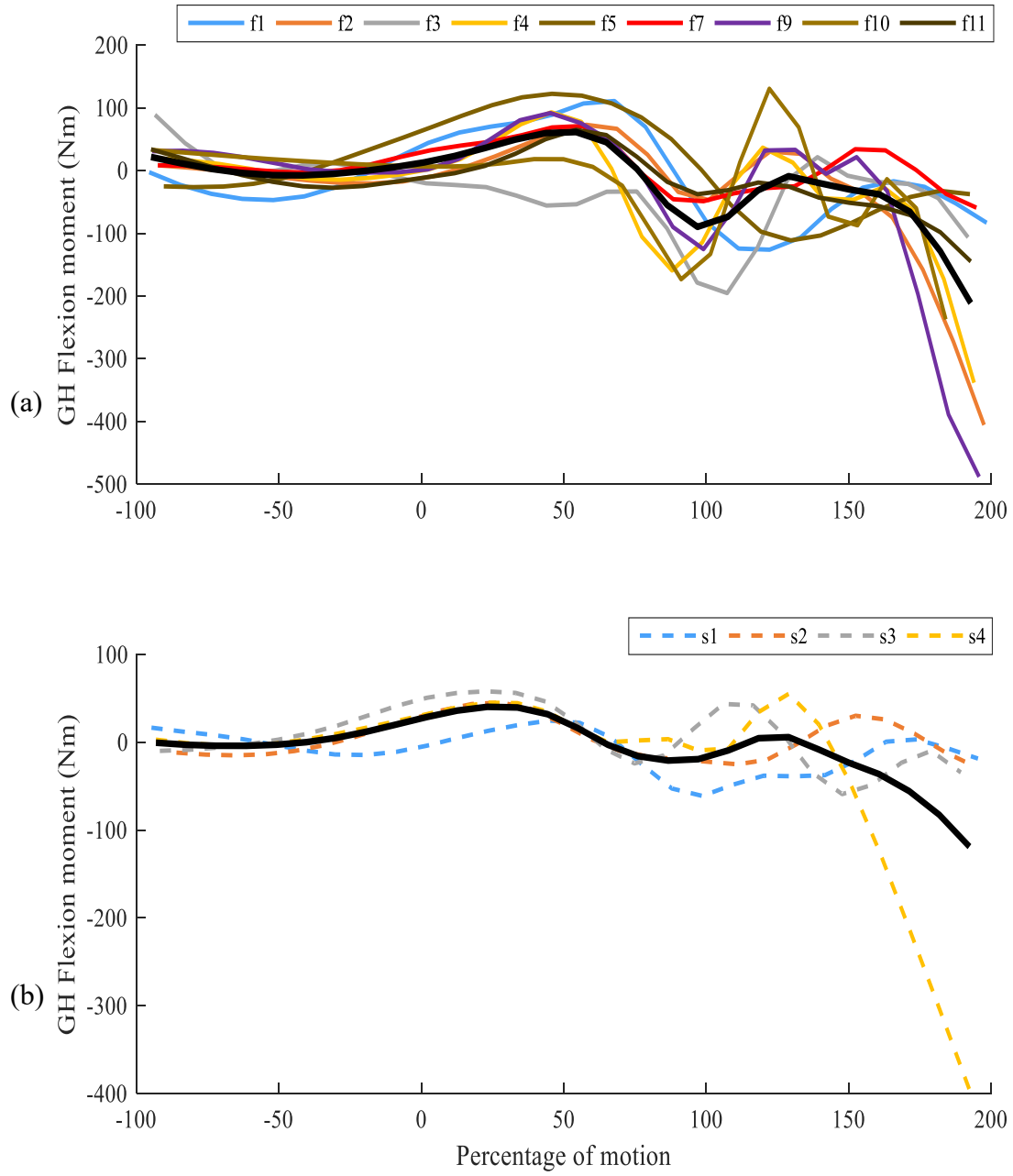

Figure 7.19 GH flexion rotation moment for (a) fast and (b) slow bowlers, stock over. Mean rotation moment is indicated by a black line.

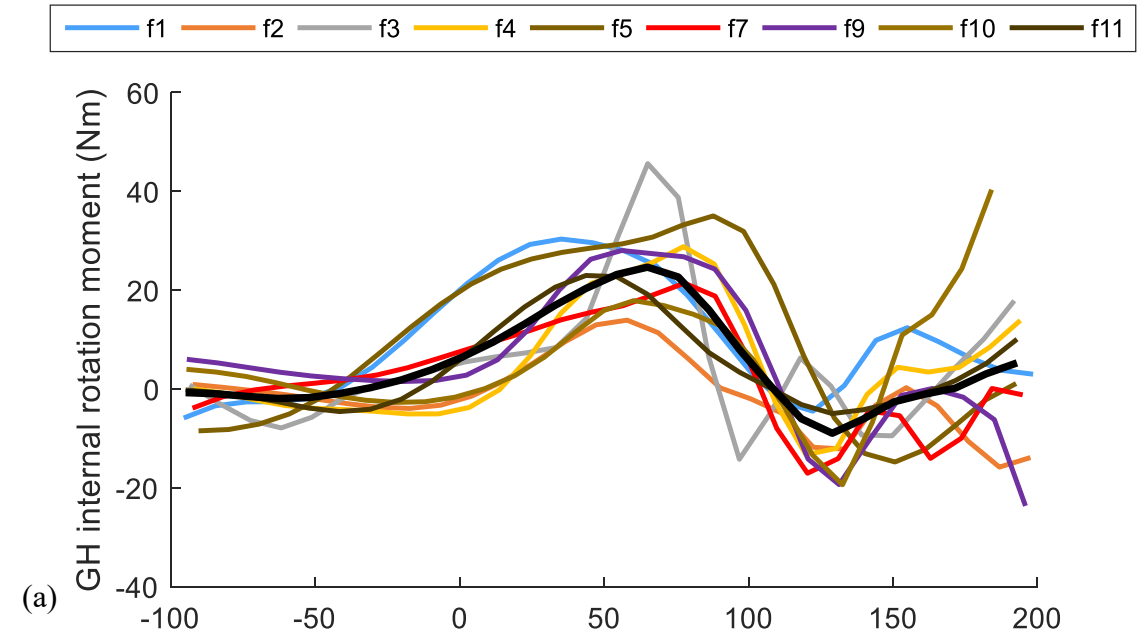

(a)

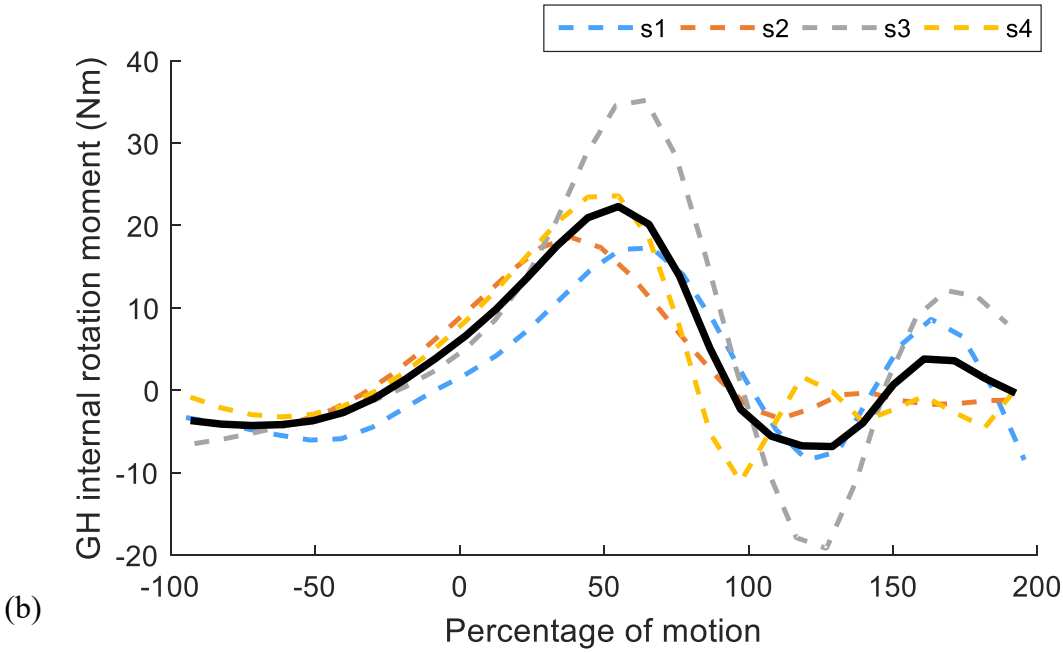

(b)

Figure 7.20 GH internal rotation moment for (a) fast and (b) slow bowlers, stock over. Mean internal rotation moment is indicated by a black line.

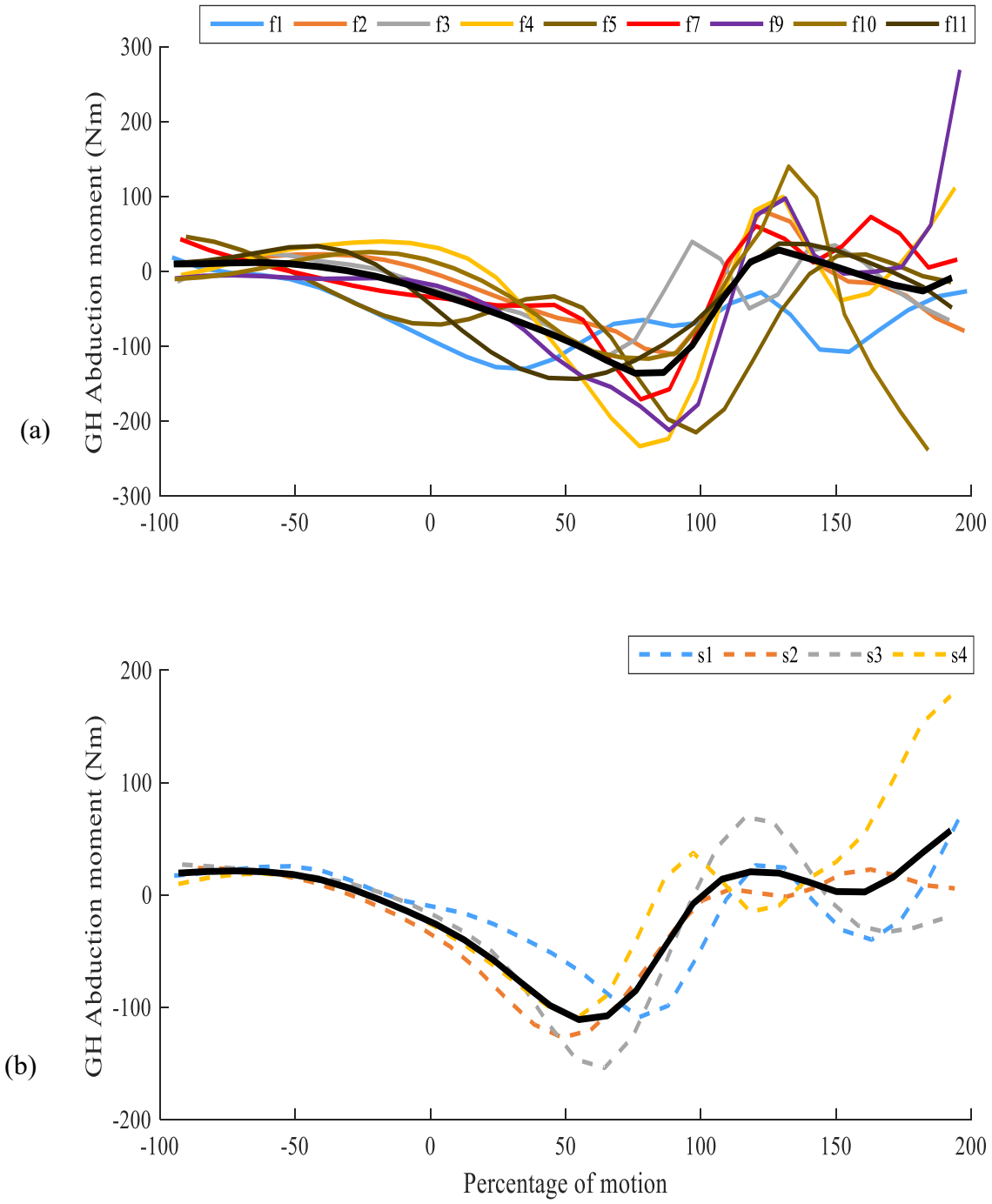

Figure 7.21 GH abduction rotation moment for (a) fast and (b) slow bowlers, stock over. Mean rotation moment is indicated by a black line.

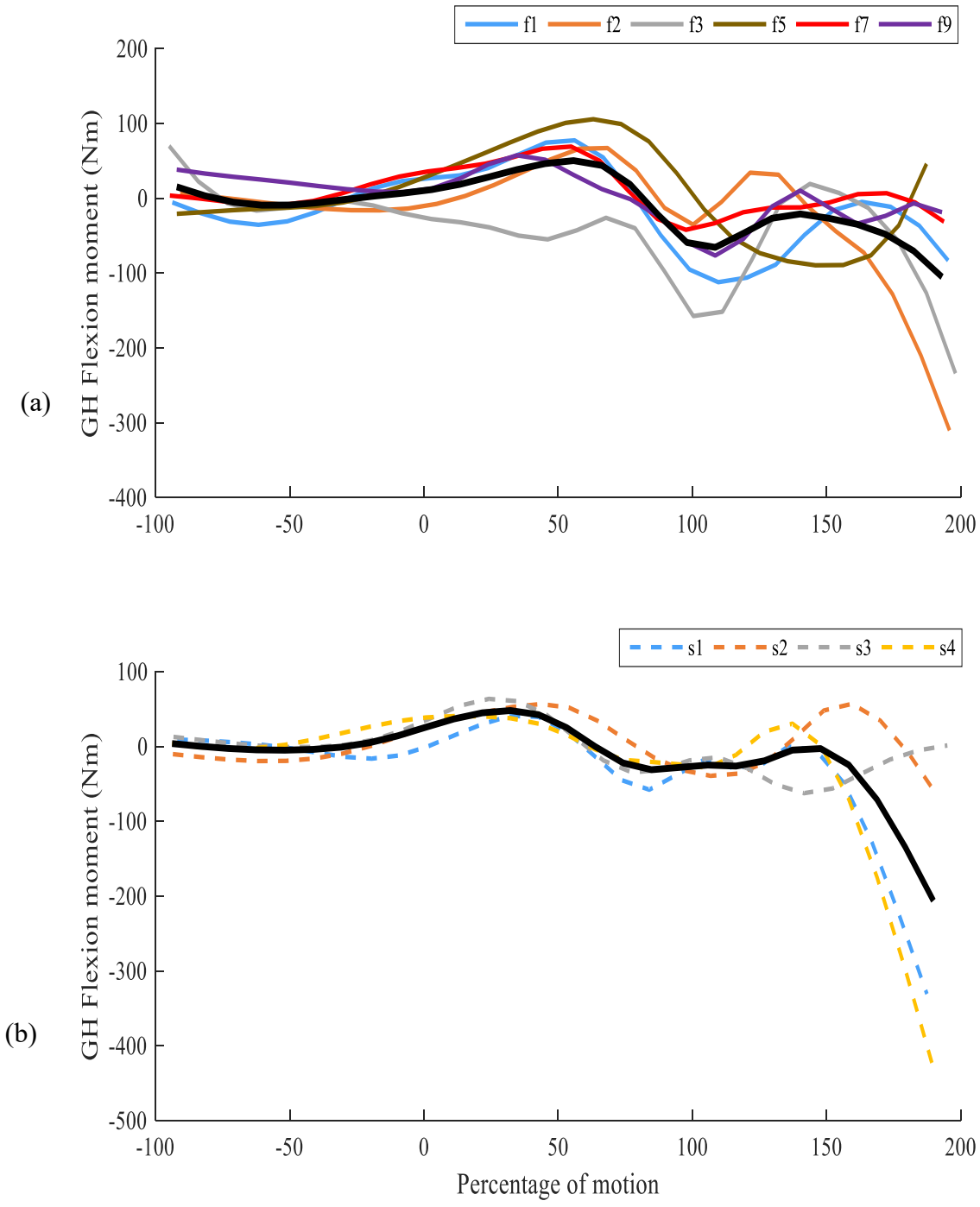

Figure 7.22 GH flexion rotation moment for (a) fast and (b) slow bowlers, variation over. Mean rotation moment is indicated by a black line.

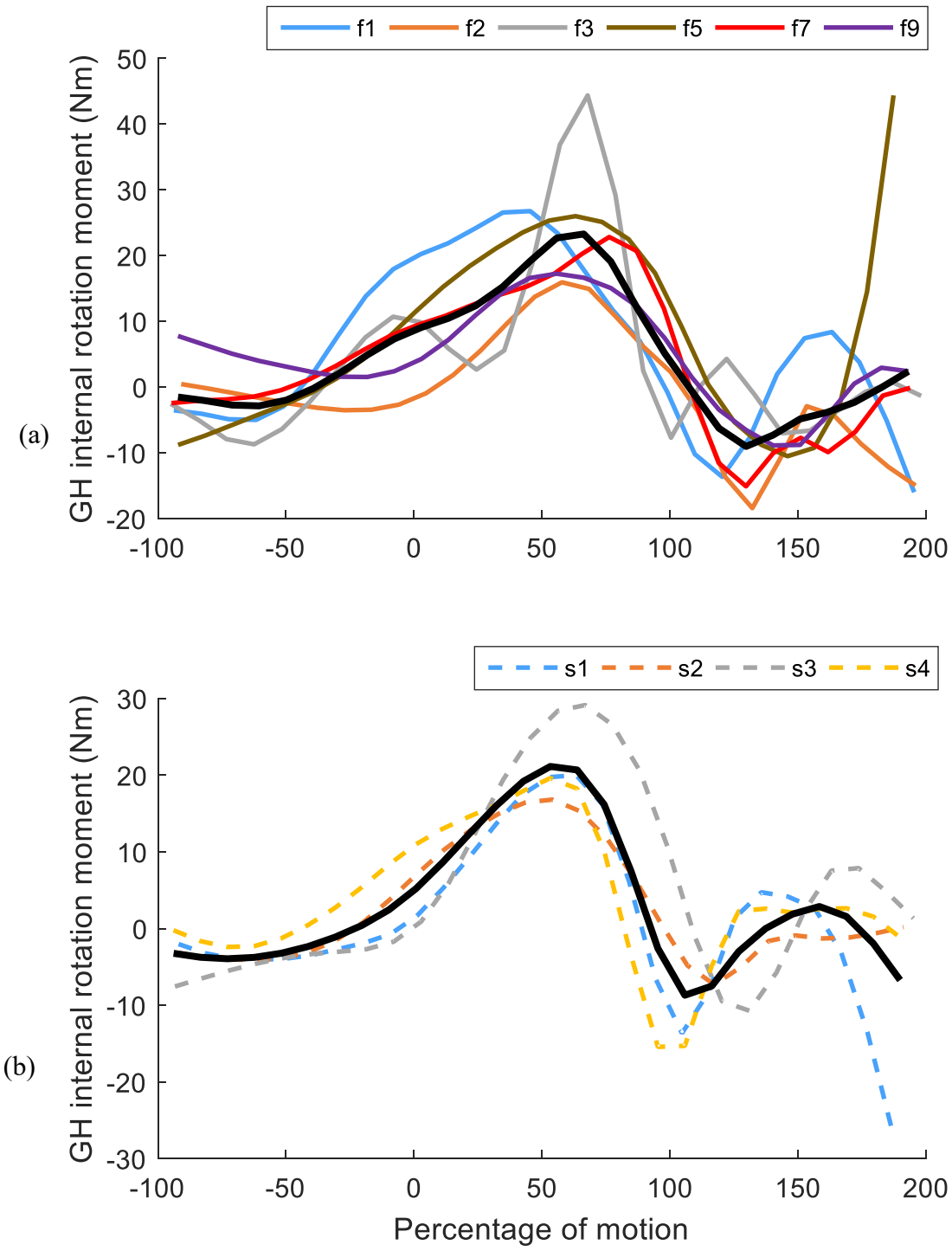

Figure 7.23 GH internal rotation moment for (a) fast and (b) slow bowlers, variation over. Mean internal rotation moment is indicated by a black line.

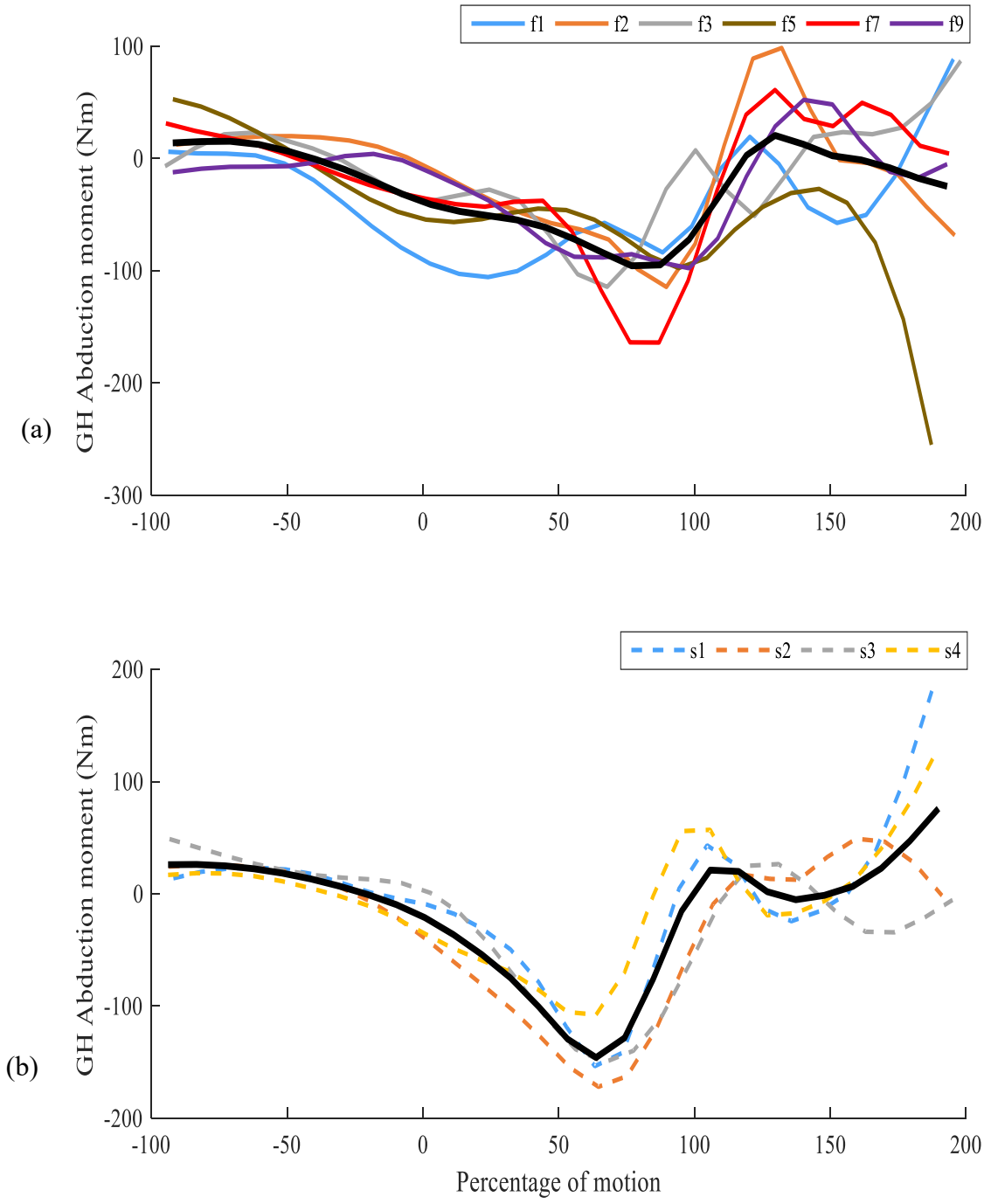

Figure 7.24 GH abduction rotation moment for (a) fast and (b) slow bowlers, variation over. Mean rotation moment is indicated by a black line.

7.4.2 Muscle forces and activation

One of the main mechanisms for resisting the distraction force at the shoulder is provided by the action of the rotator cuff muscles that dynamically stabilise the joint by creating a compressive force keeping the humeral head centred on the glenoid. As such, these muscles are investigated together with other key muscles responsible for stabilising the scapula and those that provide the driving force for movement of the humerus.

The average maximum muscle forces for both sets of bowlers (Figure 7.8) highlight the importance of the following muscles with a muscle force greater than 1 body weight: pectoralis major, rotator cuff muscles, middle and posterior deltoid, serratus anterior, latissimus dorsi, teres major, long head of the biceps and long head of the triceps. Values greater than 3 body weight were recorded for subscapularis and pectoralis major for both sets of bowlers. Figure 7.9 and Figure 7.10 show a summary of the average peak muscle forces for each bowler where a similar pattern of highly loaded muscles indicated by the peaks of these graphs is observed.

EMG studies provide a useful measurement of muscle activation patterns during activity. However, one limitation is that they are susceptible to cross talk and are not representative of maximum muscle activation levels (Laursen et al., 1998). Muscle activations (Figure 7.11 to Figure 7.16) are compared to EMG studies relating to cricket bowling for verification.

The results show moderate activity for the subscapularis, middle deltoid and approximately 17% peak activation for the supraspinatus during the delivery phase of fast bowlers (Figure 7.11). In contrast, slow bowlers had a greater anterior deltoid and teres minor activation during their delivery phase. The activity of the supraspinatus was greater in the follow through phase.

The subscapularis was previously described as having a high risk of overuse in the bowling action. The activation pattern of this muscles shows that its activation increases from upper arm horizontal to approximately 50% active in the delivery phase where it was observed that it was also eccentrically loaded, similar to what was reported by Roger et al. (1999) who related subscapularis tears to repetitive overload of the anterior musculature. These finds suggest that attention should be given to rotations from upper arm horizontal due to the important contributions of the subscapularis.

The serratus anterior together with the rhomboid muscles were most active between 50%- 100% of the motion while each of the scapula stabilising muscles showed increased activity late in

the follow through phase. There was a consistent pattern of activation for the latissimus dorsi, infraspinatus, teres major and posterior deltoid and scapula stabilising muscles in the follow through where the focus of the surround musculature at the shoulder is to control the deceleration of the arm and stabilising the joint by either eccentric or concentric contractions. This highlights the importance of these muscles during deceleration of the arm. These results show agreement with what is reported in literature where surface EMG studies on cricket bowling have shown that movement at the shoulder joint was mainly due to the actions of the deltoid and latissimus dorsi muscles (Burnden & Bartlett, 1990; Shorter et al., 2010).

The importance of the scapula stabilisers is highlighted by the action of the superior trapezius that retracts the clavicle preventing excessive internal rotation of the scapula (Ludewig & Braman, 2011), which is important in the follow through phase since measured scapula rotations showed internal rotation in this period. In addition, excessive internal rotation is also one of the kinematic variables that increase the risk of impingement. Thus the activity of this muscle is consistent with the literature.

The activation pattern of the biceps did not agree with what was reported in the literature where it is often described as more active after ball release in the follow through in overhead throwing (Rojas et al., 2009) which was also reported as being true in bowling (Burnden & Bartlett, 1990). The biceps is said to assist in providing a compressive force, especially since it is likely to be active during the bowling to control elbow extension (Stuelcken et al., 2010). Furthermore any dysfunction of the rotator cuff increases the role of the bicep brachii in providing dynamic stability (Pagnani et al., 1996) making the biceps labrum complex susceptible to overuse injury (Barrentine et al., 1998). However, in this study, the long and short head of the biceps were found to have less than 20% activation during the follow through phase.

Ahamed et al. (2014) investigated the difference between EMG signals of the biceps brachii between eight amateur fast bowlers and eight amateur spin bowlers. They reported that the bicep brachii was more active during fast bowling than spin bowling and the point of ball release. Both these findings are consistent to what is observed in this study (Figure 7.15 and Figure 7.16). These researchers went on to state that follow through phase generated a higher signal than any other portion of the bowling action. They describe that when the arm reaches its greatest external rotation in the period between front foot contact and ball release, this may account for the higher signal on the biceps brachii muscle.

7.4.3 Scapula kinematics and associated risk of impingement

Scapulothoracic and GH kinematics are summarised in Table 7-7 and Table 7-8. Previous chapters have described how altered scapula kinematics and internal rotation of the humerus present and increase risk of impingement. In addition to this, the subacromial space is reported to be the smallest at 90° humeral abduction and 45° external rotation (Graichen et al., 1999). Furthermore, the infraspinatus was found to be at risk of impingement when externally rotated in extension and arm positions in flexion and abduction while internally rotated presented the greatest risk of rotator cuff impingement (Hughes et al., 2012).

The only kinematic risk that was observed was occurred from 50% to 100% of the motion when the arm was extended and in maximum external rotation. Even though there was significant scapulothoracic internal rotation, these may not be representative of the subject's kinematics as explained in Chapter 5. Furthermore, the low activity of the supraspinatus meant that a reduction in the subacromial space presented less of an impingement risk.

Internal rotation within this study includes motion about both the glenohumeral and scapulothoracic joints. It is therefore feasible that although bowlers may have limited internal rotation at the glenohumeral joint, they can functionally adapt to this through increased scapulothoracic movement (anterior tilt and internal rotation) which aids in increasing internal rotation at the shoulder. The measurement errors of these smaller rotations meant that this analysis was not possible. If it is possible to accurately measure total scapula kinematics during bowling, future research needs to establish the contribution of the scapula during the bowling motion. Although increased scapulothoracic motion may aid the bowler in meeting the functional demands of the movement. It may act to destabilise the glenohumeral joint through altering the moment arms of the rotator cuff and other surrounding musculature.

	ST posterior tilt (°)			ST Internal rot. (°)			ST Upward rot. (°)			GH Internal rot. (°)			GH abduction (°)			Internal rot. ROM (°)
	50%	100%	150%	50%	100%	150%	50%	100%	150%	50%	100%	150%	50%	100%	150%	100%-150%
f1	-23	-26	-26	36	38	47	30	36	42	-131	-127	-57	14	36	65	71
f2	-15	-17	-14	44	49	60	31	33	48	-122	-131	-58	18	33	74	73
f3	-13	-13	-18	41	52	52	33	42	30	-155	-160	-71	40	57	66	89
f4	-15	-21	-18	39	34	38	24	28	34	-138	-136	-90	24	49	78	46
f5	-11	-16	-17	46	46	50	25	23	21	-117	-111	-115	10	32	50	-3
f7	-7	-14	-13	49	47	51	22	20	24	-109	-101	-19	40	62	81	82
f9	-19	-21	-28	46	52	55	22	25	26	-127	-134	-76	29	45	73	58
f10	-24	-18	-18	26	32	40	26	31	36	-148	-166	-84	36	47	81	83
f11	-10	-15	-12	40	56	68	37	39	47	-131	-122	-92	28	40	61	30
s1	-6	-7	-7	40	40	48	29	31	33	-133	-132	-97	38	60	75	35
s2	-12	-21	-19	27	36	49	41	37	31	-96	-81	-16	51	61	71	65
s3	-12	-13	-11	37	44	43	31	36	30	-100	-110	-51	39	53	79	59
s4	-14	-18	-17	52	53	62	36	37	38	-105	-87	-26	42	64	60	60

Table 7-7 Scapulothoracic (ST) and GH kinematics at three points in the bowling action for all bowlers, stock over. ROM-range of motion

	ST posterior tilt (°)			ST Internal rot. (°)			ST Upward rot. (°)			GH Internal rot. (°)			GH abduction (°)			Internal rot. ROM (°)
	50%	100%	150%	50%	100%	150%	50%	100%	150%	50%	100%	150%	50%	100%	150%	100%-150%
f1	-23	-28	-27	44	47	52	36	38	36	-131	-113	-72	19	47	65	28
f2	-14	-17	-13	45	51	60	31	34	47	-120	-127	-65	19	30	73	11
f3	-11	-16	-17	45	51	51	33	40	33	-159	-161	-67	39	52	64	13
f5	-9	-18	-13	46	48	54	21	19	28	-115	-110	-113	13	28	53	15
f7	-8	-14	-14	48	48	51	21	19	23	-109	-100	-34	38	56	77	18
f9	-20	-22	-27	45	53	63	24	29	29	-128	-137	-140	35	52	73	17
s1	-8	-9	-8	39	38	46	28	29	26	-131	-129	-52	34	61	66	27
s2	-6	-22	-19	24	37	50	44	36	28	-95	-77	-5	47	60	69	13
s3	-10	-11	-13	38	44	42	31	37	26	-110	-112	-69	36	54	72	18
s4	-11	-16	-16	52	53	64	35	36	38	-104	-87	-18	41	63	59	22

Table 7-8 Scapulothoracic (ST) and GH kinematics at three points in the bowling action for all bowlers, variation over. ROM-range of motion

7.4.4 Stock delivery vs variation

Kinematic analysis showed very few within subject adaptations that occurred between both overs as discussed in Chapter 5. Significant differences were related to changes in humerothoracic kinematics in increasing ball speed. This included delayed elevation of the humerus in slow bowlers and greater external rotation prior to ball release in fast bowlers. These changes were reflected in a larger GH joint moment and larger muscle forces, activations and joint forces for bowlers delivering their faster delivery. Due to the unusually large forces recorded and small sample size, conclusions on the effect of bowling a faster ball and the demands on the shoulder could not be established as any differences that may have occurred may be due to sensitivity of modelling the action or to variations between bowlers' technique.

7.4.5 Suitability of the UKNSM

It must be emphasised that the bowling action is complex occurring at high velocities hence, angular joint acceleration and decelerations at the shoulder must happen at considerable variations. Two major hindrances to the model solution were the speed and range of motion in cricket bowling. The sensitivity to fast motion was highlighted by the drastic changes in muscles forces and unsolved frames presented in Chapter 6 compared to the results presented here. Fixing this issue does not preclude other major but less apparent problems with the model. For instance, the supraspinatus muscle force for subject f3 and s1 is shown in Figure 7.25 and Figure 7.28 have near zero activation in the between 0-100%, while f1 shows a maximum muscle force of 0.95% body weight which then decreases to near zero at ball release.

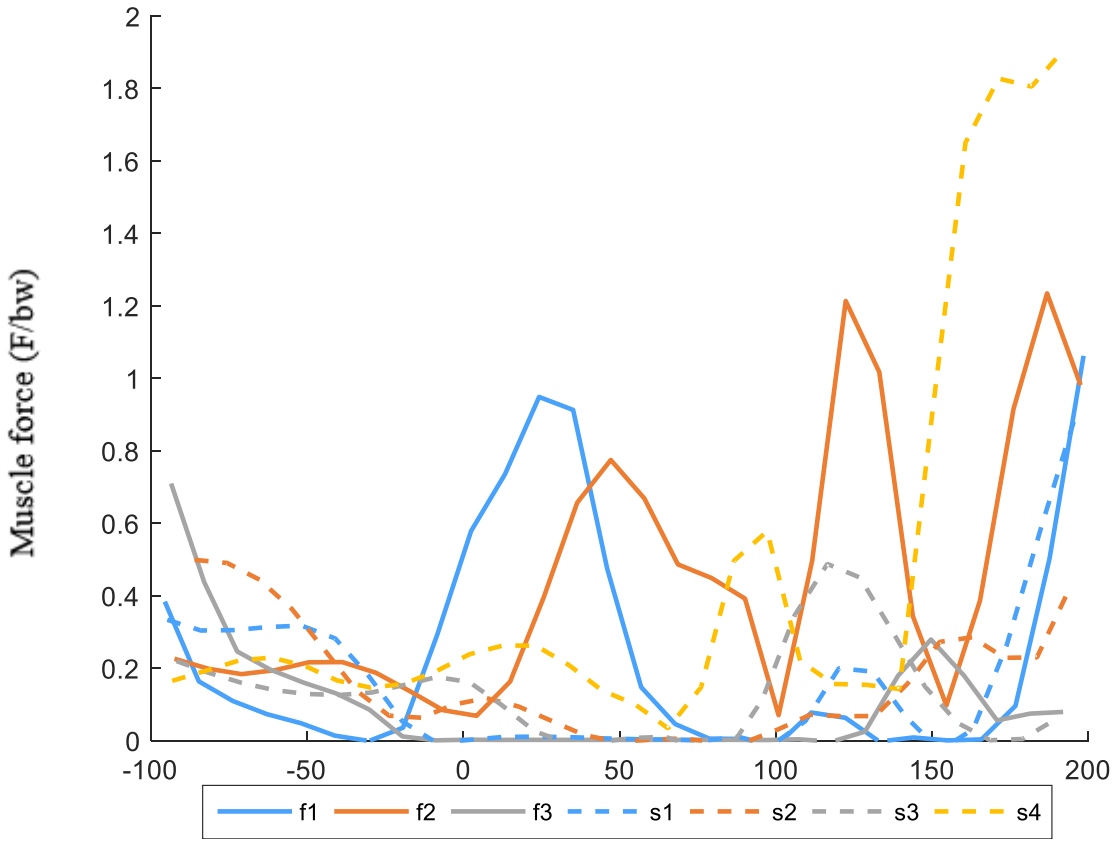

Figure 7.25 Supraspinatus normalised mean force (F/bw) for the front-on fast bowlers and slow bowlers.

Subject f3 was of particular interest since the kinematic analysis in Chapter 5 showed that they externally rotated prior to ball release, which was then followed by rapid internal rotation and elbow extension in generating ball speed. This subject was found to have the greatest external GH external rotation angle (Table 7-3) at 50% of the motion. This problem was highlighted in the original model where the extended, elevated and externally rotated arm was a major obstacle preventing the model from finding a solution. This issue is further highlighted by the gap in shoulder musculoskeletal literature where motion is simulated with the humerus in an extended, elevated and externally rotated position.

Investigation of the moment arms shows some inconsistent behaviour particularly, in flexion/extension (Figure 7.26) however, this does not explain the low activation of the supraspinatus throughout the bowling action. One possible explanation is that bowler f3 showed one of the highest externally rotated arms which might result in a line of action for this muscle

that does not contribute to joint stability. The question of whether this is physiological is unknown. With this in mind adjustments to the line of action were effected in the model, however this did not significantly improve the output of the model even though there was a greater activation in the muscle. This indicates that due to the subject's extreme kinematics the overall muscle wrapping technique employed was ineffective. The use of via points and other segment embedded wrapping objects were tested with little success due to the large range of motion.

Kinematic optimisation was found to be acceptable however, the improvements in the muscle wrapping were ultimately insufficient. The issue of the model's inability to activate the supraspinatus, one of the major contributors to GH stability was highlighted, in addition muscle forces and joint reaction forces beyond physiological limits were found due to a limitation in the model to deal with fast motion.

The obstacle-set wrapping technique used in the UKNSM, was reported to underestimate muscle moment arms; therefore, it is recommended that other more elegant and robust wrapping techniques be used such as the multi-object approach (Marsden et al., 2008) that employs multiple external wrapping objects to match a muscle line of action. One key difference to this multi-object wrapping and the one used in the UKNSM is that it considers the location of all the wrapping objects together in finding a sensible wrapping path. In contrast the muscle wrapping algorithms in the UKNSM wraps around each object individually from one effective origin to another's effective insertion and so on. Furthermore, the use of multi-object, energy-based methods where there is a physiological link between muscle fibres (elements) is recommended. Currently in the model, there are no constraints that restrict the movement within a group of elements used to represent a muscle. So, the wrapping path is calculated for each element independent on the location of the other elements of the group. Any issues in the muscle wrapping is serious since it has been shown that any small changes in moment arms have significant effects on muscle activation levels (Prinold, 2012).Considering the model has 90 muscle elements this issue is a serious one.

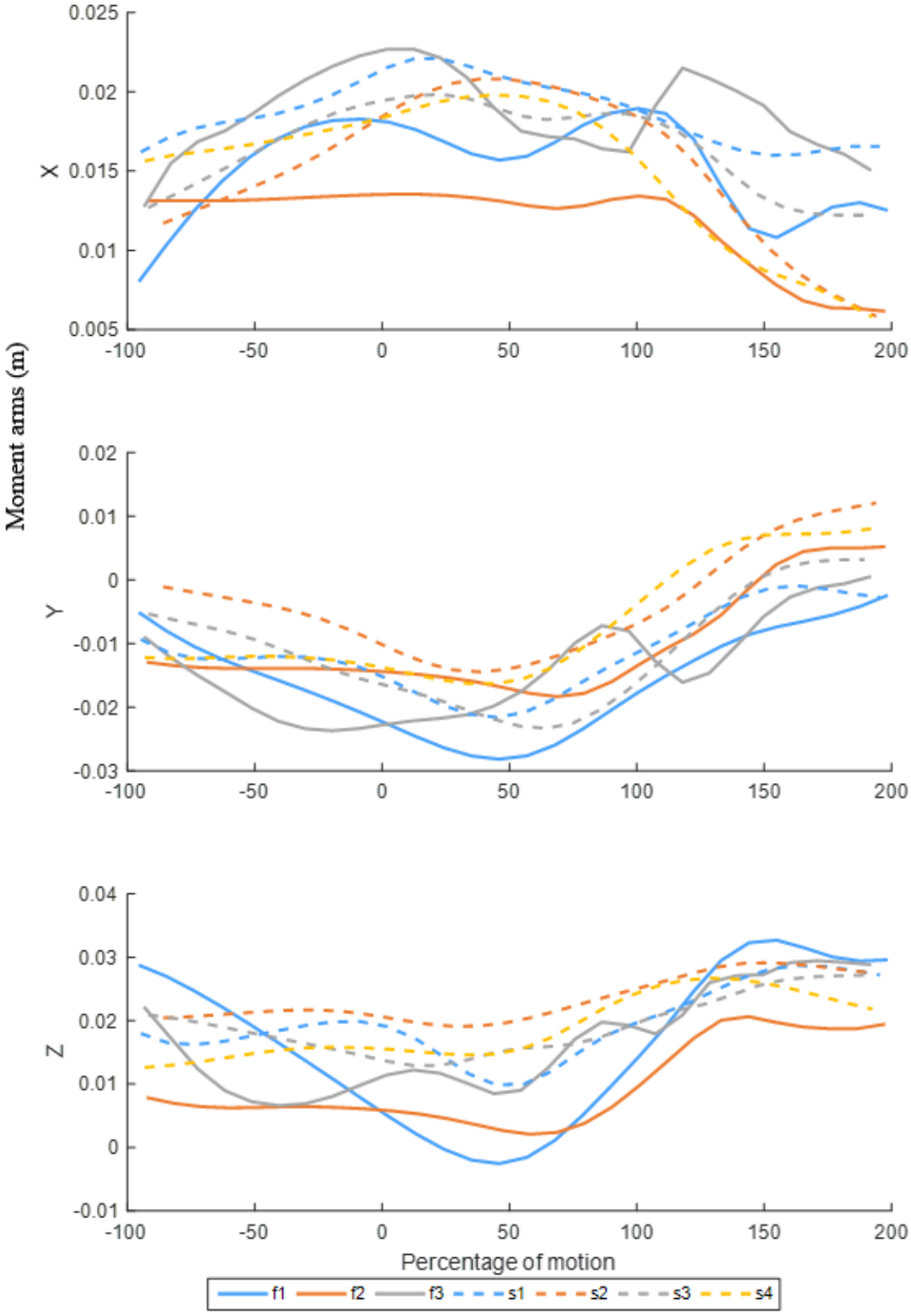

Figure 7.26 Supraspinatus moment arm in the humerus coordinate frame for front-on fast bowlers and slow bowlers.

The importance of musculature in the shoulder complex is well established to be key in maintaining the stability of the joint during motion, especially in cricket bowling where the speed and range of motion at the joint is significant. As such, the lines of action and corresponding moment arms would be key in properly simulating muscle activations during cricket. While there was agreement in the activation patterns with what is published, the significantly higher muscle joint forces and erratic behaviour of the supraspinatus limited any further analysis.

In addition to this, body segment parameters in the model were not changed. Investigation into modelling parameters used by other researchers that more appropriately match that of a younger athletic subject could be tested to look at the sensitivity of these parameters to the predicted muscle and joint forces.

The lack of consideration for muscle activation dynamics and the effects of velocity and length may have been a major limitation in such a highly dynamic task. The reason this was not considered was due to uncertainties over parameters like optimal fibre length and issues with scaling these parameters. Furthermore, the absence of the GH joint ligaments and contribution of other passive structures in the joint towards stability was not included and their importance in this motion may be significant given the large range of motion and power output at the joint.

Figure 7.27 shows a summary of the unsolved frames for each bowler. A maximum of 6 frames at each percentage of motion is possible, representing the 6 trials. The figure shows both subjects f6 and f8 who had to be eliminated from the analysis given the high number of unsolved frames within the important phases of the action. Subject f3 consistently showed an unsolved frame near 50% of the motion for five trials, in addition to showing at least 3 unsolved frames per trial. This however, does not explain the inconsistencies shown for the supraspinatus and for other subjects.

The effect of these issues in the model to properly simulate cricket bowling meant that the model outputs would be affected. Although similar muscle activation patterns were observed, compared to the literature, the muscles and joint forces were found to be significantly higher than expected. This is directly related to the increase in upper limit of the muscle forces by a factor of five in the load sharing optimisation that was used. This increase was necessary, since at lower values the model resulted in greater unsolved frames in the between 0-150% of the motion leading to erratic output of the model. The value of five was found to be the most

appropriate from a process of trial and error.

The model sensitivity to range of motion and speed of motion also meant that any key differences that may occur between bowlers would be difficult to describe and justify. Therefore, analysis was limited to describing any overall differences between both sets of bowlers with comparison to literature being key.

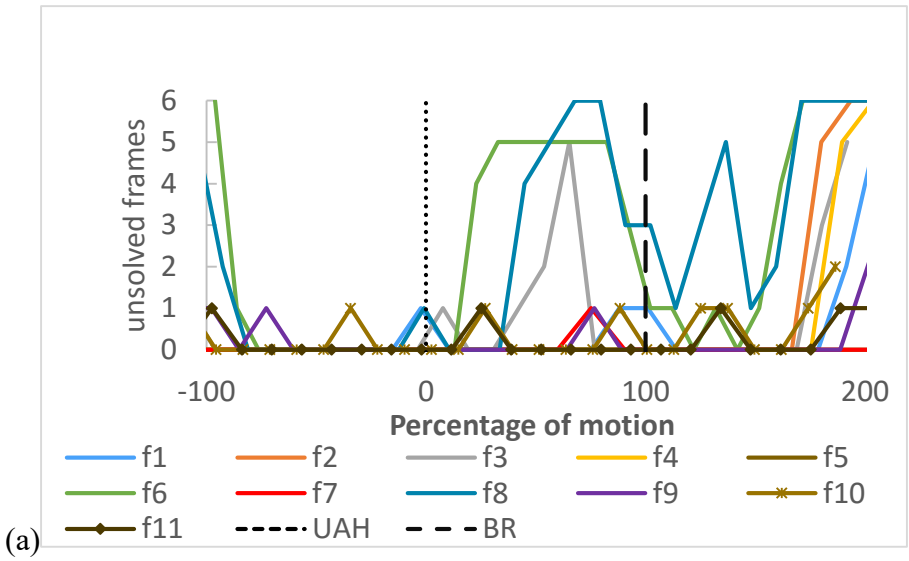

(a)

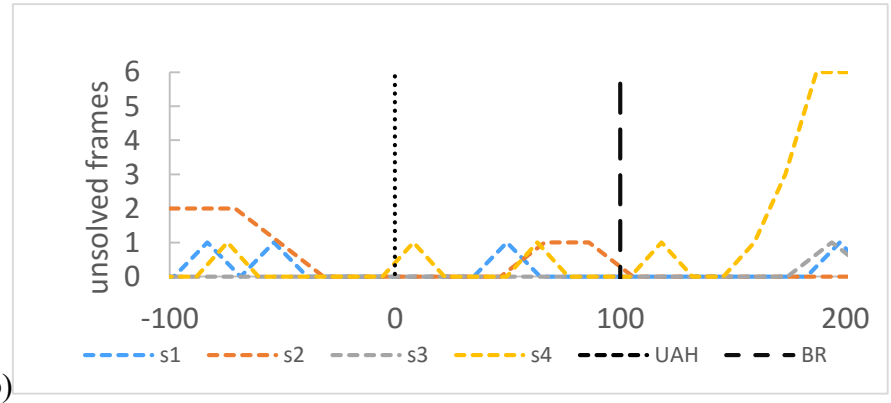

(b)

Figure 7.27 Unsolved frames for (a) fast bowlers stock over, (b) slow bowlers stock over. subjects f6 and f8 had to be removed from the analysis due to large number of unsolved frames.

Figure 7.28 illustrates the inactive supraspinatus when the arm is in an extended and externally rotation positions. The activation of the surround musculature is indicated by a bright red and thicker lines.

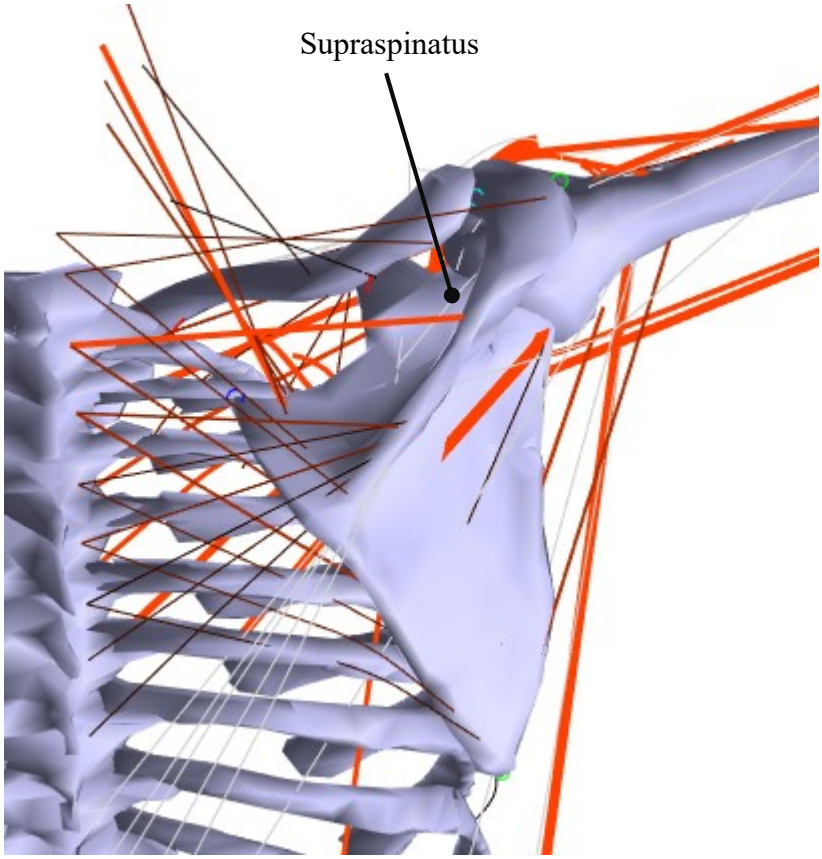

Figure 7.28 Inactive supraspinatus for subject f3 between 0%-100%. It is observed that this is due to the extreme range of external rotation and extended position of the humerus.

7.5 Conclusion

The results for GH joint forces align with what is described in the literature where bowlers were at risk of shoulder injuries due to large distraction forces. A mean peak distraction force of 7.9 body weight and 8.7 body weight for fast and spin bowlers was calculated. Analysis of the GH joint shear forces was also done, which was not reported by Stuelcken et al. (2010). Peak superior shear forces comparable in magnitude with the distraction forces were reported and indicated a risk of humeral head translation just before ball release and near 50% of the motion for fast and slow bowlers respectively. These peak forces did not scale with ball speed indicating it was dependant on the bowling technique.

The most compromising positions to joint stability was at ball release and early follow through for fast bowlers while for spin bowlers between 50% to 100% presented a greater risk of instability.

Muscles that contributed to joint stability were analysed and it was reported that the subscapularis demonstrated major contributions to joint stability during the delivery phase (0-100%) while the infraspinatus showed significant contributions in the follow through phase. The significant activation and eccentric loading of this muscle also places it at risk of overuse/fatigue leading translations of the humeral head and impingement in the region from upper arm horizontal to ball release, in accordance to the literature. The supraspinatus showed the greatest activity and contribution to joint stability in the follow through phase. The reason why the supraspinatus had lower activity during the delivery may have been due to the extended and externally rotated arm typical of all bowlers.

Regardless of the type of bowler, there was a larger internal rotation torque which substantiates the reports by Aginsky et al. (2004) who reported a functional deficiency of the external rotators and attributed injuries to muscle imbalance where the external rotators cannot oppose the large internal rotations at the GH during bowling. These findings highlight the phase 50%-100% presented a greater risk for bowlers who had imbalances between internal and external rotators of the shoulder.

The activation pattern was compared with literature showing a good agreement while also highlighting the key muscles within the two phases. One exception with what is reported in the literature is that the long head of the bicep that only showed significant activity in the bowling phase and minimal activity in the follow through phase.

The risk on impingement was assessed based on kinematics of the scapula and humerus. It was concluded that the only impinging position was just prior to ball release with the arm in an elevated and maximal external rotation. Spin bowlers were described to be at a higher risk of shoulder injuries (Gregory et al., 2002) where it was hypothesised that the GH internal rotation torque may predispose these bowlers given that the range of internal rotation for both sets of bowlers did not show any pattern. This hypothesis however was unsubstantiated. One key observation discussed the contribution of scapula internal rotation and tilt to increase internal rotation at the GH joint. Given the measurement errors associated with these smaller rotations, this analysis was not possible and highlighted an area of future work.

Final comments on the suitability of the UKNSM and issues that affected the modelling process were discussed. One major improvement that was suggested was the use of a different multi-object wrapping approach and more appropriate body segment parameters.

Chapter 8

Conclusions and future work

This chapter gives an overview of the findings of this thesis. Limitations and future work is also discussed.

8.1 Summary

Scapula kinematics has been established as key in musculoskeletal modelling of the shoulder. Thus, scapula kinematics was measured using a skin-fixed methodology during cricket bowling. Dynamic tracking of the scapula was measured for the first time in such activities. It was found that using a rigid cluster affixed across the spine of the scapula, during slow circumduction, showed good intra-subject repeatability with a mean coefficient of multiple correlation (CMC) value of 0.82 (SD 0.13), 0.94 (SD 0.03) & 0.86 (SD 0.08) for scapula internal/external (IE), up/down (UD) and posterior/anterior (PA) rotations respectively. Even though a high repeatability was found for the scapula tracker used, its accuracy in measured posterior/anterior tilt was low when validated against a scapula palpator. scapula internal/external and up/down rotations were accurate to within 6° and 6° respectively while scapula tilt had an RMS error of 8° in addition to having a poor agreement with the waveform of the palpator. Regression equations were used to improve to the capability of the scapula tracker during bowling however they were found to be unsuitable for predicting scapula kinematics for such a large range of motion.

The performance of the scapula tracker in full speed bowling trials again showed good repeatability across the 11 fast bowlers and 4 slow bowlers who were studied. There was however, significantly greater posterior/anterior tilt and internal rotation measured, showing that these measured angles were poor for the full speed trials. Fast bowlers were found to have a humerothoracic elevation angle at ball release within the range of 98°-139° and slow bowlers were within 107°-120° and were within the region that is usually described as high impingmenet risk. The action of the bowling arm followed the trend of external rotation from upper arm horizontal to ball release then internal rotation during the follow-through phase. The range of internal rotation from an externally rotated arm was found to be a change of 59° for fast bowlers and 46° for slow bowlers.

Significant differences were shown between fast and slow bowlers when it came to bowling a faster delivery. The kinematic changes that occurred were found to be closely related to generating ball speed as described by the literature. Fast bowlers showed significantly greater internal rotation from ball release to follow through while spin bowlers delayed humeral elevation while retracting the shoulder joint with the arm following behind. Another interesting technique that was found was described in one bowler who demonstrated late external rotation prior to ball release followed by rapid internal rotation of the humerus coupled with extension

of the elbow beyond the 15° legal limit. This highlights a bowling technique adaptation that may greatly stress the shoulder joint. However, investigations into this were inconclusive due to limitations of the musculoskeletal model used.

The GH range of internal rotation in the early stages of the follow through did not differ between groups, suggesting that this was due to variability in the actions of the bowlers tested within both groups. These results seemed to contradict what was reported by Gregory et al. (2002) who found that leg spin bowlers were at greater risk due to internal rotation at ball release. Instead the internal rotation torque was highlighted as being a better measurement.

An existing musculoskeletal model was improved upon for simulating cricket bowling. This included improvement in the kinematic optimisation where the introduction of new constraints allowed for a continuous kinematic solution while keeping the scapula at a physiologically sensible position, and also maintaining a similar level of errors to the measured kinematics when compared to the original models' most suitable kinematic optimisation routine.

In addition to corrections to the kinematic optimisation, muscle wrapping for key muscles anterior to the shoulder joint were corrected. These muscles included the subscapularis, anterior deltoid, pectoralis major thorax and clavicle head, coracobrachialis and short head of the biceps. Changes to the subscapularis and anterior deltoid were validated with in vivo moment arms reported in the literature while wrapping was implemented for other muscles since they did not previously wrap around the GH joint.

The model's sensitivity to the changes were demonstrated with a reduction in the unsolved frames and improvement in the model outputs, when compared to its original configuration. The model's sensitivity to the velocity of the arm was also documented where down sampling the raw marker data significantly improved the model outputs and was therefore necessary. In addition to this, the model's sensitivity to scapula internal and posterior/anterior rotations were highlighted by subjects who showed an over exaggeration in these rotations, which negatively affected the model's output leading to the elimination of these subjects from the analysis.

The motivation of this thesis was to investigate the risk of impingement injuries in bowlers where a large distraction force, internal rotation of the humerus at ball release and a front-on technique were highlighted in the literature as key predisposition factors. Limitations of the musculoskeletal model prevented any in-depth analysis to substantiate the last factor mentioned. None the less, the model has demonstrated shoulder muscle activation pattern for

bowlers during this highly dynamic and complex motion that is coherent with what is presented in literature. The analysis showed that one potentially vulnerable position was in the region between upper arm horizontal and ball release due to the location of the joint reaction force at the glenoid rim and the magntiude of this force. Also within this region, a large distraction force was reported for bowlers where the superior shear forces were large, identifying another potential mechanism for injury if the shear force is greater than the compressive joint force causing translation of the humeral head.

Musculoskeletal modelling of cricket bowling showed a similar pattern of muscle activation where the subscapularis was found to have the greatest stabilising potential of the rotator cuff muscles, especially with the arm in an elevated and externally rotated position. Supraspinatus and infraspinatus showed increased activity in the follow through. Latissimus dorsi, infraspinatus, teres major and posterior deltoid and scapula stabilising muscles showed a consistent pattern of activation during the follow through phase where they act to stabilise the joint and control the deceleration of the arm.

Predicted activation pattern for subscapularis substantiate the risk of impingement injuries due to overuse and fatigue during rotation of the arm from upper arm horizontal to ball release. In addition, muscle imbalances in the external and internal rotators were deemed crucial within this key phase in the bowling action.

Finally, modelling of the cricket bowling action inherently included modelling the GH joint in an extended position, where the humerus moves posterior to the thorax and has seen very little research. As such, the modelling methodology and issues presented in this thesis would add to the body of work in this area. Furthermore, the scapula kinematic data and regression equation present a novel dataset for describing the shoulder complex during slow circumduction of the humerus and during full speed bowling.

8.2 Limitations and future work

A number of limitations exists in the study that was presented. This included the small number of experienced bowlers who regularly compete at a high level. Further investigations should incorporate a larger sample of elite athletes particularly to substantiate the risk of front-on fast bowlers to impingement. In addition, the significant amount of external rotation in certain subjects highlighted the importance of a defined measurement protocol for humeral axial rotation during bowling. As such, it is recommended that studies be conducted to investigate

the currently available methods and their feasibility for measuring humeral axial rotations.

The absence of the hand segment and wrist joint is another limitation since the action at this joint is an important consideration when describing bowling kinematics especially for spin bowlers. The reason this was not included was that the focus of this thesis was limited to the kinematics and musculoskeletal loading at the GH joint. However to gain a better understanding of overall bowling kinematics it is recommended that the wrist joint be included.

The number of markers that was used to capture bowling kinematics may have had a slightly negative effect on the bowlers' action even if they indicated otherwise. Therefore, the bowling technique that was measured may not be representative of match conditions (for the few who competed at a high level).

Lower limb kinematics was not a major discussion topic in this thesis even though they were measured. Given the already large amount of data for the upper limb and outputs from the musculoskeletal model, it was not possible to include a full body kinematic analysis of cricketers as is often presented in literature. In addition, a large dataset was collected due to a greater number of markers used as a result of incorporating two other marker models for capturing bowling kinematics. Therefore, sensitivity studies on upper limb kinematics in cricket bowling using calculation methods and the corresponding marker set used by other researchers is possible and is recommended as future work.

The range of internal rotation at ball release was found to be variable among bowlers where the joint internal rotation torque might still prove to be a better indicator. Studies on different bowling deliveries and their influence on shoulder muscles should be conducted. This is particularly applicable in spin bowling given that there are several types of deliveries: off spin, leg spin, flipper, googly, carrom ball, top-spinner, arm-ball, doosra and teesra.

Modelling cricket bowling has proved to be a significant challenge where major limitations of the model originated from a combination of two factors specific to bowling: speed of movement and large range of movement, namely GH extension and external rotation. These issues prevented any definitive conclusions from being made based on subject specific kinematics. As such, it was recommended that an improvement in muscle wrapping was necessary with the use of multi-object, energy based methods with a physiological link between muscle fibres. Other factors that are important in musculoskeletal modelling of athletic activities include scaling of segments, particularly for the scapula and thorax since they are important factors in the

kinematic optimisation procedure and body segment parameters. Another key challenge that stems from this is the scaling of muscle and ligament attachments of the bone. Advancements in this area that may be possible to implement in future iterations of the model include the use of statistical shape modelling.

The lack of consideration for muscle activation dynamics and the effects of velocity and length may have been a major limitation in such a highly dynamic task together with a lack of GH joint ligaments and other passive structures that also aid in joint stability. However, given the issues associated with incorporating this into a musculoskeletal model and lack of literature for athletic activities that use this, it might prove to be a challenging implementation.

Although there were major limitations, the model simulations confirmed the risk of impingement in bowlers, demonstrated the importance of considering the distraction force and shear forces in bowling and showed a general pattern of muscle recruitment that were similar to other studies. The modelling process highlighted important considerations when simulating cricket bowling with recommendations being made.

References

Ackland, DC, Pak, P, Richardson, M & Pandy, MG 2008, 'Moment arms of the muscles crossing the anatomical shoulder', *Journal of Anatomy*, vol. 213, pp. 383-390.

Ackland, DC & Pandy, MG 2009, 'Lines of action and stabilizing potential of the shoulder musculature', *Journal of Anatomy*, vol. 215, pp. 184-197.

Ackland, DC & Pandy, MG 2011, 'Moment arms of the shoulder muscles during axial rotation', *Journal of Orthopaedic Research*, vol. 29, pp. 658-667.

Aginsky, K, Lategan, L & Stretch, R 2004, 'Shoulder injuries in provincial male fast bowlers - predisposing factors', *South African Journal of Sports Medicine*, vol. 16, pp. 25-28.

Aginsky, KD & Noakes, TD 2010, 'Why it is difficult to detect an illegally bowled cricket delivery with either the naked eye or usual two-dimensional video analysis.', *British journal of sports medicine*, vol. 44, pp. 420-425.

Ahamed, NU, Sundaraj, K, Ahmad, B, Rahman, M, Ali, MA & Islam, MA 2014, 'Surface electromyographic analysis of the biceps brachii muscle of cricket bowlers during bowling', *Australas Phys Eng Sci Med*, vol. 37, no. 1, pp. 83-95.

Albernethy, B 1981, 'Mechanism of skill in cricket batting', *Australian Jourlan of Sports Medicine*, vol. 13, no. 1, p. 10.

Amasay, T & Karduna, AR 2009, 'Scapular kinematics in constrained and functional upper extremity movements.', *The Journal of orthopaedic and sports physical therapy*, vol. 39, pp. 618-627.

Anderson, MK 1993, 'Isokinetic Exercise and Assessment - Perrin,Dh', *Research Quarterly for Exercise and Sport*, vol. 64, no. 4, pp. 471-472.

Anderson, MW & Alford, BA 2010, 'Overhead throwing injuries of the shoulder and elbow', *Radiol Clin North Am*, vol. 48, no. 6, pp. 1137-54.

Anglin, C & Wyss, UP 2000, 'Review of arm motion analyses.', *Proceedings of the Institution of Mechanical Engineers. Part H, Journal of engineering in medicine*, vol. 214, pp. 541-555.

Arnet, U, van Drongelen, S, van der Woude, LH & Veeger, DH 2012, 'Shoulder load during handcycling at different incline and speed conditions', *Clin Biomech (Bristol, Avon)*, vol. 27, no. 1, pp. 1-6.

Baltaci, G & Tunay, VB 2004, 'Isokinetic performance at diagonal pattern and shoulder mobility in elite overhead athletes', *Scandinavian Journal of Medicine and Science in Sports*, vol. 14, pp. 231-238.

Barnett, ND, Duncan, RD & Johnson, GR 1999, 'The measurement of three dimensional scapulohumeral kinematics--a study of reliability.', *Clinical biomechanics (Bristol, Avon)*, vol. 14, pp. 287-290.

Barre, A & Armand, S 2014, 'Biomechanical ToolKit: Open-source framework to visualize and process biomechanical data', *Comput Methods Programs Biomed*, vol. 114, no. 1, pp.

80-7.

Barrentine, SW, Fleisig, GS, Whiteside, Ja, Escamilla, RF & Andrews, JR 1998, 'Biomechanics of windmill softball pitching with implications about injury mechanisms at the shoulder and elbow.', *The Journal of orthopaedic and sports physical therapy*, vol. 28, pp. 405-415.

Bartlett, RM, Stockill, NP, Elliott, BC & Burnett, AF 1996, 'The biomechanics of fast bowling in men's cricket: A review', *Journal of Sports Sciences*, vol. 14, no. 5, pp. 403-424.

Bedi, G 2011, 'Shoulder injury in athletes', *Journal of Clinical Orthopaedics and Trauma*, vol. 2, pp. 85-92.

Bell-Jenje, T & Gray, J 2005, 'Incidence , nature and risk factors in shoulder injuries of national academy cricket players over 5 years – a retro- spective study', *South African Journal of Sports Medicine*, vol. 17, pp. 22-28.

Biryukova, EV, Roby-Brami, a, Frolov, aa & Mokhtari, M 2000, 'Kinematics of human arm reconstructed from spatial tracking system recordings', *Journal of Biomechanics*, vol. 33, pp. 985-995.

Bolsterlee, B, Veeger, HEJ & van der Helm, FCT 2014, 'Modelling clavicular and scapular kinematics: From measurement to simulation', *Medical and Biological Engineering and Computing*, vol. 52, pp. 283-291.

Bonnefoy-Mazure, a, Slawinski, J, Riquet, a, Lévèque, JM, Miller, C & Chèze, L 2010, 'Rotation sequence is an important factor in shoulder kinematics. Application to the elite players' flat serves', *Journal of Biomechanics*, vol. 43, pp. 2022-2025.

Burnden, AM & Bartlett, RM 1990, 'An electromyographical analysis of fast-medium bowling in cricket', in *8th ISEK Conference, Baltimore*, pp. 475-460.

Burnett, aF, Barrett, CJ, Marshall, RN, Elliott, BC & Day, RE 1998, 'Three-dimensional measurement of lumbar spine kinematics for fast bowlers in cricket', *Clinical Biomechanics*, vol. 13, pp. 574-583.

Camomilla, V, Cereatti, A, Vannozzi, G & Cappozzo, A 2006, 'An optimized protocol for hip joint centre determination using the functional method', *J Biomech*, vol. 39, no. 6, pp. 1096-106.

Cappello, A, Cappozzo, A, La Palombara, PF, Lucchetti, L & Leardini, A 1997, 'Multiple anatomical landmark calibration for optimal bone pose estimation', *Human Movement Science*, vol. 16, pp. 259-274.

Cappello, A, Stagni, R, Fantozzi, S & Leardini, A 2005, 'Soft tissue artifact compensation in knee kinematics by double anatomical landmark calibration: Performance of a novel method during selected motor tasks', *IEEE Transactions on Biomedical Engineering*, vol. 52, pp. 992-998.

Cappozzo, A, Catani, F, Della Croce, U & Leardini, A 1995, 'Position and Orientation in-Space of Bones during Movement - Anatomical Frame Definition and Determination', *Clinical Biomechanics*, vol. 10, no. 4, pp. 171-178.

Cappozzo, A, Catani, F, Leardini, a, Benedetti, MG & Della Croce, U 1996, 'Position and

orientation in space of bones during movement: Experimental artefacts', *Clinical Biomechanics*, vol. 11, pp. 90-100.

Charlton, IW 2003, A model for prediction of the forces at the glenohumeral join, thesis, University of Newcastle upon Tyne.

Charlton, IW & Johnson, GR 2006, 'A model for the prediction of the forces at the glenohumeral joint.', *Proceedings of the Institution of Mechanical Engineers. Part H, Journal of engineering in medicine*, vol. 220, pp. 801-812.

Chèze, L, Fregly, BJ & Dimnet, J 1995, 'A solidification procedure to facilitate kinematic analyses based on video system data', *Journal of Biomechanics*, vol. 28, pp. 879-884.

Chin, A, Elliott, B, Alderson, J, Lloyd, D & Foster, D 2009, 'The off-break and "doosra": kinematic variations of elite and sub-elite bowlers in creating ball spin in cricket bowling', *Sports Biomech*, vol. 8, no. 3, pp. 187-98.

Chin, A, Lloyd, D, Alderson, J, Elliott, B & Mills, P 2010, 'A marker-based mean finite helical axis model to determine elbow rotation axes and kinematics in vivo', *J Appl Biomech*, vol. 26, no. 3, pp. 305-15.

Chu, Y, Akins, J, Lovalekar, M, Tashman, S, Lephart, S & Sell, T 2012, 'Validation of a video-based motion analysis technique in 3-D dynamic scapular kinematic measurements', *Journal of Biomechanics*, vol. 45, pp. 2462-2466.

Cleather, DI & Bull, AM 2010, 'Lower-extremity musculoskeletal geometry affects the calculation of patellofemoral forces in vertical jumping and weightlifting', *Proc Inst Mech Eng H*, vol. 224, no. 9, pp. 1073-83.

Codine, P, Bernard, PL, Pocholle, M, Benaim, C & Brun, V 1997, 'Influence of sports discipline on shoulder rotator cuff balance', *Med Sci Sports Exerc*, vol. 29, no. 11, pp. 1400-5.

Crockett, HC, Gross, LB, Wilk, KE, Schwartz, ML, Reed, J, O'Mara, J, Reilly, MT, Dugas, JR, Meister, K, Lyman, S & Andrews, JR 2002, 'Osseous adaptation and range of motion at the glenohumeral joint in professional baseball pitchers', *Am J Sports Med*, vol. 30, no. 1, pp. 20-6.

Cutti, AG, Cappello, A & Davalli, A 2006, 'In vivo validation of a new technique that compensates for soft tissue artefact in the upper-arm: Preliminary results', *Clinical Biomechanics*, vol. 21, pp. 13-19.

Cutti, AG, Giovanardi, A, Rocchi, L, Davalli, A & Sacchetti, R 2008, 'Ambulatory measurement of shoulder and elbow kinematics through inertial and magnetic sensors', *Medical and Biological Engineering and Computing*, vol. 46, pp. 169-178.

Cutti, AG, Paolini, G, Troncossi, M, Cappello, A & Davalli, A 2005, 'Soft tissue artefact assessment in humeral axial rotation', *Gait and Posture*, vol. 21, pp. 341-349.

De Groot, JH 1997, 'The variability of shoulder motions recorded by means of palpation', *Clinical Biomechanics*, vol. 12, pp. 461-472.

De Groot, JH 1998, The shoulder: a kinematic and dynamic analysis of motion and loading, thesis, Delft University of Technology.

De Groot, JH 1999, 'The scapulo-humeral rhythm: effects of 2-D roentgen projection', *Clin Biomech (Bristol, Avon)*, vol. 14, no. 1, pp. 63-8.

De Leva, P 1996, 'Adjustments to zatsiorsky-seluyanov's segment inertia parameters', *Journal of Biomechanics*, vol. 29, pp. 1223-1230.

Duck, TR, Dunning, CE, Armstrong, AD, Johnson, Ja & King, GJW 2003, 'Application of screw displacement axes to quantify elbow instability', *Clinical Biomechanics*, vol. 18, pp. 303-310.

Ebaugh, DD, McClure, PW & Karduna, AR 2005, 'Three-dimensional scapulothoracic motion during active and passive arm elevation', *Clinical Biomechanics*, vol. 20, pp. 700-709.

Edoarado, *Anatomical planes*. Available from: <http://commons.wikimedia.org/wiki/File:Anatomical_Coronal_Plane-en.svg>.

Eftaxiopoulou, T 2011, Measuring elbow kinematics in cricket bowling, thesis, Imperial College London.

Eftaxiopoulou, T, Gupte, CM, Dear, JP & Bull, AM 2013, 'The effect of digitisation of the humeral epicondyles on quantifying elbow kinematics during cricket bowling', *J Sports Sci*, vol. 31, no. 15, pp. 1722-30.

Ellenbecker, TS, Roetert, EP, Bailie, DS, Davies, GJ & Brown, SW 2002, 'Glenohumeral joint total rotation range of motion in elite tennis players and baseball pitchers', *Med Sci Sports Exerc*, vol. 34, no. 12, pp. 2052-6.

Elliott, BC & Foster, DH 1984, 'A Biomechanical analysis of the front-on and side-on fast bowling techniques', *Journal of Human Movement Studies*, vol. 10, pp. 83-94.

Euler, L 1776, ' Formula generales pro translatione quacunque corporum rigidorum', *Novi commentarii Academiae Scientiarum Imperialis Petropolitanae*, pp. 189-207.

Fayad, F, Hoffmann, G, Hanneton, S, Yazbeck, C, Lefevre-colau, MM, Poiraudeau, S, Revel, M & Roby-Brami, a 2006, '3-D scapular kinematics during arm elevation: Effect of motion velocity', *Clinical Biomechanics*, vol. 21, pp. 932-941.

Ferdinands, R, Marshall, RN & Kersting, U 2010, 'Centre of mass kinematics of fast bowling in cricket', *Sports Biomech*, vol. 9, no. 3, pp. 139-52.

Ferrari, A, Cutti, AG & Cappello, A 2010, 'A new formulation of the coefficient of multiple correlation to assess the similarity of waveforms measured synchronously by different motion analysis protocols', *Gait and Posture*, vol. 31, pp. 540-542.

Finch, CF, Elliott, BC & McGrath, AC 1999, 'Measures to prevent cricket injuries: an overview', *Sports Med*, vol. 28, no. 4, pp. 263-72.

Foster, D, John, D, Elliott, B, Ackland, T & Fitch, K 1989, 'Back injuries to fast bowlers in cricket: a prospective study', *Br J Sports Med*, vol. 23, no. 3, pp. 150-4.

Freehill, MT, Ebel, BG, Archer, KR, Bancells, RL, Wilckens, JH, McFarland, EG & Cosgarea, AJ 2011, 'Glenohumeral range of motion in major league pitchers: changes over the playing season', *Sports Health*, vol. 3, no. 1, pp. 97-104.

Frost, A & Michael Robinson, C 2006, 'The painful shoulder', *Surgery (Oxford)*, vol. 24, pp. 363-367.

Gamage, SSHU & Lasenby, J 2002, 'New least squares solutions for estimating the average centre of rotation and the axis of rotation', *Journal of Biomechanics*, vol. 35, pp. 87-93.

Garofalo, P, Cutti, AG, Filippi, MV, Cavazza, S, Ferrari, A, Cappello, A & Davalli, A 2009, 'Inter-operator reliability and prediction bands of a novel protocol to measure the coordinated movements of shoulder-girdle and humerus in clinical settings', *Med Biol Eng Comput*, vol. 47, no. 5, pp. 475-86.

GetData Graph Digitizer 2013, ed.^eds 2.26.

Giles, K & Musa, I 2008, 'A survey of glenohumeral joint rotational range and non-specific shoulder pain in elite cricketers', *Physical Therapy in Sport*, vol. 9, pp. 109-116.

Glazier, PS, Paradisis, GP & Cooper, SM 2000, 'Anthropometric and kinematic influences on release speed in men's fast-medium bowling.', *Journal of sports sciences*, vol. 18, pp. 1013-1021.

Graichen, H, Bonel, H, Stammberger, T, Haubner, M, Rohrer, H, Englmeier, KH, Reiser, M & Eckstein, F 1999, 'Three-dimensional analysis of the width of the subacromial space in healthy subjects and patients with impingement syndrome', *AJR Am J Roentgenol*, vol. 172, no. 4, pp. 1081-6.

Green, Ra, Taylor, NF, Watson, L & Ardern, C 2013, 'Altered scapula position in elite young cricketers with shoulder problems', *Journal of Science and Medicine in Sport*, vol. 16, pp. 22-27.

Gregory, PL, Batt, ME & Wallace, WA 2002, 'Comparing injuries of spin bowling with fast bowling in young cricketers', *Clin J Sport Med*, vol. 12, no. 2, pp. 107-12.

Grey, H 2008, *Gray's Anatomy: The Anatomical Basis of Clinical Practice*, 40th edn, Elsevier Limited, Spain.

Hess, SA, Richardson, C, Darnell, R, Friis, P, Lisle, D & Myers, P 2005, 'Timing of rotator cuff activation during shoulder external rotation in throwers with and without symptoms of pain', *J Orthop Sports Phys Ther*, vol. 35, no. 12, pp. 812-20.

Hill, aM, Bull, aMJ, Wallace, aL & Johnson, GR 2008, 'Qualitative and quantitative descriptions of glenohumeral motion', *Gait and Posture*, vol. 27, pp. 177-188.

Hughes, PC, Green, Ra & Taylor, NF 2012, 'Measurement of subacromial impingement of the rotator cuff', *Journal of Science and Medicine in Sport*, vol. 15, pp. 2-7.

Hughes, RE & An, KN 1996, 'Force analysis of rotator cuff muscles', *Clin Orthop Relat Res*, no. 330, pp. 75-83.

Hurov, J 2009, 'Anatomy and Mechanics of the Shoulder: Review of Current Concepts', *Journal of Hand Therapy*, vol. 22, pp. 328-343.

Hussain, I 2011, 'Biomechanical Analysis of Flex Elbow on Bowling Speed in Cricket', vol. 2.

Johnson, GR & Pandyan, AD 2005, 'The activity in the three regions of the trapezius under

controlled loading conditions--an experimental and modelling study', *Clin Biomech (Bristol, Avon)*, vol. 20, no. 2, pp. 155-61.

Johnson, GR, Spalding, D, Nowitzke, A & Bogduk, N 1996, 'Modelling the muscles of the scapula morphometric and coordinate data and functional implications', *J Biomech*, vol. 29, no. 8, pp. 1039-51.

Johnson, GR, Stuart, PR & Mitchell, S 1993, 'A method for the measurement of three-dimensional scapular movement', *Clinical Biomechanics*, vol. 8, pp. 269-273.

Kadaba, MP, Ramakrishnan, HK, Wootten, ME, Gainey, J, Gorton, G & Cochran, GV 1989, 'Repeatability of kinematic, kinetic, and electromyographic data in normal adult gait', *J Orthop Res*, vol. 7, no. 6, pp. 849-60.

Karduna, AR, McClure, PW & Michener, La 2000, 'Scapular kinematics: Effects of altering the Euler angle sequence of rotations', *Journal of Biomechanics*, vol. 33, pp. 1063-1068.

Karduna, AR, McClure, PW, Michener, LA & Sennett, B 2001, 'Dynamic measurements of three-dimensional scapular kinematics: a validation study', *J Biomech Eng*, vol. 123, no. 2, pp. 184-90.

Kibler, WB 1998, 'The role of the scapula in athletic shoulder function', *Am J Sports Med*, vol. 26, no. 2, pp. 325-37.

Klein Horsman, MD, Koopman, HFJM, van der Helm, FCT, Prosé, LP & Veeger, HEJ 2007, 'Morphological muscle and joint parameters for musculoskeletal modelling of the lower extremity', *Clinical Biomechanics*, vol. 22, pp. 239-247.

Laursen, B, Jensen, BR, Nemeth, G & Sjogaard, G 1998, 'A model predicting individual shoulder muscle forces based on relationship between electromyographic and 3D external forces in static position', *J Biomech*, vol. 31, no. 8, pp. 731-9.

Leardini, A, Chiari, A, Della Croce, U & Cappozzo, A 2005, 'Human movement analysis using stereophotogrammetry Part 3. Soft tissue artifact assessment and compensation', *Gait and Posture*, vol. 21, pp. 212-225.

Leary, T & White, Ja 2000, 'Acute injury incidence in professional county club cricket players (1985-1995).', *British journal of sports medicine*, vol. 34, pp. 145-147.

Ledger, M, Leeks, N, Ackland, T & Wang, A 2005, 'Short malunions of the clavicle: an anatomic and functional study', *J Shoulder Elbow Surg*, vol. 14, no. 4, pp. 349-54.

Lee, SB, Kim, KJ, O'Driscoll, SW, Morrey, BF & An, KN 2000, 'Dynamic glenohumeral stability provided by the rotator cuff muscles in the mid-range and end-range of motion. A study in cadavera', *J Bone Joint Surg Am*, vol. 82, no. 6, pp. 849-57.

Lempereur, M, Brochard, S, Burdin, V & Rémy-néris, O 2010, 'Difference between palpation and optoelectronics recording of scapular motion.', *Computer methods in biomechanics and biomedical engineering*, vol. 13, pp. 49-57.

Lempereur, M, Brochard, S, Leboeuf, F & Rémy-Néris, O 2014, 'Validity and reliability of 3D marker based scapular motion analysis: A systematic review', *Journal of Biomechanics*, vol. 47, pp. 2219-2230.

Lempereur, M, Brochard, S & Remy-Neris, O 2011, 'Accuracy of scapular motion by double calibration', *Computer Methods in Biomechanics and Biomedical Engineering*, vol. 14, pp. 37-39.

Lloyd, D, Alderson, J, Elliott, B, Hong, Y & Johns, DP 2000a, *Biomechanics in Testing the Legality of a Bowling Action in Cricket*.

Lloyd, DG, Alderson, J & Elliott, BC 2000b, 'An upper limb kinematic model for the examination of cricket bowling: a case study of Mutiah Muralitharan', *J Sports Sci*, vol. 18, no. 12, pp. 975-82.

Lovern, B, Stroud, La, Evans, RO, Evans, SL & Holt, Ca 2009, 'Dynamic tracking of the scapula using skin-mounted markers.', *Proceedings of the Institution of Mechanical Engineers. Part H, Journal of engineering in medicine*, vol. 223, pp. 823-831.

Ludewig, PM & Braman, JP 2011, 'Shoulder impingement: biomechanical considerations in rehabilitation', *Man Ther*, vol. 16, no. 1, pp. 33-9.

Ludewig, PM & Cook, TM 2000, 'Alterations in shoulder kinematics and associated muscle activity in people with symptoms of shoulder impingement', *Phys Ther*, vol. 80, no. 3, pp. 276-91.

Ludewig, PM, Hassett, DR, LaPrade, RF, Camargo, PR & Braman, JP 2010, 'Comparison of scapular local coordinate systems', *Clinical Biomechanics*, vol. 25, pp. 415-421.

Ludewig, PM, Phadke, V, Braman, JP, Hassett, DR, Cieminski, CJ & LaPrade, RF 2009, 'Motion of the shoulder complex during multiplanar humeral elevation.', *The Journal of bone and joint surgery. American volume*, vol. 91, pp. 378-389.

Lukasiewicz, AC, McClure, P, Michener, L, Pratt, N & Sennett, B 1999, 'Comparison of 3-dimensional scapular position and orientation between subjects with and without shoulder impingement', *J Orthop Sports Phys Ther*, vol. 29, no. 10, pp. 574-83; discussion 584-6.

Mansingh, a, Harper, L, Headley, S, King-Mowatt, J & Mansingh, G 2006, 'Injuries in West Indies cricket 2003-2004.', *British journal of sports medicine*, vol. 40, pp. 119-123; discussion 119-123.

Marsden, SP, Swailes, DC & Johnson, GR 2008, 'Algorithms for exact multi-object muscle wrapping and application to the deltoid muscle wrapping around the humerus.', *Proceedings of the Institution of Mechanical Engineers. Part H, Journal of engineering in medicine*, vol. 222, pp. 1081-1095.

Marshall, R & Ferdinands, R 2003, 'The effect of a flexed elbow on bowling speed in cricket', *Sports Biomech*, vol. 2, no. 1, pp. 65-71.

Masjedi, M & Johnson, GR 2011, 'Alteration of scapula lateral rotation for subjects with the reversed anatomy shoulder replacement and its influence on glenohumeral joint contact force', *Proc Inst Mech Eng H*, vol. 225, no. 1, pp. 38-47.

Matsui, K, Shimada, K & Andrew, PD 2006, 'Deviation of skin marker from bone target during movement of the scapula', *Journal of Orthopaedic Science*, vol. 11, pp. 180-184.

MCC, *Laws of Cricket*. Available from: <http://www.lords.org/laws-and-spirit/laws-of-

cricket/laws/law-24-no-ball,50,ar.html>. [4th October].

McClure, PW, Michener, La, Sennett, BJ & Karduna, AR 2001, 'Direct 3-dimensional measurement of scapular kinematics during dynamic movements in vivo', *Journal of Shoulder and Elbow Surgery*, vol. 10, pp. 269-277.

McQuade, KJ & Smidt, GL 1998, 'Dynamic scapulohumeral rhythm: the effects of external resistance during elevation of the arm in the scapular plane.', *The Journal of orthopaedic and sports physical therapy*, vol. 27, pp. 125-133.

Meister, K 2000, 'Injuries to the shoulder in the throwing athlete. Part one: Biomechanics/pathophysiology/classification of injury', *Am J Sports Med*, vol. 28, no. 2, pp. 265-75.

Meskers, CG, Vermeulen, HM, de Groot, JH, van Der Helm, FC & Rozing, PM 1998, '3D shoulder position measurements using a six-degree-of-freedom electromagnetic tracking device', *Clin Biomech (Bristol, Avon)*, vol. 13, no. 4-5, pp. 280-292.

Meyer, KE, Saether, EE, Soiney, EK, Shebeck, MS, Paddock, KL & Ludewig, PM 2008, 'Three-dimensional scapular kinematics during the throwing motion', *J Appl Biomech*, vol. 24, no. 1, pp. 24-34.

Moynes, DR, Perry, J, Antonelli, DJ & Jobe, FW 1986, 'Electromyography and Motion Analysis of the Upper Extremity in Sports', *Physical Therapy*, vol. 66, no. 12, pp. 1905-1911.

Myers, JB, Laudner, KG, Pasquale, MR, Bradley, JP & Lephart, SM 2005, 'Scapular position and orientation in throwing athletes.', *The American journal of sports medicine*, vol. 33, pp. 263-271.

Myers, JB, Laudner, KG, Pasquale, MR, Bradley, JP & Lephart, SM 2006, 'Glenohumeral range of motion deficits and posterior shoulder tightness in throwers with pathologic internal impingement.', *The American journal of sports medicine*, vol. 34, pp. 385-391.

Ng, YFG & Lam, PCW 2002, 'A Study of Antagonist/Agonist Isokinetic Work Ratios of Shoulder Rotators in Men Who Play Badminton', *journal of Orthopaedic & Sports Physical Therapy*, vol. 32, pp. 399-404.

Nikooyan, AA, Veeger, HE, Chadwick, EK, Praagman, M & Helm, FC 2011, 'Development of a comprehensive musculoskeletal model of the shoulder and elbow', *Med Biol Eng Comput*, vol. 49, no. 12, pp. 1425-35.

Nikooyan, aa, Veeger, HEJ, Westerhoff, P, Graichen, F, Bergmann, G & van der Helm, FCT 2010, 'Validation of the Delft Shoulder and Elbow Model using in-vivo glenohumeral joint contact forces', *Journal of Biomechanics*, vol. 43, pp. 3007-3014.

Noffal, GJ 2003, 'Isokinetic eccentric-to-concentric strength ratios of the shoulder rotator muscles in throwers and nonthrowers.', *The American journal of sports medicine*, vol. 31, pp. 537-541.

Orchard, J, James, T, Alcott, E, Carter, S & Farhart, P 2002, 'Injuries in Australian cricket at first class level 1995/1996 to 2000/2001', *Br J Sports Med*, vol. 36, no. 4, pp. 270-4; discussion 275.

Orchard, JJ, T; Kountouris,A; Portus,M 2010, 'Changes to injury porifle (and recommended cricket injury definitions) based on the increased frequncy of Twenty20 cricket matches', *Open Access Journal of Sport Medicine*

Page, P 2011, 'Shoulder muscle imbalance and subacromial impingement syndrome in overhead athletes', *Int J Sports Phys Ther*, vol. 6, no. 1, pp. 51-8.

Pagnani, MJ, Deng, XH, Warren, RF, Torzilli, PA & O'Brien, SJ 1996, 'Role of the long head of the biceps brachii in glenohumeral stability: a biomechanical study in cadavera', *J Shoulder Elbow Surg*, vol. 5, no. 4, pp. 255-62.

Paley, KJ, Jobe, FW, Pink, MM, Kvitne, RS & ElAttrache, NS 2000, 'Arthroscopic findings in the overhand throwing athlete: evidence for posterior internal impingement of the rotator cuff', *Arthroscopy*, vol. 16, no. 1, pp. 35-40.

Pandis, P 2013, Musculoskeletal Biomechanics of the shoulder in functional activities, thesis, Imperial College London.

Portus, M, Mason, BR, Elliott, BC, Pfitzner, MC & Done, RP 2004, 'Technique factors related to ball release speed and trunk injuries in high performance cricket fast bowlers', *Sports Biomech*, vol. 3, no. 2, pp. 263-84.

Primal, *Upper limb anatomy*. Available from: <http://anatomy.tv/new_home.aspx>. [12th October].

Prinold, JA, Shaheen, AF & Bull, AM 2011, 'Skin-fixed scapula trackers: a comparison of two dynamic methods across a range of calibration positions', *J Biomech*, vol. 44, no. 10, pp. 2004-7.

Prinold, JaI 2012, The scapula in musculoskeletal modelling of extreme activities, thesis, Imperial College London.

Prinold, JaI & Bull, AMJ 2014, 'Scaling and kinematics optimisation of the scapula and thorax in upper limb musculoskeletal models', *Journal of Biomechanics*, vol. 47, pp. 2813-2819.

Prinold, JaI & Bull, aMJ 2015, 'Scapula kinematics of pull-up techniques: avoiding impingement risk with training changes', *British journal of sports medicine*, pp. 4-10.

Pronk, GM & van der Helm, FC 1991, 'The palpator: an instrument for measuring the positions of bones in three dimensions', *J Med Eng Technol*, vol. 15, no. 1, pp. 15-20.

Pronk, GM, van der Helm, FC & Rozendaal, LA 1993, 'Interaction between the joints in the shoulder mechanism: the function of the costoclavicular, conoid and trapezoid ligaments', *Proc Inst Mech Eng H*, vol. 207, no. 4, pp. 219-29.

Ranson, C & Gregory, PL 2008, 'Shoulder injury in professional cricketers', *Physical Therapy in Sport*, vol. 9, pp. 34-39.

Ranson, CA, Burnett, AF, King, M, Patel, N & O'Sullivan, PB 2008, 'The relationship between bowling action classification and three-dimensional lower trunk motion in fast bowlers in cricket', *J Sports Sci*, vol. 26, no. 3, pp. 267-76.

Rasmussen, J, Damsgaard, M & Voigt, M 2001, 'Muscle recruitment by the min/max criterion

-- a comparative numerical study', *J Biomech*, vol. 34, no. 3, pp. 409-15.

Roberts, CS, Davila, JN, Hushek, SG, Tillett, ED & Corrigan, TM 2002, 'Magnetic resonance imaging analysis of the subacromial space in the impingement sign positions', *J Shoulder Elbow Surg*, vol. 11, no. 6, pp. 595-9.

Rockwood, CA 2009, *The shoulder. Vol. 1*, 4th edn, 2 vols, Saunders, Philadelphia, Pa. ; [London].

Roger, B, Skaf, A, Hooper, AW, Lektrakul, N, Yeh, L & Resnick, D 1999, 'Imaging findings in the dominant shoulder of throwing athletes: comparison of radiography, arthrography, CT arthrography, and MR arthrography with arthroscopic correlation', *AJR Am J Roentgenol*, vol. 172, no. 5, pp. 1371-80.

Rojas, IL, Provencher, MT, Bhatia, S, Foucher, KC, Bach, BR, Jr., Romeo, AA, Wimmer, MA & Verma, NN 2009, 'Biceps activity during windmill softball pitching: injury implications and comparison with overhand throwing', *Am J Sports Med*, vol. 37, no. 3, pp. 558-65.

Sapega, AA 1990, 'Muscle Performance Evaluation in Orthopedic Practice', *Journal of Bone and Joint Surgery-American Volume*, vol. 72A, no. 10, pp. 1562-1574.

Senk, M & Cheze, L 2010, 'A new method for motion capture of the scapula using an optoelectronic tracking device: a feasibility study', *Comput Methods Biomech Biomed Engin*, vol. 13, no. 3, pp. 397-401.

Šenk, M & Chèze, L 2006, 'Rotation sequence as an important factor in shoulder kinematics', *Clinical Biomechanics*, vol. 21, pp. 3-8.

Seo, YJ, Yoo, YS, Noh, KC, Song, SY, Lee, YB, Kim, HJ & Kim, HY 2012, 'Dynamic function of coracoclavicular ligament at different shoulder abduction angles: a study using a 3-dimensional finite element model', *Arthroscopy*, vol. 28, no. 6, pp. 778-87.

Shaheen, AF 2010, Tracking scapular movement, thesis, Imperial College London.

Shaheen, AF, Alexander, CM & Bull, AM 2011a, 'Tracking the scapula using the scapula locator with and without feedback from pressure-sensors: A comparative study', *J Biomech*, vol. 44, no. 8, pp. 1633-6.

Shaheen, aF, Alexander, CM & Bull, aMJ 2011b, 'Effects of attachment position and shoulder orientation during calibration on the accuracy of the acromial tracker', *Journal of Biomechanics*, vol. 44, pp. 1410-1413.

Shaheen, AF, Villa, C, Lee, YN, Bull, AM & Alexander, CM 2013, 'Scapular taping alters kinematics in asymptomatic subjects', *J Electromyogr Kinesiol*, vol. 23, no. 2, pp. 326-33.

Shorter, K, Smith, N, Lauder, M & Khoury, P 2010, 'a Preliminary Electromyographic Investigation Into Shoulder Muscle Activity in Cricket Seam Bowling', pp. 1-4.

Soderkvist, I & Wedin, PA 1993, 'Determining the movements of the skeleton using well-configured markers', *J Biomech*, vol. 26, no. 12, pp. 1473-7.

Southgate, DF, Cleather, DJ, Weinert-Aplin, RA & Bull, AM 2012, 'The sensitivity of a lower

limb model to axial rotation offsets and muscle bounds at the knee', *Proc Inst Mech Eng H*, vol. 226, no. 9, pp. 660-9.

Southgate, DFL, Hill, AM, Alexander, S, Wallace, AL, Hansen, UN & Bull, AMJ 2009, 'The range of axial rotation of the glenohumeral joint', *Journal of Biomechanics*, vol. 42, pp. 1307-1312.

Spindler, KP, Dovan, TT & McCarty, EC 2001, 'Assessment and management of the painful shoulder.', *Clinical cornerstone*, vol. 3, pp. 26-37.

Spitzer, VM & Whitlock, DG 1998, 'The Visible Human Dataset: the anatomical platform for human simulation', *Anat Rec*, vol. 253, no. 2, pp. 49-57.

Steel, FL & Tomlinson, JD 1958, 'The carrying angle in man', *J Anat*, vol. 92, no. 2, pp. 315-7.

Stokdijk, M, Meskers, CGM, Veeger, HEJ, De Boer, Ya & Rozing, PM 1999, 'Determination of the optimal elbow axis for evaluation of placement of prostheses', *Clinical Biomechanics*, vol. 14, pp. 177-184.

Stretch, RA 2003, 'Cricket injuries: a longitudinal study of the nature of injuries to South African cricketers', *Br J Sports Med*, vol. 37, no. 3, pp. 250-3; discussion 253.

Stronach, B, Cronin, J & Portus, M 2014, 'Part 1: Biomechanics, Injury Surveillance, and Predictors of Injury for Cricket Fast Bowlers', *Strength & Conditioning Journal*, vol. 1, pp. 65-72.

Stuelcken, MC, Ferdinands, RED, Ginn, Ka & Sinclair, PJ 2010, 'The shoulder distraction force in cricket fast bowling', *Journal of Applied Biomechanics*, vol. 26, pp. 373-377.

Stuelcken, MC, Ginn, Ka & Sinclair, PJ 2008, 'Shoulder strength and range of motion in elite female cricket fast bowlers with and without a history of shoulder pain', *Journal of Science and Medicine in Sport*, vol. 11, pp. 575-580.

Sugamoto, K, Harada, T, Machida, A, Inui, H, Miyamoto, T, Takeuchi, E, Yoshikawa, H & Ochi, T 2002, 'Scapulohumeral rhythm: relationship between motion velocity and rhythm', *Clin Orthop Relat Res*, no. 401, pp. 119-24.

Sundaram, B 2012, 'Original Research Glenohumeral Rotational Range of Motion Differences Between Fast Bowlers and Spin', vol. 7, pp. 576-585.

Terry, GC & Chopp, TM 2000, 'Functional anatomy of the shoulder', *J Athl Train*, vol. 35, no. 3, pp. 248-55.

Thompson, N 2015, *Shoulder Impingement Syndrome And Tears of the Rotator Cuff*.

Tortora, GJ & Derrickson, B 2011, *Principles of anatomy & physiology. Volume 1, Organization, support and movemenet, and control systems of the uman body*, 13th edn, 1 vols, Wiley, Hoboken, N.J.

Tyler, TF, Nicholas, SJ, Roy, T & Gleim, GW 2000, 'Quantification of posterior capsule tightness and motion loss in patients with shoulder impingement.', *The American journal of sports medicine*, vol. 28, pp. 668-673.

van Andel, C, van Hutten, K, Eversdijk, M, Veeger, D & Harlaar, J 2009, 'Recording scapular

motion using an acromion marker cluster', *Gait and Posture*, vol. 29, pp. 123-128.

van der Helm, FC & Pronk, GM 1995, 'Three-dimensional recording and description of motions of the shoulder mechanism', *J Biomech Eng*, vol. 117, no. 1, pp. 27-40.

Van der Helm, FC, Veeger, HE, Pronk, GM, Van der Woude, LH & Rozendal, RH 1992, 'Geometry parameters for musculoskeletal modelling of the shoulder system', *J Biomech*, vol. 25, no. 2, pp. 129-44.

van Drongelen, S, van der Woude, LH & Veeger, HE 2011, 'Load on the shoulder complex during wheelchair propulsion and weight relief lifting', *Clin Biomech (Bristol, Avon)*, vol. 26, no. 5, pp. 452-7.

Van Roy, P, Baeyens, JP, Fauvart, D, Lanssiers, R & Clarijs, JP 2005, 'Arthro-kinematics of the elbow: study of the carrying angle.', *Ergonomics*, vol. 48, pp. 1645-1656.

Veeger, HE & van der Helm, FC 2007, 'Shoulder function: the perfect compromise between mobility and stability', *J Biomech*, vol. 40, no. 10, pp. 2119-29.

Veeger, HE, van der Helm, FC & Rozendal, RH 1993, 'Orientation of the scapula in a simulated wheelchair push', *Clin Biomech (Bristol, Avon)*, vol. 8, no. 2, pp. 81-90.

Veeger, HEJ, Yu, B, An, KN & Rozendal, RH 1997, 'Parameters for modeling the upper extremity', *Journal of Biomechanics*, vol. 30, pp. 647-652.

Veldpaus, FE, Woltring, HJ & Dortmans, LJMG 1988, 'A Least-Squares Algorithm for the Equiform Transformation from Spatial Marker Coordinates', *Journal of Biomechanics*, vol. 21, no. 1, pp. 45-54.

Vorndran, D, *montage showing the final stage of the run-up of fast bowler Mitchell Johnson*. Available from: <https://en.wikipedia.org/wiki/Run-up_%28cricket%29#/media/File:Run-Up_study_of_Mitchell_Johnson_100311_1.jpg>.

Warner, JJ, Micheli, LJ, Arslanian, LE, Kennedy, J & Kennedy, R 1992, 'Scapulothoracic motion in normal shoulders and shoulders with glenohumeral instability and impingement syndrome. A study using Moire topographic analysis', *Clin Orthop Relat Res*, no. 285, pp. 191-9.

Werner, SL, Gill, TJ, Murray, TA, Cook, TD & Hawkins, RJ 2001, 'Relationships between throwing mechanics and shoulder distraction in professional baseball pitchers', *Am J Sports Med*, vol. 29, no. 3, pp. 354-8.

Wilk, KE, Andrews, JR, Arrigo, CA, Keirns, MA & Erber, DJ 1993, 'The Strength Characteristics of Internal and External Rotator Muscles in Professional Baseball Pitchers', *American Journal of Sports Medicine*, vol. 21, no. 1, pp. 61-66.

Wilk, KE, Obma, P, Simpson, CD, Cain, EL, Dugas, JR & Andrews, JR 2009, 'Shoulder injuries in the overhead athlete', *J Orthop Sports Phys Ther*, vol. 39, no. 2, pp. 38-54.

Williams, GR, Jr., Shakil, M, Klimkiewicz, J & Iannotti, JP 1999, 'Anatomy of the scapulothoracic articulation', *Clin Orthop Relat Res*, no. 359, pp. 237-46.

Williams, GR & Kelley, M 2000, 'Management of rotator cuff and impingement injuries in the

athlete', *J Athl Train*, vol. 35, no. 3, pp. 300-15.

Winters, JM & Stark, L 1985, 'Analysis of fundamental human movement patterns through the use of in-depth antagonistic muscle models', *IEEE Trans Biomed Eng*, vol. 32, no. 10, pp. 826-39.

Woltring, HJ, Huiskes, R, Delange, A & Veldpaus, FE 1985, 'Finite Centroid and Helical Axis Estimation from Noisy Landmark Measurements in the Study of Human Joint Kinematics', *Journal of Biomechanics*, vol. 18, no. 5, pp. 379-389.

Woolmer, B, Noakes, T & Moffett, H 2008, *Bob Woolmer's art and science of cricket*, Struik ;New Holland distributor, Cape Town

Worthington, PJ, King, Ma & Ranson, Ca 2013, 'Relationships between fast bowling technique and ball release speed in cricket', *Journal of Applied Biomechanics*, vol. 29, pp. 78-84.

Wu, G, Siegler, S, Allard, P, Kirtley, C, Leardini, A, Rosenbaum, D, Whittle, M, D'Lima, DD, Cristofolini, L, Witte, H, Schmid, O & Stokes, I 2002, 'ISB recommendation on definitions of joint coordinate system of various joints for the reporting of human joint motion--part I: ankle, hip, and spine. International Society of Biomechanics.', *Journal of biomechanics*, vol. 35, pp. 543-548.

Wu, G, Van Der Helm, FCT, Veeger, HEJ, Makhsous, M, Van Roy, P, Anglin, C, Nagels, J, Karduna, AR, McQuade, K, Wang, X, Werner, FW & Buchholz, B 2005, 'ISB recommendation on definitions of joint coordinate systems of various joints for the reporting of human joint motion - Part II: Shoulder, elbow, wrist and hand', *Journal of Biomechanics*, vol. 38, pp. 981-992.

Yanagawa, T, Goodwin, CJ, Shelburne, KB, Giphart, JE, Torry, MR & Pandy, MG 2008, 'Contributions of the individual muscles of the shoulder to glenohumeral joint stability during abduction', *J Biomech Eng*, vol. 130, no. 2, p. 021024.

Yano, Y, Hamada, J, Tamai, K, Yoshizaki, K, Sahara, R, Fujiwara, T & Nohara, Y 2010, 'Different scapular kinematics in healthy subjects during arm elevation and lowering: glenohumeral and scapulothoracic patterns', *J Shoulder Elbow Surg*, vol. 19, no. 2, pp. 209-15.

Yeadon, MR & King, MA 2015, 'The effect of marker placement around the elbow on calculated elbow extension during bowling in cricket', *J Sports Sci*, vol. 33, no. 16, pp. 1658-66.

Zhang, YU, J;Liu,G 2011, 'The Influence of Cricket Bowler’s Joint Rotations on Ball Release Speed', *2011 International Conference on Human Health and Biomedical Engineering*.

Appendix 1 Total body kinematic curves

Bowlers f7 and s1 were left-handers, as such joint kinematics are reported as the bowling side, non–bowling side, front foot and back foot. Left-handers deliver with the left foot being the back foot and front foot being the right. The opposite is true for right-handers. Joint rotation conventions for left-handers were adjusted so that positive rotations were the same clinical description with that of a right-hander. This was done for all the rotations except thorax relative to the pelvis since the clinical description used describe rotations to the left or right sides.

Fast bowlers stock over

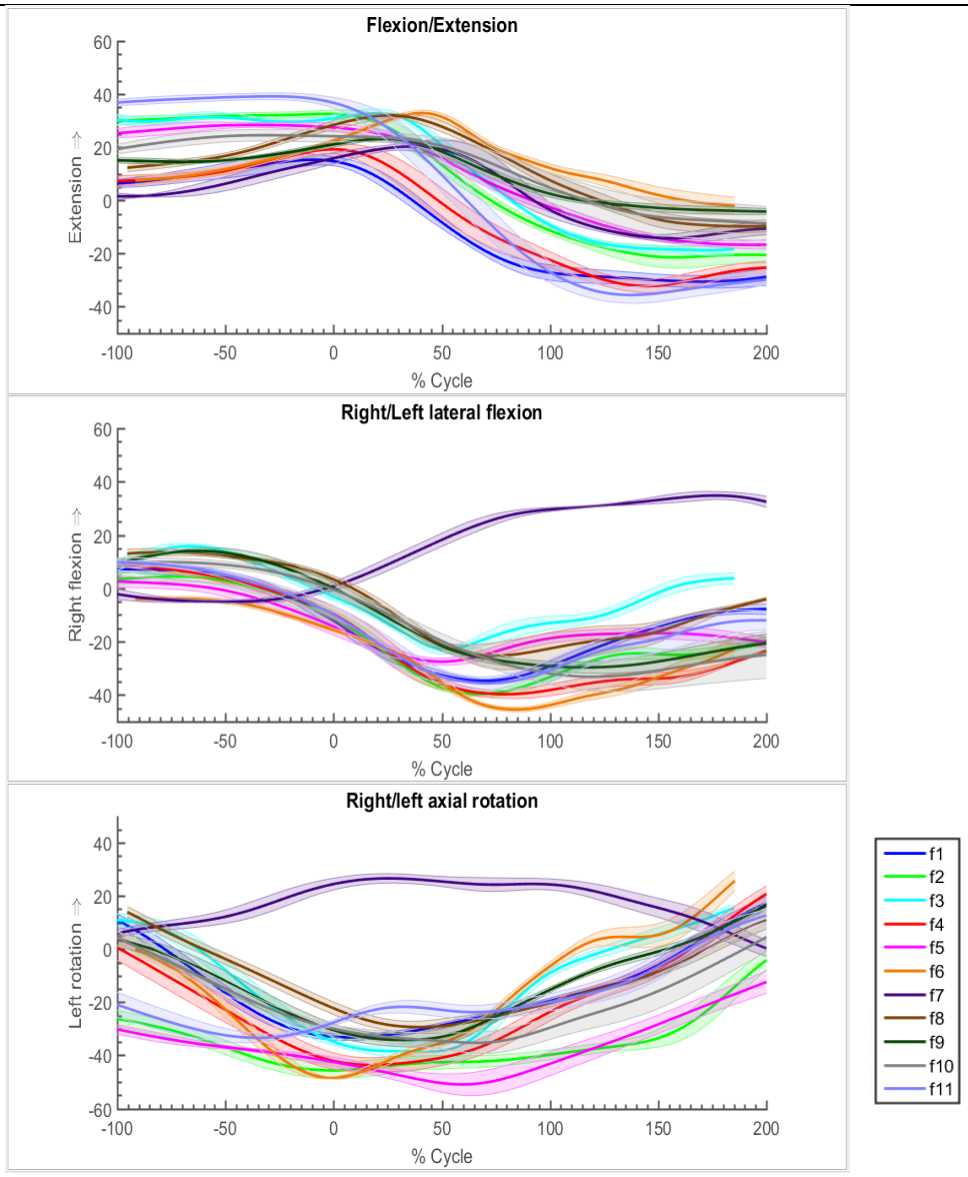

Figure 1.1 Thorax relative to pelvis, fast bowlers-stock over.

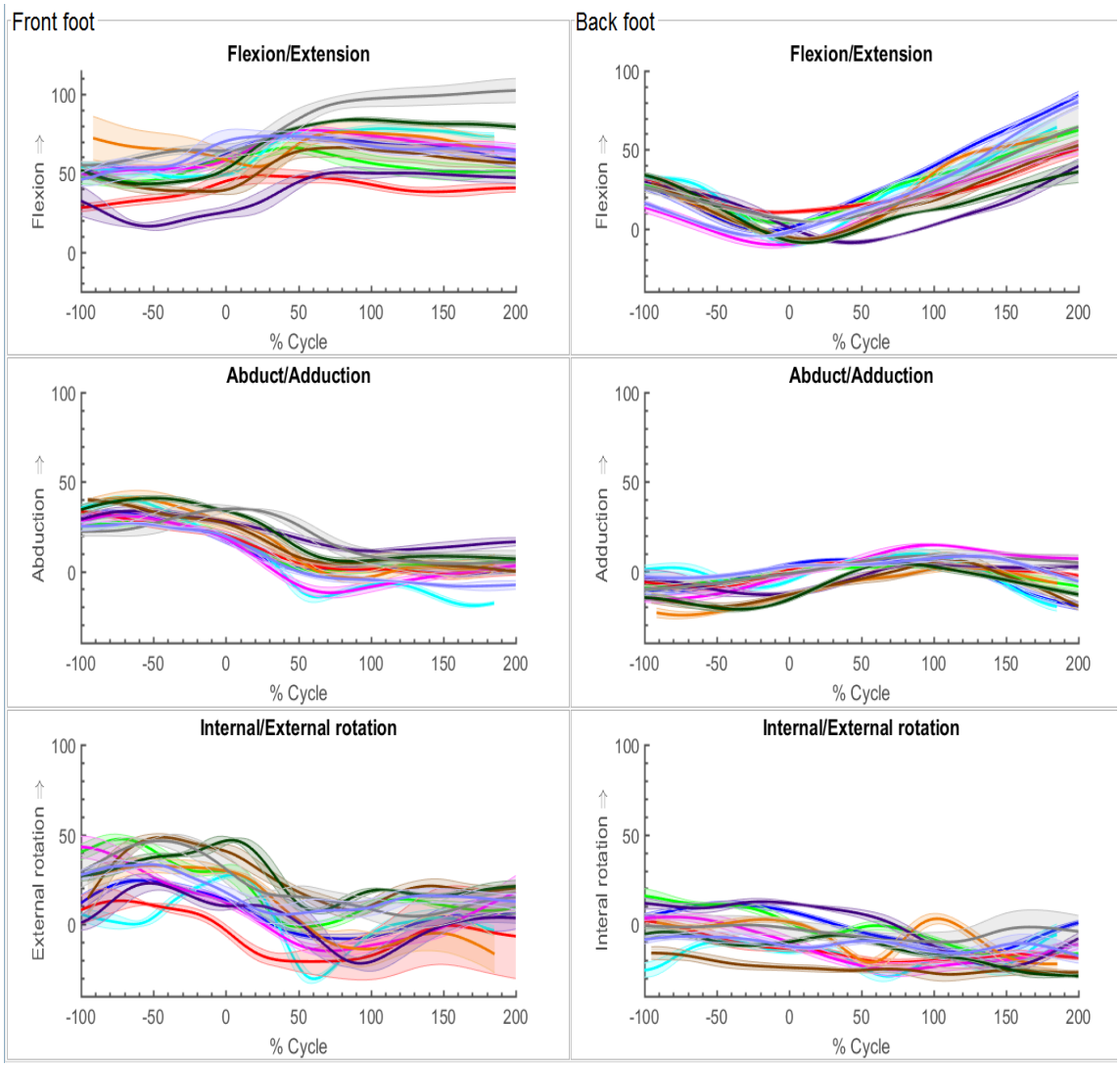

Figure 1.2 Hip joint, fast bowlers-stock over.

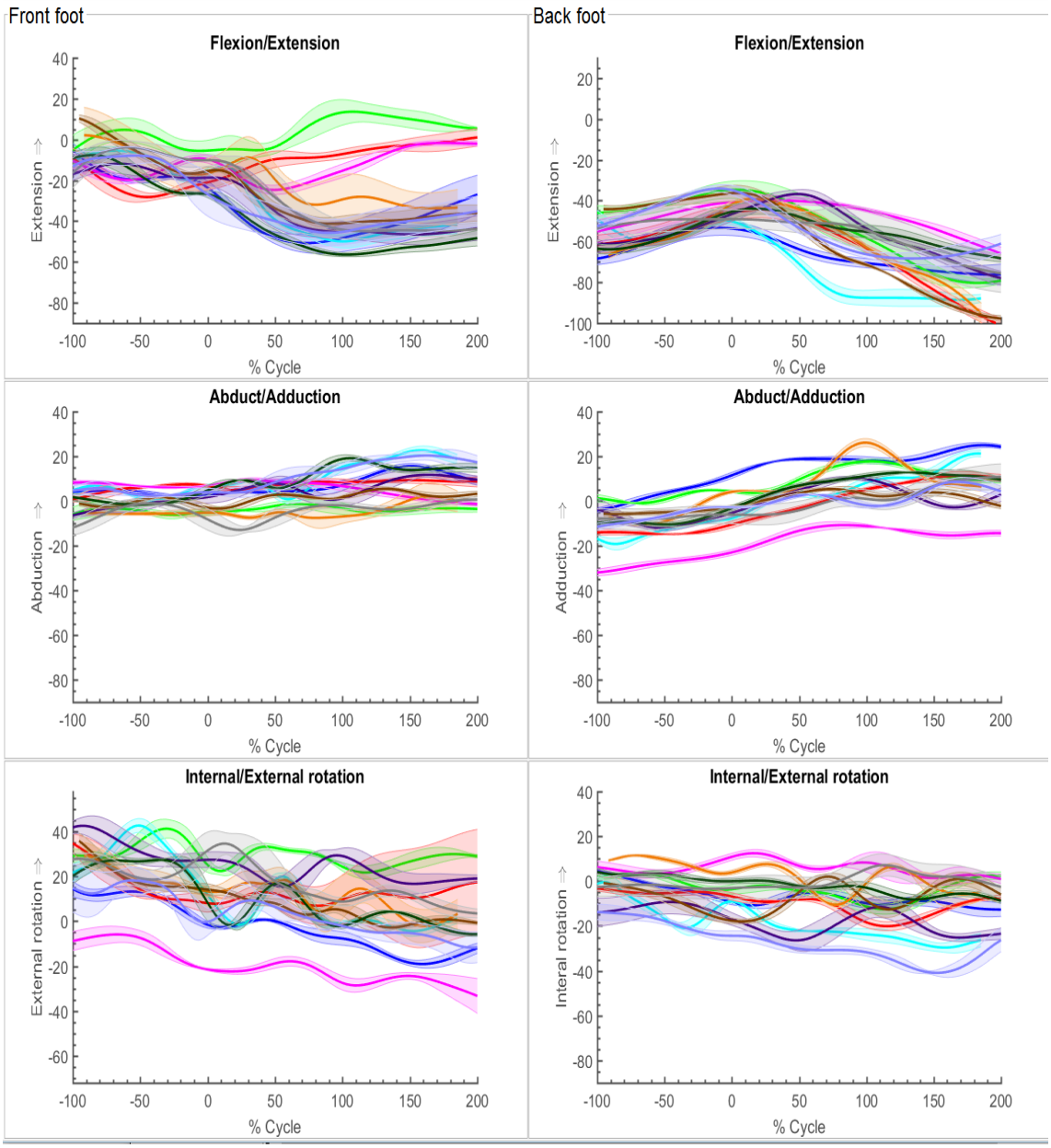

Figure 1.3 Knee joint, fast bowlers-stock over.

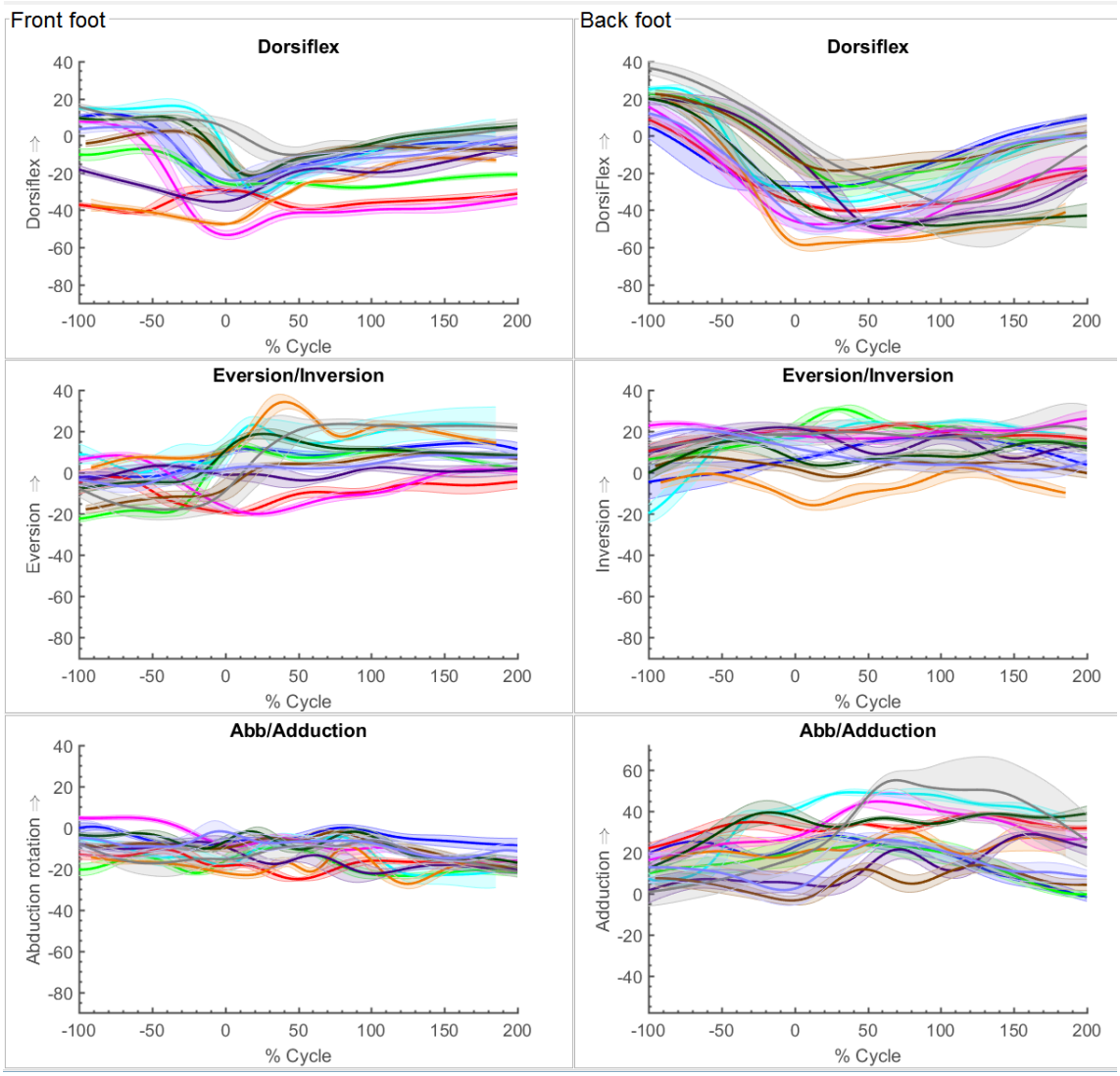

Figure 1.4 Ankle joint, fast bowlers-stock over.

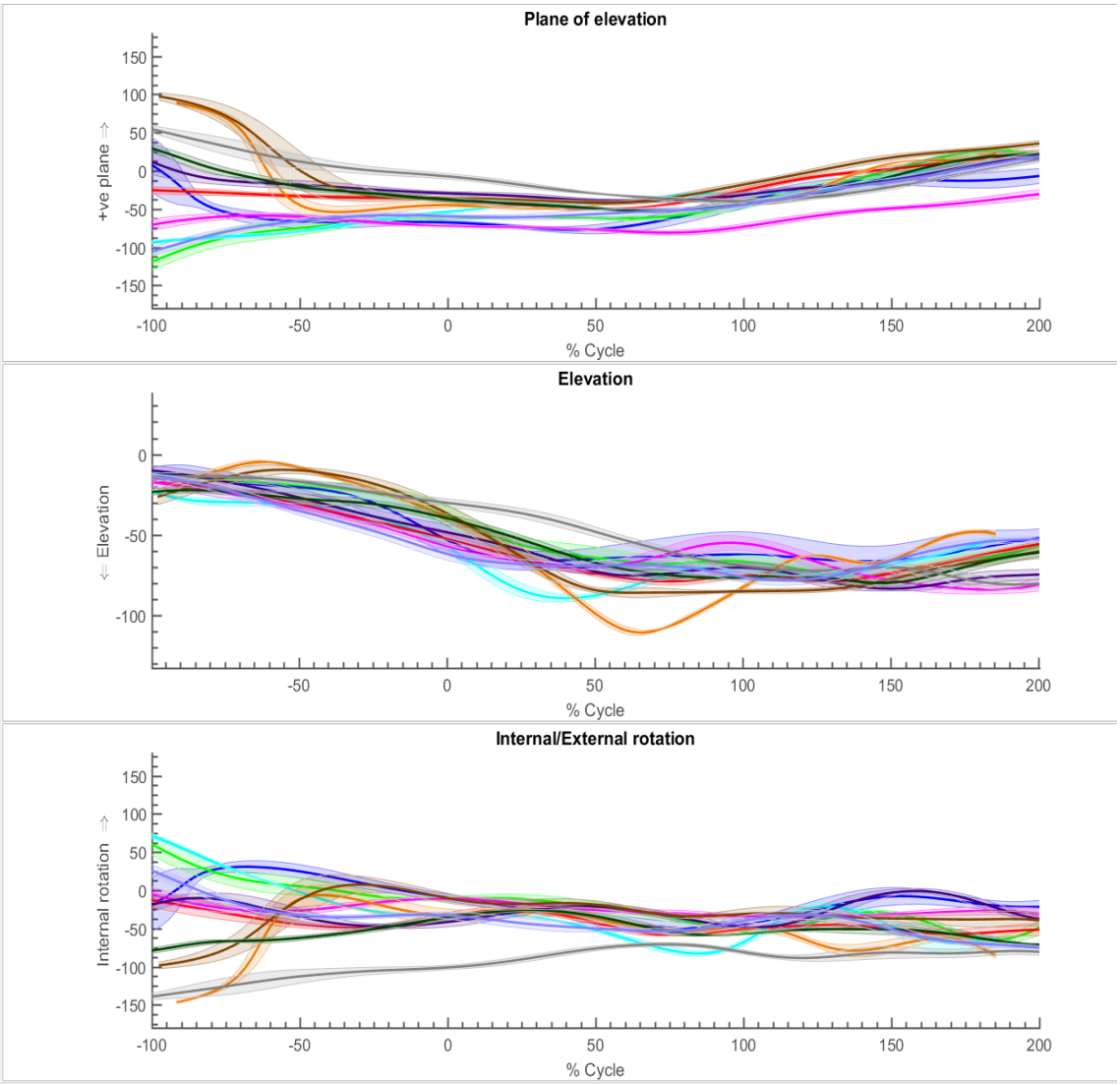

Figure 1.5 Glenohumeral joint, fast bowlers-stock over.

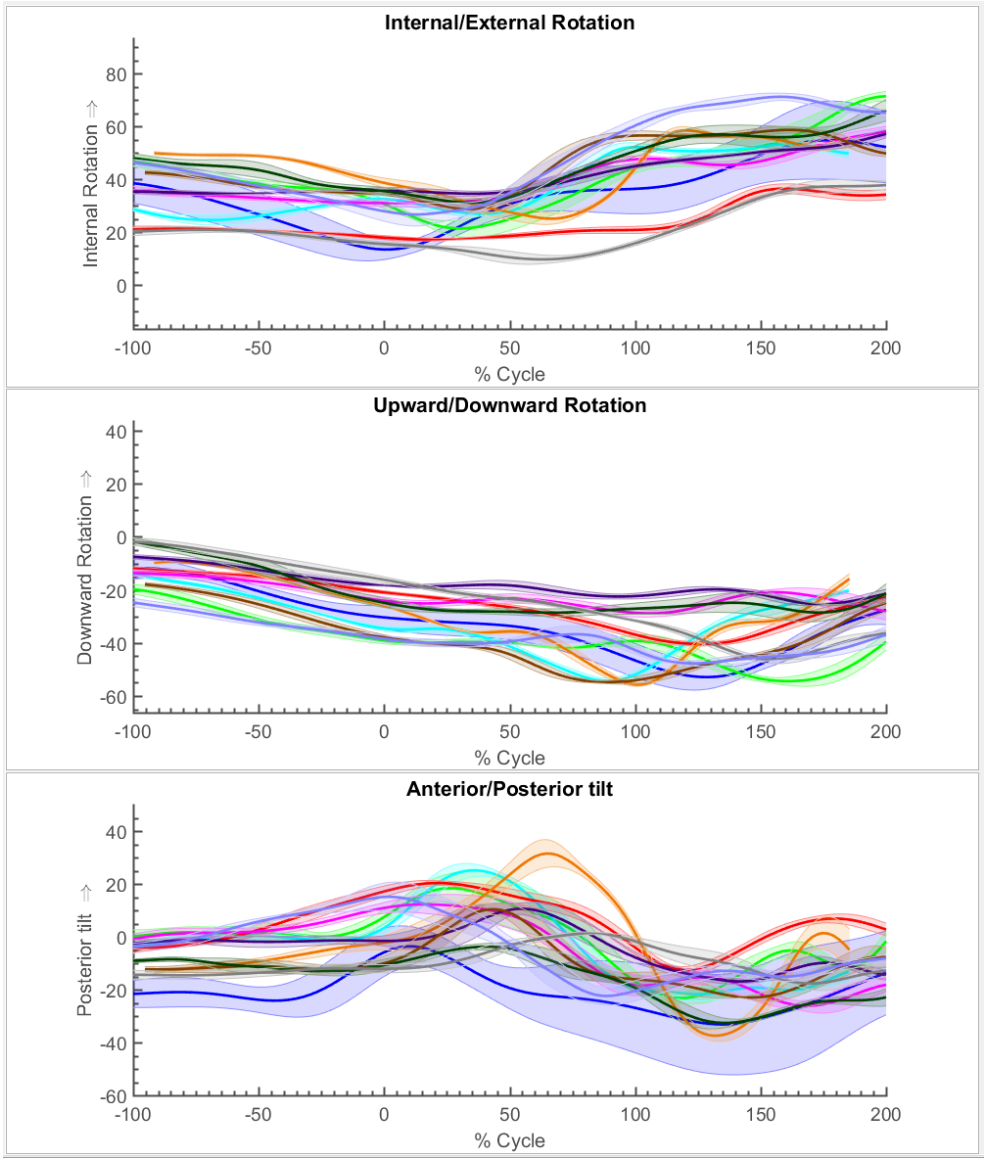

Figure 1.6 Scapulothoracic rotations, fast bowlers-stock over.

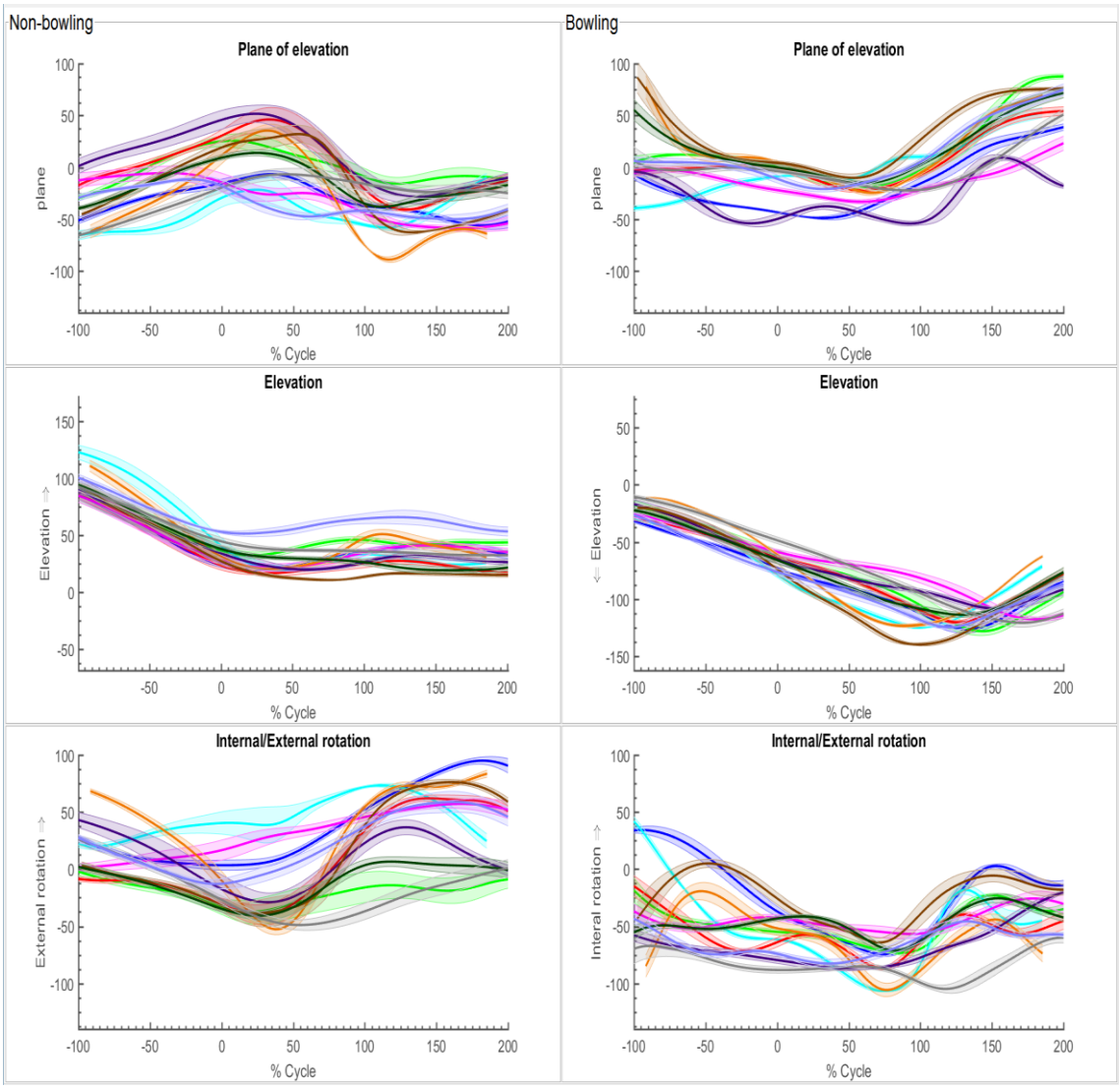

Figure 1.7 Humerothoracic rotations, fast bowlers-stock over.

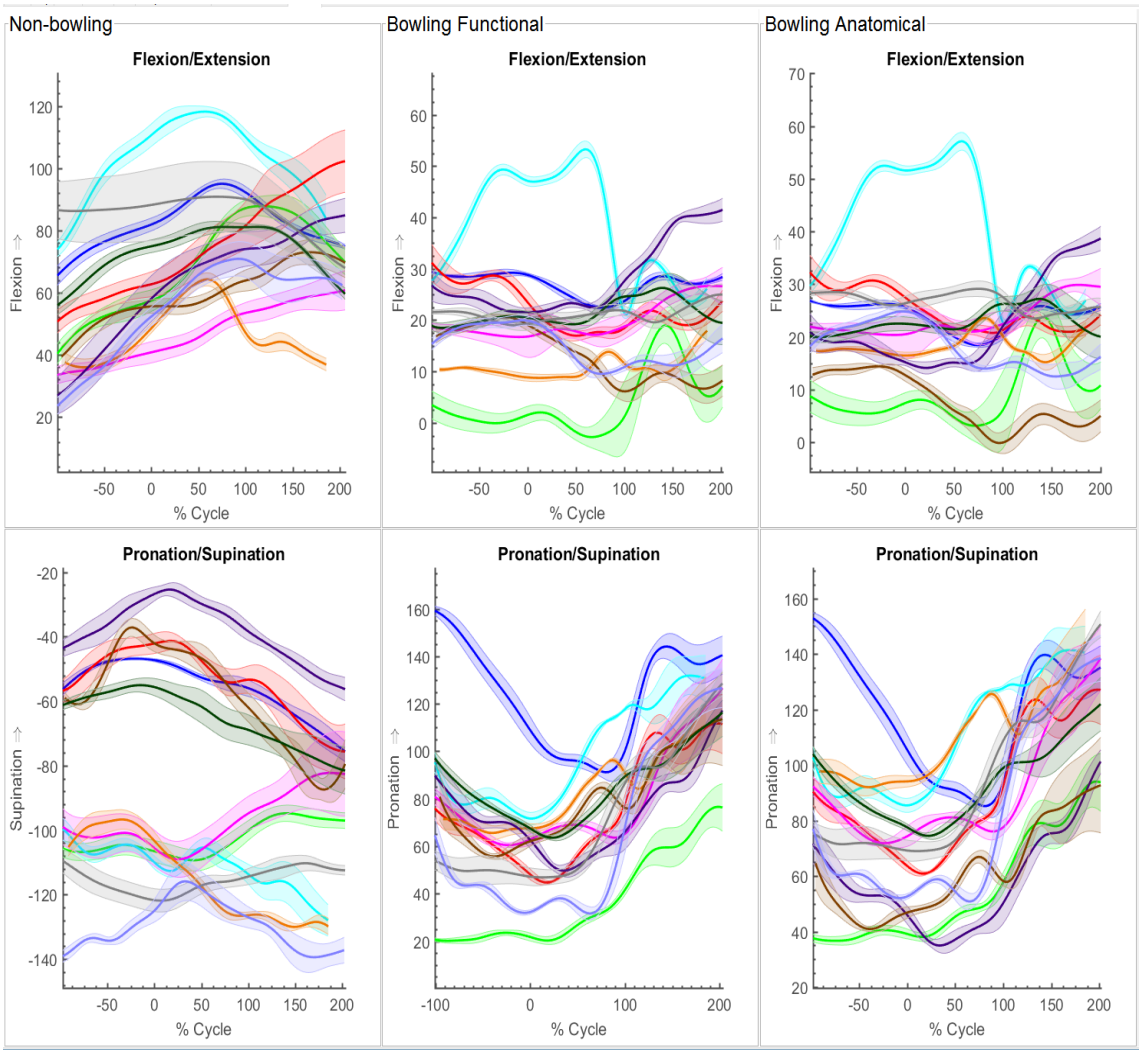

Figure 1.8 Elbow joint, fast bowlers-stock over.

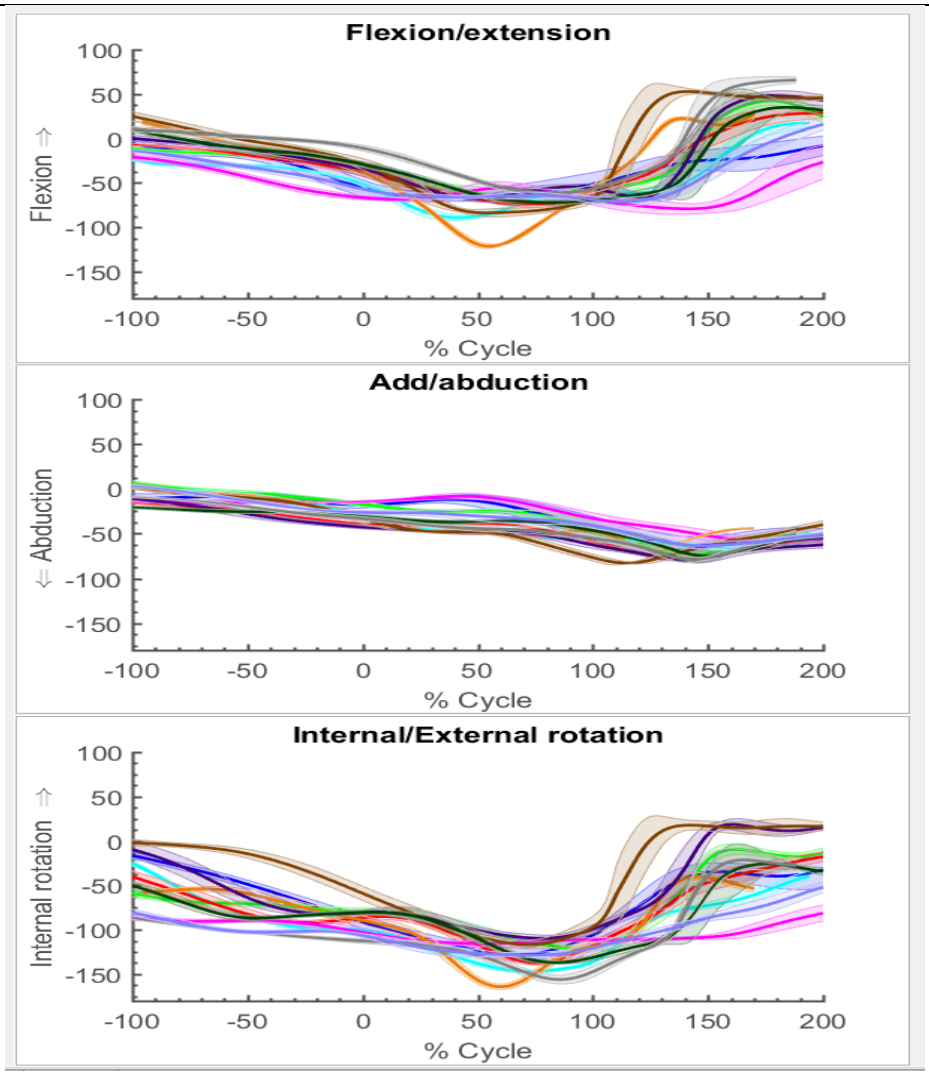

Figure 1.9 Alternative GH joint kinematics using Euler sequence ZXY, fast bowlers stock over

Fast bowlers variation over

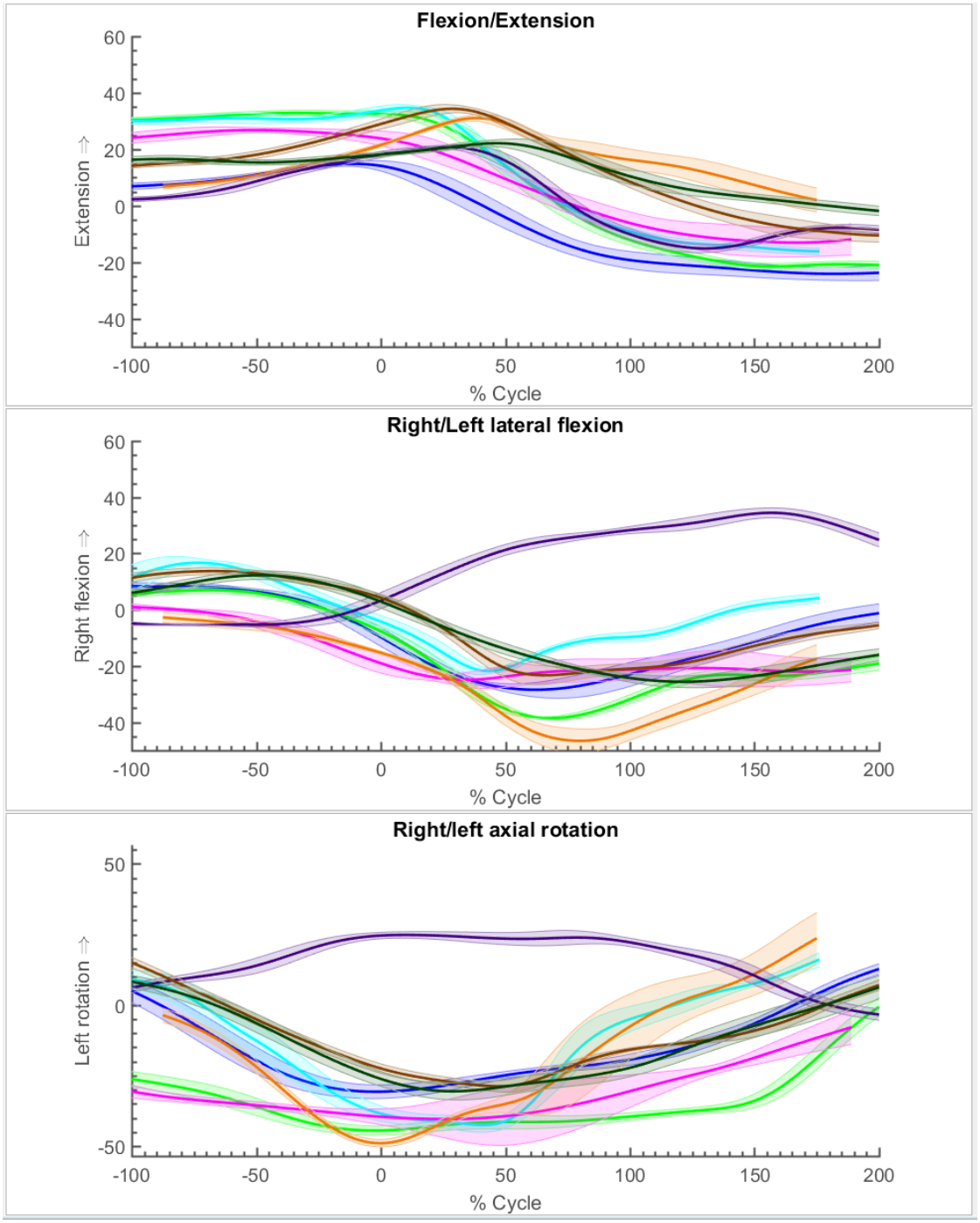

Figure 1.10 Thorax relative to pelvis, fast bowlers-variation over.

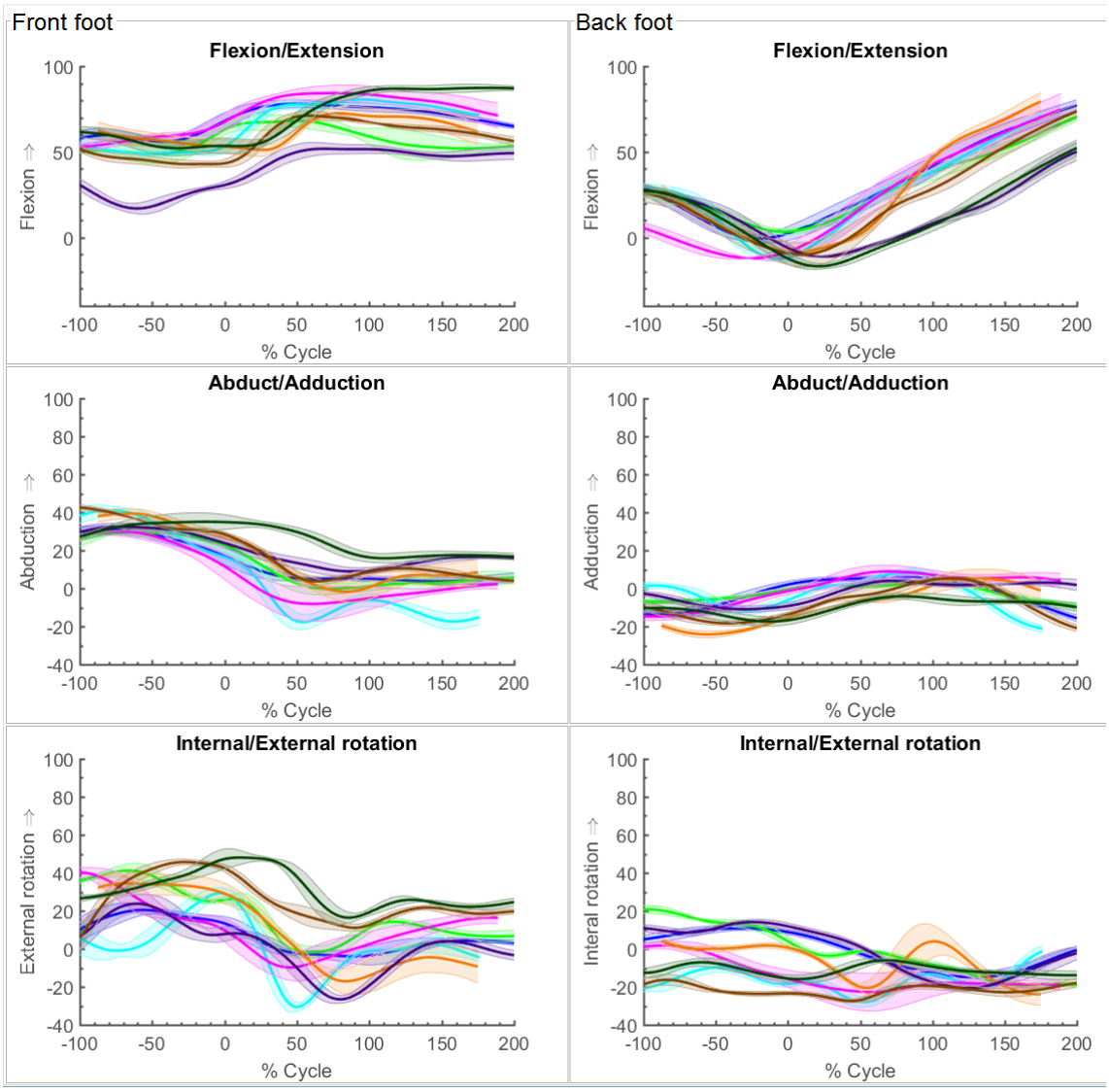

Figure 1.11 Hip joint, fast bowlers-variation over.

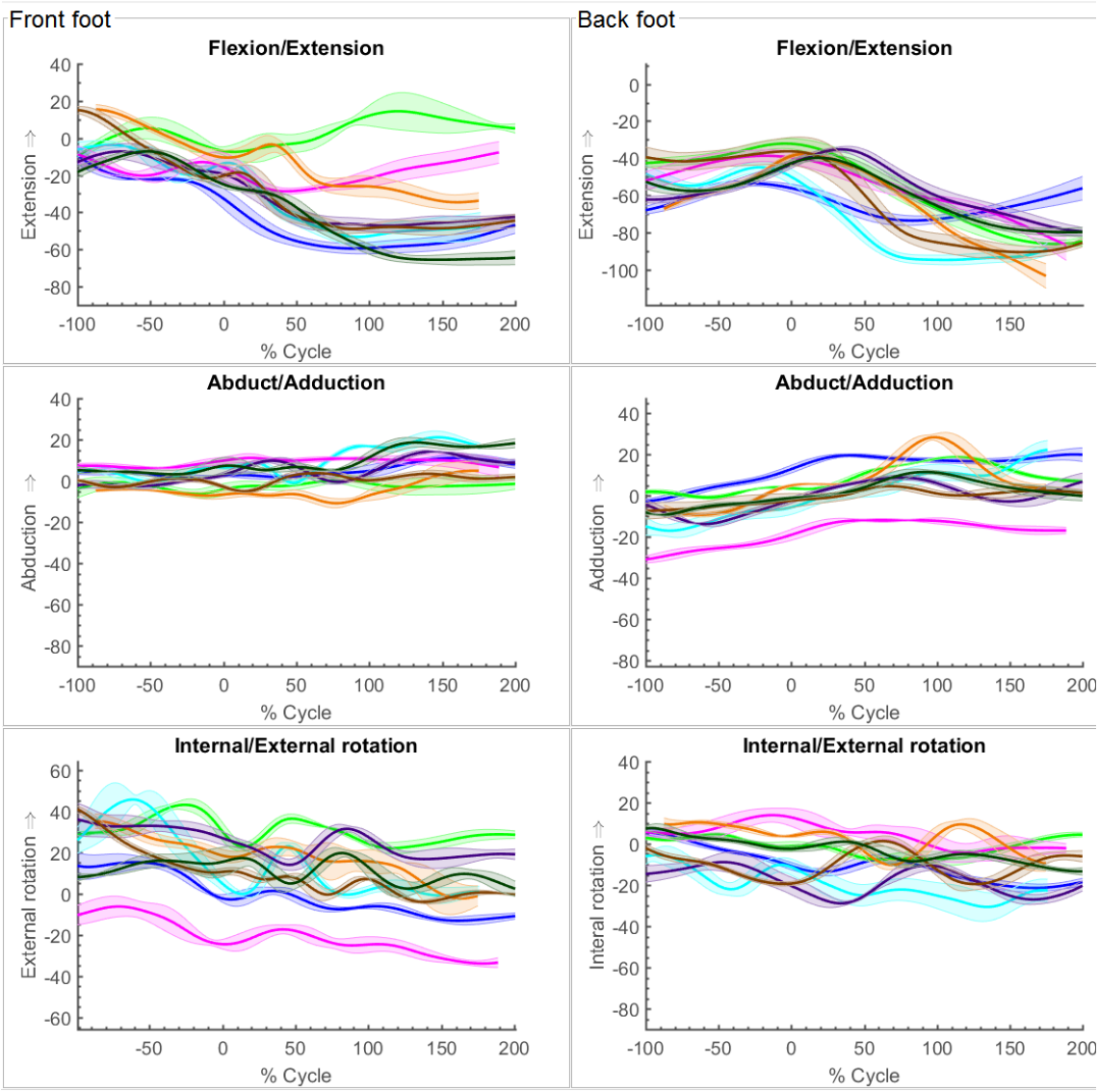

Figure 1.12 Knee joint, fast bowlers-variation over.

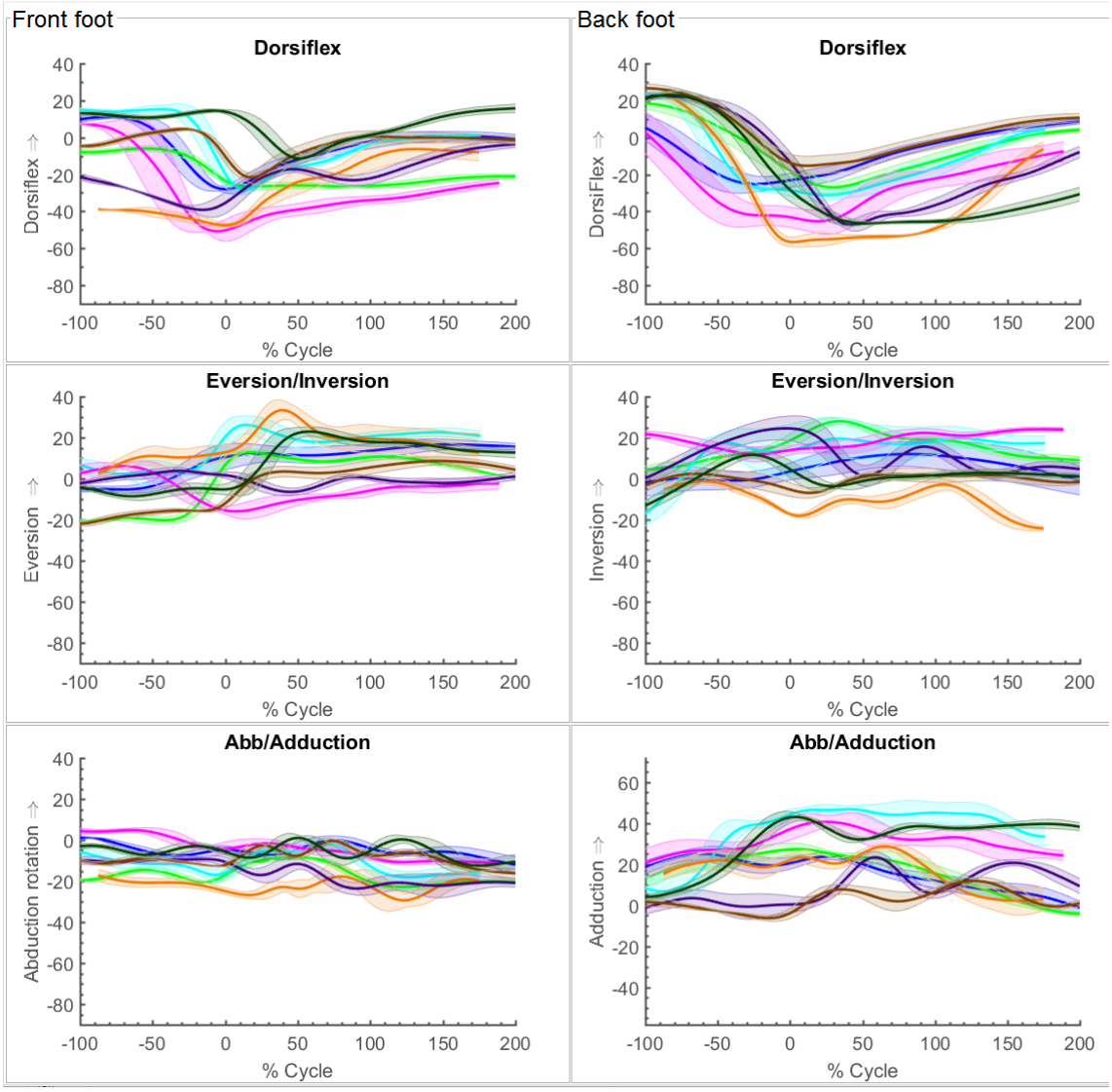

Figure 1.13 Ankle joint, fast bowlers-variation over.

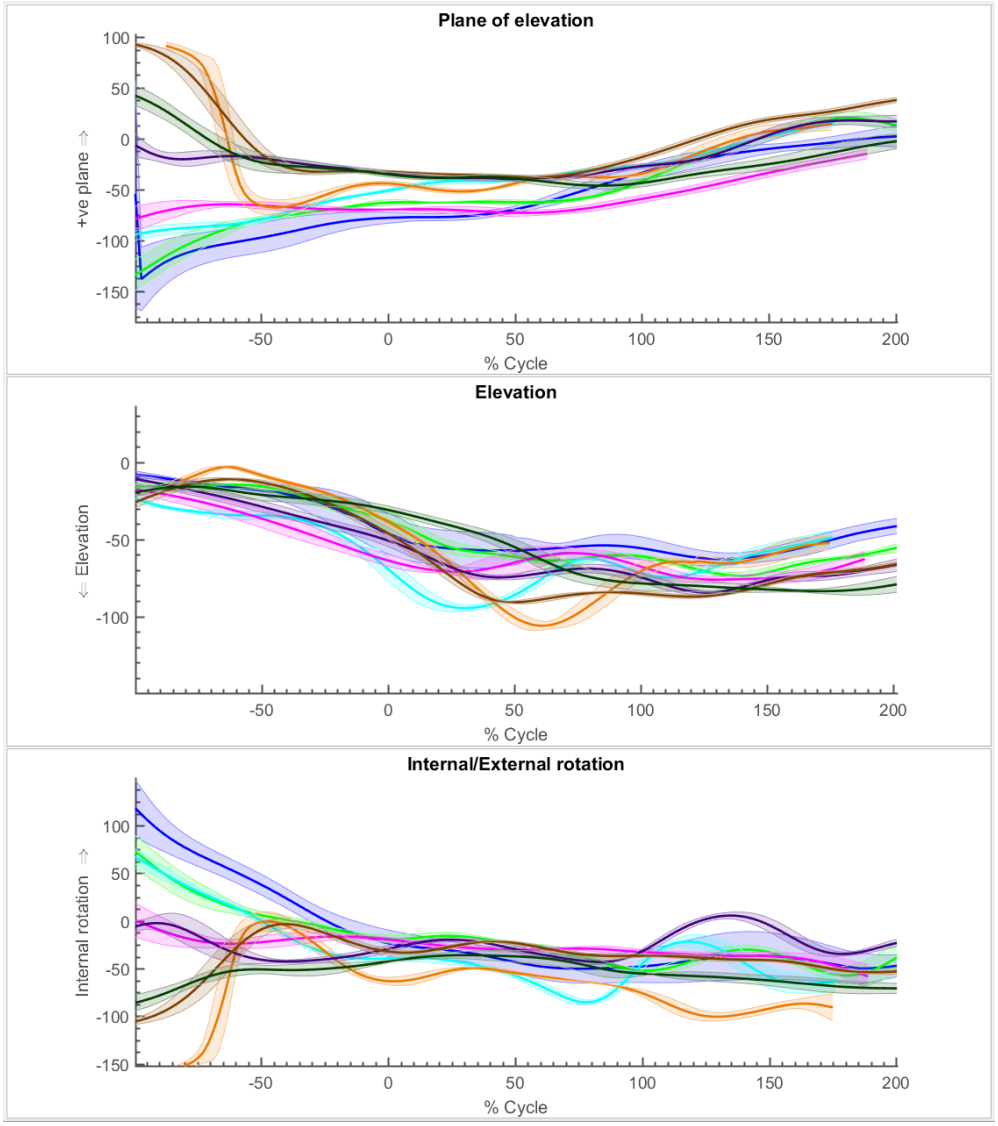

Figure 1.14 Glenohumeral joint, fast bowlers-variation over.

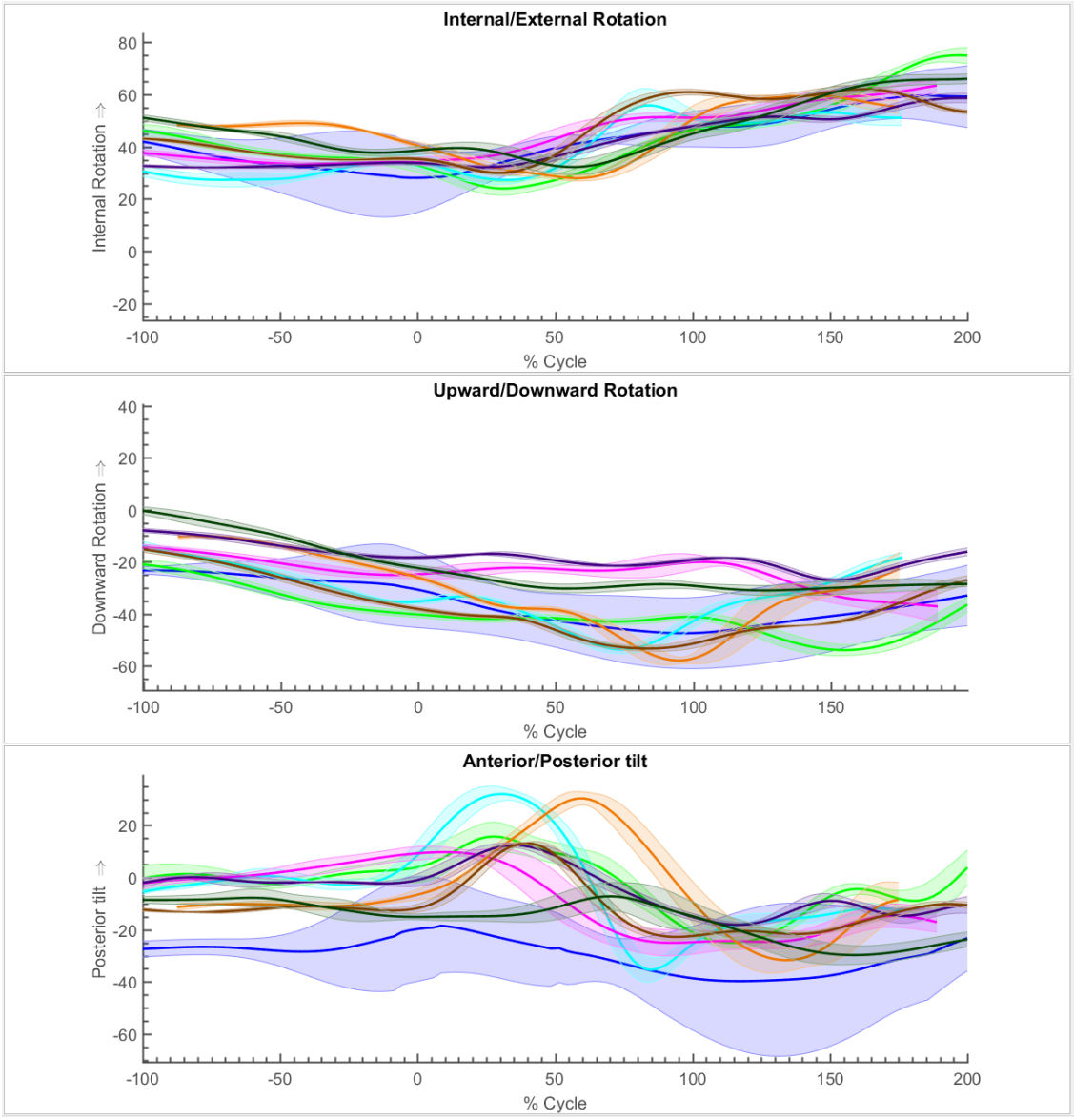

Figure 1.15 Scapulothoracic rotations, fast bowlers-variation over.

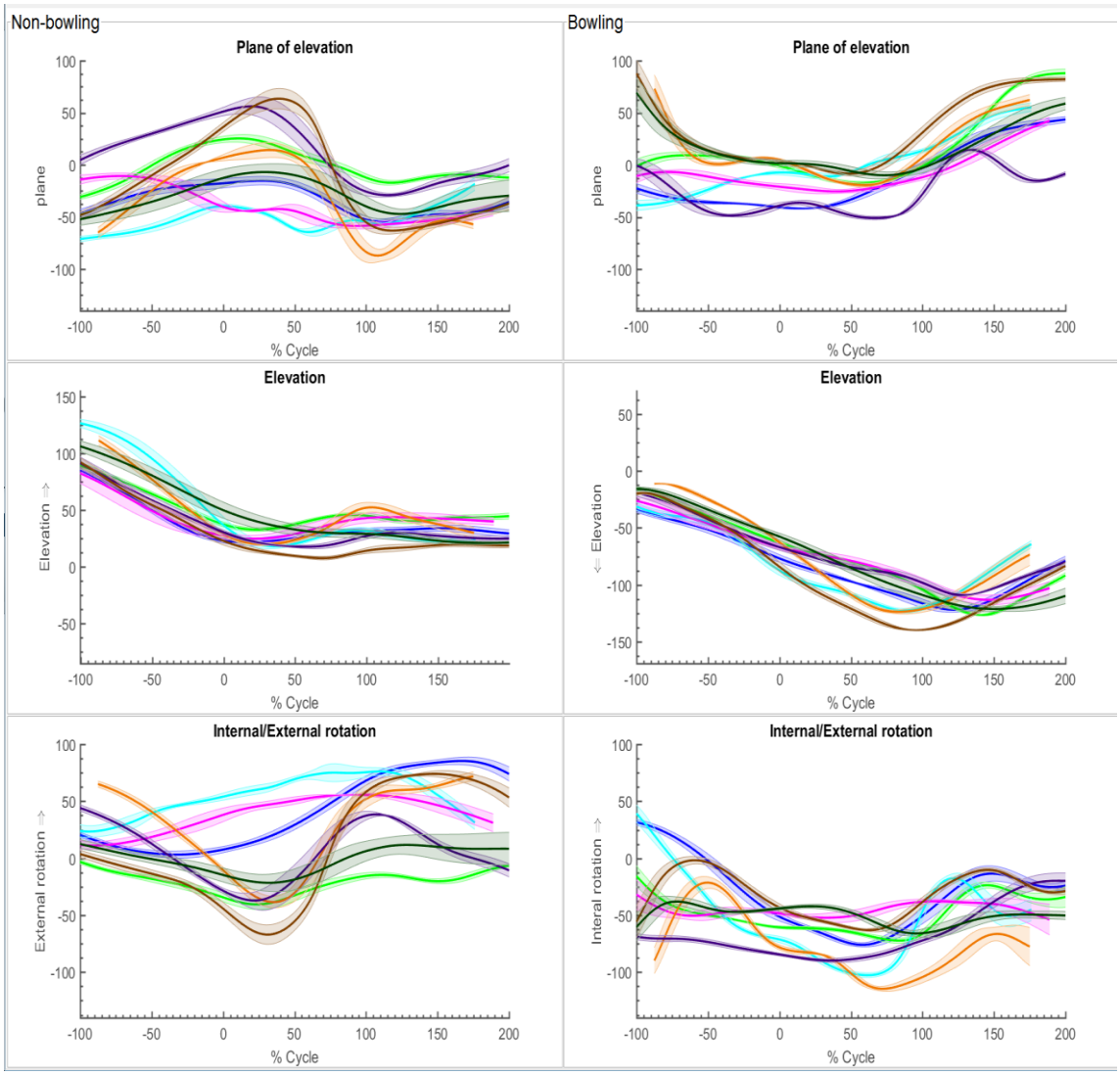

Figure 1.16 Humerothoracic rotations, fast bowlers-variation over.

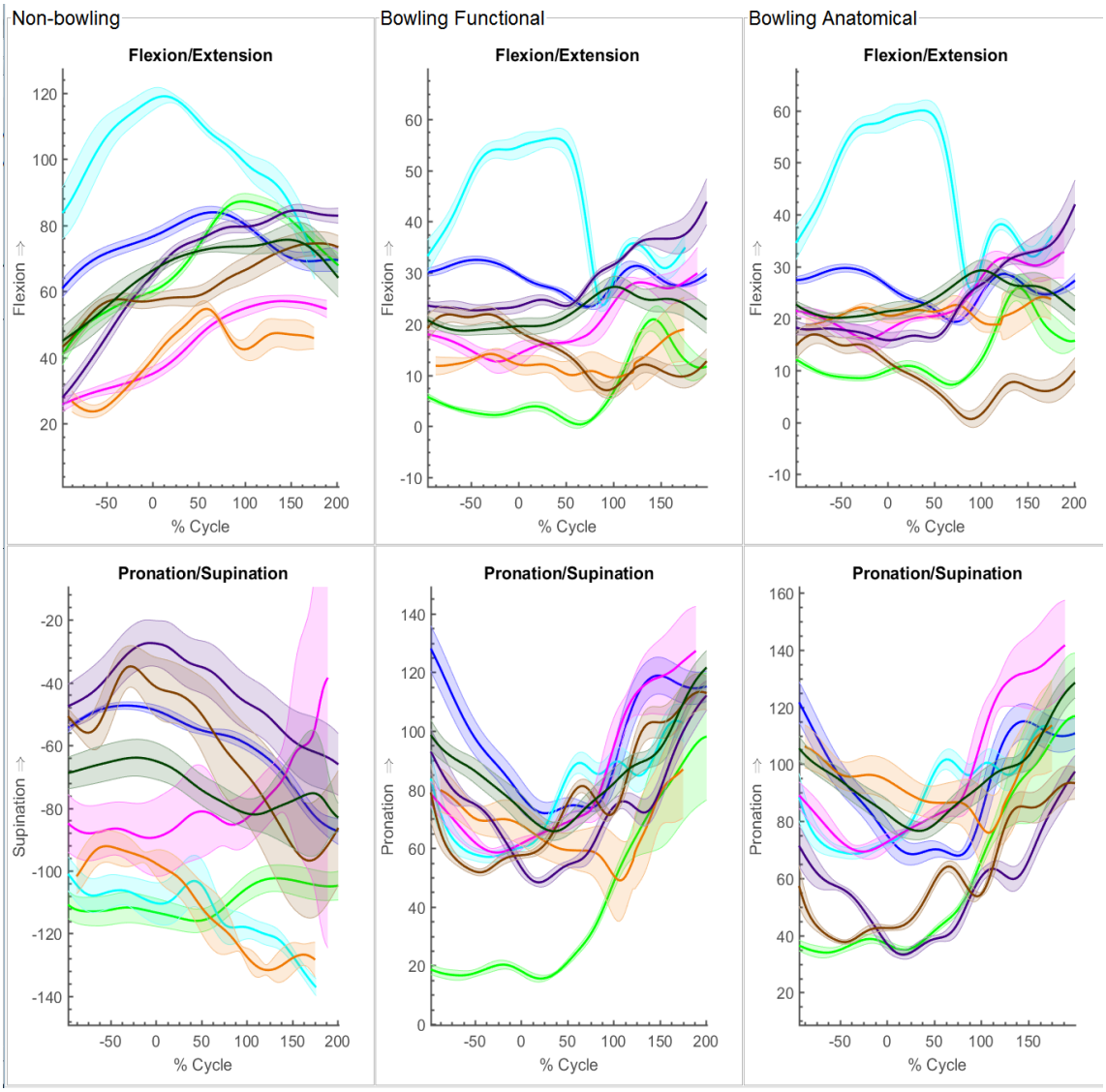

Figure 1.17 Elbow joint , fast bowlers-variation over.

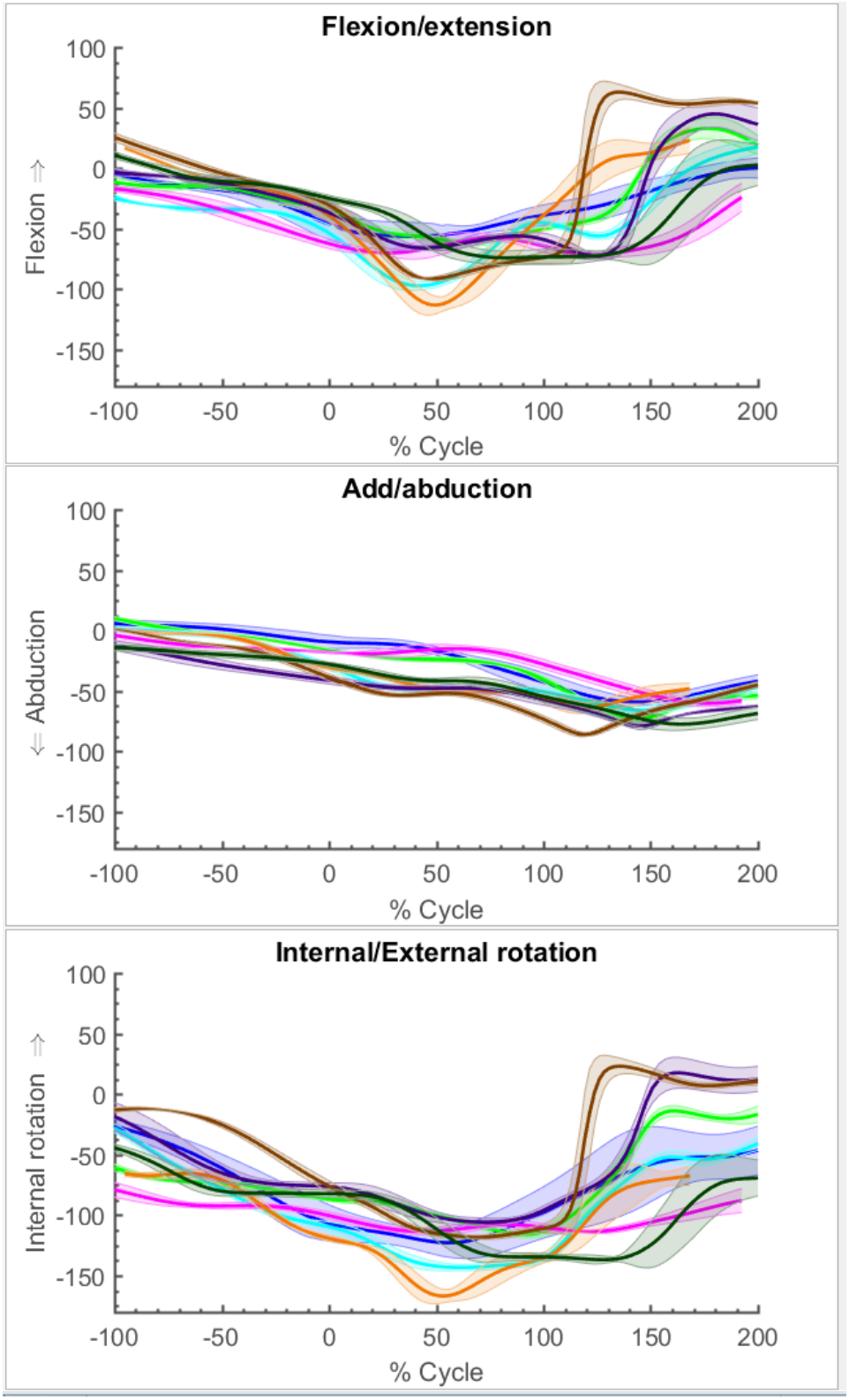

Figure 1.18 Alternative GH joint kinematics using Euler sequence ZXY, fast bowlers variation over

Slow bowlers stock delivery

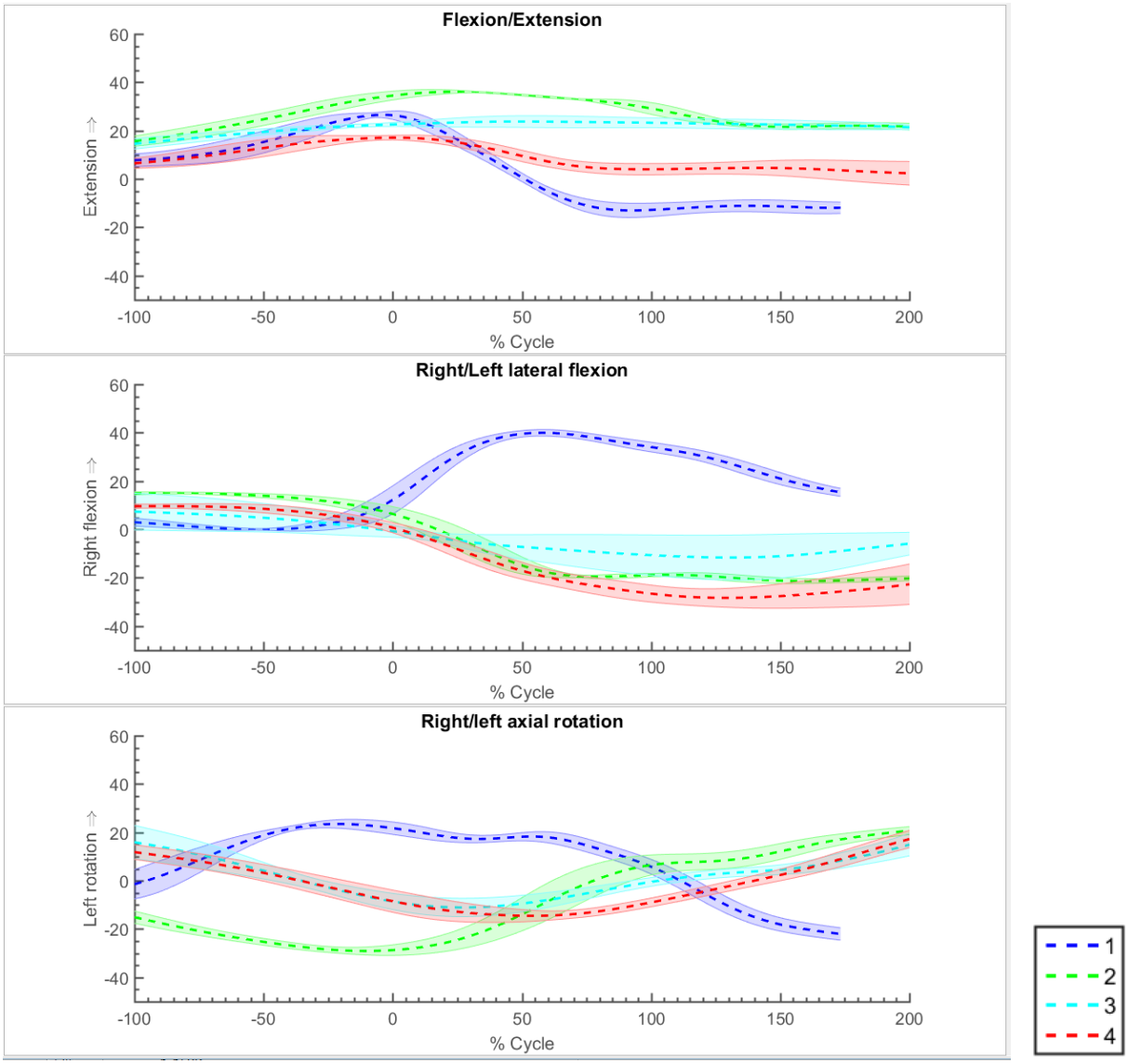

Figure 1.19 Thorax relative to pelvis, slow bowlers-stock over.

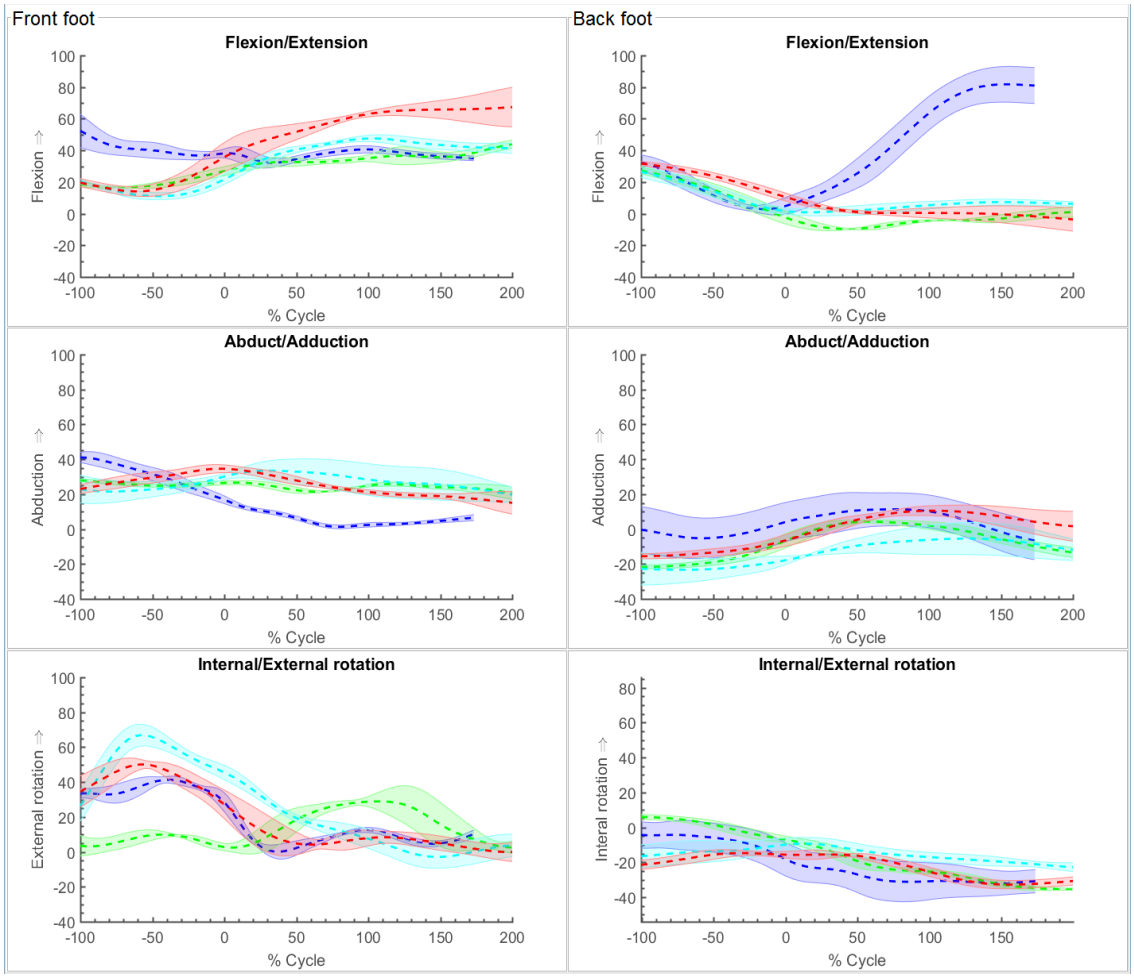

Figure 1.20 Hip joint, slow bowlers-stock over.

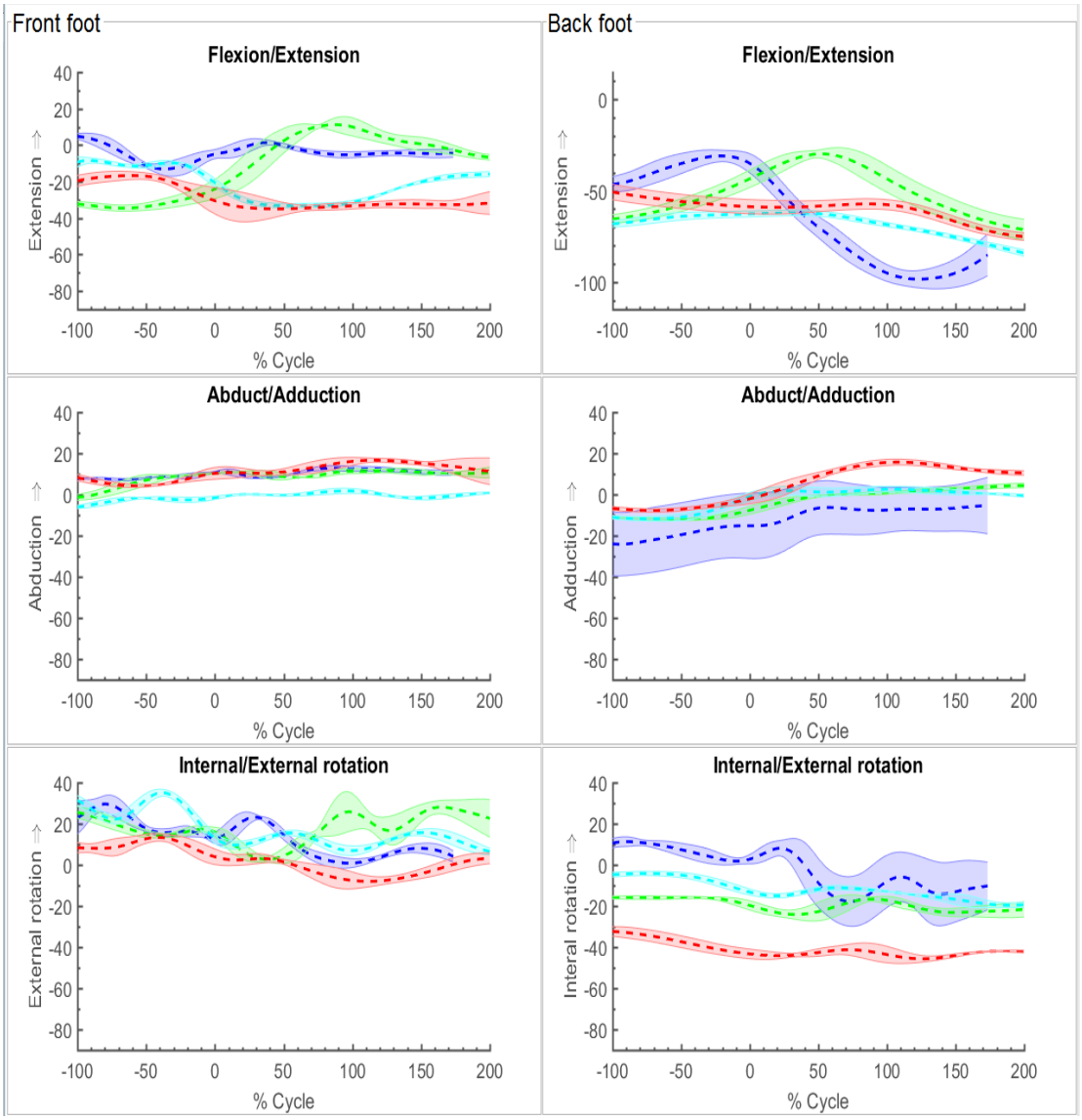

Figure 1.21 Knee joint, slow bowlers-stock over.

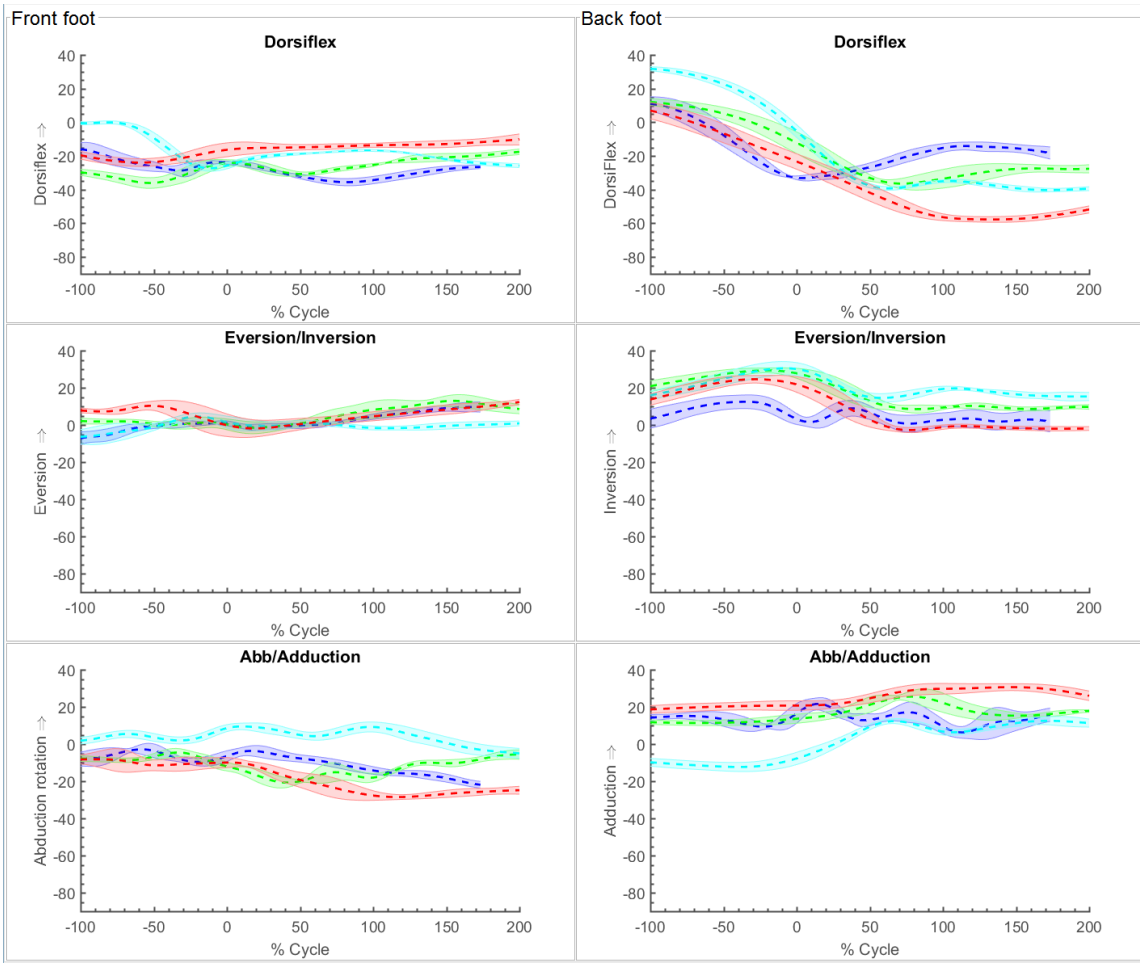

Figure 1.22 Ankle joint, slow bowlers-stock over.

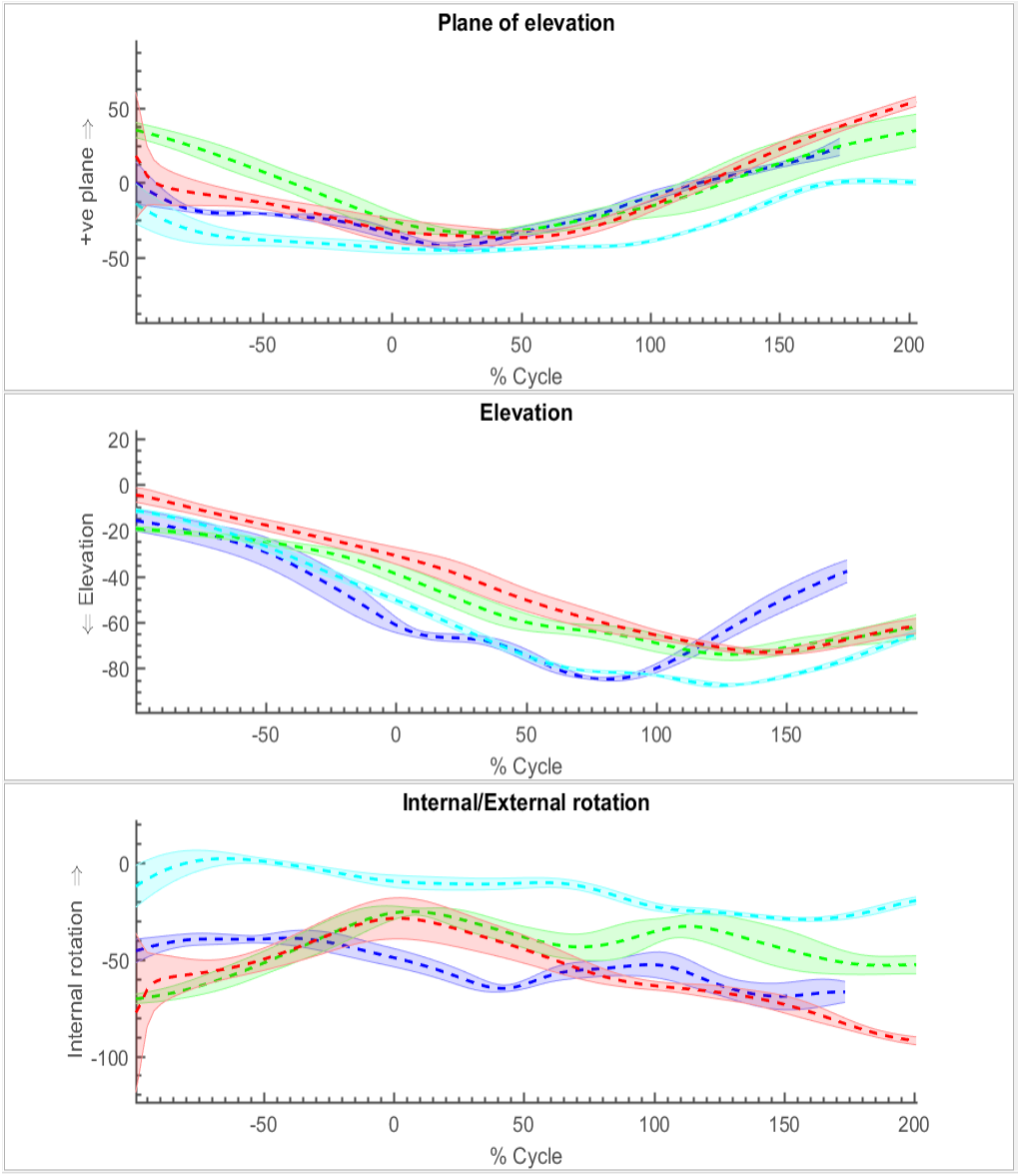

Figure 1.23 Glenohumeral joint, slow bowlers-stock over.

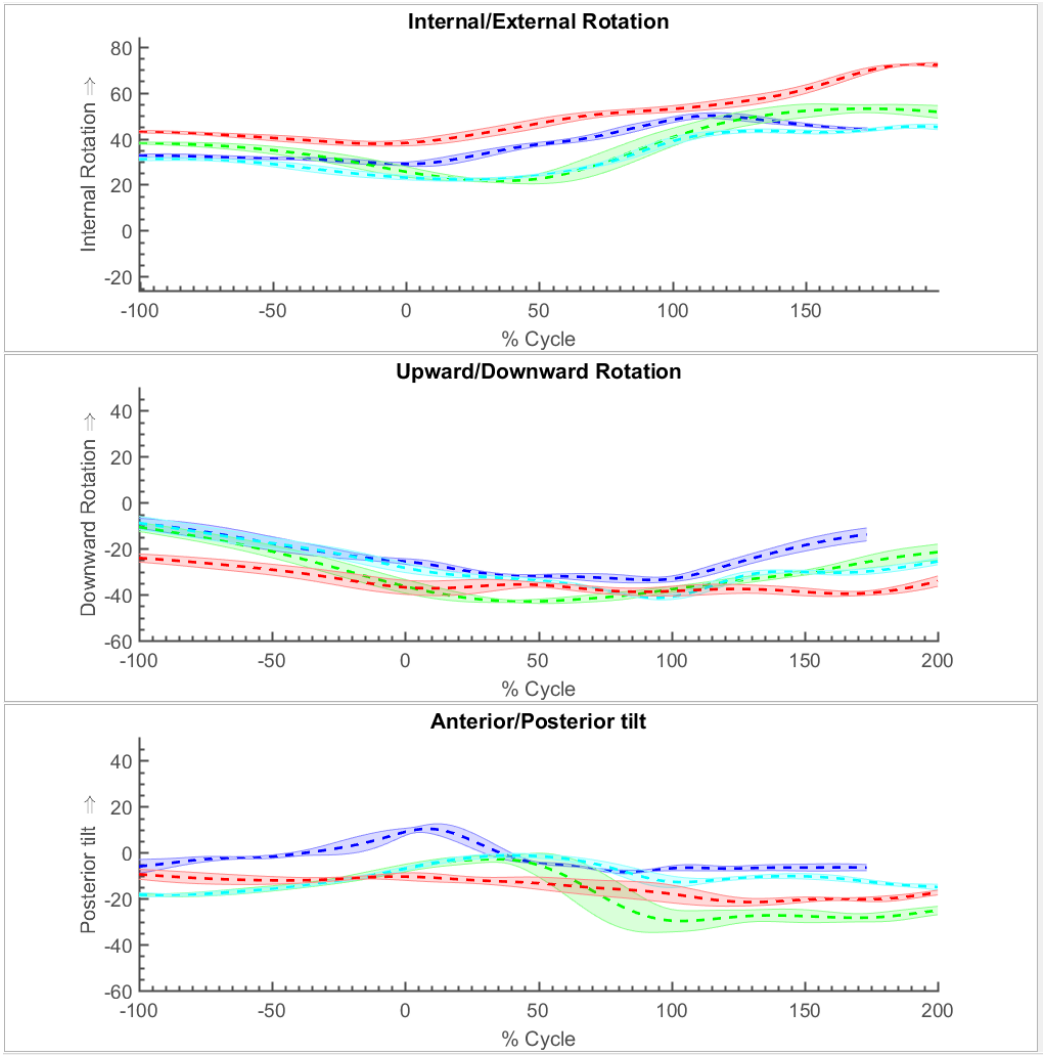

Figure 1.24 Scapulothoracic rotations, slow bowlers-stock over.

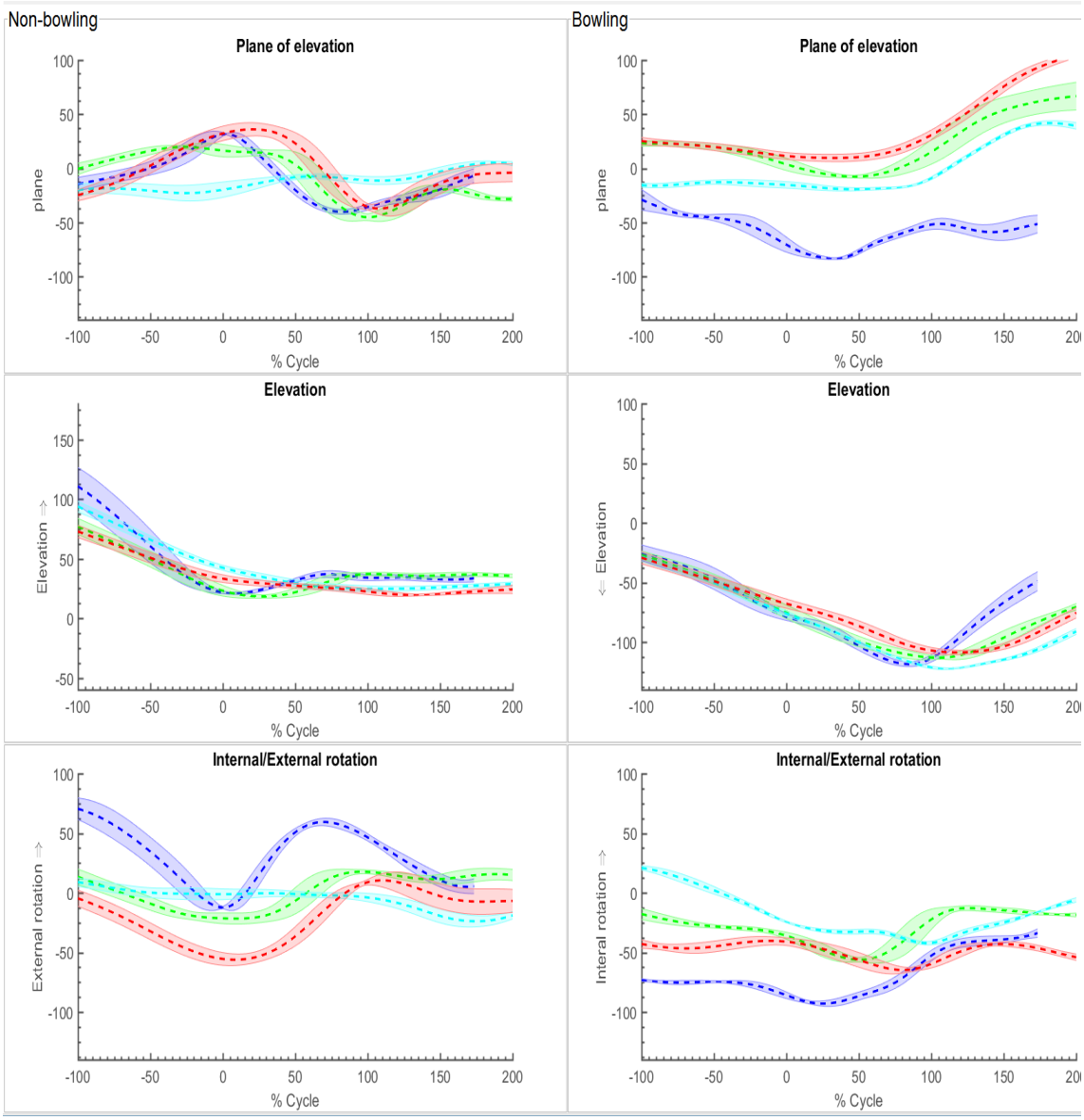

Figure 1.25 Humerothoracic rotations, slow bowlers-stock over.

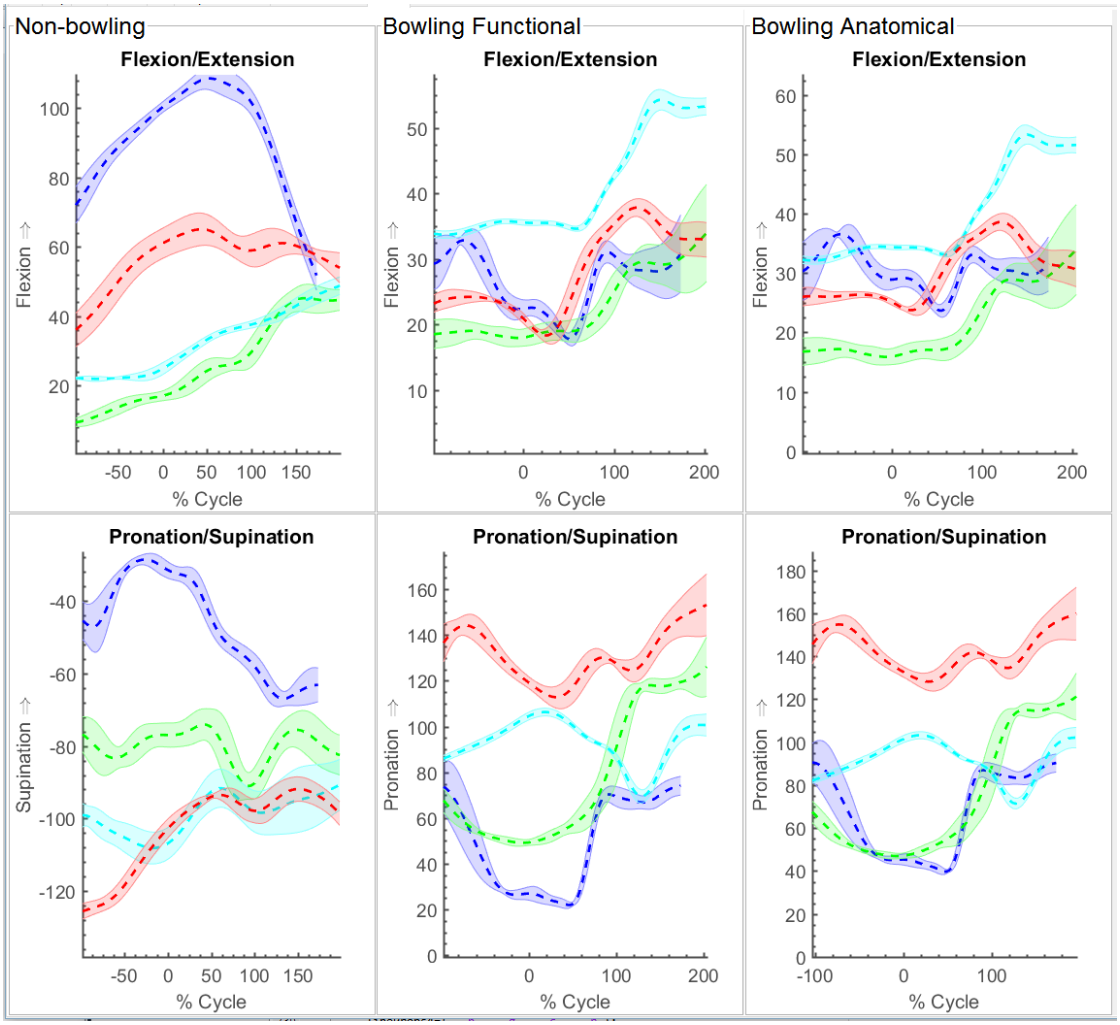

Figure 1.26 Elbow joint, slow bowlers-stock over.

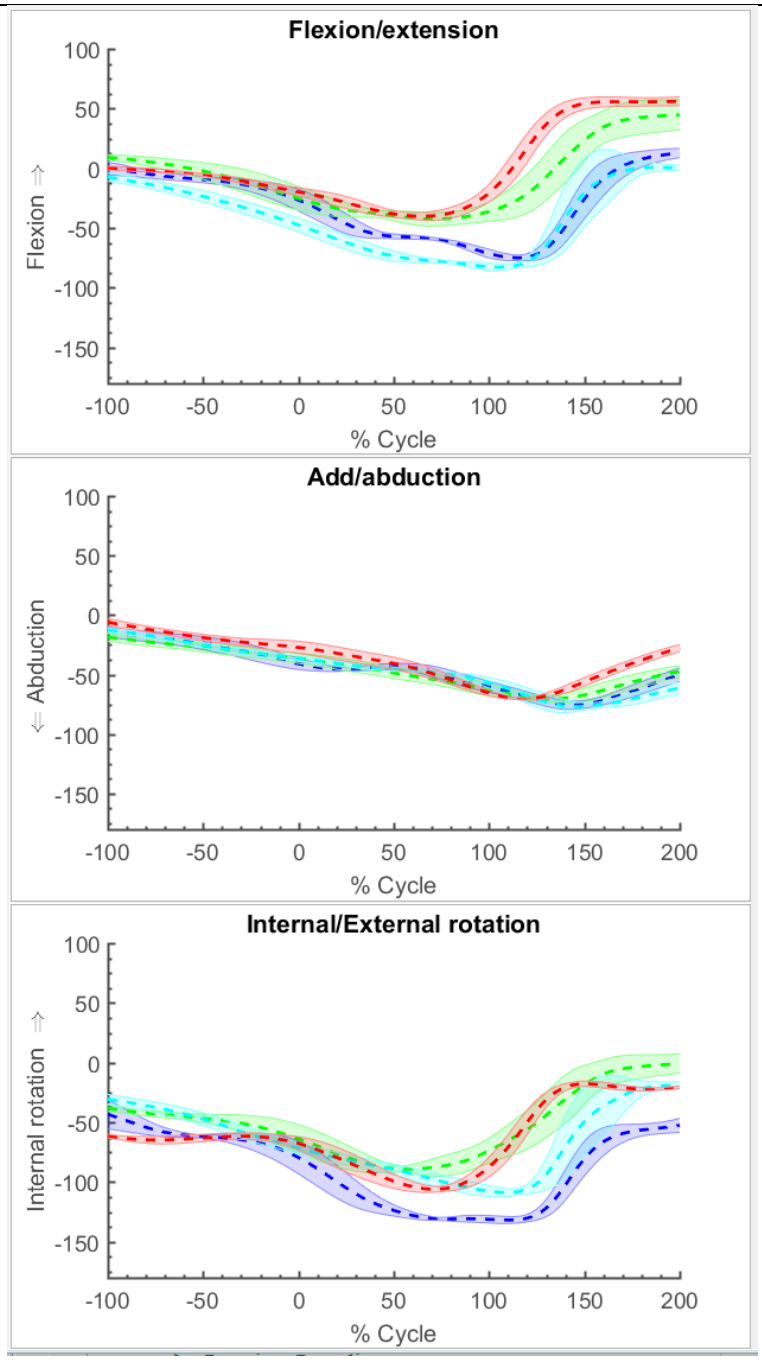

Figure 1.27 Alternative GH joint kinematics using Euler sequence ZXY, slow bowlers stock over

Slow bowlers variation over

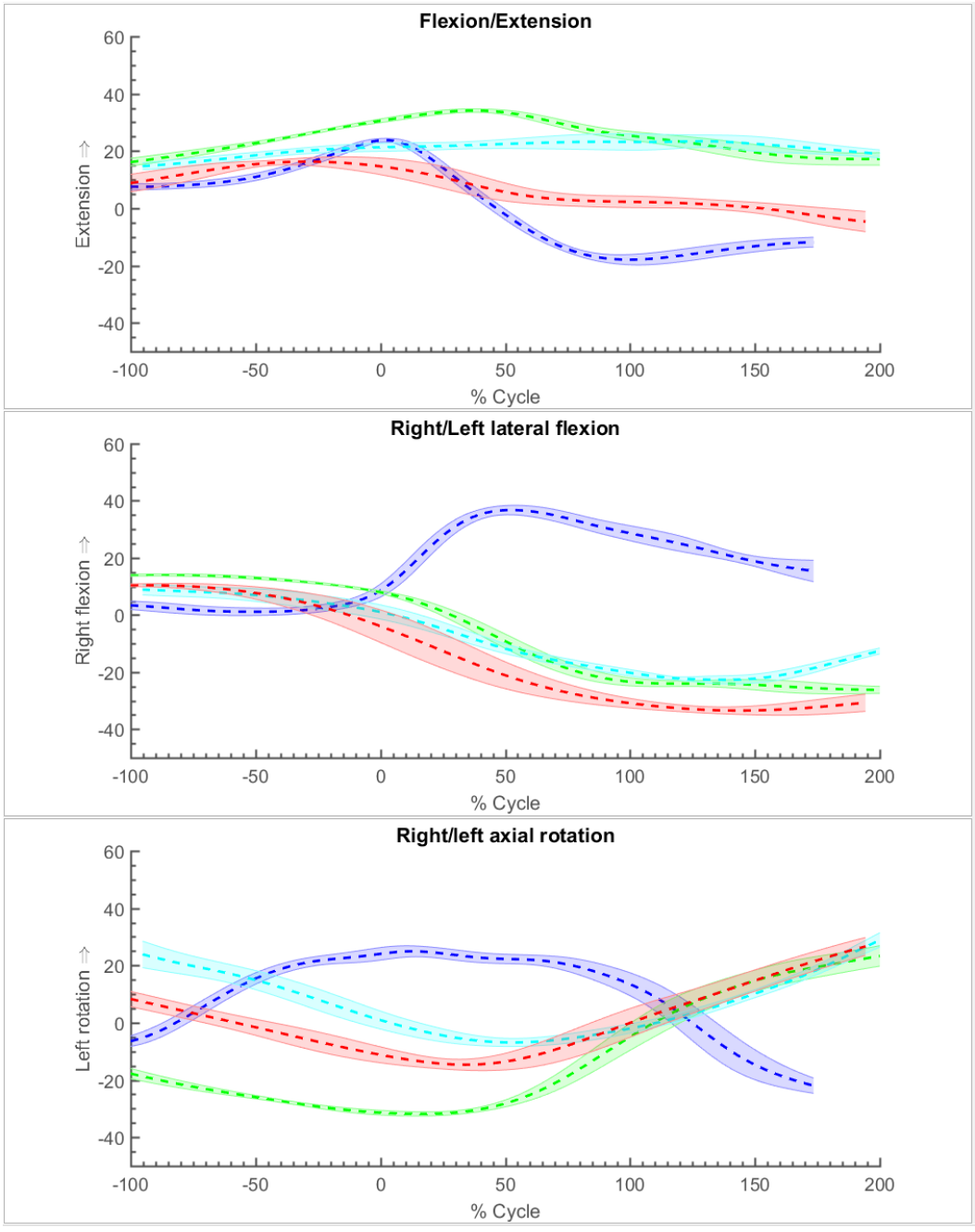

Figure 1.28 Thorax relative to pelvis, slow bowlers-variation over.

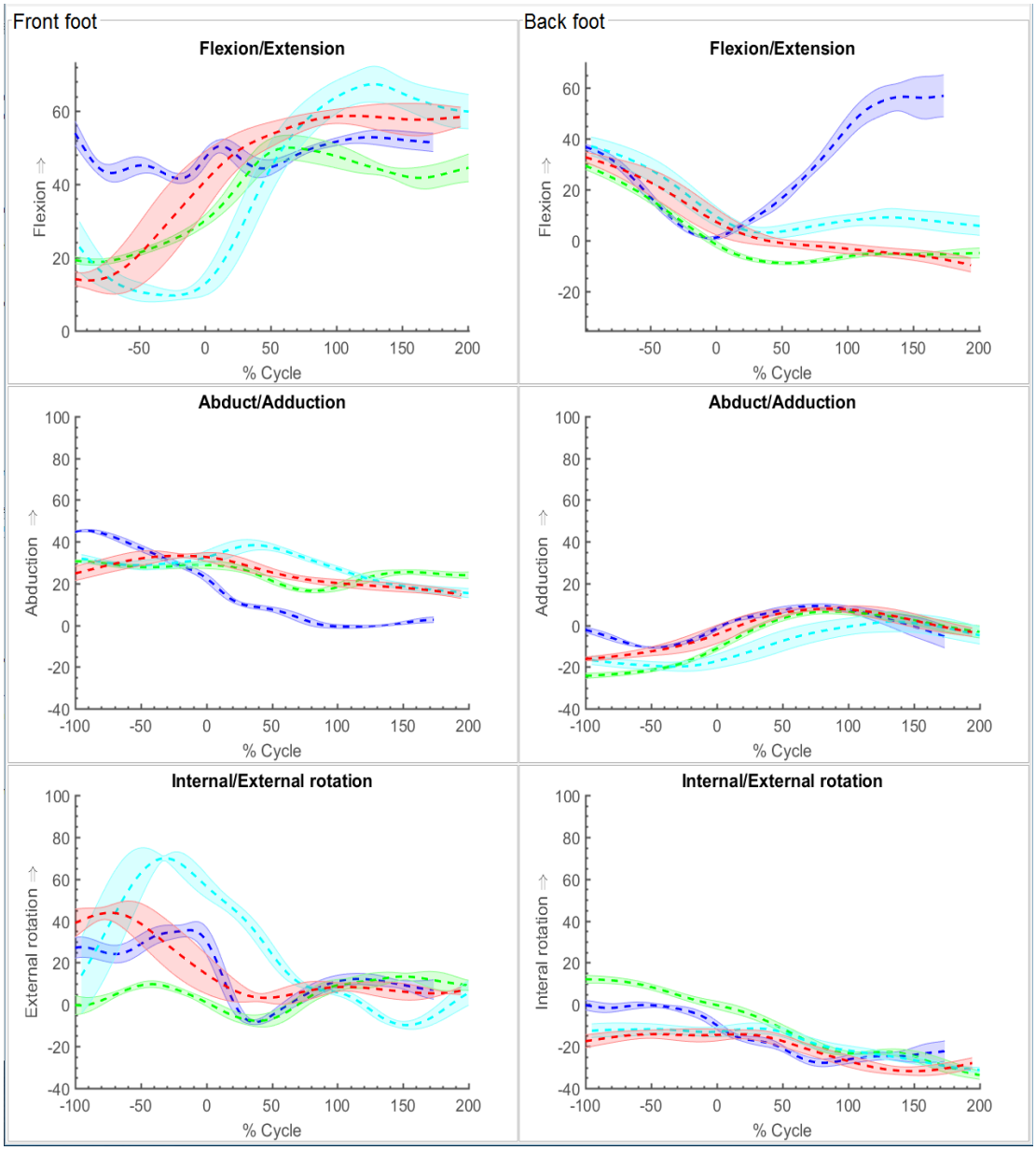

Figure 1.29 Hip joint, slow bowlers-variation over.

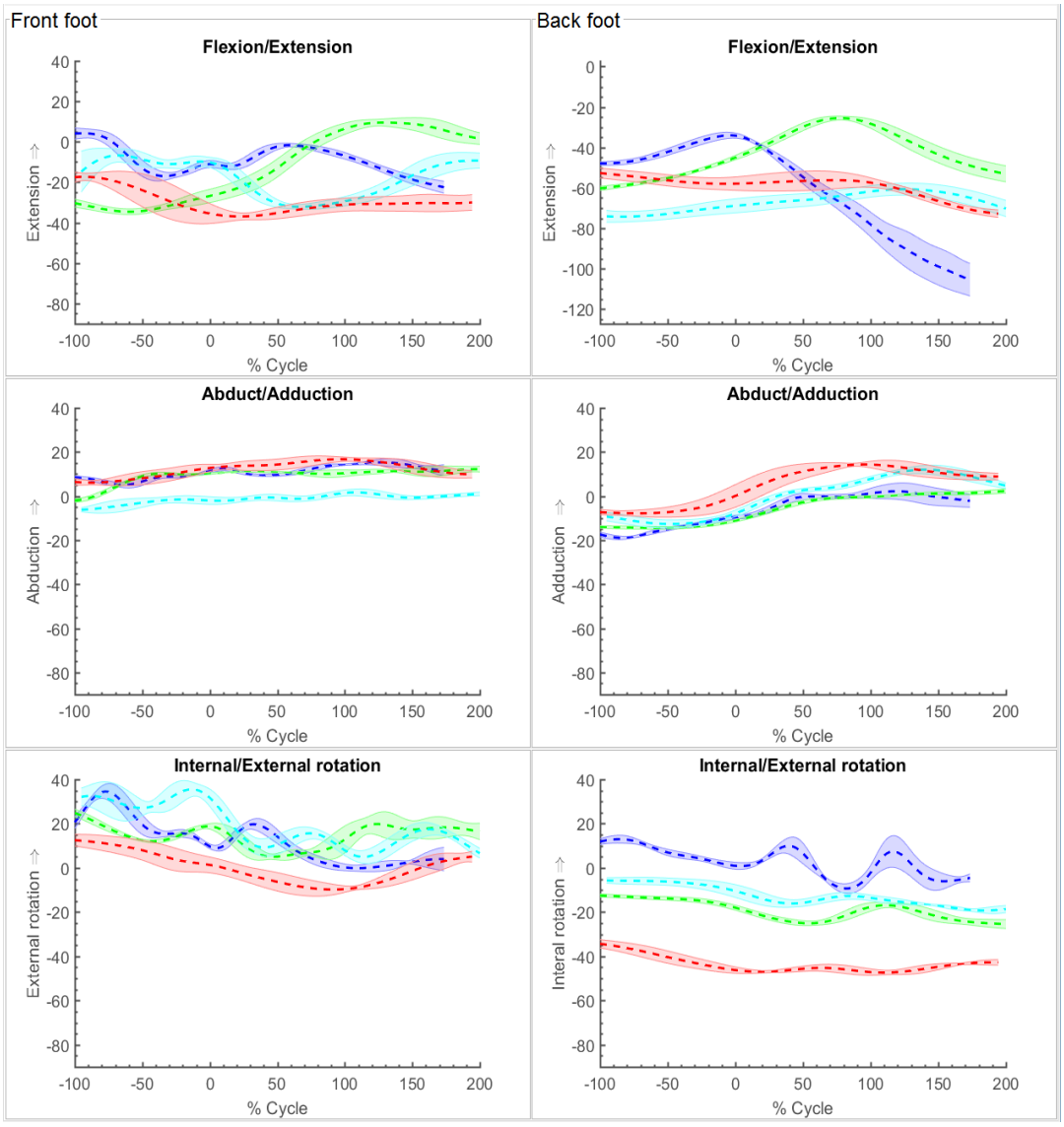

Figure 1.30 Knee joint, slow bowlers-variation over.

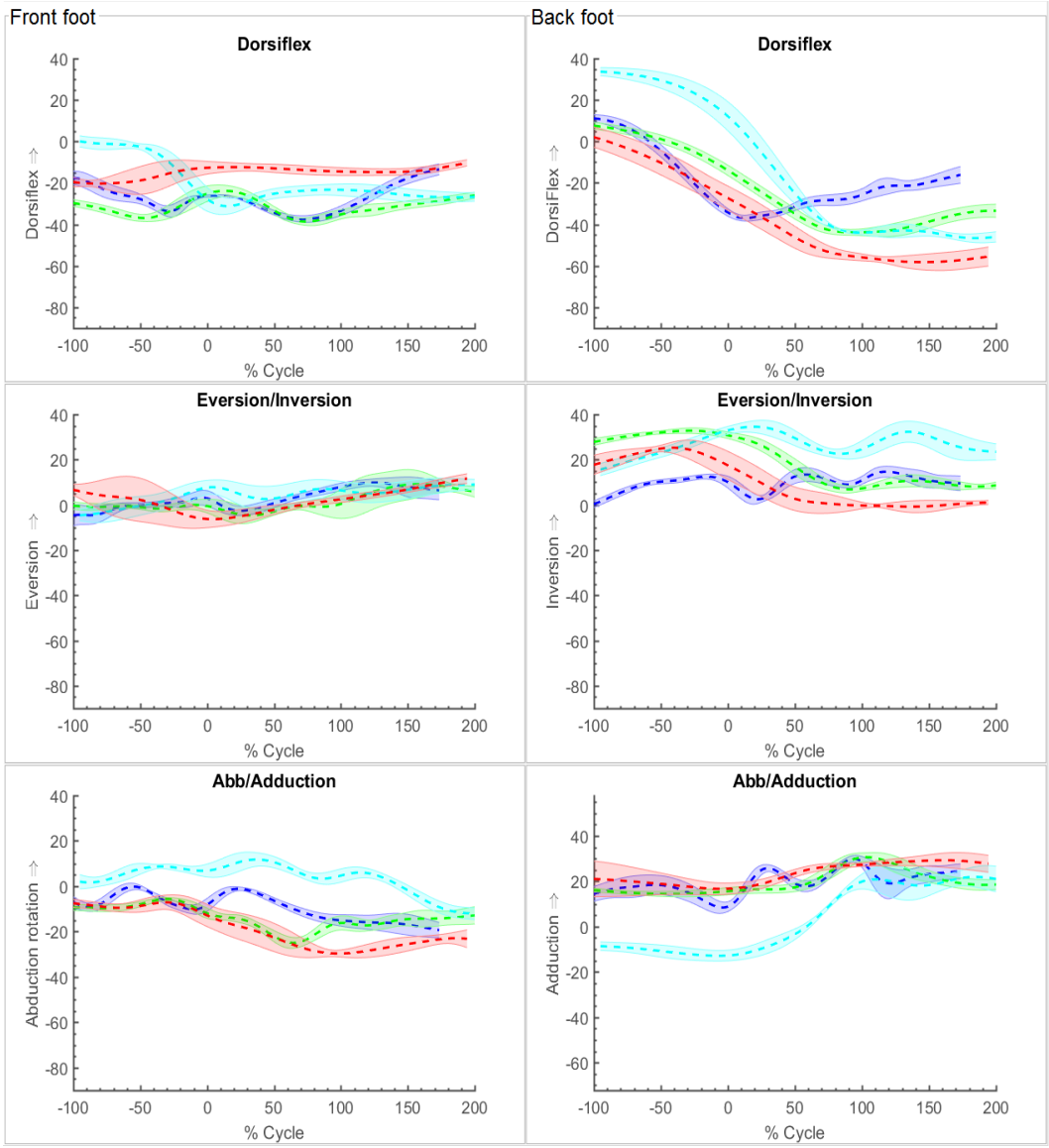

Figure 1.31 Ankle joint, slow bowlers-variation over.

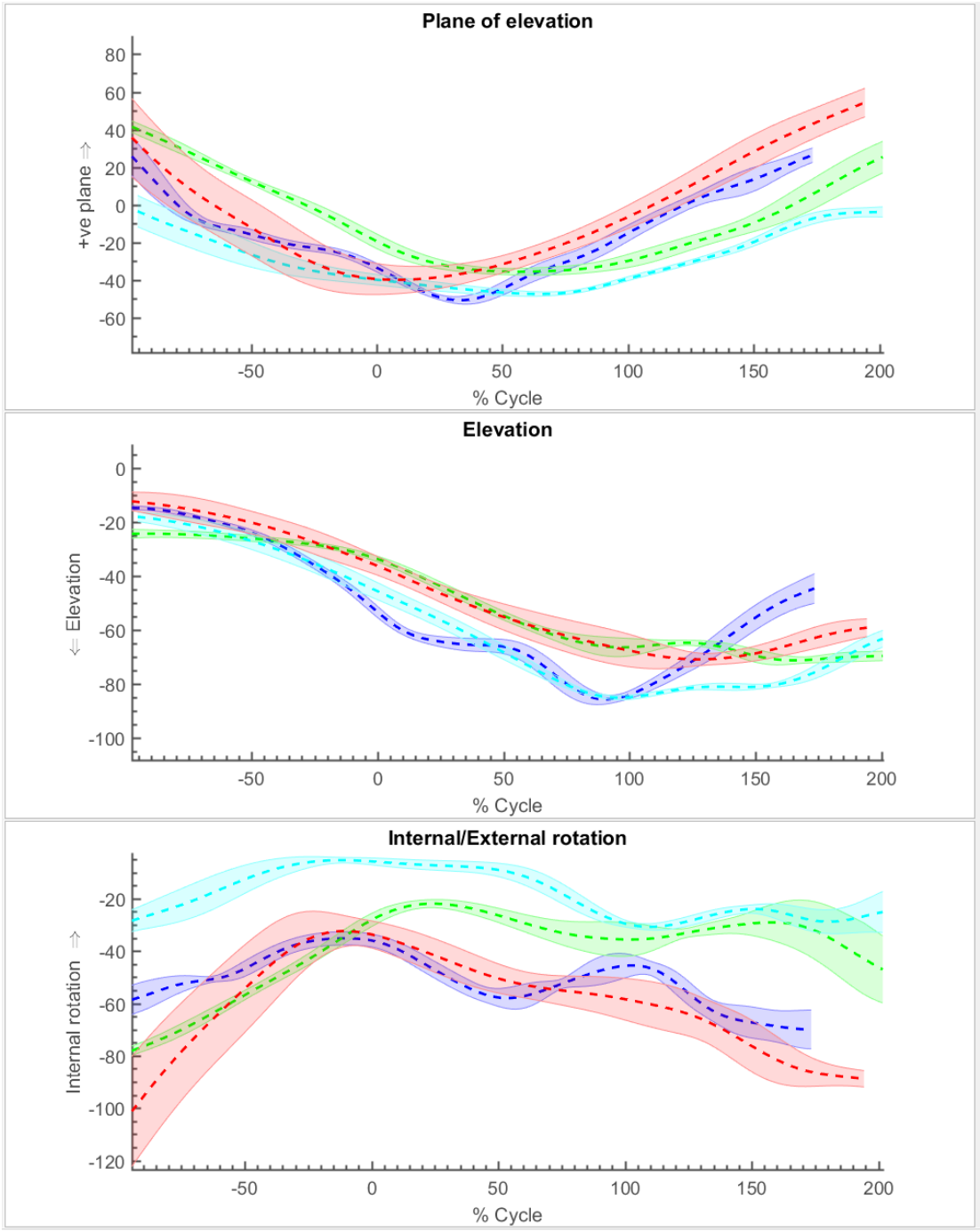

Figure 1.32 Glenohumeral joint, slow bowlers-variation over.

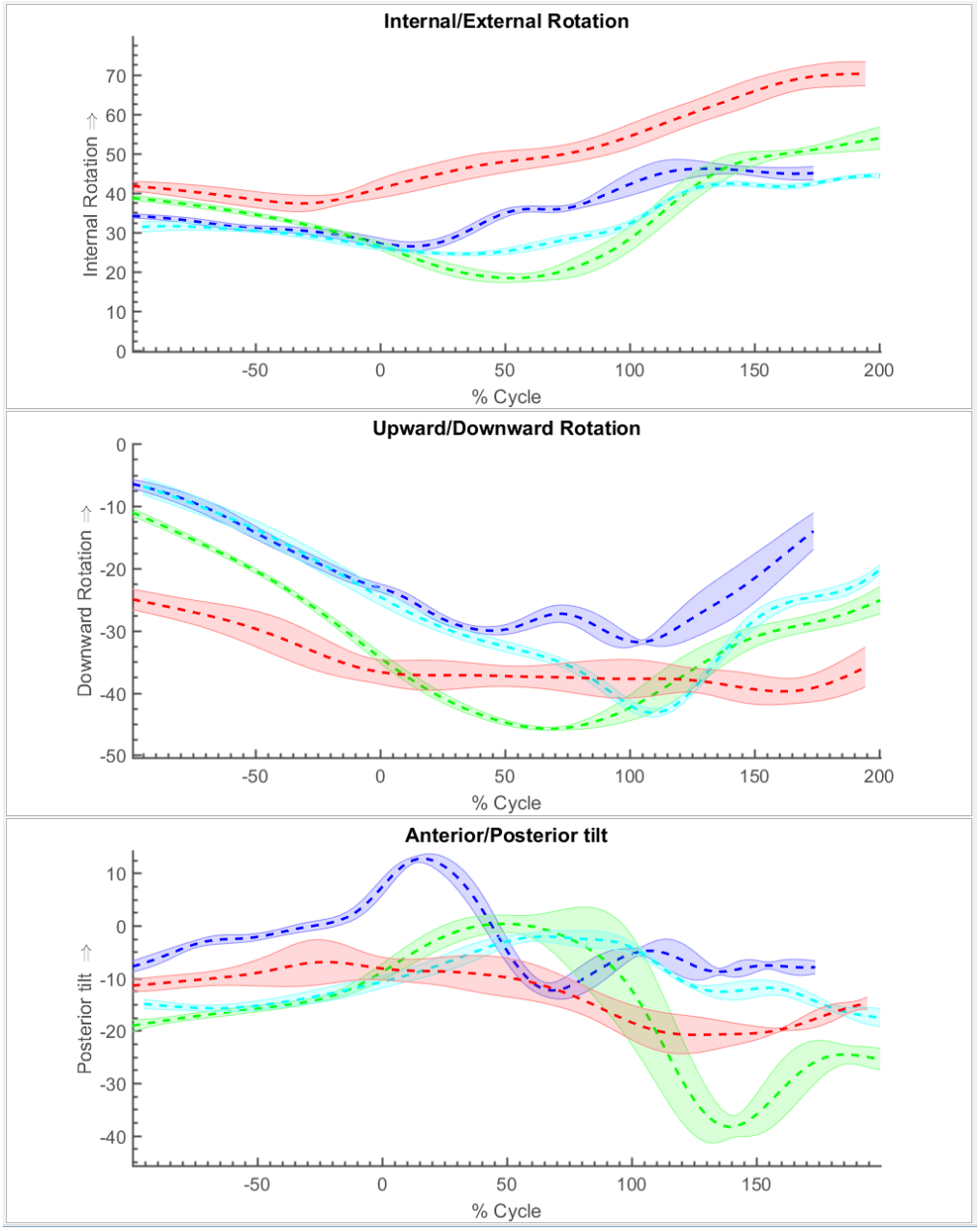

Figure 1.33 Scapulothoracic rotations, slow bowlers-variation over.

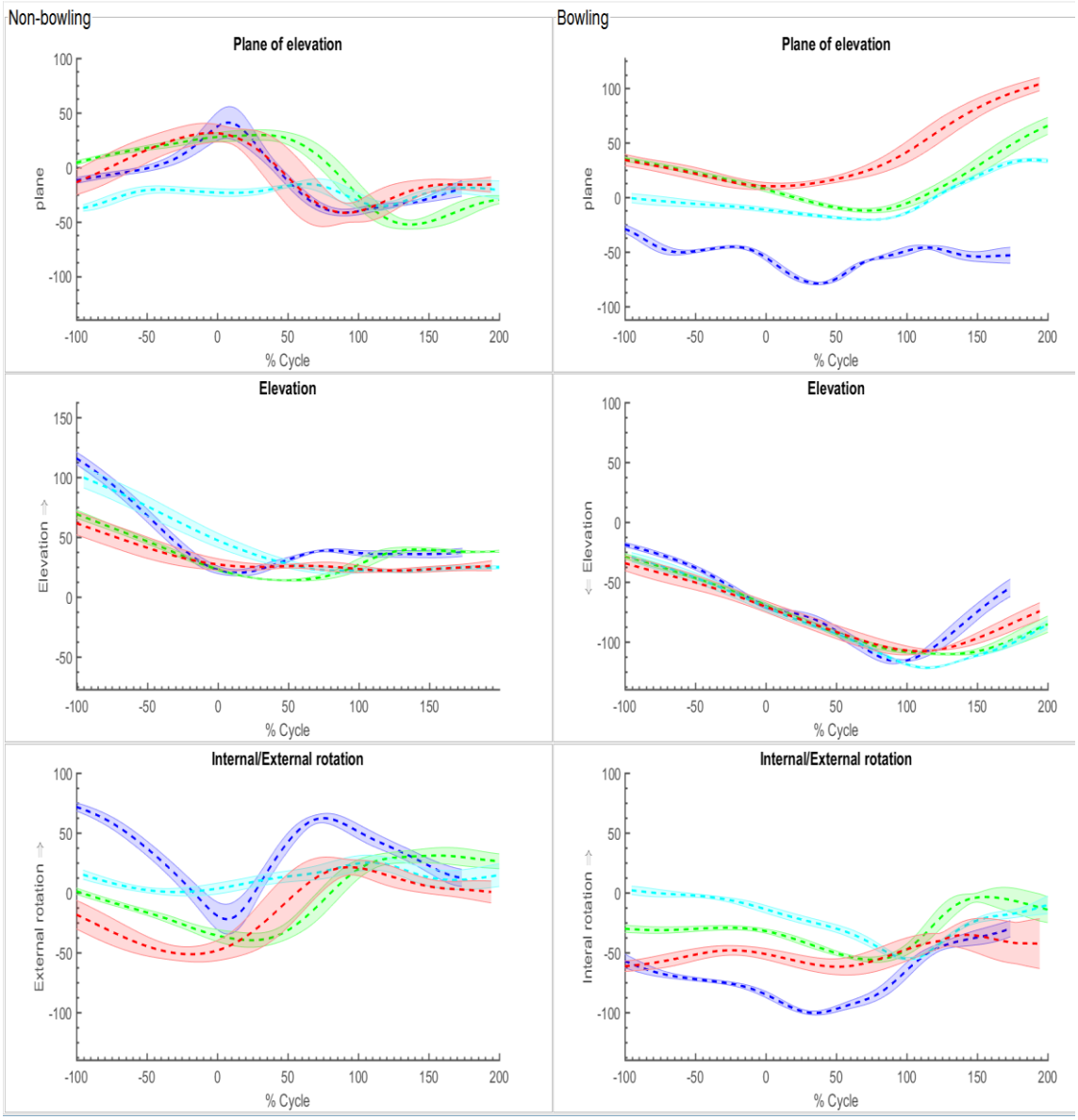

Figure 1.34 Humerothoracic rotations, slow bowlers-variation over.

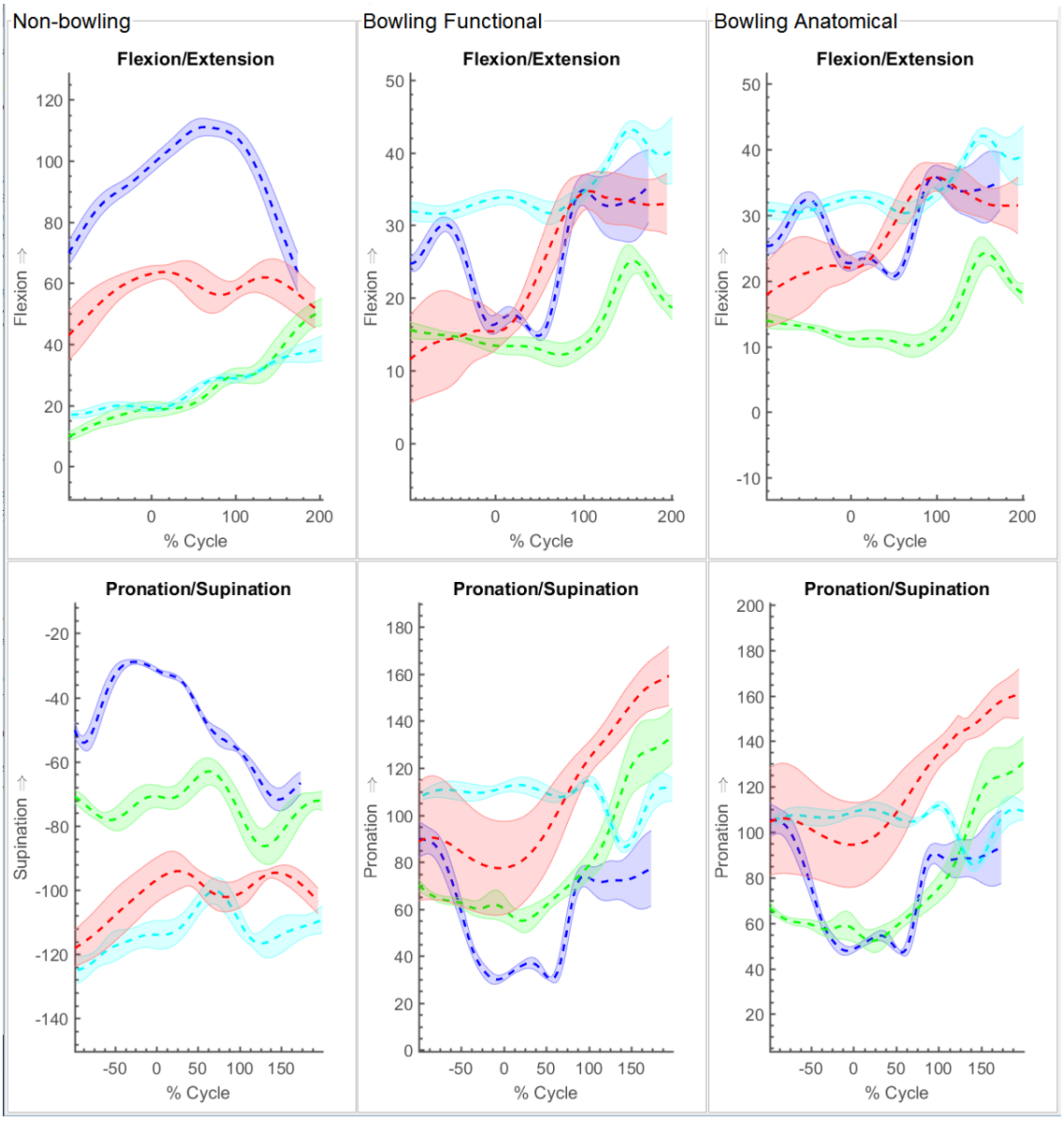

Figure 1.35 Elbow joint, slow bowlers-variation over.

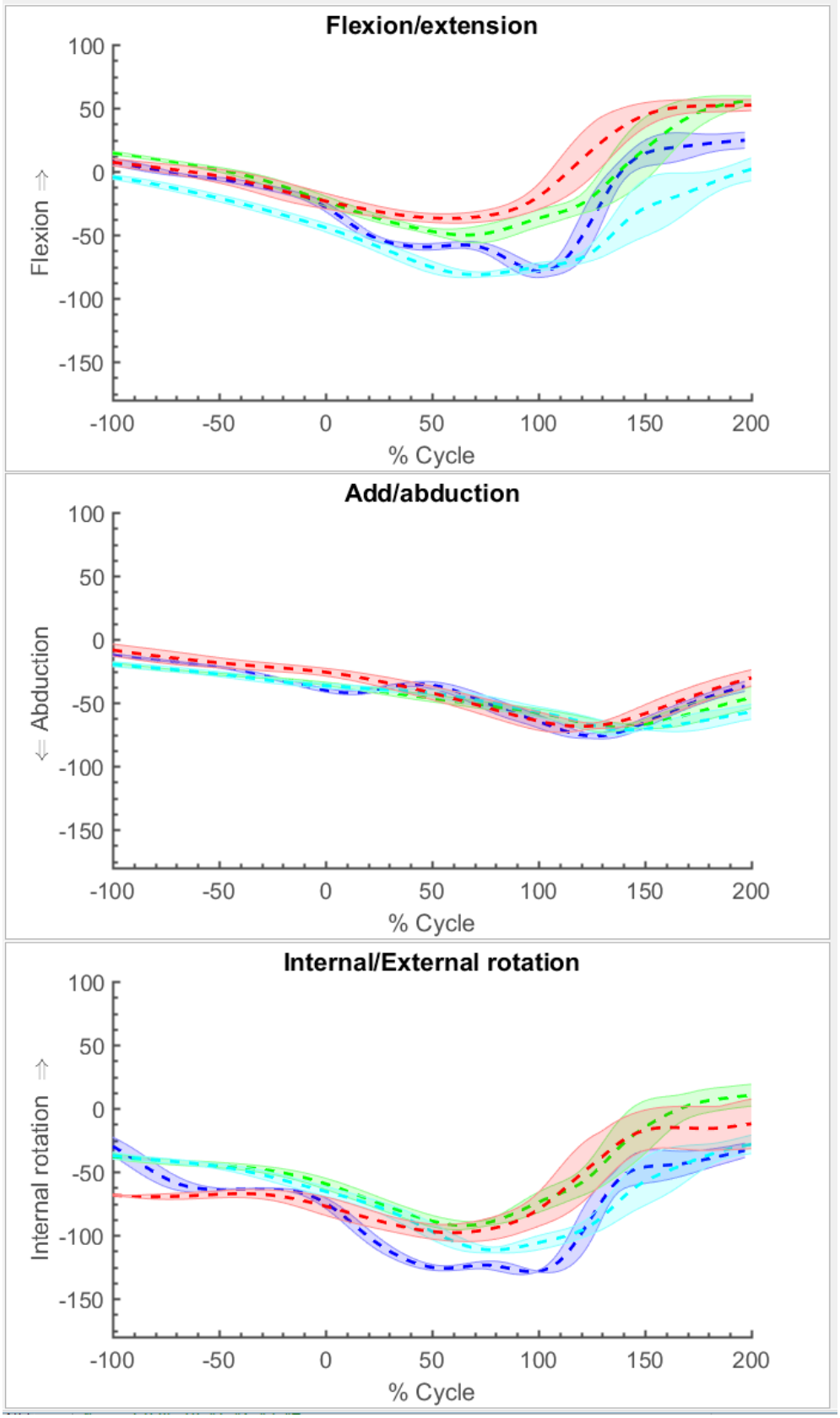

Figure 1.36 Alternative GH joint kinematics using Euler sequence ZXY, slow bowlers variation over

Appendix 2 Motion capture model

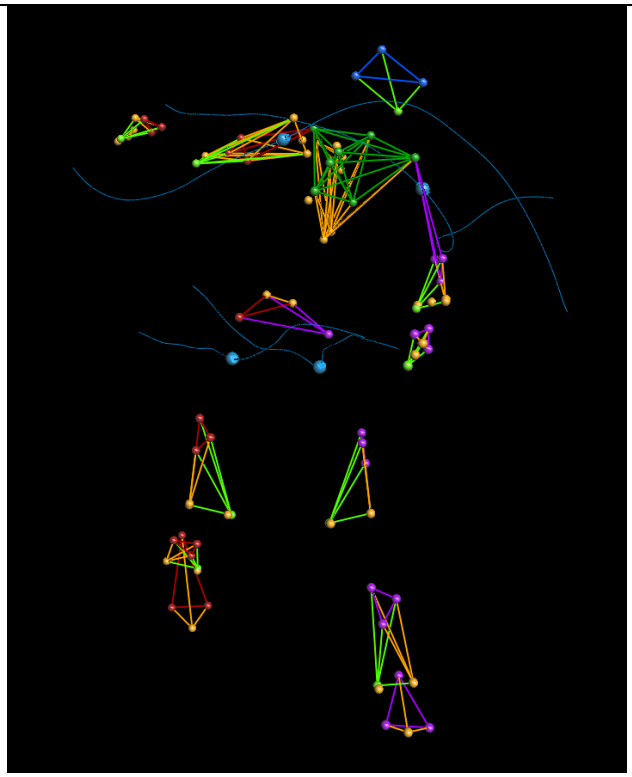

Figure 2.1 Example of the glenohumeral and hip joint centres calculated

Appendix 3 correct moment arms for the pectoralis muscle

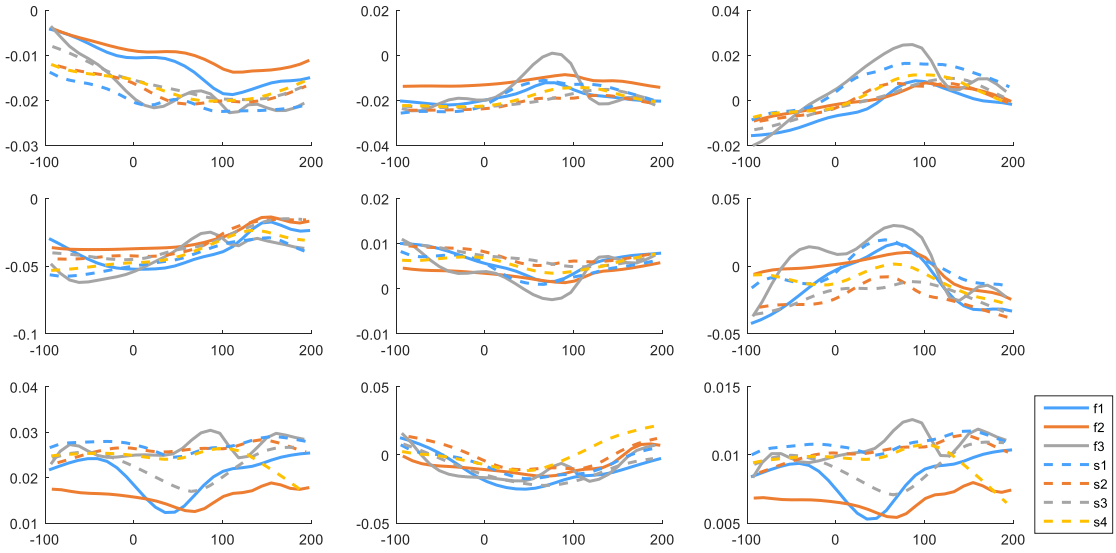

Figure 3.1 Pectoralis major clavicle (3 elements) moment arm during bowling for 3 fast bowlers and 4 slow bowlers

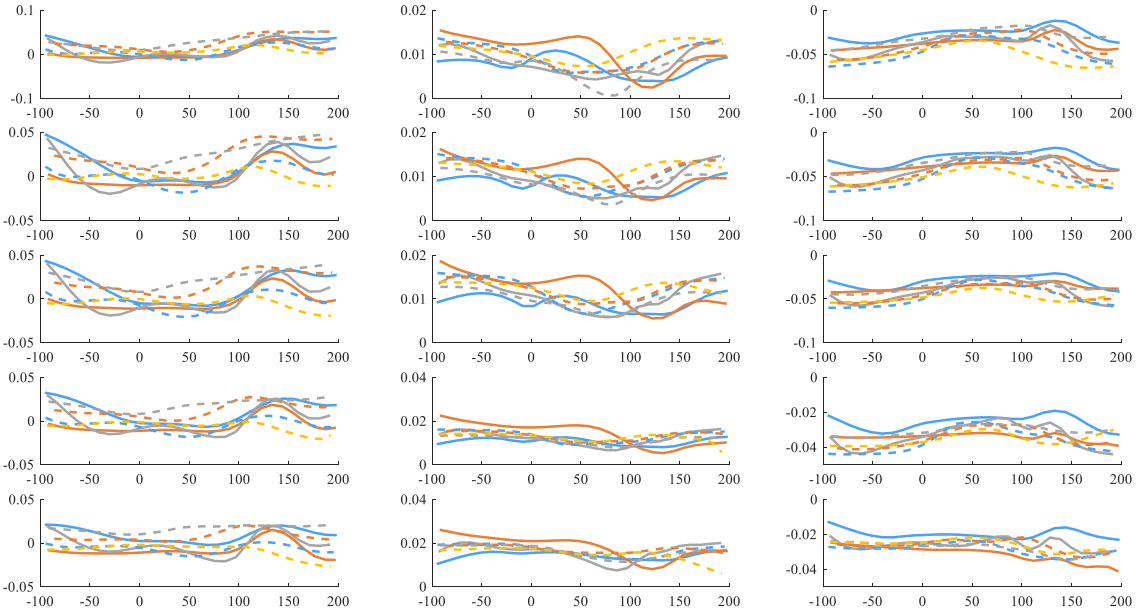

Figure 3.2 Pectoralis major thorax (5 elements) moment arm during bowling for 3 fast bowlers and 4 slow bowlers